



UNIVERSIDAD DE CHILE
FACULTAD DE CIENCIAS FÍSICAS Y MATEMÁTICAS
DEPARTAMENTO DE INGENIERÍA MATEMÁTICA

**CONTRIBUTIONS TO OPTIMIZATION IN ENERGY:
FROM BILEVEL OPTIMIZATION TO OPTIMAL DESIGN
OF RENEWABLE ENERGY PLANT**

**TESIS PARA OPTAR AL GRADO DE
DOCTOR EN CIENCIAS DE LA INGENIERÍA, MENCIÓN
MODELACIÓN MATEMÁTICA**

DANIEL LASLUIA CASTAÑO

Profesores Guía:
Didier Aussel
Héctor Ramírez Cabrera

Profesor Co-Guía:
David Salas Videla

Miembros de la comisión:

Olivier Beaudé
Alejandro Jofré Cáceres
Pierre Neveu
Freddy Ordóñez Malla
Claudia Sagastizábal

Este trabajo ha sido en cotutela con la Universidad de Perpiñán Via Domitia y parcialmente financiado por ANID-2020/21201478, CMM ANID BASAL FB10005, SOLSTICE project ANR-10-LABX-0022, FONDECYT-ANID 11220586 y 1201982.

SANTIAGO DE CHILE
2024

RESUMEN DE LA TESIS PARA OPTAR
AL GRADO DE DOCTOR EN CIENCIAS DE LA INGENIERÍA,
MENCION MODELACIÓN MATEMÁTICA
POR: DANIEL LASLUIA CASTAÑO
FECHA: 2024
PROF. GUÍA: SR. HÉCTOR RAMÍREZ Y SR. DIDIER AUSSEL

CONTRIBUCIONES A LA OPTIMIZACIÓN EN ENERGÍA: DESDE LA
OPTIMIZACIÓN BINIVEL AL DISEÑO ÓPTIMO DE PLANTAS DE ENERGÍA
RENOVABLE

En este trabajo de tesis, desarrollamos y aplicamos técnicas de optimización en el diseño y gestión de energía. En primer lugar, nos enfocamos en la optimización binivel y desarrollamos nuevo análisis teórico para single-leader-multi-follower games con restricciones de cardinalidad. Luego, se aplica a la localización óptima de estaciones de carga por vehículos eléctricos. La segunda parte está dedicada a la optimización económica de plantas solares desde una perspectiva a largo plazo, así como desde una perspectiva a corto plazo. Se desarrolla un enfoque innovador de optimización global que combina el diseño óptimo de almacenamiento y la operación óptima en un contexto de mercado. Luego, a escala a corto plazo, se analiza el control óptimo de la producción de energía de una planta solar.

RESUMEN DE LA TESIS PARA OPTAR
AL GRADO DE DOCTOR EN CIENCIAS DE LA INGENIERÍA,
MENCION MODELACION MATEMATICA
POR: DANIEL LASLUISA CASTAÑO
FECHA: 2024
PROF. GUÍA: SR. HÉCTOR RAMÍREZ Y SR. DIDIER AUSSEL

CONTRIBUTIONS TO OPTIMIZATION IN ENERGY: FROM BILEVEL
OPTIMIZATION TO OPTIMAL DESIGN OF RENEWABLE ENERGY PLANT

In this thesis work, we develop and apply optimization techniques in energy design and management. First we focus on bilevel optimization and developed new theoretical analysis for single-leader-multi-follower games with cardinality constraints. It is then applied to optimal location of charging stations for electric vehicles. The second part is dedicated to economic optimization of solar power plants from a long term as well as from a short term perspective. Innovating global optimization approach mixing optimal design of storage and optimal operation in a market context is developed. Then at a short term scale, the optimal control of energy production of a solar power plant is analysed.

Acknowledgements

I want to express my deepest gratitude to all the people who significantly contributed to the completion of this thesis work. First and foremost, I thank my family for their unwavering support and for being my constant source of inspiration, as well as my friends for their constant encouragement, understanding, and for providing me with moments of distraction and joy during the most challenging times. Furthermore, I want to express my gratitude to my esteemed professors, whose wisdom, guidance, and advice have been fundamental in the development of this work. Their dedication and commitment to academic excellence have been a constant source of motivation and learning. To each and every one of you, my heartfelt thanks. This achievement would not have been possible without your unwavering support.

Table of content

Front cover (sp-en)	
1 Introduction (English and French version)	1
1.1 Part I: Bilevel games and cardinality constraints	2
1.2 Part II: Economic Efficiency of Concentrated Solar Power plants .	4
1.3 Thesis structure and development	8
1.4 Partie I: Jeux biniveaux et contraintes de cardinalité	9
1.5 Partie II: Efficacité Économique des Centrales Solaires à Concentra- tion	12
1.6 Structure et développement de la thèse	16
I Bilevel games and cardinality constraints	17
2 Preliminaries	18
2.1 Introduction	18
2.2 Definitions and notations	20
2.3 The Generalized Nash Equilibrium problem (GNEP)	22
2.4 Single-leader-multi-follower game (SLMFG)	22
2.5 Cardinality Constraint	24
2.6 MPCC Reformulation	25
2.7 SOS1	26
3 Single-Leader Multi-Follower games with cardinality constraints and their application to a location problem	27
3.1 SLMF games with upper-level cardinality constraints	27
3.1.1 Problem formulation and existence result	27
3.1.2 Reformulations	30
3.1.3 Lower-level cardinality constraints	35
3.2 SLMF games with mixed cardinality constraints	36
3.2.1 Existence of solutions and MPCC reformulation	37
3.2.2 Further results for the linear case	40
3.3 Application to Facility location problems with cardinality constraints	42
3.3.1 Upper-level and mixed formulations	43
3.3.2 Methodology	45
3.3.3 Numerical experiments and results	46

3.4	Simulations	47
3.5	Conclusion	59
II Economic Efficiency of Concentrated Solar Power plants		60
4	Preliminaries	61
4.1	Introduction	61
4.2	Black-box model	63
4.2.1	The Solar Resource and the Solar Field	64
4.2.2	The Steam Rankine Cycle or Power Block	65
4.2.3	Storage System	67
4.3	Spot Market	69
4.4	Economic Criteria	70
4.4.1	Levelized Cost of Energy (LCOE)	70
4.4.2	Net Present Value (NPV)	70
4.4.3	Internal Rate of Return (IRR)	71
4.4.4	Conventional PayBack (CPB)	71
4.5	Production Strategies	71
4.6	Optimization Algorithms	72
4.6.1	Interior point - Matlab	72
4.6.2	Bocop	72
5	Multidimensional analysis for the techno-economic study of the CSP plant with different storage systems	74
5.1	Control problem	74
5.1.1	From Control problem to the Optimization Problem	75
5.2	Optimization Problem	79
5.2.1	Modeling - Storage System	79
5.2.2	Objective Function	89
5.2.3	Bounds	93
5.2.4	Structure of the optimization problem	94
5.3	Results and Discussion	98
5.3.1	Computational Implementation	99
5.3.2	LCOE sensitivity to discharge duration	99
5.3.3	Sensitivity analysis based on NPV criterion	101
5.3.4	Conventional Payback	107
5.3.5	Internal Rate of Return	108
5.3.6	Comparison of some typical profiles	109
5.4	Conclusion	112
6	Optimal Operation of a CSP plant under DNI perturbations using switch controls	114
6.1	Dynamics of the reduced plant model	115
6.2	Plant dynamics with Switch Control	119
6.3	Optimal control problem	120
6.3.1	Objective functional	121

6.3.2	Control Problem	122
6.4	Simulations - Search for the optimal shutdown.	123
6.4.1	Case 1: Useful thermal power Without perturbations	125
6.4.2	Case 2: Useful thermal power with continuous perturbation	126
6.4.3	Case 3: Useful thermal power with discontinuous perturbations	129
6.5	Conclusion	132
7	Final Conclusion	133
III	Bibliography	135

List of Figures

1.1	Facility location problem, graphic representation.	2
1.2	Black box model for a CSP plant. Left image taken from [56].	4
1.3	Meta-model for CSP optimal design	5
1.4	Representation of incident solar radiation (DNI) on a cloudy day.	7
1.5	Problème de localisation des installations, représentation graphique.	10
1.6	Modèle de boîte noire pour une centrale solaire à concentration. Image de gauche tirée de [56].	12
1.7	Méta-modèle pour la conception optimale de CSP	13
1.8	Représentation du rayonnement solaire incident (DNI) par temps nuageux.	14
3.1	Optimal gap for each of the problems in each case.	49
3.2	Execution time for each of the problems in each case.	49
3.3	Each bar corresponds to the number of built facilities of type a_1 , a_2 or a_3 , for the different problems, these are, from left to right, 1-Upper-Profit, 2-Mixed-Profit, 3-Upper-SW, 4-Mixed-SW.	50
3.4	Values for the different functional objectives in each case study.	51
4.1	Concentrated Solar Power Plant (CSP plant). Image from [118].	62
4.2	Scheme of the black-box model for a Concentrated Solar Power plant. The red circuit represents the main heat-transfer loop.	63
4.3	Data and Interpolation model - Summer day. California, SM = 2.5.	65
4.4	Data and Interpolation model - Summer day. Sevilla, SM = 2.5.	65
4.5	Schema in production phase.	67
4.6	Concentrated Solar Power Plan with thermochemical storage.	68
5.1	Example of a Pre-scenario for one day, one Storage phase, one Storage-Production phase and two Discharges phases.	76
5.2	Two-tank molten salt storage. Scheme in Storage phase.	80
5.3	Two-tank molten salt storage. Scheme in Storage-Production phase.	81
5.4	Two-tank molten salt storage. Schema in Discharge phase.	82
5.5	Concentrated Solar power plant with Thermochemical storage, including the thermal integration (original Figure from [124]).	84
5.6	Thermochemical storage system. Schema in Storage phase. Copied from [124].	86
5.7	Thermochemical storage system. Schema in Storage-Production phase. Copied from [124].	87
5.8	Thermochemical storage system. Schema in Discharge phase. Copied from [124].	88

5.9	LCOE values, changing the discharge duration with the classic strategy, $SM = 2.5$, $N = 30$ years and $\iota_r = 3\%$. PP scenario.	100
5.10	LCOE values, changing the discharge duration with the classic strategy, $SM = 2.5$, $N = 30$ years and $\iota_r = 3\%$. PO scenario.	101
5.11	NPV values, changing the discharge duration with the classic strategy, $SM = 2.5$, $N = 30$ years and $\iota_r = 3\%$. Price-Pessimistic scenario.	102
5.12	NPV values, changing the discharge duration with the classic strategy, $SM = 2.5$, $N = 30$ years and $\iota_r = 3\%$. Price-Optimistic scenario.	103
5.13	Winter season, Thermochemical system with Price Chasing strategy - 1 Discharge phase.	103
5.14	Winter season, Thermochemical system with Price Chasing strategy - 2 Discharge phases.	104
5.15	Summer season, Thermochemical system with Price Chasing strategy - 1 Discharge phase.	104
5.16	Summer season, Thermochemical system with Price Chasing strategy - 2 Discharge phases.	105
5.17	Winter season, Two-tank storage system with Classical production strategy.	106
5.18	Summer season, Two-tank storage system with Classical production strategy.	106
5.19	Thermochemical system, Price Chasing strategy with one and two Discharge phases, different values for cost parameter β , $SM = 2.5$, $\iota_r = 3\%$ and PP scenario.	107
5.20	Thermochemical system, Price Chasing strategy with one and two Discharge phases, different values for cost parameter β , $SM = 2.5$, $\iota_r = 3\%$ and PO scenario.	107
5.21	These simulations correspond to the Classical and Price Chasing strategies with both storage systems. $SM = 2.5$, $N = 30$ years and PM scenario.	108
5.22	These curves correspond to the different storage systems with the Price Chasing and Classical operation strategies. $SM = 2.5$, $\iota_r = 3\%$ and PP scenario.	110
5.23	These curves correspond to the different storage systems with the Price Chasing and Classical operation strategies. $SM = 2.5$, $\iota_r = 3\%$ and PO scenario.	110
6.1	Scheme of a CSP plant reduced model.	116
6.2	Methodology to find the optimal shutdown.	123
6.3	Exogenous functions. Useful thermal power and price function.	125
6.4	state variables and complementary functions of temperatures T_1 , T_2 , T_3 and T_4 , without shutdown of the Rankine cycle.	125
6.5	Control variables, mass flows \dot{m}_{SF} and \dot{m}_R , without shutdown of the Rankine cycle.	126
6.6	Electrical power in a nominal range of 40 to 55 MW, without shutdown of the Rankine cycle.	126
6.7	Exogenous functions. Useful thermal power and price function.	127
6.8	State variables and complementary functions of temperatures T_1 , T_2 , T_3 and T_4	128
6.9	Control variable, mass flows with shutdown of the Rankine cycle at time $t=5.83$ (5 hours and 50 minutes), during 20 minutes.	128
6.10	Mass in the cold and hot tanks and electric power.	129
6.11	Exogenous functions. Useful thermal power and price function.	129

6.12	Control variable, mass flows with shutdown of the Rankine cycle at time $t=5.83$ (5 hours and 50 minutes), during 20 minutes.	130
6.13	State variables and complementary functions of temperatures T_1 , T_2 , T_3 and T_4	131
6.14	Mass in the cold and hot tanks and electric power.	131

List of Tables

3.1	Bilevel problems with cardinality constraints at the upper level and mixed, considering different objective functions for the company.	45
3.2	Type of facilities.	46
3.3	Description of facilities.	47
3.4	Each component of the vector $[n_1, n_2, n_3]$ represents the number of built facilities according to type a_1, a_2 and a_3 , respectively.	48
3.5	Optimality gap.	52
3.6	Execution time.	53
3.7	Distribution for cars in facilities.	54
3.8	Values in [USD] for the configuration Upper-Profit. The Social Welfare is given by the sum of the profit of the leader and the benefit of the followers.	55
3.9	Values in [USD] for the configuration Upper-SW. The Social Welfare is given by the sum of the profit of the leader and the benefit of the followers.	56
3.10	Values in [USD] for the configuration Mixed-Profit. The Social Welfare is given by the sum of the profit of the leader and the benefit of the followers.	57
3.11	Values in [USD] for the configuration Mixed-SW. The Social Welfare is given by the sum of the profit of the leader and the benefit of the followers.	58
4.1	Coefficients of the quadratic regressions.	67
5.1	Storage phase - Conditions for temperatures and mass flows.	81
5.2	Storage-Production phase assumptions.	81
5.3	Discharge phase assumptions.	83
5.4	Optimization problem variables bounds.	94
5.5	Thermochemical reactor system with Classical strategy, $\beta = 1$	101
5.6	Thermochemical reactor system with Classical strategy, $\beta = 2$	102
5.7	Two-tank system with Classical strategy.	102
5.8	Economic results considering different β for Thermochemical storage system and Price Chasing strategy with one Discharge phase. $SM = 2.5, N = 30$ years and $\iota_r = 3\%$	105
5.9	Economic results considering different β for Thermochemical storage system and Price Chasing strategy with two Discharge phases. $SM = 2.5, N = 30$ years and $\iota_r = 3\%$	105
5.10	Economic results for the Two-tank system considering different strategies of production and the PO price scenario. $SM = 2.5, N = 30$ years and $\iota_r = 3\%$	106

5.11	Economic results for Thermochemical and Two-tank storage system (with Price Chasing strategy, one Discharge phase), considering different years. . .	109
6.1	Complementary functions.	117
6.2	Parameters and notations.	118
6.3	State and control variables.	118
6.4	Parameters and notations.	124
6.5	Case 2, time and economic results. For every fixed duration value, only the optimal Initial time is displayed.	127
6.6	Case 3, time and economic results. For every fixed duration value, only the optimal Inicial time is displayed.	130

Chapter 1

Introduction (English and French version)

When speaking of the "optimal design" of energy units, that is production plants or delivery plants (charging stations for electric vehicles, renewable energy plants....), one can understand this problem in many different ways. Some examples are:

- 1) determining the "best" physical characteristics/design for an energy unit, where best can be understood from an economical point of view, by an exergy approach or other criterion;
- 2) determining the optimal location to built this energy unit. Here again "optimal" can cover the evaluation of costs, benefits, quality of service...;
- 3) determining the "best" way to operate the energy unit, that is when to store, when to produce/to stop producing or when to offer a delivery;

and many others. This kind of analysis is of course fundamental in an investment decision perspective or to compare different configurations. But it is also very important for the design of demand-side management interactions (for example in Smart-grid, microgrids and virtual power plants).

In this thesis work we will address the three following cases: in a first part (chapters 2 and 3), motivated by the determination of optimal location of charging stations for electric vehicles (point 2) above), we will focus on the study of bilevel problems intrinsically including cardinality constraints.

In the second part of this manuscript (chapters 4, 5 and 6), we will concentrate both on the optimal design of a concentrated solar plant in the context of prices determined by energy market and on its operation at a long term (Chapter 5), thus addressing points 1) and 3) above. The short term operation with irradiance perturbations will be considered in Chapter 6.

In Chapter 2, respectively Chapter 4, preliminary notions, context and notation will be recalled/fixed concerning bilevel optimization, respectively on concentrated solar plants. Finally, a brief summary of the structure of the whole development in this research work is

given in Conclusion/Chapter 7.

1.1 Part I: Bilevel games and cardinality constraints

In recent years, the automobile industry has witnessed a significant shift towards sustainable transportation solutions. One of the most notable advancements in this regard is the growing popularity of electric cars. Electric vehicles (EVs) have become a viable alternative to traditional gasoline cars, offering numerous benefits in terms of environmental impact, energy efficiency, and technological innovation. Some of the factors that have favored this growth include:

- The increasing awareness of environmental issues, such as climate change and air pollution, has led to a rise in demand for cleaner and more sustainable vehicles [32, 89].
- The continuous development of battery technology has improved the range of electric cars, alleviating concerns about the limited distance they can travel between charges (for example, an electric car with a 60 kWh battery and an efficiency of 4 miles/kWh can travel approximately 240 miles).
- Many governments provide significant financial incentives for the purchase of electric cars, such as tax credits, tax discounts, and subsidies, to encourage the adoption of cleaner technologies.
- The deployment of a broader and more accessible charging infrastructure has alleviated concerns about the availability of charging stations, making electric cars more practical for a larger number of people.

In contrast, as an increasing number of electric vehicle owners proceed to charge their cars, higher demand is generated in the charge service, exerting a direct influence on the planning and management of the electrical infrastructure.

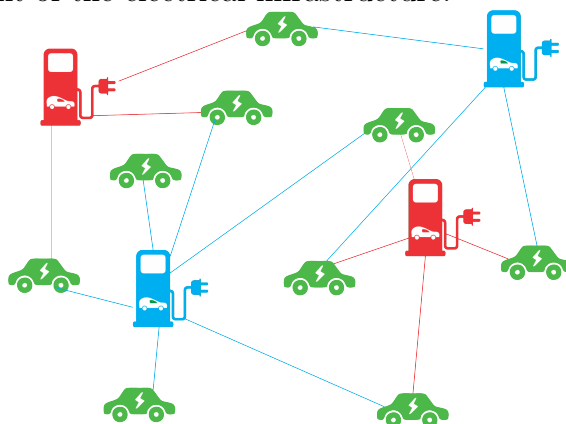


Figure 1.1: Facility location problem, graphic representation.

The development of charging infrastructure drives the demand for increased capacity in the electrical grid, requiring strategic planning when locating charging stations. A well-established charging network not only has the potential to promote the growth of the EV market by alleviating concerns about the availability of charging points but also intensifies the requirement for an expanded charging network, as the rising number of EVs contributes to such a demand. Additionally, the charging patterns of electric vehicles can have a significant

impact on daily electricity demand [97, 70, 37]. In this regard, based on the supply capacity of each facility simultaneously, the implementation of tariffs or incentives for charging at different facilities may be key to balancing the load on the electrical grid [37].

The theory of bilevel optimization focuses on problems with two levels of decision-making, akin to a leader and a follower. In the context of facility location problem (see Figure 1.1), this entails a company (leader) making strategic decisions regarding location, while followers (cars in this case) react. This perspective allows for the joint optimization of strategic and tactical decisions, encompassing both facility location and the reactions of participants in the market. Now, in confronting the challenge of facility location, the additional complexity of considering the limited capacity of facilities for car supply is introduced, which could be translated into cardinality constraints in a bilevel problem. Let us recall that cardinality constraints are constraints on the maximum number of non zero components of given vector variables. However it turns out that bilevel problems with cardinality constraints have never been considered in the literature. We develop here the first elements of the theory on these problems.

In the Single-Leader-Multi-Follower (SLMF) games, a designated leader engages with a group of followers, each playing a crucial role in the decision-making process. The leader, orchestrates her choices, while the followers respond by solving a (generalized) Nash equilibrium problem that is parameterized by the leader’s decision variable.

A common approach to tackle the complexities of Single-Leader-Multi-Follower games involves reformulating them as single-level optimization problems. This reformulation is rooted in the natural variational formulation of the lower-level game played by the followers. Leveraging standard convexity and continuity assumptions, a vector emerges as an equilibrium point for the lower-level game if and only if it satisfies the coupled Karush-Kuhn-Tucker (KKT) optimality conditions associated with each follower’s optimization problem.

The resulting optimization problem seamlessly fits into the realm of *Mathematical Programming with Complementarity Constraints (MPCC)*. This classification arises naturally as complementarity equations play a pivotal role in the Karush-Kuhn-Tucker-based variational formulations. The study of Single-Leader-Multi-Follower games within the MPCC framework provides a powerful analytical lens, facilitating a deeper understanding of the intricate relationships and strategic interactions within hierarchical decision-making structures.

We will present three case studies for these type of problems: those with cardinality constraints at the upper level, at the lower level, and a third mixed case. We begin by the first case study, which maintains a structure that preserves key properties to ensure the existence of solutions. In [23], for a single-level optimization problem with cardinality constraints, the authors pose a reformulation of the original problem and prove equivalence of global optima between the two optimization problems. Rebounding on this proposal, we introduce a novel approach to the bilevel problem with cardinality constraints at the upper level and establish the equivalence between global solutions in both approaches. In the second case, with cardinality constraints at the lower level, there is a significant complexity in analyzing solution existence due to the loss of convexity in the lower-level constraint set. Therefore, we

propose a "mixed" approach, in which expressions corresponding to cardinality constraints are distributed across both levels, preserving fundamental properties that guarantee solution existence. Finally, we describe a detailed methodology for the numerical resolution of these bi-level problems, situated within the context of the issue of locating electric vehicle charging facilities.

1.2 Part II: Economic Efficiency of Concentrated Solar Power plants

For the problem of optimal design of solar thermal plants, a multidimensional analysis will be carried out, which consists of choosing the best configuration of each of the components (for a certain type of Solar Captor, storage system and Rankine cycle) together with other economic factors, in order to maximize the performance of the plant over a useful life horizon. However, the concept of optimizing the performance is not uniquely defined and several parameters need to be settled before an optimization model can be posed. Based on the black-box model (described in Chapter 4), we will address, in a general way, multidimensional analysis for a CSP plant with different thermal storage systems.

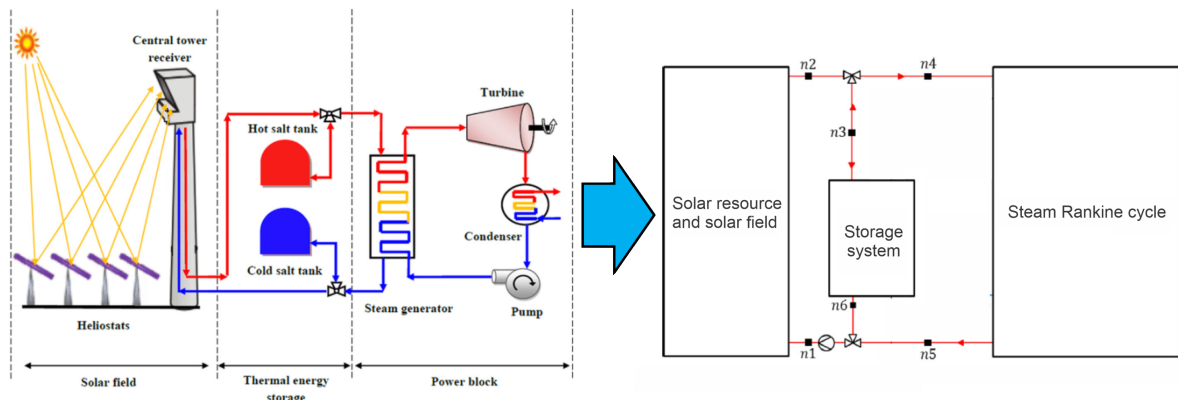


Figure 1.2: Black box model for a CSP plant. Left image taken from [56].

For a solar power plant to be profitable depends largely on the storage system [123, 110]. According to the characteristics and functionalities of the storage systems that will be considered in this part of the investigative work, one of the objectives is to optimize the dimensions and operations for each of these systems. On the other hand, to evaluate the profitability and viability of a CSP plant together with a storage system, many studies consider the economic indicator LCOE [5, 34]. Nevertheless, in a SPOT market context, it does not work to consider this type of indicator, since it does not take into account incomes, which can also be different depending on the type of storage system and production strategy. Hence the need to consider other economic indicators to evaluate a CSP plant project that may vary according to physical and economic conditions. Therefore, we will be considering them in a SPOT market context, where we will be working with a non-constant price function, which means that the operation of the plant can change the economic benefit of the plant. In addi-

tion to the LCOE indicator, in this work we consider indicators such as: NPV (Net Present Value), IRR (Internal Rate of Return), and CPB (Conventional Payback), since they capture both the production capacity of the plant and the impact of production strategies [124, 125]. Another consideration to be analyzed is the variation of electricity market prices, which will influence the income and costs generated by the plant, i.e., particularly according to the economic indicator under consideration, the economic benefit will be slightly or strongly affected. The previously described paradigm gives way to different optimization problems, each one involving two distinct sets of variables that are optimized simultaneously: the physical variables corresponding to the type of storage, and the operational/strategic variables, which define storage/production strategies according to the desired objective. Because some of the variables correspond to the operational use of the storage (and are therefore functions), this maximization (or minimization) problem is actually an optimal control problem. However, solving an optimal control problem could be quite difficult. Moreover, due to the discontinuous nature of some functions, computational difficulties may arise. Therefore, in this part the notion of pre-scenarios will be used. This concept, first formulated in [124], allows us to transform the optimal control problem into a "classical" mathematical programming problem, which consists in fixing the number and order of the different operation phases of the plant, inducing a real parameterization of the admissible operations of the CSP plant of the admissible operations of the CSP plant.

To address this problem, the first objective to develop will be to build a metamodel whose usefulness can be summarized in Figure 1.3: First, the exogenous parameters like the DNI function, lifetime of the plant, and the price function $\lambda(\cdot)$ are set; then each black-box component is chosen, where the parameters to optimize are identified as variables of the optimization problem, and finally, through the black-box model, the optimization problem is constructed to optimize the chosen economic criterion under a pre-fixed operation strategy.

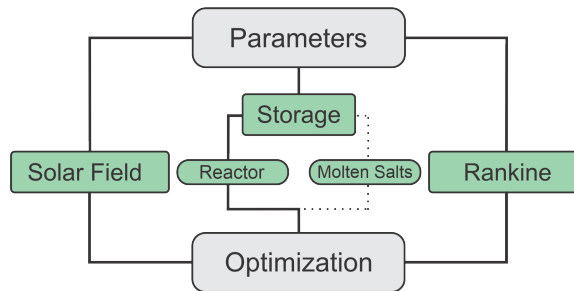


Figure 1.3: Meta-model for CSP optimal design

The resolution of the optimization problems that will be developed in the Chapter 5 follows the alignments proposed in [124], these are: a prototype solar thermal plant is considered, which will be optimized over a lifetime of N years. During this time, each year is assumed to behave exactly the same with respect to the others, so only one year is optimized, and then repeated N times. This repetition takes into account an economic devaluation, which is captured by a discount rate. The model year is divided into periods (e.g. when divided into four, each would represent a season) and each period is represented by a cyclical stage, which is repeated. The optimization of the model year consists of maximizing (or minimizing) the physical variables of the storage and the operation of the solar thermal power plant in each

cyclic stage in order to maximize (or minimize) the economic criterion. So in a first instance we will proceed in the creation and implementation of an algorithm for the maximization (or minimization) of the economical indicators for the prototype solar thermal power plant. This type of modeling will allow a comparative study between different integrated storage systems, to show the efficiency of each one of them, as well as different prices scenarios, economic criteria and operation strategies depending on the assumptions and sought objectives.

When designing a CSP plant, the effect of operation strategies is taken into account *in average*, since the lifetime horizon doesn't allow to have reliable forecasting on the variations of weather conditions or fluctuations of prices. However, if one wants to address the problem of optimal operation of an already existing CSP plant, this approach is not valid for a long time. Instead, it is necessary to consider the short-term problem of optimal operation under the light of optimal control theory. The operation of a central receiver CSP plant is conceived for maximizing the energy harvesting. To do so, the heliostats follow an aiming strategy seeking to ensure a high radiation flux in the solar receiver. Although the laws of thermodynamics allow achieving higher conversion efficiencies as the temperature raises, the materials used in the absorber, as well as the thermal stability of the heat transfer fluid define the temperature operational range. For instance, the molten salts mixtures commonly used in CSP plants, present a thermal stability limit around 560°C and a freezing point of around 290°C [131]. For avoiding freezing events, CSP plants commonly use heat tracers in the pipes and/or directly in the storage tanks. In order to keep the temperature level lower than the thermal stability, but high enough for maintaining high conversion efficiency, most of CSP plants consider a perfect mass flow rate control. This control scheme considers that the mass flow rate of heat transfer fluid (HTF) is varied to maintain a constant design outlet temperature at the receiver. This operation mode is commonly activated during stable periods of DNI, such as during clear-sky days or periods with low variability. However, during intermittent cloudy days or periods with high DNI variability (see Figure 1.4), a fixed mass flow rate control is implemented. In this control scheme, the HTF outlet temperature is calculated to maintain a constant HTF mass flow rate in the receiver, allowing the HTF outlet temperature to vary within a safety limit during variable conditions of DNI, and ensuring the receiver integrity [149]. In this context, critical scenarios with significant variations of the DNI will be explored, where the daily operation of a CSP plant must meet two fundamental criteria: first, optimize economic objectives, and second, maintain safe temperatures in the face of DNI instability events.

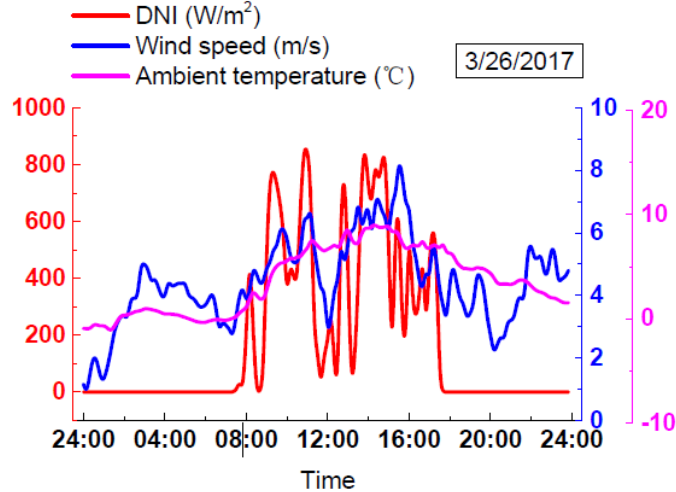


Figure 1.4: Representation of incident solar radiation (DNI) on a cloudy day.

For this problem, we will start adapting the quasi-static Black-box model of Section 2 to a dynamic one, identifying the controllable variables as well as the transition dynamics that govern the system. We will focus on the dynamics of the heat-transfer fluid which is the most sensitive element under DNI instability, and consider simplified dynamics for each of the blackbox component. This simplification will allow us to derive a well-posed dynamic for the variation of temperatures and mass-flow rates of the system. Once a black-box dynamic system is derived, we can address the optimal operation problem, starting by solving a perfect-information setting. Imagine first that for a short-term period of time $[0, H]$, like a day or a week, both the DNI function and the price curve are known. In order to optimize the operation of the plant for a chosen economic criterion, we count with two types of objects: the first one stands for the Dynamic constraints, the whole problem of DNI instability is to maintain the conditions on the heat-transfer fluid within its limit temperatures to avoid damages. Thus, for every time $t \in [0, H]$ and every point $x \in L$ (where L is the one-dimensional model of the heat-transfer system), we need to ensure that

$$T_{\min} \leq T(t, x) \leq T_{\max}, \quad (1.2.1)$$

where $T(t, x)$ denotes the temperature of the HTF at point x and at time t .

The second one represents Controllable variables. The plant has many variables that determine how the different functioning modes will be executed, and they can be modified over time. For example, during the storage process, the consumed power of the storage system q_s and the mass flow rate \dot{m} are controllable (see eq. (4.2.1)). The value of $\dot{m}(t)$ is controlled by a pump and $q_s(t)$ is controlled by internal variables of the storage system.

Among the challenges currently faced by Concentrated Solar Power (CSP) plants, a significant issue is interference in the concentration of solar rays, primarily caused by the passage of clouds between the sun and the mirrors. The actions that the plant must take in these scenarios include, for example, the selective defocusing of certain mirrors and adjustments to mass flow velocities—increasing them in response to the decrease in concentrated heat at

the receiver and vice versa.

In critical situations, the most practical measure for the plant is to shut down, thus avoiding excessive costs associated with electricity production. Therefore, in the last part (Chapter 6, we will focus on considering critical scenarios characterized by disturbances in solar irradiation concentration. From these critical scenarios, we will apply optimal control theory to determine optimal shutdown policies.

1.3 Thesis structure and development

The first part of the thesis consists of two chapters, identified as Chapter 2 and 3. In the first one, fundamental concepts, which will be used in Chapter 3: convex optimization, generalized Nash equilibrium problems, bilevel problems, cardinality constraints, among others. Subsequently, in Chapter 3, results related to the analysis of Single-Leader-Multi-Follower (SLMFG) including cardinality constraints are developed. Finally, in Section 3.3, the application of these results is illustrated in the well-known Facility Location Problem, treating it as a binomial problem.

The second part of the thesis is made up of three chapters. In Chapter 4, essential concepts are presented to address the issues related to optimal design and operation of a CSP plant. It begins with a brief introduction to the problem to be addressed, followed by the presentation of a black-box model that allows the representation of a CSP plant and each of its components (Solar Field, Storage System, and Rankine Cycle). Furthermore, relevant parameters related to the geographical and economic characteristics specific to the location of the plant project are detailed. For this purpose, functions capturing variations associated with solar irradiation and prices in the electricity market are employed (see Section 4.2 and 4.3). In Chapter 5, dedicated to the comparative study with various storage systems, economic indicators, and operation strategies are considered and detailed in sections 4.2, 4.4, and 4.5, respectively. Finally, in Chapter 6, the optimal operation problem is addressed, in which optimal control problems are proposed, considering a reduced model of the CSP plant (keeping the three-component structure).

The developments presented in chapter 5 correspond to an article accepted for publication in *Journal of Energy Storage* (2024).

Résumé en français

Lorsque l'on parle de "conception optimale" des unités énergétiques, c'est-à-dire des installations de production ou de distribution d'énergie (stations de recharge pour véhicules électriques, centrales d'énergie renouvelable, etc.), on peut comprendre ce problème de plusieurs manières différentes. Quelques exemples sont les suivants:

- 1) déterminer les "meilleures" caractéristiques physiques/conception d'une unité énergétique, où "meilleures" peuvent être comprises d'un point de vue économique, par une approche exergétique ou autre;
- 2) déterminer l'emplacement optimal pour construire cette unité énergétique. Ici encore, le terme "optimal" peut recouvrir l'évaluation des coûts, des bénéfices, de la qualité de service...;
- 3) déterminer la "meilleure" façon d'exploiter l'unité énergétique, c'est-à-dire quand stocker, quand produire/arrêter de produire;

et bien d'autres encore. Ce type d'analyse est bien sûr fondamental dans une perspective de décision d'investissement ou pour comparer différentes configurations. Mais il est également très important pour la conception des interactions de gestion de la demande (par exemple dans le Smart-grid, micro-réseaux et centrales électriques virtuelles).

Dans ce travail de thèse, nous aborderons les trois cas suivants: dans une première partie (chapitres 2 and 3), motivée par la détermination de l'emplacement optimal des stations de recharge pour les véhicules électriques (point 2) ci-dessus), nous nous concentrerons sur l'étude de problèmes à deux niveaux incluant intrinsèquement des contraintes de cardinalité. Dans la deuxième partie de ce manuscrit (chapitres 4, 5 and 6), nous nous concentrerons à la fois sur la conception optimale d'une centrale solaire concentrée dans un contexte de prix déterminés par le marché de l'énergie et sur son fonctionnement à long terme (chapitre 5), abordant ainsi les points 1) et 3) ci-dessus. Le fonctionnement à court terme avec des perturbations de l'irradiation sera examiné au chapitre 6.

Au chapitre 2, respectivement au chapitre 4, les notions préliminaires, le contexte et la notation seront rappelés/fixés en ce qui concerne l'optimisation à deux niveaux (respectivement sur les centrales solaires à concentration).

1.4 Partie I: Jeux biniveaux et contraintes de cardinalité

Ces dernières années, l'industrie automobile a connu une évolution significative vers des solutions de transport durables. L'une des avancées les plus notables à cet égard est la popularité croissante des voitures électriques. Les véhicules électriques (VE) sont devenus une alternative viable aux voitures à essence traditionnelles, offrant de nombreux avantages en termes d'impact sur l'environnement, d'efficacité énergétique et d'innovation technologique. Voici quelques-uns des facteurs qui ont favorisé cette croissance:

- La prise de conscience croissante des problèmes environnementaux, tels que le changement climatique et la pollution de l'air, a conduit à une augmentation de la demande de véhicules plus propres et plus durables [32, 89].

- Le développement continu de la technologie des batteries a amélioré l'autonomie des voitures électriques, atténuant les inquiétudes concernant la distance limitée qu'elles peuvent parcourir entre deux charges (par exemple, une voiture électrique avec une batterie de 60 kWh et un rendement de 4 miles/kWh peut parcourir environ 240 miles).
- De nombreux gouvernements offrent des incitations financières importantes pour l'achat de voitures électriques, telles que des crédits d'impôt, des réductions fiscales et des subventions, afin d'encourager l'adoption de technologies plus propres;
- Le déploiement d'une infrastructure de recharge plus large et plus accessible a atténué les inquiétudes concernant la disponibilité des stations de recharge, rendant les voitures électriques plus pratiques pour un plus grand nombre de personnes.

En revanche, lorsqu'un nombre croissant de propriétaires de véhicules électriques procèdent à la recharge de leur voiture, une demande plus importante est générée dans le service de recharge, ce qui exerce une influence directe sur la planification et la gestion de l'infrastructure électrique.

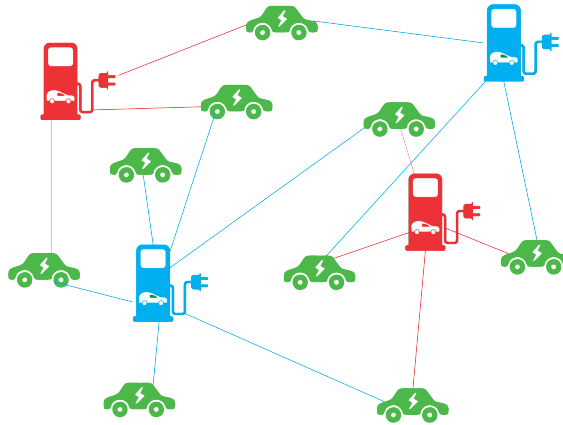


Figure 1.5: Problème de localisation des installations, représentation graphique.

Le développement de l'infrastructure de recharge stimule la demande d'augmentation de la capacité du réseau électrique, ce qui nécessite une planification stratégique de l'emplacement des stations de recharge. Un réseau de recharge bien établi peut non seulement favoriser la croissance du marché des véhicules électriques en apaisant les inquiétudes concernant la disponibilité des points de recharge, mais aussi intensifier le besoin d'un réseau de recharge étendu, car le nombre croissant de VE contribue à une telle demande. En outre, les habitudes de recharge VE's électriques peuvent avoir un impact significatif sur la demande quotidienne d'électricité [97, 70, 37]. À cet égard, en se basant sur la capacité d'approvisionnement de chaque installation simultanément, la mise en place de tarifs ou d'incitations à la recharge dans différentes installations pourrait être essentielle pour équilibrer la charge sur le réseau électrique [37].

La théorie de l'optimisation biniveau se concentre sur les problèmes comportant deux niveaux de prise de décision, à l'instar d'un leader et d'un suiveur. Dans le contexte du problème de localisation des installations (voir la figure 1.5), cela implique qu'une entreprise (leader) prenne des décisions stratégiques concernant la localisation, tandis que les suiveurs (propriétaires de véhicules dans ce cas) réagissent. Cette perspective permet d'optimiser conjointement les décisions stratégiques et tactiques, en tenant compte à la fois de l'emplacement

des installations et des réactions des acteurs du marché. En relevant le défi de la localisation des installations, on introduit la complexité supplémentaire de la prise en compte de la capacité limitée des installations pour l’approvisionnement en voitures, ce qui se traduit par des contraintes de cardinalité dans un problème à deux niveaux. Hors il s’avère que les problèmes bivariés avec contraintes de cardinalité n’ont jamais été considérés dans la littérature. Nous en développons ici les premiers éléments.

Dans les jeux SLMF (Single-Leader-Multi-Follower), un leader est en interaction avec un groupe de suiveurs, chacun jouant un rôle crucial dans le processus de prise de décision. Le leader, représenté par la variable de décision $x \in \mathbb{R}^p$, orchestre ses choix, tandis que les suiveurs répondent en résolvant un problème d’équilibre de Nash (généralisé) qui est paramétré par la variable de décision du leader. Une approche courante pour aborder les complexités des jeux à un seul meneur et plusieurs suiveurs consiste à les reformuler comme des problèmes d’optimisation à un seul niveau. Cette reformulation s’appuie sur la formulation variationnelle naturelle du jeu de niveau inférieur joué par les suiveurs. En s’appuyant sur les hypothèses standard de convexité et de continuité, un vecteur $y \in \mathbb{R}^q$ apparaît comme un point d’équilibre pour le jeu de niveau inférieur si et seulement s’il satisfait aux conditions d’optimalité couplées de Karush-Kuhn-Tucker (KKT) associées au problème d’optimisation de chaque suiveur.

Le problème d’optimisation qui en résulte s’inscrit parfaitement dans le domaine de la *Programmation Mathématique avec Contraintes de Complémentarité (MPCC)*. Cette classification découle naturellement du fait que les équations de complémentarité jouent un rôle central dans les formulations variationnelles basées sur Karush-Kuhn-Tucker. L’étude des jeux à un seul leader et à plusieurs suiveurs via les MPCC facilite une compréhension plus profonde des relations complexes et des interactions stratégiques au sein des structures de prise de décision hiérarchiques.

Nous présenterons trois études de cas pour ce type de problèmes: ceux avec des contraintes de cardinalité au niveau supérieur, au niveau inférieur, et un troisième cas mixte. Nous commençons par la première étude de cas, qui maintient une structure qui préserve des propriétés clés pour garantir l’existence de solutions. Dans [23], pour un problème d’optimisation à un seul niveau avec des contraintes de cardinalité, les auteurs posent une reformulation du problème original et prouvent l’équivalence des optima globaux entre les deux problèmes d’optimisation. Sur la base de cette proposition, nous introduisons une nouvelle approche pour le problème à deux niveaux avec des contraintes de cardinalité au niveau supérieur et établissons l’équivalence entre les solutions globales dans les deux approches. Dans le second cas, avec des contraintes de cardinalité au niveau inférieur, l’analyse de l’existence d’une solution est très complexe en raison de la perte de convexité de l’ensemble de contraintes du niveau inférieur. Nous proposons donc une approche "mixte", dans laquelle les expressions correspondant aux contraintes de cardinalité sont réparties entre les deux niveaux, tout en préservant les propriétés fondamentales qui garantissent l’existence de la solution. Enfin, nous décrivons une méthodologie détaillée pour la résolution numérique de ces problèmes à deux niveaux, dans le contexte de la localisation des installations de recharge des véhicules

électriques.

1.5 Partie II: Efficacité Économique des Centrales Solaires à Concentration

Pour le problème de la conception optimale des centrales solaires thermiques, une analyse multidimensionnelle sera effectuée, qui consiste à choisir la meilleure configuration de chacun des composants (pour un certain type de capteur solaire, de système de stockage et de cycle de Rankine) avec d'autres facteurs économiques, afin de maximiser la performance de la centrale sur une durée de vie utile. Cependant, le concept d'optimisation des performances n'est pas défini de manière unique et plusieurs paramètres doivent être définis avant qu'un modèle d'optimisation puisse être posé. Sur la base du modèle de boîte noire (décrit dans le Chapitre 4), nous aborderons, d'une manière générale, l'analyse multidimensionnelle pour une centrale CSP avec différents systèmes de stockage thermique.

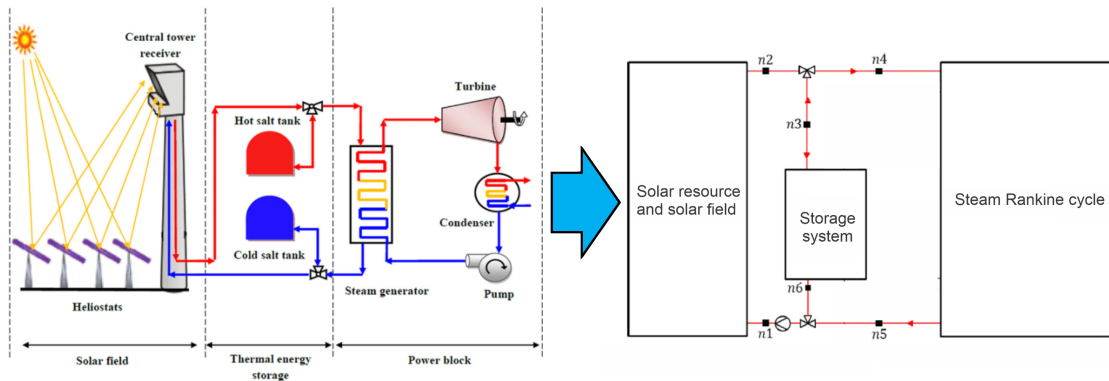


Figure 1.6: Modèle de boîte noire pour une centrale solaire à concentration. Image de gauche tirée de [56].

La rentabilité d'une centrale solaire dépend en grande partie du système de stockage. Selon les caractéristiques et les fonctionnalités des systèmes de stockage qui seront examinés dans cette partie du travail d'investigation, l'un des objectifs est d'optimiser les dimensions et les opérations pour chacun de ces systèmes. D'autre part, pour évaluer la rentabilité et la viabilité d'une centrale CSP associée à un système de stockage, de nombreuses études prennent en compte l'indicateur économique LCOE [5, 34]. Néanmoins, dans un contexte de marché SPOT, ce type d'indicateur ne fonctionne pas, car il ne prend pas en compte les revenus, qui peuvent également être différents en fonction du type de système de stockage et de la stratégie de production. D'où la nécessité de prendre en compte d'autres indicateurs économiques pour évaluer un projet de centrale solaire à concentration, qui peuvent varier en fonction des conditions physiques et économiques. Nous les examinerons donc dans le contexte du marché SPOT, où nous travaillerons avec une fonction de prix non constante, ce qui signifie que l'exploitation de la centrale peut modifier le bénéfice économique de la centrale. Outre l'indicateur LCOE, nous considérons dans ce travail des indicateurs tels que: NPV (Net Present Value), IRR (Internal Rate of Return), et CPB (Conventional Payback), puisqu'ils capturent à la fois la capacité de production de l'usine et l'impact des stratégies de produc-

tion [124, 125]. Une autre considération à analyser est la variation des prix du marché de l'électricité, qui influencera les revenus et les coûts générés par la centrale, c'est-à-dire qu'en fonction de l'indicateur économique considéré, le bénéfice économique sera légèrement ou fortement affecté. Cela donne donc lieu à différents problèmes d'optimisation, chacun impliquant deux ensembles distincts de variables qui sont optimisées simultanément: les variables physiques correspondant au type de stockage, et les variables opérationnelles/stratégiques, qui définissent les stratégies de stockage/production en fonction de l'objectif souhaité. Comme certaines des variables correspondent à l'utilisation opérationnelle du stockage (et sont donc des fonctions), ce problème de maximisation (ou de minimisation) est en fait un problème de contrôle optimal. Cependant, la résolution d'un problème de contrôle optimal peut s'avérer très difficile. De plus, en raison de la nature discontinue de certaines fonctions, des difficultés de calcul peuvent survenir. C'est pourquoi, dans cette partie, nous utiliserons la notion de pré-scénarios, qui a été formulée dans [124], grâce à laquelle le problème de contrôle optimal peut être transformé en un problème de programmation mathématique "classique", qui consiste à fixer le nombre et l'ordre des différentes phases de fonctionnement de l'installation, induisant un véritable paramétrage des opérations admissibles de l'installation de DSP. des opérations admissibles de la centrale CSP.

Pour aborder ce problème, le premier objectif à développer sera de construire un méta-modèle dont le fonctionnement peut être résumé dans la Figure 1.3: tout d'abord, les paramètres exogènes comme la fonction DNI, la durée de vie de la centrale et la fonction de prix $\lambda(\cdot)$ sont définis; puis chaque composant de boîte noire est choisi, où les paramètres à optimiser sont identifiés comme variables du problème d'optimisation, et enfin, à travers le modèle de boîte noire, le problème d'optimisation est construit pour optimiser le critère économique choisi selon une stratégie d'exploitation prédéfinie.

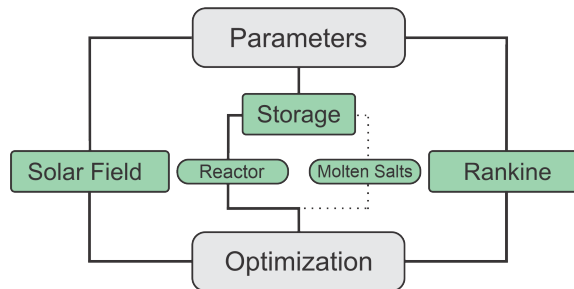


Figure 1.7: Méta-modèle pour la conception optimale de CSP

La résolution des problèmes d'optimisation qui seront développés dans le chapitre 5 suit une stratégie proposée dans [124], à savoir: un prototype d'installation solaire thermique est considéré, qui sera optimisé sur une durée de vie de N années. Pendant cette période, on suppose que chaque année se comporte exactement de la même manière par rapport aux autres, de sorte qu'une seule année est optimisée, puis répétée N fois. Cette répétition tient compte d'une dévaluation économique, capturée par un taux d'actualisation. L'année modèle est divisée en périodes (par exemple, si elle est divisée en quatre, chacune représente une saison) et chaque période est représentée par une étape cyclique, qui est répétée. L'optimisation de l'année modèle consiste à maximiser (ou minimiser) les variables physiques du stockage et les variables de l'exploitation de la centrale solaire thermique dans chaque étape cyclique afin

de maximiser (ou minimiser) le critère économique. Ce type de modélisation permettra une étude comparative entre différents systèmes de stockage intégrés, afin de montrer l'efficacité de chacun d'entre eux, ainsi que différents scénarios de prix, critères économiques et stratégies d'exploitation en fonction des hypothèses et des objectifs recherchés.

Lors de la conception d'une centrale solaire à concentration, l'effet des stratégies d'exploitation est pris en compte *en moyenne*, puisque l'horizon de la durée de vie ne permet pas d'avoir des prévisions fiables sur les variations des conditions météorologiques ou les fluctuations des prix. Cependant, si l'on veut aborder le problème de l'exploitation optimale d'une centrale solaire à concentration déjà existante, cette approche n'est plus suffisante. Au lieu de cela, il est nécessaire d'examiner le problème à court terme de l'exploitation optimale via la théorie du contrôle optimal.

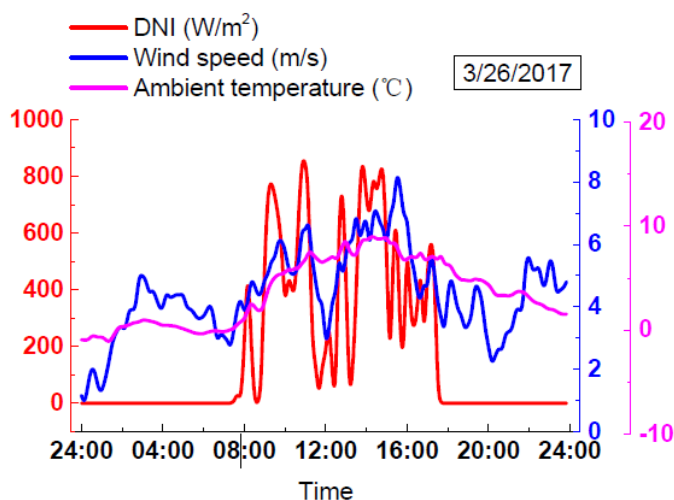


Figure 1.8: Représentation du rayonnement solaire incident (DNI) par temps nuageux.

Le fonctionnement d'une centrale CSP à récepteur central est conçu pour maximiser la récolte d'énergie. Pour ce faire, les héliostats suivent une stratégie d'orientation visant à assurer un flux de rayonnement élevé dans le récepteur solaire. Bien que les lois de la thermodynamique permettent d'obtenir des rendements de conversion plus élevés à mesure que la température augmente, les matériaux utilisés dans l'absorbeur, ainsi que la stabilité thermique du fluide caloporteur, définissent la plage opérationnelle de température. Par exemple, les mélanges de sels fondus couramment utilisés dans les centrales CSP présentent une limite de stabilité thermique autour de 560°C et un point de congélation autour de 290°C [131]. Pour éviter les épisodes de gel, les centrales solaires à concentration utilisent généralement des traceurs de chaleur dans les conduites et/ou directement dans les réservoirs de stockage. Afin de maintenir le niveau de température inférieur à la stabilité thermique, mais suffisamment élevé pour maintenir un rendement de conversion élevé, la plupart des centrales solaires à concentration envisagent un contrôle parfait du débit massique. Ce schéma de contrôle considère que le débit massique du fluide de transfert de chaleur (HTF, pour son acronyme en anglais) est modifié pour maintenir une température de sortie constante au niveau du récepteur. Ce mode de fonctionnement est généralement activé pendant les périodes stables de l'indice DNI, comme les jours de ciel clair ou les périodes de faible variabilité. Toutefois, pendant les journées nuageuses intermittentes ou les périodes de forte variabilité du DNI (voir la figure 1.8), une commande de débit massique fixe est mise en œuvre. Dans ce schéma

de contrôle, la température de sortie du HTF est calculée pour maintenir un débit massique constant du HTF dans le récepteur, ce qui permet à la température de sortie du HTF de varier dans une limite de sécurité dans des conditions variables de DNI, et d'assurer l'intégrité du récepteur [149]. Dans ce contexte, nous considérerons des scénarios critiques impliquant des variations significatives du DNI, où le fonctionnement quotidien d'une centrale CSP doit répondre à deux critères fondamentaux: premièrement, optimiser les objectifs économiques, et deuxièmement, maintenir des températures sûres face à des événements d'instabilité du DNI.

Pour ce problème, nous commencerons par adapter le modèle "quasi-statique boîte noire" présenté au Chapitre 4 à un modèle dynamique, en identifiant les variables contrôlables ainsi que la dynamique de transition qui régit le système. Nous nous concentrerons sur la dynamique du fluide caloporteur, qui est l'élément le plus sensible en cas d'instabilité DNI, et nous considérerons une dynamique simplifiée pour chacun des composants de la boîte noire. Cette simplification nous permettra de dériver une dynamique bien posée pour la variation des températures et des débits massiques du système. Une fois que le système dynamique de la boîte noire est dérivé, nous pouvons aborder le problème de l'exploitation optimale, en commençant par résoudre un cadre d'information parfaite. Imaginons tout d'abord que pour une période à court terme $[0, H]$, comme un jour ou une semaine, la fonction DNI et la courbe des prix sont toutes deux connues. Afin d'optimiser le fonctionnement de l'usine pour un critère économique choisi, nous disposons de deux types d'objets: le premier représente les contraintes dynamiques, le problème de l'instabilité du DNI étant de maintenir les conditions sur le fluide caloporteur dans ses températures limites afin d'éviter les dommages. Ainsi, pour chaque temps $t \in [0, H]$ et chaque point $x \in L$ (où L est le modèle unidimensionnel du système de transfert de chaleur), nous devons nous assurer que

$$T_{\min} \leq T(t, x) \leq T_{\max}, \quad (1.5.1)$$

où $T(t, x)$ représente la température du HTF au point x et à l'instant t .

La seconde représente les variables de contrôle. L'installation comporte de nombreuses variables qui déterminent la manière dont les différents modes de fonctionnement seront exécutés, et elles peuvent être modifiées au fil du temps. Par exemple, pendant le processus de stockage, la puissance consommée du système de stockage q_S et le débit massique \dot{m} sont contrôlables (voir eq. (4.2.1)). La valeur de $\dot{m}(t)$ est contrôlée par une pompe et $q_S(t)$ est contrôlé par des variables internes du système de stockage.

Parmi les défis auxquels sont actuellement confrontées les centrales solaires à concentration (CSP), un problème important est l'interférence dans la concentration des rayons solaires, principalement causée par le passage des nuages entre le soleil et les miroirs. Les mesures que l'usine doit prendre dans ces scénarios comprennent, par exemple, la défocalisation sélective de certains miroirs et l'ajustement des vitesses d'écoulement de la masse - en les augmentant en réponse à la diminution de la chaleur concentrée au niveau du récepteur et vice-versa.

Dans les situations critiques, la mesure la plus pratique pour la centrale est de s'arrêter, ce qui permet d'éviter les coûts excessifs liés à la production d'électricité. Par conséquent,

dans ce chapitre, nous nous concentrerons sur l'examen de scénarios critiques caractérisés par des perturbations de la concentration de l'irradiation solaire. À partir de ces scénarios critiques, nous appliquerons la théorie du contrôle optimal pour déterminer les politiques d'arrêt optimales.

1.6 Structure et développement de la thèse

La première partie de la thèse se compose de deux chapitres, appelés 2 et 3. Dans le premier, sont rappelés les concepts fondamentaux qui seront utilisés dans le Chapitre 3: optimisation convexe, problèmes d'équilibre de Nash généralisé, problèmes binomiaux, contraintes de cardinalité, entre autres. Ensuite, dans le Chapitre 3, une analyse des problèmes Single-Leader-Multi-Follower (SLMFG) incluant des contraintes de cardinalité est développée. Puis l'application de ces résultats est illustrée dans le célèbre problème de localisation des installations, en le traitant comme un problème biniveau.

La deuxième partie de la thèse est composée de trois chapitres. Dans le Chapitre 4, les concepts essentiels sont présentés pour aborder les questions liées à la conception et à l'exploitation optimales d'une centrale CSP. Il commence par une brève introduction au problème à traiter, suivie par la présentation d'un modèle de boîte noire qui permet la représentation d'une centrale CSP et de chacun de ses composants (champ solaire, système de stockage et cycle de Rankine). En outre, les paramètres pertinents liés aux caractéristiques géographiques et économiques spécifiques à l'emplacement du projet de centrale sont détaillés. À cette fin, des fonctions capturant les variations associées à l'irradiation solaire et aux prix sur le marché de l'électricité sont utilisées (voir les Sections 4.2 et 4.3). Le Chapitre 5, consacré à l'étude comparative de divers systèmes de stockage, des indicateurs économiques et des stratégies d'exploitation sont examinés et détaillés dans les sections 4.2, 4.4, et 4.5, respectivement. Enfin, le Chapitre 6 aborde le problème de l'exploitation optimale, dans lequel des problèmes de contrôle optimal sont proposés, en tenant compte d'un modèle réduit de la centrale CSP (en conservant la structure à trois composants

Les développements présentés au chapitre 5 ont fait l'objet d'un article accepté pour publication dans *Journal of Energy Storage* (2024).

Part I

Bilevel games and cardinality constraints

Chapter 2

Preliminaries

This chapter introduces the theoretical foundations for the development of the first part of the research. In Section 2.1, a brief introduction to bilevel games is provided, focusing particularly on Single-Leader Multi-Follower (SLMF) games, whose structure will be used to address the challenges of considering cardinality constraints at different levels (upper and lower). Subsequently, in Section 2.2, specific notations implemented for this work will be presented. Finally, we present the preliminaries for the understanding and development of the theoretical and numerical results.

2.1 Introduction

Single-Leader Multi-Follower (SLMF) games, introduced in [106], are bilevel games where one agent, the leader, interacts with a group of other agents, the followers, under a hierarchical structure. The leader decides her decision variable $x \in \mathbb{R}^p$, and the followers react by solving a (generalized) Nash equilibrium problem, parametrized by x . The leader, by knowing the equilibrium problem of the followers, anticipates their reaction, and takes it into account during her decision process.

The games where only one follower is considered are known as Stackelberg games, they have been largely studied during the last decades, and their applications are now well spread along many interdisciplinary fields (see, e.g., [122, 43, 14, 82] for some recent reviews and advances on the field). The case where multiple followers are involved is considerably more challenging, and therefore it still have a lot of open problems (see, e.g., [9, 73]).

A usual method to try to solve a Single-Leader-Multi-Follower game is to reformulate it as a single-level optimization problem, based on the natural variational formulation of the lower-level game played by the followers. Under standard convexity assumptions, one has that a vector $y \in \mathbb{R}^q$ is an equilibrium point for the lower-level game if and only if it solves the coupled Karush-Kuhn-Tucker optimality conditions of each follower's optimization problem [42]. The resulting problem fits into the class of *Mathematical Programming with Complementarity*

Constraints (MPCC), since the complementarity equations naturally appear in KKT-based variational formulations. Recall that a complementarity constraint involving a vector variable x is of the form

$$T_1(x) \cdot T_2(x) = 0, \quad (2.1.1)$$

where $T_1, T_2 : \mathbb{R}^n \rightarrow \mathbb{R}$ are two affine maps. As an illustration, the most common (but not the only) complementarity constraint is given by complementary slackness in linear programming. The MPCC reduction is classic in the literature of bilevel programming and it can be found in monographs like [41, 40] for the case of one follower, and in [9] for the general SLMF game. It is nevertheless important to say that specific qualification conditions one used to guarantee that the associated MPCC is a reformulation of the initial SLMF game.

In this part, the objective is to study a particular class of SLMF games, involving the so-called *cardinality constraints*. A cardinality constraint over a vector variable $z \in \mathbb{R}^n$ has the form of

$$\|z\|_0 = |\{i \in \{1, \dots, n\} : z_i \neq 0\}| \leq K, \quad (2.1.2)$$

where K is a positive (integer) constant and $|A|$ denotes the cardinality of the set A . The function $\|\cdot\|_0$ is known as the ℓ_0 -norm (or ℓ_0 -pseudonorm) and it counts the number of nonzero entries of a vector. It is commonly used in mathematical programming to model sparsity. However, due to its structure, the ℓ_0 -norm is hard to deal with. While most common approaches in the literature consist in replacing the ℓ_0 -norm by an alternative with more regularity properties (such as the ℓ_1 -norm), recent studies have tackled mathematical programming problems involving the ℓ_0 -norm directly. Some examples are: [54], where the minimization of the ℓ_0 -norm is tackled by a complementarity constraint reformulation; [28], where hidden convexity properties of the ℓ_0 -norm are explored; and [29], where the ℓ_0 -norm is studied through the lens of generalized convexity.

A very important contribution to deal with optimization problems with cardinality constraints was developed in [23, 133], where the constraint (2.1.2) was equivalently written as complementarity constraints as follows:

$$\|z\|_0 \leq K \iff \exists u \in [0, 1]^n \text{ such that } \begin{cases} \sum_{i=1}^n u_i \geq n - K, \text{ and} \\ \forall i \in \{1, \dots, n\}, u_i z_i = 0. \end{cases} \quad (2.1.3)$$

This idea has been deeply exploited to provide constraints qualification, algorithms, first-order optimality conditions, sequential methods, etc. We refer the reader to the recent works [55, 22, 79, 88, 87, 115] and the references therein. But to our knowledge bilevel problems with cardinality conditions have never been studied.

Here, we will study SLMF games with cardinality constraints based on the following straightforward remark: the MPCC reformulation of SLMF games, and the reformulation (2.1.3) of (single-level) optimization problems with cardinality constraints follow the same structure, namely, they encode the ‘‘hard’’ constraints by means of new variables (multipliers) and complementarity constraints. The main caveat, as we will see later on, is that cardinality constraints in SLMF games induce feasibility issues, regardless if they are considered as

coupling constraints for the leader, or shared constraints for the followers.

2.2 Definitions and notations

For any integer $n \in \mathbb{N}$, we write $[n] = \{1, \dots, n\}$. From now on, we will work over finite-dimensional euclidean spaces \mathbb{R}^n , endowed with their respective usual inner products $\langle \cdot, \cdot \rangle$ and their induced euclidean norms. For any two vectors $a, b \in \mathbb{R}^n$, we write $a \odot b$ to denote their Hadamard product, that is, $a \odot b = (a_i b_i : i \in [n])$. We will write $\mathbb{1} \in \mathbb{R}^n$ as the vector of 1-entries of \mathbb{R}^n , that is, the vector given by $\mathbb{1}_i = 1$ for every $i \in [n]$. Abusing notation, we will use the $\mathbb{1}$ to denote the corresponding vector of 1-entries regardless the dimension of the space.

For extended-real valued function $f : \mathbb{R}^n \rightarrow \mathbb{R} \cup \{+\infty\}$, we denote by $\text{dom}(f)$ the (effective) domain of f , that is, $\text{dom} f = \{x \in \mathbb{R}^n : f(x) < +\infty\}$. For a given $\gamma \in \mathbb{R}$, we denote by $[f \leq \gamma]$ the sublevel set of f of value γ . Recall that the function f is said to be

- *convex* if $f(\lambda x + (1 - \lambda)y) \leq \lambda f(x) + (1 - \lambda)f(y)$ for each $x, y \in \text{dom}(f)$ and $\lambda \in [0, 1]$.
- *quasiconvex* if $f(\lambda x + (1 - \lambda)y) \leq \max\{f(x), f(y)\}$, for each $x, y \in \text{dom}(f)$ and $\lambda \in [0, 1]$.

It is well-known that every convex function is quasiconvex, and a function f is quasiconvex if and only if the sublevel sets $[f \leq \gamma]$ are all convex (see, e.g., [4]).

A function $h : \mathbb{R}^n \rightarrow \mathbb{R}$ is said to be *weakly analytic* if for any two vectors $x, y \in \mathbb{R}^n$, the following implication holds:

$$t \in \mathbb{R} \mapsto h(x + ty) \text{ is constant over an open interval} \implies h(x + ty) = h(x), \text{ for all } t \in \mathbb{R}. \quad (2.2.1)$$

In other words, h is weakly analytic if, whenever it is constant over a segment, it must be constant over the whole line containing that segment. Of course, analytic function, such as affine functions, are weakly analytic (see, e.g., [11]).

Let X and Y be two non-empty sets, and let us denote by $\mathcal{P}(Y)$ the power set of Y . A multifunction (also known as correspondence) F is a function $F : X \rightarrow \mathcal{P}(Y)$, that is, a function which, for every $x \in X$, assigns a set $F(x) \subseteq Y$. We denote such a multifunction as $F : X \rightrightarrows Y$.

Whenever X and Y are metric spaces, following [3], we say that:

- A multifunction $F : X \rightrightarrows Y$ is *upper semicontinuous* at a point $x_0 \in X$ if, for each neighbourhood V of $F(x_0)$ in Y , there exists a neighbourhood U of x_0 in X such that

$$F(x) \subset V, \quad \forall x \in U.$$

- A multifunction $F : X \rightrightarrows Y$ is *lower semicontinuous* at a point $x_0 \in X$ if, for each open

set $V \subset Y$ for which $F(x_0) \cap V \neq \emptyset$ there exists a neighbourhood U of x_0 such that

$$F(x) \cap V \neq \emptyset, \quad \forall x \in U.$$

We define the domain of F and the graph of F as $\text{dom}F = \{x \in X : F(x) \neq \emptyset\}$, and $\text{gph}F = \{(x, y) \in X \times Y : y \in F(x)\}$, respectively. We say that F is closed if its graph is closed as a subset of $X \times Y$.

The following proposition, that will be used in the sequel, establishes that parametric sets given by separable weakly analytic constraints are lower semicontinuous (in fact, they enjoy further continuity properties, see, e.g., [11, Theorem 4.3.5] or [119]).

Proposition 2.2.1 ([11, Theorem 3.3.3]). *Let $X \subset \mathbb{R}^n$ be a closed set, and consider a multifunction $F : X \rightrightarrows \mathbb{R}^m$ given by*

$$F(x) = \{y \in \mathbb{R}^m : g_k(y) \leq \varphi_k(x), \forall k \in [m]\},$$

where, for each $k \in [m]$, $g_k : \mathbb{R}^m \rightarrow \mathbb{R}$ and $\varphi_k : \mathbb{R}^n \rightarrow \mathbb{R}$ are continuous functions. If additionally the functions $\{g_k\}_{k \in [m]}$ are convex and weakly analytic, then the multifunction F is lower semicontinuous.

Convex optimization and constraint qualification:

Let us consider an abstract optimization problem

$$\min_{z \in \Omega} f(z), \tag{2.2.2}$$

with the feasibility domain, Ω , defined as in terms of a set of constraints. This is,

$$\Omega = \{z \mid g_k(z) \leq 0, k = 1, \dots, p\}, \tag{2.2.3}$$

where, for each $k \in \{1, \dots, p\}$, the function $g_k : \mathbb{R}^n \rightarrow \mathbb{R}$ is continuous. In this work, we focus only on convex smooth problems, that is, we will assume that the objective function is of class \mathcal{C}^1 and convex, and all constraint functions are of class \mathcal{C}^1 and quasiconvex. In particular, this yields that the feasible sets Ω that we consider are always convex and closed.

For $z \in \Omega$, we consider *normal cone* of Ω at z , denoted by $N_\Omega(z)$, as in the sense of convex analysis, that is,

$$N_\Omega(z) = \{\nu \in \mathbb{R}^n : \langle \nu, y - z \rangle \leq 0, \forall y \in \Omega\}.$$

We will say that the set Ω with its representation (2.2.3) verifies the *Guignard's Constraint Qualification* (see [65], or [126]) at $z \in \Omega$ if

$$N_\Omega(z) = \left\{ \sum_{k=1}^p \lambda_k \nabla g_k(z) \mid \lambda \odot g(z) = 0, \lambda \geq 0 \right\} \tag{2.2.4}$$

There exist many sufficient conditions to ensure that Ω verifies (2.2.4). In particular, if all functions g_k are affine, then (2.2.4) holds (see, e.g., [126]).

2.3 The Generalized Nash Equilibrium problem (GNEP)

A Generalized Nash Equilibrium Problem (GNEP for short) is a noncooperative game considering a finite numbers of players and each of the players solves an optimization problem parameterized by the decision of the other players. These optimization problems form feasibility sets of decisions that influence the individual choices of the players, causing each player to seek a strategy that maximizes his own profit, given the expected behavior of the other players. Consider a finite set $I := \{1, 2, \dots, N\}$ of players, with $N \in \mathbb{N}$. Each player $i \in I$ controls a variable/strategy $z_i \in \mathbb{R}^{n_i}$, and

$$z := (z_1, \dots, z_N) \in \mathbb{R}^n, \quad n := n_1 + \dots + n_N,$$

is the vector of joint strategies of all the players. As usual, we will denote $z = (z_i, z_{-i})$ to emphasise the decision variable of player i within the aggregated decision vector z . The index $-i$ corresponds to the set of opponents of player $i \in I$ and we also write $n_{-i} := n - n_i$. The set of possible strategies for the player i given by the opponents' joint strategy $z_{-i} \in \mathbb{R}^{n_{-i}}$ is denoted by $Z_i(z_{-i})$. That is, the constraints for player i are given by a multifunction $Z_{-i} : \mathbb{R}^{n_{-i}} \rightrightarrows \mathbb{R}^{n_i}$.

Given the strategy z_{-i} , the player i chooses a strategy z_i such that it solves the following optimization problem

$$\begin{aligned} \min_{z_i} \quad & f_i(z_i, z_{-i}) \\ \text{s.t.} \quad & z_i \in Z_i(z_{-i}). \end{aligned} \tag{2.3.1}$$

with $f_i : \mathbb{R}^{n_i} \times \mathbb{R}^{n_{-i}} \mapsto \mathbb{R}$ the cost function. A solution \bar{z} of the (GNEP), called a generalized Nash equilibrium, is a vector of $\prod_i Z_i(\bar{z}_{-i})$ such that, for any i , \bar{z}_i solves the problem (2.3.1). A Nash Equilibrium Problem (NEP) is a particular case of a GNEP, where the set-valued maps Z_i are constant maps (they do not depend on opponents strategies) [7].

2.4 Single-leader-multi-follower game (SLMFG)

We consider a game of $M + 1$ agents with one leader and M followers, where the latter are indexed by $i \in [M]$. We will say that the leader controls a variable $x \in \mathbb{R}^p$, while each follower $i \in [M]$ controls a variable $y_i \in \mathbb{R}^{q_i}$. Let $q = \sum_{i=1}^M q_i$.

Remark 2.4.1. In what follows, we will reserve the index letter i exclusively to denote the i th follower. Thus, for a vector $u \in \mathbb{R}^q$, we write u_i to denote the vector in \mathbb{R}^{q_i} corresponding to the coordinates in u associated to the i th follower. To denote coordinates of a vector or a function, we will use other indexes, such as k or j .

For the leader's problem, the objective function, which depends on all variables, is denoted by $\theta : \mathbb{R}^p \times \mathbb{R}^q \mapsto \mathbb{R}$. We denote by X the feasible set for the leader's decision variable x . For each follower $i \in I$, following (2.2.2)-(2.2.3), we denote by $f_i : \mathbb{R}^p \times \mathbb{R}^{q_i} \times \mathbb{R}^{q_{-i}} \mapsto \mathbb{R}$ their cost function, and by $g_i : \mathbb{R}^p \times \mathbb{R}^{q_i} \times \mathbb{R}^{q_{-i}} \mapsto \mathbb{R}^{m_i}$ their constraint function, both functions depending on the variables of all players (x, y_i, y_{-i}) . We write $p = \sum_{i=1}^M p_i$. We denote by

$Y_i : X \times \mathbb{R}^p \times \mathbb{R}^{q-i} \rightrightarrows \mathbb{R}^{q_i}$ the feasibility set-valued map of follower i : given a leader's decision x , and the vector of decisions of the other followers, y_{-i} , the set $Y_i(x, y_{-i})$ is given by

$$(x, y_{-i}) \mapsto Y_i(x, y_{-i}) := \{y_i : g_i(x, y_i, y_{-i}) \leq 0\}. \quad (2.4.1)$$

In the rest of this chapter and the next one, we will indistinctly use the notation $g_i(x, y_i, y_{-i}) \leq 0$ or $y_i \in Y_i(x, y_{-i})$ to refer to the constraints of the i th follower. The general SLMF game is defined in the following way:

$\begin{array}{ll} \min_{x,y} & \theta(x, y) \\ \text{s.t.} & \begin{cases} x \in X, \\ G(x, y) \leq 0, \\ y \in GNEP(x). \end{cases} \end{array}$	$\begin{array}{ll} \min_{y_i} & f_i(x, y_i, y_{-i}) \\ \text{s.t.} & y_i \in Y_i(x, y_{-i}). \end{array}$	(2.4.2)
Leader	i th Follower	

where $G : \mathbb{R}^p \times \mathbb{R}^q \rightarrow \mathbb{R}^r$ is a continuous function, and $GNEP(x)$ is the solution set-valued map of generalized Nash equilibrium problem of the followers parametrized by x (see, e.g. [58, 106]). Recall that the solution of the GNEP of the followers is given by

$$y \in GNEP(x) \iff \forall i \in [M], y_i \in \operatorname{argmin}\{f_i(x, z, y_{-i}) : z \in Y_i(x, y_{-i})\}. \quad (2.4.3)$$

In (2.4.2), the constraints $G(x, y) \leq 0$ are known as *coupling constraints*, since they are present only in the leader problem. They induce an extra difficulty for feasibility: indeed the leader that must verify feasibility of $x \in X$ considering that

$$x \in X \text{ is feasible} \iff \{y : G(x, y) \leq 0\} \cap GNEP(x) \neq \emptyset,$$

while followers do not take into account the coupling constraint $G(x, y) \leq 0$ when they solve their equilibrium problem. Finally, formulation (2.4.2) is known as optimistic, since the leader can choose, in between the equilibrium point $y \in GNEP(x)$ the most favorable to it. Other formulations, such as the classic pessimistic approach (see, e.g. [9]) or the resent Bayesian approach (see [119]), are available in the literature, but they are out of the scope of this work.

One of the most relevant results for this work part is the one presented in [9], where the authors prove the existence of solutions for SLMFG. In the following, we will quote this important result.

Theorem 2.4.2. (Aussel-Svensson, 2018). *Assume that,*

- a) θ is lower semi-continuous and X is closed,

- b) for each $i \in M$, f_i is continuous,
- c) for each $i \in M$, Y_i is lower semi-continuous relatively to its non-empty domain and has closed graph, and
- d) θ is coercive or, X is compact and at least for one i , the graph of Y_i are uniformly bounded,

If the graph of the lower level GNEP is non-empty, then the SLMFG admits an optimistic equilibrium.

In the original theorem of Aussel-Svensson [9], assumption d) was written with images, but this is an error and graph should be considered.

2.5 Cardinality Constraint

In the field of optimization, decision-makers often encounter situations where they need to select a limited number of elements from a given set to achieve an optimal outcome. This kind of constraint, known as "cardinality constraints", plays a crucial role in various optimization problems across different [23, 127, 10]. Cardinality constraints impose restrictions on the number of variables that can take non-zero values (see 2.1.2) or participate in the solution of an optimization problem. They are particularly common in combinatorial optimization, machine learning, portfolio optimization, and resource allocation, among others [57, 94, 30, 127].

A general cardinality constrained problem is of the form

$$\begin{aligned} \min_x \quad & F(x) \\ \text{s.t.} \quad & \begin{cases} x \in X, \\ \|x\|_0 \leq K \end{cases} \end{aligned} \tag{2.5.1}$$

where $F : \mathbb{R}^n \rightarrow \mathbb{R}$ is a continuously differentiable function, $X \subset \mathbb{R}^n$ is a subset determined by any further constraints on x , K is a natural number and $\|x\|_0$ is the number of nonzero elements in the vector x (also called l_0 -norm). Of course it is assumed that $K < n$, otherwise the cardinality constraint would be superfluous. The problems represented by (2.5.1) are inherently nonconvex because, even if all the functions involved are convex, the feasible region remains nonconvex. Additionally, problem (2.5.1) cannot be treated as a nonlinear program due to the discontinuity of the function $\|x\|_0$. Problem (2.5.1) has been extensively studied, see [23, 121, 141, 22, 54]

In [23], the authors first present a formulation of the problem (2.5.1) as a standard nonlinear program (NLP) with complementary-type constraints, using some binary variables. Then they demonstrate that the standard relaxation of these binary variables has the nice property that its solutions remain equivalent to the solutions of the original cardinality-constrained problem (2.5.1). Additionally, they discuss the stationary conditions of the NLP reformulation and mention that the usual constraint qualification conditions are often violated in their NLP reformulation. So let us recall We will now present the binary-mixed reformulation for

problem (2.5.1) and the theorem that guarantees the equivalence of the solutions of the two problems (in the sense of global minimum).

The mixed-integer reformulation for the problem (2.5.1) is the following:

$$\begin{aligned} \min_{x,u} \quad & F(x) \\ \text{s.t.} \quad & \begin{cases} x \in X, \\ \mathbf{1}^\top u \geq n - K, \\ x \odot u = 0, \quad u \in \{0, 1\}^n, \end{cases} \end{aligned} \quad (2.5.2)$$

with a new variable $u \in \mathbb{R}^n$ and the expression $\mathbf{1}$, represents the ones vector of n components.

Theorem 2.5.1. (Burdakov, Kanzow and Schwartz, 2016) [23]. *A vector $x^* \in \mathbb{R}^n$ is a solution of problem (2.5.1), if and only if there exists a vector $u^* \in \mathbb{R}^n$ such that (x^*, u^*) solves the mixed-integer problem (2.5.2).*

2.6 MPCC Reformulation

In general terms, the utility of reformulating a problem is to place it within a framework where there is a well-developed theory to find a solution (or equilibrium) and/or to better understand the properties of the problem. A classical reformulation of SLMFG consists in replacing the lower-level *GNEP* with a parametric KKT conditions of each of the followers, obtaining a Mathematical Program with Complementarity Constraints (MPCC).

The KKT optimality conditions associated to each follower's problem described in (2.4.2) is that, (y_i, μ_i) from follower i satisfying

$$\begin{cases} \nabla_{y_i} f_i(x, y_i, y_{-i}) + \sum_{k=1}^{p_i} \mu_{ik} \nabla_{y_i} g_{ik}(x, y_i, y_{-i}) = 0, \\ g_i(x, y) \leq 0 \\ \mu_{ik} g_{ik}(x, y_i) = 0, \\ \mu_{ik} \geq 0, k = 1, \dots, p_i. \end{cases} \quad (2.6.1)$$

Let $\text{KKT}(x)$ be denoted as the set of solutions of KKT conditions of all the followers, that is, (y, μ) such that, given the parameters (x, y_{-i}) for each $i = 1, \dots, N$, (y_i, μ_i) , solves the KKT system (2.6.1). Then, a global optimal solution for the MPCC reformulation of a SLMF game is a vector (\bar{x}, \bar{y}) that solves the following problem

$$\begin{aligned} \min_{x,y} \quad & \theta(x, y) \\ \text{s.t.} \quad & \begin{cases} x \in X, \\ G(x, y) \leq 0, \\ y \in \text{KKT}(x). \end{cases} \end{aligned} \quad (2.6.2)$$

For this type of reformulations, there are numerical resolution methods, for instance in [61, 67, 95].

Now, it is important to precise the correspondence or relationship between the global solutions of the original problem (2.4.2) and its MPCC reformulation (2.6.2). For this, we must analyze the lower level constraints qualification for the existence of Lagrange multipliers. In other words, to ensure the equivalence between the global solutions of the problem (2.4.2) and its reformulation (2.6.2), there are several qualification constraints that have to be verified [51, 9]. However, under some basic assumptions on the objective functions and constraints of the lower-level (with respect to differentiability and convexity [7]), along with techniques developed in [8], it is possible to reduce the conditions to be verified, resulting in the fact that $GNEP(x) = KKT(x)$, $\forall x \in X$, which implies the equivalence between global solutions.

2.7 SOS1

By Special Ordered Set of type One (SOS1) one describes a collection of values in which one value at most can have a non-zero value. The values in an SOS1 are not subject to any other discrete conditions and are grouped together consecutively in the data [13].

The sets SOS1 are commonly used to represent a set of mutually exclusive alternatives that are ordered in increasing values of size, cost, or some other relevant unit. This representation is an extension of the separable programming model that deals with discrete variables. This representation extends discrete programming from the separable programming model. It is important to note that this representation assumes that a non-linear function represented in this way has a single value within the range of its argument.

This method has been implemented to computationally solve the MPCC reformulations (see Subsection 2.6) of the linear bilevel problems. For this, the complementary conditions are omitted initially and then branch on them instead [83]. More recently, in [6], it has been known that the SOS1 method is also very efficient to solve SLMF games in which the constraints of the followers are linear.

Chapter 3

Single-Leader Multi-Follower games with cardinality constraints and their application to a location problem

In this chapter, we will analyze SLMF games with cardinality constraints. In Section 3.1, we will address the case of problems with cardinality constraints at the upper level, through existence results, reformulations of the original problem and, finally, examples illustrating the complexity of ensuring existence results for a bilevel problem with cardinality constraints at the lower level will be presented. Then, in Section 3.2, an alternative approach will be used: the cardinality constraints will be split between the lower and the upper levels. Existence results and an equivalent reformulation will be presented. Finally, to illustrate the applicability of the aforementioned results, formulations for the well-known facility location problem will be developed and simulated.

3.1 SLMF games with upper-level cardinality constraints

In this section, we begin by illustrating the structure of bilevel problems with cardinality constraints at the upper level. Subsequently, we prove the existence of solutions and introduce a reformulation of the original problem, which will facilitate the establishment of equivalence results for global solutions.

3.1.1 Problem formulation and existence result

The focus is here to consider a SLMF game where the coupling constraint $G(x, y) \leq 0$ is a cardinality constraint. That is, we will study the problem

$\begin{aligned} \min_{x,y} \quad & \theta(x, y) \\ \text{s.t.} \quad & \begin{cases} x \in X, \\ \ y\ _0 \leq K \\ y \in GNEP(x) \end{cases} \end{aligned}$	$\begin{aligned} \min_{y_i} \quad & f_i(x, y_i, y_{-i}) \\ \text{s.t.} \quad & g_i(x, y_i, y_{-i}) \leq 0. \end{aligned}$	(3.1.1)
Leader	<i>i</i> th Follower	

Remark 3.1.1. For the sake of simplicity, in this section we consider a single (global) cardinality constraint $\|y\|_0 \leq K$. However, for any partition $\mathcal{S} = \{s_1, \dots, s_r\}$ of the involved index set $\{(i, j) : i \in [M], j \in [q_i]\}$, we can consider a sequence of “independent” cardinality constraints of the form

$$\|y_{s_l}\|_0 \leq K_l, \quad \forall l \in [r], \quad (3.1.2)$$

where $y_{s_l} = (y_{i,j} : (i, j) \in s_l)$. The results of this section can be directly extended to this general case.

The main problem with formulations with cardinality constraints in the upper level, is that the constraint $\|y\|_0 \leq K$ is a coupling constraint. This might lead to infeasibility, even if the equilibrium set $GNEP(x)$ is nonempty for every $x \in X$, as the following example shows.

Example 3.1.2 (Infeasibility at the upper level problem by the cardinality constraint). We consider the leader’s problem as

$$\begin{aligned} \min_{x,y} \quad & x \\ \text{s.t.} \quad & \begin{cases} x \in [1, 2] \\ \|y\|_0 \leq 1 \\ y \in GNEP(x) \end{cases} \end{aligned} \quad (3.1.3)$$

while the followers’ equilibrium problem, for which $GNEP(x)$ is the solution set, is given by

$\begin{aligned} \min_{y_1} \quad & y_1 \\ \text{s.t.} \quad & \begin{cases} x \leq 2y_1 \\ y_1 \in [0, 1] \end{cases} \end{aligned}$	$\begin{aligned} \min_{y_2} \quad & -y_2 \\ \text{s.t.} \quad & \begin{cases} y_2 \leq y_1 \\ y_2 \in [0, 1] \end{cases} \end{aligned}$	(3.1.4)
Follower 1	Follower 2	

It is not hard to check that for any $x \in [1, 2]$, the followers’ equilibrium problem has a unique solution given by $(y_1(x), y_2(x)) = (x/2, x/2)$. Thus, the solution map $x \mapsto GNEP(x)$ enjoys several amenable properties: it is single-valued, continuous, linear and nonempty for every leader’s decision. However, the upper-level problem is clearly infeasible. \diamond

However, if one assumes that there is at least one feasible point for the leader, one can replicate the standard existence result of [7].

Theorem 3.1.3. *Consider problem (3.1.1) and assume that*

- (i) θ is lower semicontinuous and X is closed.
- (ii) for each $i \in [M]$, f_i is continuous.
- (iii) for each $i \in [M]$, the graph of Y_i are uniformly bounded, and X is bounded.
- (iv) for each follower $i \in [M]$, the set-valued map Y_i is lower semicontinuous with nonempty closed graph.

Then, either the SLMF game (3.1.1) is infeasible, or it admits a solution.

PROOF. Let us assume that (3.1.1) is feasible, that the feasible set of the leader's problem

$$\mathcal{F} := \{(x, y) \in X \times \mathbb{R}^m \mid \|y\|_0 \leq K, y \in GNEP(x)\} \quad (3.1.5)$$

is nonempty. It thus remains to show that in this case, there is a solution for (3.1.1). It follows the same lines as in [7] and is included here for sake of completeness.

To do so, we will prove first that the set-valued map GNEP has closed graph, thus defining a closed constraint set for the leader. Let us observe that we can write

$$GNEP(x) = \bigcap_{i=1}^M S_i(x)$$

with

$$S_i(x) := \{(y_i, y_{-i}) \mid y_i \in \operatorname{argmin}_z \{f_i(x, z, y_{-i}) \mid z_i \in Y_i(x, y_{-i})\}\}.$$

Thus it is sufficient to prove that each of the maps $S_i : X \rightrightarrows \mathbb{R}^q$ has closed graph. Let us fix $i \in [M]$ and take sequences $(x_k)_k$ in \mathbb{R}^p and $(y_k)_k$ in \mathbb{R}^q converging respectively to x and y , and such that $y_k \in S_i(x_k)$ for all $k \in \mathbb{N}$. We want to prove that $y \in S_i(x)$. Note that

$$(x_k, y_k) \in \operatorname{gph} S_i \implies y_{i,k} \in Y_i(x_k, y_{-i,k}) \implies (x_k, y_k) \in \operatorname{gph} Y_i,$$

and thus, since Y_i has closed graph, we get that $y_i \in Y_i(x, y_{-i})$. Take $z_i \in Y_i(x, y_{-i})$. By lower semicontinuity of the set-valued map Y_i , we know that (up to subsequences) that there exist $z_{i,k} \in Y_i(x_k, y_{-i,k})$ such that $z_{i,k} \rightarrow z_i$. Since $y_k \in S_i(x_k)$ then

$$f_i(x_k, y_{i,k}, y_{-i,k}) \leq f_i(x_k, z_{i,k}, y_{-i,k}), \forall k \in \mathbb{N}.$$

Taking limit as $k \rightarrow \infty$, since f_i is continuous, it gives $f_i(x, y_i, y_{-i}) \leq f_i(x, z_i, y_{-i})$. Since z_i was arbitrarily chosen from $Y_i(x, y_{-i})$, we conclude that $y \in S_i(x)$. Thus $S_i(x)$ is closed and hence, GNEP has closed graph.

Observe also that $GNEP$ is also uniformly bounded, since

$$GNEP(x) = \bigcap_{i=1}^M S_i(x) \subset \{y \in \mathbb{R}^q \mid y_i \in Y_i(x, y_{-i})\},$$

and the right-hand set is uniformly bounded, thanks to hypothesis (iii). Thus, noting that $\{(x, y) : x \in X, \|y\|_0 \leq K\}$ is closed, we get that the set

$$\mathcal{F} = \{(x, y) : x \in X, \|y\|_0 \leq K\} \cap \text{gph}(GNEP)$$

is compact. Since the objective function θ is lower semicontinuous, it follows that the optimization problem of the leader in (3.1.1) has a solution, by a mild application of Weierstrass theorem. \square

As usual, if the objective of the leader is coercive, that is, if $\theta(x, y) \rightarrow +\infty$ as $\|(x, y)\| \rightarrow +\infty$, then we can remove hypothesis (iii) from Theorem 3.1.3, and obtain the same result. Note also that, Theorem 3.1.3 coincides with Theorem 3.1 of [7] in the case of trivial cardinality constraints (that is, $K = q$), and so, that is why the proof follows the same strategy.

An important feature of this result is that for many optimization problems, infeasibility can be checked numerically. Indeed, if one can reformulate the SLMF game to a single-level optimization problem, classic ready-to-go algorithms should be able to decide infeasibility or to provide a (global/local) solution. This property allows us to skip the step of checking existence, and pass directly to computation: either we will find the solution or we will get a certificate of infeasibility.

In the next subsection, we are going to present a first reformulation of the problem with cardinality constraints in the upper level (3.1.1), and then discuss the relationship between the feasible set of the problem (3.1.1) and the ones of its first reformulation.

3.1.2 Reformulations

Since $GNEP(x)$ always stands for the solution set of the followers' equilibrium problem, as given in (3.1.1), we will only write the leader's problem, where the constraint $y \in GNEP(x)$ captures the interaction with the followers, as in (2.4.3).

Now, following [23, 133], we can rewrite the cardinality constraint of (3.1.1), by including a new variable $u \in \mathbb{R}^q$ and using (2.1.3) as follows:

$$\begin{aligned} \min_{x, y, u} \quad & \theta(x, y) \\ \text{s.t.} \quad & \begin{cases} x \in X, \\ y \in GNEP(x) \\ \mathbf{1}^\top u \geq q - K \\ u \odot y = 0, \quad u \in [0, 1]^q \end{cases} \end{aligned} \tag{3.1.6}$$

This reformulation is in fact equivalent (in the sense of global minimizers) to (3.1.1), as the following proposition shows.

Proposition 3.1.4. *A vector $(x, y) \in \mathbb{R}^n \times \mathbb{R}^q$ is feasible for (3.1.1) if and only if there is a vector $u \in \mathbb{R}^q$ such that (x, y, u) is feasible for (3.1.6).*

Moreover, a vector $(x^*, y^*) \in \mathbb{R}^n \times \mathbb{R}^q$ is a global solution of problem (3.1.1) if and only if there exist a vector $u^* \in \mathbb{R}^q$ such that (x^*, y^*, u^*) is a global solution of reformulated problem (3.1.6).

PROOF. Since the objective functions of both problems are the same and do not depend on the variable u , it suffices to show only the first part of the proposition.

First assume that (x, y) is feasible for (3.1.1). Then, due to $\|y\|_0 \leq K$, let us define the vector $u \in \mathbb{R}^q$ defined componentwise by

$$\forall k \in [q], \quad u_k = \begin{cases} 0 & \text{if } y_k \neq 0, \\ 1 & \text{if } y_k = 0. \end{cases} \quad (3.1.7)$$

Recall that, according to Remark 2.4.1, y_k stands for the k th coordinate of the aggregated vector y , without referring any follower. Then, u satisfies $u \in [0, 1]^q$, $\mathbf{1}^\top u \geq q - K$, and $u_k y_k = 0$ for all $k \in [q]$. Hence (x, y, u) is feasible for problem (3.1.6).

Now, for the reverse implication, suppose that there exists $u \in \mathbb{R}^q$ such that (x, y, u) is feasible for (3.1.6). Then define the index set $J := \{k : u_k > 0\} \subset [q]$. Since, by assumption, $u \in [0, 1]^q$ and $\mathbf{1}^\top u \geq q - K$, it follows that $|J| \geq q - K$. Furthermore, using $u \odot y = 0$, we see that $y_i = 0$ at least for all $i \in J$. Hence $\|y\|_0 \leq K$. By hypothesis we have $y \in GNEP(x)$. Thus, (x, y) is feasible for problem (3.1.1). The proof is then complete. \square

Remark 3.1.5. Note that it is immediate to extend the previous result to the case of a reformulation of the problem (3.1.1) considering $u \in \{0, 1\}^q$ instead of $u \in [0, 1]^q$. The first part of the proof remains the same, while for the second part, it is enough to define the set of indices $J := \{k : u_k = 1\}$.

If we consider local minimizers, the equivalence between (3.1.1) and (3.1.6) does not hold anymore. Nevertheless, we still can get one implication.

Proposition 3.1.6. *Let $(x^*, y^*) \in \mathbb{R}^n \times \mathbb{R}^m$ a local solution of (3.1.1). Then there exists a vector $u^* \in \mathbb{R}^q$ such that the vector (x^*, y^*, u^*) is also a local solution of (3.1.6).*

PROOF. Let u^* be a vector defined componentwise by

$$\forall k \in [q], \quad u_k^* := \begin{cases} 0 & \text{if } y_k^* \neq 0, \\ 1 & \text{if } y_k^* = 0. \end{cases} \quad (3.1.8)$$

Again, according to Remark 2.4.1, y_k stands for the k th coordinate of the aggregated vector y , without referring any follower. We have that $u_k^* = 1$ if and only if $y_k^* = 0$ and hence $\mathbf{1}^\top u^* = q - \|y^*\|_0 \geq q - K$. It's clear that (x^*, y^*, u^*) is feasible for problem (3.1.6). We will show that (x^*, y^*, u^*) is a local minimum of (3.1.6). To this end, we can note that there exists $r_1 > 0$, such that

$$f(x, y) \geq f(x^*, y^*) \quad \forall (x, y) \in B_{r_1}(x^*, y^*), \text{ such that } y \in GNEP(x), \quad \|y\|_0 \leq K,$$

due to the assumed local optimality of (x^*, y^*) for the problem (3.1.1). Furthermore, let us choose $r_2 = 1/2$. We have $u_k > 0$ for all $u \in B_{r_2}(u^*)$ and all $k \in [q]$ such that $u_k^* > 0$. The previous observation lead to the following inclusion

$$\{k : u_k = 0\} \subseteq \{k : u_k^* = 0\}, \quad \forall u \in B_{r_2}(u^*) \quad (3.1.9)$$

Now, taking $r := \min\{r_1, r_2\}$, and let $(x, y, u) \in B_r(x^*, y^*) \times B_r(u^*)$ be a feasible vector for problem (3.1.6). In particular, we have $x \in X$ and $y \in GNEP(x)$. The inclusion (3.1.9) implies that for every $k \in [q]$,

$$y_k \neq 0 \implies u_k = 0 \implies u_k^* = 0 \implies y_k^* \neq 0$$

which entails $\|y\|_0 \leq \|y^*\|_0$. Hence (x, y) is feasible for problem (3.1.1). Since we have $(x, y) \in B_{r_1}(x^*, y^*)$, we obtain $f(x, y) \geq f(x^*, y^*)$ from local optimality of (x^*, y^*) of the problem (3.1.1). Therefore, (x^*, y^*, u^*) is a local minimum of problem (3.1.6). The proof is then completed. \square

This proposition is tight, in the sense that the converse implication does not hold. Here, the local minima of problem (3.1.6) might fail to induce local minima of (3.1.1). The obstruction is that the variable u in the reformulation (3.1.6) acts as a multiplier inducing partitions of the space: while the overall feasible set might be connected, it is possible to locally separate a point where some coordinate u_k is strictly positive from those where it is zero. Similar issues have been identified in the classic MPCC reformulation of bilevel programming problems (see, e.g., [39, Example 3.4]). The following example illustrates this fact.

Example 3.1.7. Consider the problem

$$\begin{aligned} \min_{x,y} \quad & y_1 - 2y_2 \\ \text{s.t} \quad & \begin{cases} x \in [0, 1], \\ y \in GNEP(x) \\ \|y\|_0 \leq 1, \end{cases} \end{aligned}$$

and assume that for every $x \in [0, 1]$, $GNEP(x) = [0, 1]^2$. For any $x \in [0, 1]$, the point $(x, 0, 1)$ is a global minimizer, while clearly $(x, 0, 0)$ is not a local optimum. Now, the reformulation (3.1.6) of this problem is given by

$$\begin{aligned} \min_{x,y,u} \quad & y_1 - 2y_2 \\ \text{s.t} \quad & \begin{cases} x \in [0, 1], \\ y \in GNEP(x) \\ u_1 + u_2 \geq 1 \\ u \odot y = 0, \quad u \in [0, 1]^2. \end{cases} \end{aligned}$$

Here, for any $x^* \in [0, 1]$, the point (x^*, y^*, u^*) with $y^* = (0, 0)$ and $u^* = (0, 1)$ is a local optimum. Indeed, fix any $r = 1/2$ and pick any $(x, y, u) \in B_r(x^*, y^*, u^*)$ that is feasible for the reformulated problem. Then, necessarily $u_2 \geq 1/2$ and so $y_2 = 0$. Then,

$$y_1 - 2y_2 = y_1 \geq 0 = y_1^* - 2y_2^*,$$

and the conclusion follows. \diamond

The observation that the variable u of (3.1.6) acts as a multiplier similar to the classic MPCC reformulation of SLMF games is in fact rather powerful. Indeed, we can profit from this observation to produce a second single-level reformulation of (3.1.1) without cardinality constraints, which still is a mathematical programming problem with complementarity constraint, as the classic MPCC reformulation and the reformulation (3.1.6). We will just replace the lower-level (generalized) Nash equilibrium problem of (3.1.6) by the concatenation of the associated parametric KKT conditions of each of the followers.

Recalling that the constraint set $Y_i(x, y_{-i})$ is given by functional inequalities as in (2.4.1), we can consider the Lagrangian function for the i th follower as

$$L_i(x, y, u, \lambda_i) := f_i(x, y, u) + \sum_{k=1}^{m_i} \lambda_{ik} g_{ik}(x, y, u),$$

where $\lambda_i = (\lambda_{i,1}, \dots, \lambda_{i,m_i})$ stands for the vector of Lagrange multipliers. The MPCC reformulation for problem (3.1.6) is:

$$\begin{aligned} & \min_{x,y,u,\lambda} \theta(x, y) \\ & \text{s.t.} \quad \begin{cases} x \in X, \\ \mathbb{1}^\top u \geq q - K, \\ u \odot y = 0, u \in [0, 1]^q, \\ \forall i \in [M], \begin{cases} \nabla_{y_i} f_i(x, y) + \sum_{k=1}^{m_i} \lambda_{ik} \nabla_{y_i} g_{ik}(x, y) = 0, \\ g_i(x, y) \leq 0, \\ \lambda_i \odot g_i(x, y) = 0, \\ \lambda_i \geq 0. \end{cases} \end{cases} \end{cases} \quad (3.1.10) \end{aligned}$$

Note that, since the lower-level problems of (3.1.6) are not affected by the variable u (which is used only to rewrite the cardinality constraint), the same KKT equations from (3.1.10) are used to provide a MPCC reformulation of (3.1.1) maintaining cardinality constraints. However, we focus our attention only in (3.1.6) and (3.1.10), since our main goal is to avoid cardinality constraints, in the spirit of [23, 133].

We finish this subsection with the next theorem, which is one of our main results, providing the equivalence of all problems we have written so far, in the sense of global solutions. Even though the proof follows standard arguments, we include it here for the sake of completeness.

Theorem 3.1.8. *Consider problem (3.1.1) and assume the following hypotheses:*

- (H₁) (Follower Differentiability) For any follower $i \in [M]$ and any $(x, y_{-i}) \in X \times \mathbb{R}^{q-i}$, $f_i(x, \cdot, y_{-i})$ and $g_i(x, \cdot, y_{-i})$ are differentiable.
- (H₂) (Follower Convexity) For any follower $i \in [M]$ and any $(x, y_{-i}) \in X \times \mathbb{R}^{q-i}$, $f_i(x, \cdot, y_{-i})$ is convex, and the components of $g_i(x, \cdot, y_{-i})$ are quasiconvex functions.
- (H₃) (Guignard's CQ) for each leader's strategy $x \in X$, for each follower $i \in [M]$, and for each joint strategy $y = (y_i, y_{-i})$ which is feasible for all followers, equation (2.2.4) holds for $\Omega = Y_i(x, y_{-i})$ at y_i , with its representation (2.4.1).

Then, for any $(\bar{x}, \bar{y}) \in \mathbb{R}^p \times \mathbb{R}^q$, the following assertions are equivalent:

- (i) (\bar{x}, \bar{y}) is a feasible point (respectively, a global solution) of (3.1.1).
- (ii) $\exists \bar{u} \in [0, 1]^q$, such that $(\bar{x}, \bar{y}, \bar{u})$ is a feasible point (respectively, a global solution) of (3.1.6).
- (iii) $\exists \bar{\lambda} \in \mathbb{R}^m, \exists \bar{u} \in [0, 1]^q$, such that $(\bar{x}, \bar{y}, \bar{u}, \bar{\lambda})$ is a feasible point (respectively, a global solution) of (3.1.10).

PROOF. The equivalence between (i) and (ii) is given in Proposition 3.1.4. To show that (ii) \iff (iii), it is enough to show that

$$(x, y, u) \text{ is feasible for (3.1.6)} \iff \exists \lambda \in \mathbb{R}^m \text{ such that } (x, y, u, \lambda) \text{ is feasible for (3.1.10)}.$$

Suppose first that (x, y, u) is feasible for (3.1.6). Then, $y \in GNEP(x)$ and so we have that for every $i \in [M]$, $y_i \in \operatorname{argmin}_z \{f_i(x, z, y_{-i}) \mid z \in Y_i(x, y_{-i})\}$. Since $Y_i(x, y_{-i})$ is convex, we get that

$$-\nabla_{y_i} f_i(x, y_i, y_{-i}) \in N_{Y_i(x, y_{-i})}(y_i).$$

Then, hypothesis (H₃) allows us to apply formula (2.2.4) to $N_{Y_i(x, y_{-i})}(y_i)$, ensuring that there exists a multiplier $\lambda_i \in \mathbb{R}^{q_i}$ satisfying the Karush-Kuhn-Tucker conditions for the problem of the i th follower given by (x, y_{-i}) , at y_i . Then, by writing $\lambda = (\lambda_1, \dots, \lambda_M)$, we conclude that (x, y, u, λ) is feasible for (3.1.10).

For the converse, suppose now that (x, y, u, λ) is feasible for (3.1.10). Then, for $i \in [M]$, $\lambda_i \in \mathbb{R}^{q_i}$ is a multiplier satisfying the Karush-Kuhn-Tucker conditions for the problem of the i th follower given by (x, y_{-i}) , at y_i . Let $z \in Y_i(x, y_{-i})$ and fix $k \in \{1, \dots, m_i\}$. Since $g_{ik}(x, \cdot, y_{-i})$ is quasiconvex, we have that the segment $[y_i, z]$ is contained in the sublevel set $[g_{ik}(x, \cdot, y_{-i}) \leq 0]$. Then,

$$\langle \nabla_{y_i} g_{ik}(x, y_i, y_{-i}), z - y_i \rangle = \lim_{t \rightarrow 0} \frac{g_{ik}(x, y_i + t(z - y_i), y_{-i}) - g_{ik}(x, y_i, y_{-i})}{t} \leq 0.$$

Since $z \in Y_i(x, y_{-i})$ and $k \in \{1, \dots, m_i\}$ are arbitrary, we deduce that

$$-\nabla_{y_i} f_i(x, y_i, y_{-i}) = \sum_{k=1}^{m_i} \lambda_{ik} \nabla_{y_i} g_{ik}(x, y_i, y_{-i}) \in N_{Y_i(x, y_{-i})}(y_i).$$

Thus, convexity of f_i , entails that $y_i \in \operatorname{argmin}_z \{f_i(x, z, y_{-i}) \mid z \in Y_i(x, y_{-i})\}$. Since this holds for every $i \in [M]$, we conclude that $y \in GNEP(x)$, and so (x, y, u) is feasible for (3.1.6), finishing the proof. \square

3.1.3 Lower-level cardinality constraints

Even though our main focus is problem (3.1.1), in this subsection we will present the formulation of the bilevel problem with cardinality constraints at the lower-level. Such formulation considers the cardinality constraint as a shared constraint for the followers, and so it is written as

$\begin{aligned} \min_{x,y} \quad & \theta(x, y) \\ \text{s.t.} \quad & \begin{cases} x \in X, \\ y \in GNEP_0(x) \end{cases} \end{aligned}$	$\begin{aligned} \min_{y_i} \quad & f_i(x, y_i, y_{-i}) \\ \text{s.t.} \quad & \begin{cases} y_i \in Y_i(x, y_{-i}). \\ \ y\ _0 \leq K \end{cases} \end{aligned}$	(3.1.11)
Leader	<i>i</i> th Follower	

Here, we denote $GNEP_0(x)$ as the equilibrium set of the followers' problem, when including the cardinality constraints. This problem is challenging to handle due to the loss of convexity in the set of constraints for the followers and it is left out of the scope of our work.

Nonetheless, we provide here an example that illustrates how the cardinality constraint at the lower-level leads to the loss of lower semicontinuity of the leader's objective functional even for very regular data.

Example 3.1.9 (Failing lower semicontinuity with lower-level cardinality constraints).

$\begin{aligned} \min_{x,y} \quad & x + y_1 + y_2 \\ \text{s.t.} \quad & \begin{cases} x \in [0, 1], \\ y \in GNEP_0(x) \end{cases} \end{aligned}$	$\begin{aligned} \min_{y_1} \quad & y_1 + y_2 \\ \text{s.t.} \quad & \begin{cases} y_1 + y_2 \leq 1 \\ y_1 \geq x \\ \ y\ _0 \leq 1 \\ y_1 \geq 0 \end{cases} \end{aligned}$	$\begin{aligned} \min_{y_2} \quad & -y_1 - y_2 \\ \text{s.t.} \quad & \begin{cases} y_1 + y_2 \leq 1 \\ \ y\ _0 \leq 1 \\ y_2 \geq 0 \end{cases} \end{aligned}$	(3.1.12)
Leader	Follower 1	Follower 2	

The solution of the parametric $GNEP$ without considering the constraint $\|y\|_0 \leq 1$ in the followers problem is given by

$$GNEP(x) = \{(x, 1 - x)\} \text{ for all } x \in [0, 1]. \quad (3.1.13)$$

Now, the solution of the parametric $GNEP$ considering the constraint $\|y\|_0 \leq 1$, is

$$GNEP_0(x) = \begin{cases} \{(x, 0)\} & \text{if } x \in (0, 1] \\ \{(0, 1)\} & \text{if } x = 0. \end{cases} \quad (3.1.14)$$

Even though all data are linear, the function $\theta(x, y) = x + y_1 + y_2$ in the leader problem from (3.1.12) fails to be lower semicontinuous when it is restricted to the feasible set. Indeed, $\theta(x, y(x)) = \theta(x, x, 0) = 2x$ if $x > 0$, and $\theta(0, y(0)) = \theta(0, 0, 1) = 1$. \diamond

The main reason for the lack of lower semicontinuity is not the function θ itself, but rather the lack of lower semicontinuity of the constraints maps $(x, y_{-i}) \mapsto Y_i(x, y_{-i})$. If one aims to address SLMF games with lower-level cardinality constraints, probably dealing with the loss of lower semicontinuity of the constraints maps might be the most difficult obstruction.

3.2 SLMF games with mixed cardinality constraints

As illustrated in the Example 3.1.2, problems of the form (3.1.1) can become infeasible due to the fact that the leader does not have control over the decisions of the followers. Passing the cardinality constraints to the follower, as we discussed previously, can break the regularity of the upper-level problem (as illustrated in Example 3.1.9). In this section, however, we propose a mixed formulation considering the reformulation (3.1.6), where the vector u is used to represent the cardinality constraint partially distributed between the leader and the followers. Specifically, we propose to consider the following formulation:

$\begin{aligned} \min_{x, y, u} \quad & \theta(x, y) \\ \text{s.t.} \quad & \begin{cases} x \in X, \\ y \in GNEP(x, u) \\ \mathbf{1}^\top u \geq q - K \\ u \in [0, 1]^q \end{cases} \end{aligned}$	$\begin{aligned} \min_{y_i} \quad & f_i(x, y_i, y_{-i}) \\ \text{s.t.} \quad & \begin{cases} g_i(x, y_i, y_{-i}) \leq 0, \\ u_i \odot y_i = 0. \end{cases} \end{aligned}$	(3.2.1)
Leader	<i>i</i> th Follower	

Recall that, according to Remark 2.4.1, the vector $u_i \in \mathbb{R}^{q_i}$ stands for the components of vector $u \in \mathbb{R}^q$ associated to the i th follower. Consistently, the vector $u \in \mathbb{R}^q$ is written as $u = (u_i : i \in [M]) \in \prod_{i=1}^M \mathbb{R}^{q_i}$, since each part u_i acts only on the i th follower's problem. Now, $GNEP(x, u)$ stands for the solution set of the new equilibrium problem of the followers.

Problem (3.2.1) can be interpreted as follows: the leader is given a new interdiction variable $u \in [0, 1]^q$, through which she can force any subset of followers' variables to be zero. The cardinality constraint is then ensured by demanding the leader to force at least $q - K$ followers' variables to be zero, or equivalently, to allow at most K followers' variables to be nonzero. After the interdiction is decided by the leader, the followers solve their new equilibrium problem, respecting that any interdicted variable must be zero.

3.2.1 Existence of solutions and MPCC reformulation

The main difficulty in order to be able to prove the existence of solutions for the mixed cardinality problem (3.2.1), is that the new constraint $u_i \odot y_i = 0$ can break the lower semicontinuity of the constraint map of the follower, similar to what happens in Example 3.1.9. To solve this issue, we need to restrict ourselves to a setting where the constraint map Y_i is compatible with the new constraint $u_i \odot y_i = 0$. For this, let's consider the particular case where the constraint functions $g_i(x, y_i, y_{-i})$, for $i \in [M]$ can be written as

$$g_i(x, y_i, y_{-i}) = \hat{g}_i(y_i) - \varphi_i(x, y_{-i}),$$

where $\hat{g}_i : \mathbb{R}^{q_i} \rightarrow \mathbb{R}^{m_i}$ is componentwise convex, weakly analytic and continuous (see Chapter 2, Section 2.2), and $\varphi_i : \mathbb{R}^p \times \mathbb{R}^{q-i} \rightarrow \mathbb{R}^{m_i}$ is continuous.

Theorem 3.2.1. *Consider problem (3.2.1) and assume that*

- (i) θ is lower semicontinuous and X is closed.
- (ii) for each $i \in [M]$, f_i is continuous.
- (iii) for each $i \in [M]$, the images of Y_i , are uniformly bounded, and X is bounded.
- (iv) for each $i \in [M]$, $g_i(x, y_i, y_{-i}) = \hat{g}_i(y_i) - \varphi_i(x, y_{-i})$, where \hat{g}_i is componentwise convex, weakly analytic and continuous, and φ_i is continuous.

Then, either problem (3.2.1) is infeasible, or it admits a solution.

PROOF. Wlog, we will suppose that the feasible set of the leader's problem

$$\mathcal{F} := \{(x, u, y) \in X \times [0, 1]^q \times \mathbb{R}^q \mid \mathbf{1}^\top u \geq q - K, y \in GNEP(x, u)\} \quad (3.2.2)$$

is nonempty. So we only need to show that (3.2.1) admits a solution in this case.

To do so, let $(x, u, y) \in X \times [0, 1]^q \times \mathbb{R}^q$ be a feasible point for (3.2.1). Note that taking \bar{u} as

$$\forall k \in [q], \bar{u}_k := \begin{cases} 0 & \text{if } u_k = 0 \\ 1 & \text{if } u_k > 0. \end{cases} \quad (3.2.3)$$

then (x, \bar{u}, y) is feasible for the problem (3.2.1) and the objective value for the leader is the same, since it doesn't depend on u .

Fixing $u \in \{0, 1\}^q = \prod_{i=1}^M \{0, 1\}^{q_i}$, we consider for every $i \in [M]$ the set

$$Z_i^u(x, y_{-i}) = Y_i(x, y_{-i}) \cap \{y_i \in \mathbb{R}^{m_i} \mid u_i \odot y_i = 0\}, \quad (3.2.4)$$

and we define $Z^u(x, y) = \prod_{i=1}^M Z_i^u(x, y_{-i})$. With these definitions, for every $u \in \{0, 1\}^q$, we are going to define the following problem (P_u) :

$\begin{aligned} \min_{x,y} \quad & \theta(x, y) \\ \text{s.t.} \quad & \begin{cases} x \in X_u = X \cap \text{dom}(Z^u), \\ y \in GNEP_u(x) \end{cases} \end{aligned}$	$\begin{aligned} \min_{y_i} \quad & f_i(x, y_i, y_{-i}) \\ \text{s.t.} \quad & y_i \in Z_i^u(x, y_{-i}). \end{aligned}$	(3.2.5)
Leader - (P_u)	i th Follower - (F_i^u)	

where $GNEP_u(x)$ denotes the set of Nash equilibria associated to the followers problems F_i^u .

Now, we will denote (P) as the problem (3.2.1) and we consider $v(P)$ and $v(P_u)$ the optimal values of problems (3.2.1) and (3.2.5), respectively. We claim that $v(P)$ coincides with the minimal value among the problems P_u , that is $v(P) = \min\{v(P_u) \mid u \in \{0, 1\}^q\}$. Indeed, on the one hand, if (x, u, y) is feasible for (P) with $u \in [0, 1]^q$, then (x, y) is feasible for $(P_{\bar{u}})$ where \bar{u} is given as in (3.2.3), and both points have the same objective value for their respective problems. So the value of the problem (P) satisfies

$$v(P) \geq \min\{v(P_u) \mid u \in \{0, 1\}^q\}.$$

On the other hand, if (x, y) is feasible for (P_u) for some $u \in \{0, 1\}^q$, then (x, y, u) must be feasible for (P) . Indeed, this follows directly by the observation that $y \in GNEP(x, u)$ if and only if $y \in GNEP_u(x)$. Thus,

$$v(P) \leq \min\{v(P_u) \mid u \in \{0, 1\}^q\},$$

and the claim is proven. Now, in order to prove the existence of solutions for (P) it is enough to show that for every $u \in \{0, 1\}^q$, one has that (P_u) is either infeasible or it admits a solution. To do so, it is enough to verify that each problem (P_u) verifies the hypotheses of Theorem 3.1 of [7], that is, it verifies the hypotheses (i) – (iv) of Theorem 3.1.3.

Indeed, fix $u \in \{0, 1\}^q$ and assume that (3.2.5) is feasible. Trivially, hypotheses (i) and (ii) of Theorem 3.1.3 hold. Note that, from (iii), we have that the images Y_i are uniformly bounded and so the images of Z_i^u are uniformly bounded, as well. Thus, (P_u) also verifies hypothesis (iii) of 3.1.3. Moreover, we can write

$$Z_i^u(x, y_{-i}) := \{z \mid h_i(z) \leq \phi(x, y_{-i})\},$$

with

$$h_y(z) = \begin{pmatrix} \hat{g}_i(z) \\ u_i \odot z \\ -u_i \odot z \end{pmatrix} \text{ and } \phi(x, y_{-i}) = \begin{pmatrix} \varphi_i(x, y_{-i}) \\ 0 \\ 0 \end{pmatrix}.$$

Since the mappings $y_i \mapsto u_i \odot y_i$ are componentwise linear with respect to (y_i) , we get that hypothesis (iv) entails that h_i is componentwise convex, weakly analytic and continuous and that ϕ is continuous. Thus, of Theorem 3.3.3 of [11] (see Proposition 2.2.1 above), we have

that the multifunction Z_i^u defined in (3.2.4) is lower semicontinuous and has closed graph. Therefore, hypothesis (iv) of Theorem 3.1.3 holds.

Now, all the hypotheses of Theorem 3.1 of [7] are satisfied, thus (P_u) admits a solution. Since problem (3.2.1) is feasible by hypothesis, at least one of the problems (P_u) must be feasible as well. Then, to determine the solution of the problem (3.2.1), it is enough to take the best point (x^*, y^*, u) among the $u \in \{0, 1\}^q$ for which the problem (P_u) is feasible. This concludes the proof since there is a finite number of such u . \square

Similarly as we did in Subsection 3.1.2, we will consider the MPCC reformulation of Problem (3.2.1). The Lagrangian function to the i th follower is given by

$$L_i(x, y, u, \lambda_i, \nu_i) := f_i(x, y, u) + \nu_i^\top (u_i \odot y_i) + \sum_{k=1}^{m_i} \lambda_{ik} g_{ik}(x, y, u),$$

and so, the MPCC reformulation is given by

$$\begin{aligned} \min_{x, y, u, \lambda, \nu} \quad & \theta(x, y) \\ \text{s.t.} \quad & \left\{ \begin{array}{l} x \in X, \\ \mathbf{1}^\top u \geq q - K, \\ u \in [0, 1]^q, \\ \forall i \in [M], \left\{ \begin{array}{l} \nabla_{y_i} f_i(x, y) + \sum_{k=1}^{m_i} \lambda_{ik} \nabla_{y_i} g_{ik}(x, y) + \nu_i \odot u_i = 0, \\ \lambda_{ik} g_{ik}(x, y) \geq 0, \\ g_{ik}(x, y) \leq 0, \\ u_i \odot y_i = 0, \\ \lambda_{ik} \geq 0. \end{array} \right. \end{array} \right. \end{array} \quad (3.2.6)$$

By following a similar strategy as in Subsection 3.1.2, we can establish the following corollary.

Corollary 3.2.2. *Consider Problem (3.2.1) and assume the following hypotheses:*

- (H₁) (Follower Differentiability) *For any follower $i \in [M]$ and any $(x, y_{-i}) \in X \times \mathbb{R}^{q-i}$, $f_i(x, \cdot, y_{-i})$ and $g_i(x, \cdot, y_{-i})$ are differentiable.*
- (H₂) (Follower Convexity) *For any follower $i \in [M]$ and any $(x, y_{-i}) \in X \times \mathbb{R}^{q-i}$, $f_i(x, \cdot, y_{-i})$ is convex, and the components of $g_i(x, \cdot, y_{-i})$ are quasiconvex functions.*
- (H₃) (Guignard's CQ) *for each leader's strategy $x \in X$, for each follower $i \in [M]$, and for each joint strategy $y = (y_i, y_{-i})$ which is feasible for all followers, equation (2.2.4) holds for $\Omega = \{z : g_i(x, z, y_{-i}) \leq 0, u_i \odot z = 0\}$ at y_i .*

Then, for every $(\bar{x}, \bar{y}) \in \mathbb{R}^p \times \mathbb{R}^q$, the following assertions are equivalent:

- (i) $\exists \bar{u} \in [0, 1]^q$ such that $(\bar{x}, \bar{y}, \bar{u})$ is a feasible point (respectively, a global solution) of (3.2.1).

(ii) $\exists \bar{\lambda} \in \mathbb{R}^m, \exists \bar{u} \in [0, 1]^q$ such that $(\bar{x}, \bar{y}, \bar{u}, \bar{\lambda})$ is a feasible point (respectively, a global solution) of (3.2.6).

The main limitation with this last corollary, is that the constraint qualification (2.2.4) is required on the new feasible sets $\{z : g_i(x, z, y_{-i}) \leq 0, u_i \odot z = 0\}$, which might be hard to verify, since it is not automatically inherited from the original constraint sets $Y_i(x, y_{-i}) = \{z : g_i(x, z, y_{-i}) \leq 0\}$. Moreover, the constraints associated to the derivatives of the Lagrangian, that is,

$$\nabla_{y_i} f_i(x, y) + \sum_{k=1}^{m_i} \lambda_{ik} \nabla_{y_i} g_{ik}(x, y) + \nu_i \odot u_i = 0,$$

are complicated constraints, since they are at least quadratic due to the term $\nu_i \odot u_i$, and they are not complementarity constraints. However, these two problems can easily be solved in the special case of linear problems.

3.2.2 Further results for the linear case

We refer to problem (3.2.1) (or problem (3.1.1)) as linear or possessing linear data if

1. $X = \{x : Ax \leq b\}$, for some matrix A and a vector b of appropriate dimensions;
2. $\theta(x, y) = c^\top x + d^\top y$, for some vectors $c \in \mathbb{R}^p$ and $d \in \mathbb{R}^q$;
3. For each $i \in [M]$, there exist matrices B_i, C_i, D_i of appropriate dimensions and a vector $\gamma_i \in \mathbb{R}^{m_i}$ such that $g_i(x, y_i, y_{-i}) = B_i x + C_i y_i + D_i y_{-i} - \gamma_i$;
4. For each $i \in [M]$, there exists a function $\alpha_i : \mathbb{R}^p \times \mathbb{R}^{q-i} \rightarrow \mathbb{R}^{q_i}$ and a vector $\beta_i \in \mathbb{R}^{q_i}$ such that $f_i(x, y_i, y_{-i}) = \alpha_i(x, y_{-i})^\top y_i + \beta_i^\top (y_i \odot y_i)$.

Observe that we are admitting the followers' functions to be either linear with respect to y_i (if $\beta_i = 0$) or quadratic, since $\beta_i^\top (y_i \odot y_i) = \sum_{j=1}^{q_i} \beta_{ij} y_{ij}^2$. The abuse of the word "linear" comes from the fact that the gradient map $y_i \mapsto \nabla_{y_i} f(x, y_i, y_{-i})$ will be affine if the map α_i is affine.

Note that in this case, the constraint sets $\{z : g_i(x, z, y_{-i}) \leq 0, u_i \odot y_i = 0\}$ verify the linear constraint qualification (see, e.g., [126]), since all constraints are linear. Thus, (2.2.4) is verified and Corollary 3.2.2 applies: the linear problem (3.2.1) is either infeasible or it admits a solution.

Now, to search for a solution, we need to consider the MPCC reformulation (3.2.6), which

takes the form

$$\begin{aligned}
& \min_{x,y,u,\lambda,\nu} c^\top x + d^\top y \\
& \text{s.t.} \quad \left\{ \begin{array}{l} Ax \leq b, \\ \mathbf{1}^\top u \geq q - K, \\ u \in [0, 1]^q, \\ \forall i \in [M], \left\{ \begin{array}{l} \alpha_i(x, y_{-i}) + \sum_{k=1}^{m_i} C_i^\top \lambda_{ik} + \nu_i \odot u_i = 0, \\ \lambda_{ik}(B_i x + C_i y_i + D_i y_{-i} - \beta_i) = 0, \\ B_i x + C_i y_i + D_i y_{-i} \leq \beta_i, \\ u_i \odot y_i = 0, \\ \lambda_{ik} \geq 0. \end{array} \right. \end{array} \right. \quad (3.2.7)
\end{aligned}$$

Note that, assuming that all α_i functions are affine maps, problem (3.2.7) is almost a linear programming problem with complementarity constraints: the only constraint that does not fit in this setting is the one associated to the derivatives of the Lagrangian functions.

For Linear Programming problems with complementarity constraints, one could apply the usual Branch-and-Bound algorithm. In fact, complementarity constraints and binary variables can be treated in the same way using SOS1 constraints (see, e.g. [84, 6]), and so Branch-and-Bound also applies for Mixed-Integer Linear Programming problems with complementarity constraints.

Motivated by this observation and by the fact that, following Remark 3.1.5, one can force the variable $u \in [0, 1]^q$ to be an integer vector in $\{0, 1\}^q$, we establish the following proposition, which is the last reformulation of this work.

Proposition 3.2.3. *Consider problem (3.2.7), and the alternative formulation*

$$\begin{aligned}
& \min_{x,y,u,\lambda,\eta} c^\top x + d^\top y \\
& \text{s.t.} \quad \left\{ \begin{array}{l} Ax \leq b, \\ \mathbf{1}^\top u \geq q - K, \\ u \in \{0, 1\}^q, \\ \forall i \in [M], \left\{ \begin{array}{l} \alpha_i(x, y_{-i}) + \sum_{k=1}^{m_i} C_i^\top \lambda_{ik} + \eta_i = 0, \\ \lambda_{ik}(B_i x + C_i y_i + D_i y_{-i} - \beta_i) = 0, \\ B_i x + C_i y_i + D_i y_{-i} \leq \beta_i, \\ u_i \odot y_i = 0, \\ \eta_i \odot (\mathbf{1} - u_i) = 0, \\ \lambda_{ik} \geq 0. \end{array} \right. \end{array} \right. \quad (3.2.8)
\end{aligned}$$

Then, for every point $(\bar{x}, \bar{y}) \in \mathbb{R}^p \times \mathbb{R}^q$, the following assertions are equivalent:

- (a) $\exists(u, \lambda, \nu) \in [0, 1]^q \times \mathbb{R}_+^m \times \mathbb{R}^q$ such that $(\bar{x}, \bar{y}, u, \lambda, \nu)$ is a feasible point (respectively, a global solution) of (3.2.7).
- (b) $\exists(u, \lambda, \eta) \in \{0, 1\}^q \times \mathbb{R}_+^m \times \mathbb{R}^q$ such that $(\bar{x}, \bar{y}, u, \lambda, \eta)$ is a feasible point (respectively, a global solution) of (3.2.8).

In particular, if the functions α_i are affine, problem (3.2.8) is a mixed-integer linear programming problem with complementarity constraints.

PROOF. We will only show the equivalence between feasible sets, since the equivalence between global solutions follows from this first equivalence and the fact that the objective function is the same on both problems, depending only for the (x, y) variables.

(a) \implies (b): consider \bar{u} as in (3.2.3), that is: for each $k \in [q]$, $\bar{u}_k = 1$ if $u_k > 0$, and $\bar{u}_k = 0$ if $u_k = 0$. Then, we can consider η defined from ν as follows:

$$\forall k \in [q], \eta_k = \begin{cases} \nu_k \cdot u_k & \text{if } u_k > 0, \\ 0 & \text{if } u_k = 0. \end{cases}$$

Then, for every $k \in [q]$, we have that $\eta_k > 0 \iff 1 - \bar{u}_k = 0$, and that $\eta_k = \nu_k \cdot u_k$. With these observations, we can directly replace u by \bar{u} and $\nu_i \odot u_i$ by η_i (for each follower $i \in [M]$) in problem (3.2.7), deducing that $(\bar{x}, \bar{y}, \bar{u}, \lambda, \eta)$ is feasible for problem (3.2.8).

(b) \implies (a): it is enough to define $y = \nu \odot u$, since the inclusion $u \in \{0, 1\}^q$ and the constraints $\eta_i \odot (\mathbf{1} - u_i) = 0$ allows to write:

$$\nu_i \odot u_i = \eta_i \odot u_i \odot u_i = \eta_i, \quad \forall i \in [M].$$

Replacing η by $\nu \odot u$, the constraints $(\nu_i \odot u_i) \odot (\mathbf{1} - u_i) = 0$ become trivial in problem (3.2.8), and so we deduce that $(\bar{x}, \bar{y}, u, \lambda, \nu)$ is feasible for problem (3.2.8). The proof is now completed. \square

3.3 Application to Facility location problems with cardinality constraints

In order to illustrate the theory presented in the previous sections, in this final section we provide a concrete example consisting in a variant of the *Facility Location problem* [96, 36]. This problem is a classic example in Mixed-Integer programming primers, and it is very relevant in several applications. In particular, we focus on electric mobility and the need to optimize the charging infrastructure.

The problem we consider is the following: in a city, a company (the leader) is required to build charging stations for electric vehicles, within a list of strategic locations, indexed by the set $S = \{1, \dots, s\}$. The company must take into account a set of consumers with electric cars (followers), indexed by $I = \{1, \dots, i\}$, who will charge their vehicles on one of the built stations once a day. Therefore, the company must decide whether to put or not a charging facility at each location $s \in S$, taking into account the decision process of the consumers.

Due to the nature of the problem, we include some variants. First, the clients are not necessarily committing to charge in the same station every day, but rather they might alternate

within a set of stations, with certain probability. Second, the clients play a *congestion game*, in the sense that their preferences are influenced by how many clients (in expectation) will choose each of the stations. And finally, due to the characteristics of charging, a station can only serve a limited number of cars per day. With this limitation, the company must be able to satisfy the demand for any scenario induced by the distribution of the clients. This last requirement is translated into a cardinality constraint.

For this problem, it is assumed that the batteries of all vehicles have the same capacity and each driver wishes to fully charge his battery; the decision to go to a specific station varies according to the preferences of each driver.

3.3.1 Upper-level and mixed formulations

In what follows, the index $i \in I$ will represent the i th client, and the index $s \in S$, will be the s th station. For each station $s \in S$, we consider:

- A parameter $a_{is} > 0$, which represents the total price of a full charge with respect to client i at station s ;
- A parameter $c_s > 0$, which represents the cost of installing the station s ;
- A parameter $K_s > 0$, which represents the number of charges that can be served by station s per day;
- A variable $x_s \in \{0, 1\}$, where $x_s = 1$ if the station is built, and $x_s = 0$, otherwise.

For each client $i \in I$ and each station $s \in S$, we consider:

- A parameter p_{is} , representing the preference to go to the station s . This preference is influenced by the price a_s , but also by implicit factors, such as the distance to home, the perception of the service, etc;
- A factor α_{is} of inconvenience due to congestion at station s ;
- A variable $y_{is} \in [0, 1]$, which determines probability of client i going to station s .

We denote by $x = (x_s : s \in S)$ the decision vector of the company, by $y_i = (y_{is} : s \in S)$ the decision vector of each client $i \in I$, and by $y = (y_{is} : i \in I, s \in S)$ the joint decision vector of all clients. With this in mind, each client $i \in I$ aims to maximize the concave function

$$y_i \mapsto f_i(x, y_i, y_{-i}) = \sum_{s \in S} \left(p_{is} - \alpha_{is} \sum_{j \in I} y_{js} \right) y_{is},$$

which is parametrized by the company's decision x and by the other clients' decision y_{-i} . We will consider two possible objective functions for the company:

- **Profit:** The company aims to maximize its revenue

$$\theta(x, y) = \sum_{s \in S} \left(T \sum_{i \in I} a_{is} y_{is} - c_s x_s \right),$$

where T is the number of days considered as lifetime of the project.

- **Welfare:** The company aims to maximize the social welfare, given by

$$\theta(x, y) = \sum_{s \in S} \left(T \sum_{i \in I} a_{is} y_{is} - c_s x_s \right) + T \sum_{i \in I} f_i(x, y),$$

where T is the number of days considered as lifetime of the project.

The formulation of the SLMF game with cardinality constraints at upper level (3.1.1) is then given by

$\begin{aligned} & \max_{x, y} \theta(x, y) \\ & \text{s.t.} \quad \begin{cases} y \in NEP(x), \\ \ y_{\bullet, s}\ _0 \leq K_s, \forall s \in S \\ x_s \in \{0, 1\}, \forall s \in S. \end{cases} \end{aligned}$	$\begin{aligned} & \max_{y_{i, \bullet}} \sum_{s \in S} (p_{is} - \alpha_{is} \sum_{j \in I} y_{js}) y_{is} \\ & \text{s.t.} \quad \begin{cases} \sum_{s \in S} y_{is} = 1, \\ y_{is} \leq x_s, \quad s \in S, \\ y_{is} \geq 0 \quad s \in S. \end{cases} \end{aligned}$	(3.3.1)
Leader	i th Follower	

Similarly, the SLMF game with mixed cardinality constraints (3.2.1) is given by

$\begin{aligned} & \max_{x, y, u} \theta(x, y) \\ & \text{s.t.} \quad \begin{cases} y \in NEP(x, u), \\ \mathbf{1}^\top u_{\bullet, s} \geq p - K_s, \forall s \in S \\ u_{is} \in [0, 1], \forall i \in I, \forall s \in S \\ x_s \in \{0, 1\}, \forall s \in S. \end{cases} \end{aligned}$	$\begin{aligned} & \max_{y_{i, \bullet}} \sum_{s \in S} (p_{is} - \alpha_{is} \sum_{j \in I} y_{js}) y_{is} \\ & \text{s.t.} \quad \begin{cases} \sum_{s \in S} y_{is} = 1, \\ y_{is} \leq x_s, \quad \forall s \in S \\ u_i \odot y_i = 0, \\ y_{is} \geq 0, \quad \forall s \in S. \end{cases} \end{aligned}$	(3.3.2)
Leader	i th Follower	

In both problems, we write NEP instead of $GNEP$, to emphasize that the equilibrium problem of the followers is a Nash equilibrium problem and not a generalized one: the followers only affect each others through the objective function and not the constraints.

Then, in this section four bilevel problems will be developed, according to two cases of cardinality constraints and two different objective functions for the company, as summarized in Table 3.1.

Finally, we include the corresponding MPCC reformulations, according to the developments of Sections 3.1 and 3.2. For problem (3.3.1), the Lagrangian associated to the i th follower is given by

$$L_i = \sum_{s \in S} \left[\left(p_{is} - \alpha_{is} \sum_{j \in I} y_{js} \right) y_{is} + \lambda_i (y_{is} - 1) + \mu_{is}^+ (y_{is} - x_s) + \mu_{is}^- (-y_{is}) \right].$$

	Profit	Social Welfare
Upper	Upper-Profit	Upper-SW
Mixed	Mixed-Profit	Mixed-SW

Table 3.1: Bilevel problems with cardinality constraints at the upper level and mixed, considering different objective functions for the company.

Thus, the associated MPCC reformulation is given by:

$$\begin{aligned}
& \min_{x,y,u,\lambda,\mu^+,\mu^-} \theta(x,y) \\
& \text{s.t.} \quad \begin{cases} x \in \{0,1\}^p, \\ \mathbf{1}^\top u_{\bullet,s} \geq p - K_s, \forall s \in S \\ u_{is} \in \{0,1\}, \forall i \in I, \forall s \in S, \\ u \odot y = 0, \forall i \in I \end{cases} \begin{cases} p_i - \alpha_i \odot (y_i + \sum_{j \in I} y_j) + \lambda_i + \mu_i^+ - \mu_i^- = 0, \\ \mu_i^+ \odot (y_i - x_s \mathbf{1}) = 0, \\ \mu_i^- \odot y_i = 0, \\ \mu_i^+, \mu_i^- \geq 0. \end{cases}
\end{aligned} \tag{3.3.3}$$

For the case of problem (3.3.2), the Lagrangian associated to the i th follower is given by

$$L_i = \sum_{s \in S} \left[\left(p_{is} - \alpha_{is} \sum_{j \in I} y_{js} \right) y_{is} + \lambda_i (y_{is} - 1) + \mu_{is}^+ (y_{is} - x_s) + \mu_{is}^- (-y_{is}) + \nu_{is} (u_{is} y_{is}) \right].$$

Thus, considering the change of variables $\eta_i = \nu_i \odot u_i$, and following Proposition 3.2.3, we get the final MPCC formulation given by:

$$\begin{aligned}
& \min_{x,y,u,\lambda,\mu^+,\mu^-, \eta} \theta(x,y) \\
& \text{s.t.} \quad \begin{cases} x \in \{0,1\}^p, \\ \mathbf{1}^\top u_{\bullet,s} \geq p - K_s, \forall s \in S \\ u_{is} \in \{0,1\}, \forall i \in I, \forall s \in S, \\ \forall i \in I \end{cases} \begin{cases} p_i - \alpha_i \odot (y_i + \sum_{j \in I} y_j) + \lambda_i + \mu_i^+ - \mu_i^- + \eta_i = 0, \\ \mu_i^+ \odot (y_i - x_s \mathbf{1}) = 0, \\ \mu_i^- \odot y_i = 0, \\ u_i \odot y_i = 0, \\ \eta_i \odot (\mathbf{1} - u_i) = 0, \\ \mu_i^+, \mu_i^- \geq 0. \end{cases}
\end{aligned} \tag{3.3.4}$$

3.3.2 Methodology

Numerical Resolution of Bilevel Problems

For the problems at hand, we employ a numerical resolution approach based on the reformulation of Mathematical Programming with Complementarity Constraints (MPCC) along with the SOS1 (Special Ordered Sets 1) method. The use of MPCC is essential for modeling and solving optimization problems where both continuous and discrete variables coexist.

Facility	1	2	3	4	5	6	7	8	9	10
Type	1	1	1	1	1	2	2	2	3	3

Table 3.2: Type of facilities.

Step-by-Step Resolution

Here, we describe step-by-step the process used to solve the bilevel problems shown in table 3.1:

- **Problem Formulation:** first, we formulate the problem of determining the location of charging facilities as a bilevel problem with cardinality constraints (see Problem 3.3.1 and 3.3.2). The upper level aims to optimize certain global decision variables, while the lower level models demand response and the allocation of vehicles to charging facilities.
- **Reformulation 1:** apply the reformulation described in Section 3.1.2, obtaining a new variable to optimize along with new equality and inequality constraints.
- **Reformulation 2 (MPCC):** apply the MPCC reformulation technique to derive complementarity relationships. This allows us to obtain a set of equations and inequalities that characterize the problem more suitably for numerical resolution (for problems 3.3.1 and 3.3.2, see formulations 3.3.3 and 3.3.4, respectively).
- **SOS1 Method:** employ the SOS1 method, finding feasible solutions for combinatorial optimization problems, ensuring the selection of the most suitable charging facility locations, each with limited capacity for electric vehicle demand.
- **Global Optimization:** finally, we combine the solutions obtained in the lower level using the SOS1 method with global optimization at the upper level to find the global optimal solution to the charging facility location problem.

3.3.3 Numerical experiments and results

In this study we consider $M = 150$ drivers/cars ($i \in I = \{1, \dots, M\}$) and ten facilities ($s \in S = \{1, \dots, 10\}$), each of which has a fixed capacity K_s , the a_s cost of fully charging the car battery at the facility s (assuming all cars have the same battery).

Each facility belongs exclusively to one type: cheap (type 1), medium (type 2) and expensive (type 3). The values of a_s and K_s depend only on the type. Additionally, the fixed construction cost [USD], also depending on the type, is given by $c_1 = 10000$ for the cheap type, $c_2 = 30000$ for the medium type, and $c_3 = 50000$ for the expensive type. The parameters of each type of facility is given in Table 3.3 while the type of each facility is precised in Table 3.2. Note that the values of the above constants, even if inspired from real life values, have been chosen to be able to enlighten the effect of cardinality constraints in this academic example. In the same line, as a simplifying assumption, we suppose that all cars charge their cars once a week on the same days. The lifespan T of this study case, thus the number of days of charging, is fixed to 52 weeks, representing one year of operation.

Type	Installation cost [USD]	Cost per charge [USD]	Capacity per day
1	$c_1 = 10000$	$a_1 = 9$	$K_1 = 20$
2	$c_2 = 30000$	$a_2 = 15$	$K_2 = 40$
3	$c_3 = 50000$	$a_3 = 28$	$K_3 = 100$

Table 3.3: Description of facilities.

On the other hand, for each facility, a random variable $\xi_s \sim \text{Lognormal}(0.1, 0.05)$ is considered, and the inconvenience of the facility are fixed as $\alpha_s = 28 \frac{\xi_s}{K_s}$, for each facility $s \in S$. For this work, the preference p_{is} is considered as follows: for each facility and each driver, we associate a random position (uniformly distributed) within the plane $[0, 1]^2$, representing the locations of the facilities and the houses of the drivers. With this, the following is calculated

$$p_{is} = \frac{1}{d_{is}} - a_s, \quad (3.3.5)$$

where d_{is} is the euclidean distance between the position of driver i and the facility s .

Fifty different experiments were performed, here called "cases", where the values for p and α were chosen randomly for each case. These values are included in the supplementary material. 100 problems were solved (50 cases, 2 configurations per case), using `Gurobi v10.0.2` [68] coupled with the `SOS1` package, with an execution time limit of 60 minutes.

3.4 Simulations

In the simulations, we conducted 50 different experiments where the values for α_s and p_{is} , with $i \in I$, $s \in S$, were randomly chosen. The problems under consideration are divided into two categories: those with cardinality constraints at the upper level (CC at the upper level) and those with mixed cardinality constraints (mixed CC). Additionally, two objective functions will be examined in these problems: Profits and Welfare, ending thus with four possible cases: Upper-Profits, Upper-SW, Mixed-Profits, and Mixed-SW (see Table 3.1).

Cases	Upper-Profit	Mixed-Profit	Upper-SW	Mixed-SW
1	[0, 0, 2]	[0, 0, 2]	[0, 0, 2]	[3, 0, 1]
2	[0, 0, 2]	[0, 0, 2]	[0, 0, 2]	[3, 0, 1]
3	[0, 0, 2]	[0, 0, 2]	[0, 0, 2]	[3, 0, 1]
4	[0, 0, 2]	[0, 0, 2]	[0, 0, 2]	[3, 0, 1]
5	[0, 0, 2]	[0, 0, 2]	[0, 0, 2]	[4, 2, 0]
6	-	[0, 0, 2]	-	[3, 0, 1]
7	-	[0, 0, 2]	-	[3, 0, 1]
8	-	[0, 0, 2]	-	[3, 0, 1]
9	[0, 0, 2]	[0, 0, 2]	[0, 0, 2]	[3, 0, 1]
10	-	[0, 0, 2]	-	[3, 0, 1]
11	-	[0, 0, 2]	-	[3, 0, 1]
12	[0, 0, 2]	[0, 0, 2]	[0, 0, 2]	[3, 0, 1]
13	[0, 0, 2]	[0, 0, 2]	[0, 0, 2]	[3, 0, 1]
14	[0, 0, 2]	[0, 0, 2]	[0, 0, 2]	[3, 0, 1]
15	[0, 0, 2]	[0, 0, 2]	[0, 0, 2]	[3, 0, 1]
16	[0, 0, 2]	[0, 0, 2]	[0, 0, 2]	[3, 0, 1]
17	[0, 0, 2]	[0, 0, 2]	[0, 0, 2]	[3, 0, 1]
18	[0, 0, 2]	[0, 0, 2]	[0, 0, 2]	[3, 0, 1]
19	[0, 0, 2]	[0, 0, 2]	[0, 0, 2]	[3, 0, 1]
20	[0, 0, 2]	[0, 0, 2]	[0, 0, 2]	[3, 0, 1]
21	-	[0, 0, 2]	-	[3, 0, 1]
22	[0, 0, 2]	[0, 0, 2]	[0, 0, 2]	[3, 0, 1]
23	-	[0, 0, 2]	-	[3, 0, 1]
24	[0, 0, 2]	[0, 0, 2]	[0, 0, 2]	[3, 0, 1]
25	[0, 0, 2]	[0, 0, 2]	[0, 0, 2]	[3, 0, 1]
26	-	[0, 0, 2]	-	[3, 0, 1]
27	[0, 0, 2]	[0, 0, 2]	[0, 0, 2]	[3, 0, 1]
28	[0, 0, 2]	[0, 0, 2]	[0, 0, 2]	[3, 0, 1]
29	[0, 0, 2]	[0, 0, 2]	[0, 0, 2]	[3, 0, 1]
30	[0, 0, 2]	[0, 0, 2]	[0, 0, 2]	[3, 0, 1]
31	[0, 0, 2]	[0, 0, 2]	[0, 0, 2]	[3, 0, 1]
32	[0, 0, 2]	[0, 0, 2]	[0, 0, 2]	[3, 0, 1]
33	[0, 0, 2]	[0, 0, 2]	[0, 0, 2]	[3, 0, 1]
34	[0, 0, 2]	[0, 0, 2]	[0, 0, 2]	[3, 0, 1]
35	[0, 0, 2]	[0, 0, 2]	[0, 0, 2]	[3, 0, 1]
36	[0, 0, 2]	[0, 0, 2]	[0, 0, 2]	[3, 0, 1]
37	[0, 0, 2]	[0, 0, 2]	[0, 0, 2]	[3, 0, 1]
38	-	[0, 0, 2]	-	[3, 0, 1]
39	[0, 0, 2]	[0, 0, 2]	[0, 0, 2]	[3, 0, 1]
40	-	[0, 0, 2]	-	[3, 0, 1]
41	[0, 0, 2]	[0, 0, 2]	[0, 0, 2]	[3, 0, 1]
42	-	[0, 0, 2]	-	[3, 0, 1]
43	[0, 0, 2]	[0, 0, 2]	[0, 0, 2]	[3, 0, 1]
44	[0, 0, 2]	[0, 0, 2]	[0, 0, 2]	[3, 0, 1]
45	-	[0, 0, 2]	-	[3, 0, 1]
46	[0, 0, 2]	[0, 0, 2]	[0, 0, 2]	[4, 2, 0]
47	-	[0, 0, 2]	-	[3, 0, 1]
48	-	[0, 0, 2]	-	[3, 0, 1]
49	[0, 0, 2]	[0, 0, 2]	[0, 0, 2]	[3, 0, 1]
50	[0, 0, 2]	[0, 0, 2]	[0, 0, 2]	[3, 0, 1]

Table 3.4: Each component of the vector $[n_1, n_2, n_3]$ represents the number of built facilities according to type a_1 , a_2 and a_3 , respectively.

In Table 3.4, we can observe how the solutions for the Mixed-Profits problem are consistently the same, namely, constructing expensive facilities. This makes sense given the problem's structure, where the leader has significant freedom in decision-making. Since the goal is to maximize profits, the outcome reflects the choice that yields the greatest benefit for the leader, without taking into account the preferences of the followers. This can be corroborated in Table 3.10, where the values of the objective functionals (Mixed-Profit) are shown, whose results, maximizing Profit, are bigger than in the case of maximizing the Social Welfare (Mixed-SW), see Table 3.11. Conversely, for the Mixed-SW problem, we can see other different solutions, ranging from building three cheap facilities and one expensive one, to building four cheap ones and two medium ones (only in cases 5 and 46). Clearly, in this case, the effect of considering the presence of users becomes apparent when maximizing both profits and the preferences of each follower.

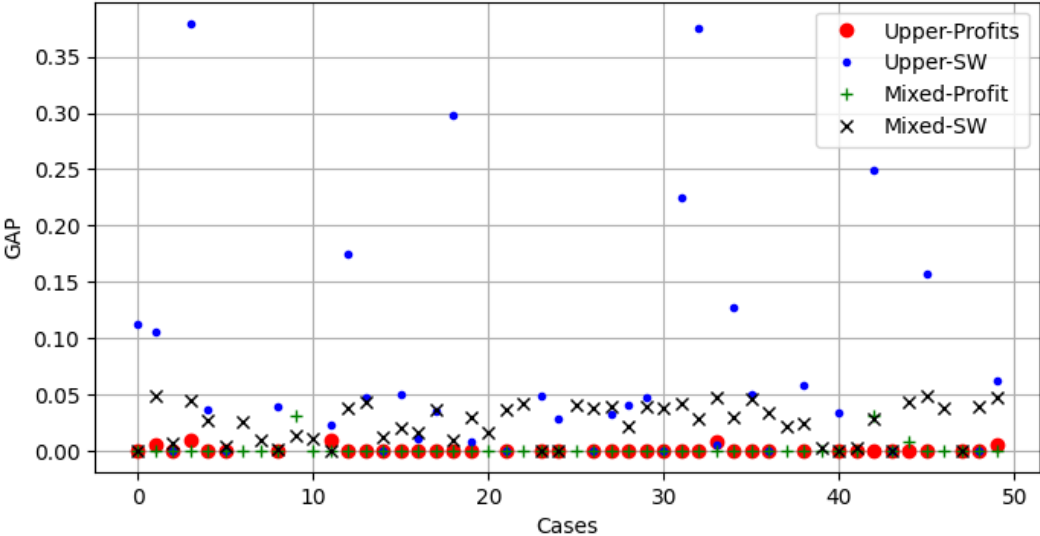


Figure 3.1: Optimal gap for each of the problems in each case.

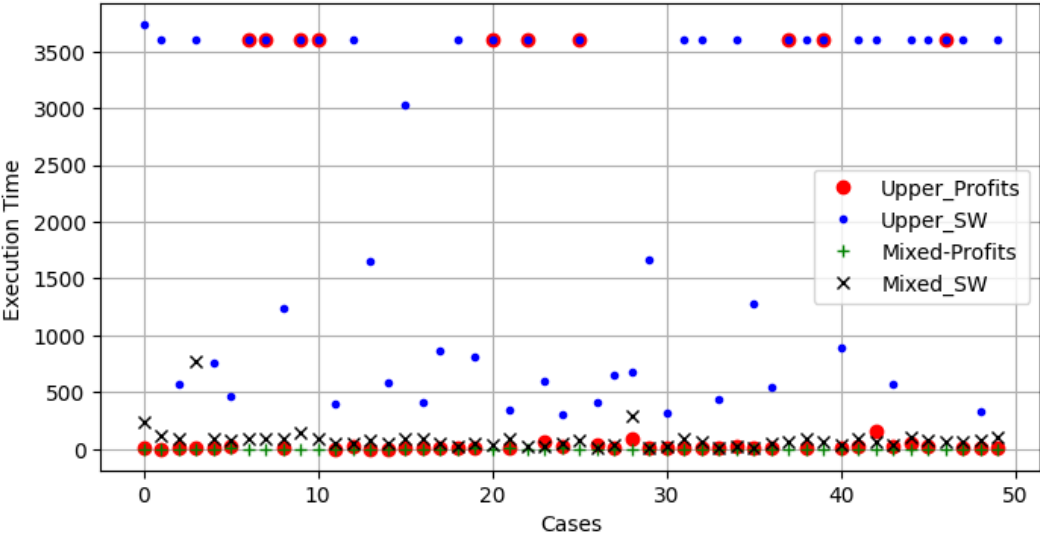


Figure 3.2: Execution time for each of the problems in each case.

In Figure 3.1, the optimality gaps are compared for each of the problems across 50 cases. A significant number of black and green characters corresponding to Mixed-Profits and Mixed-SW problems can be observed, being closer to zero. Also for the Upper-Profit problems but with a smaller number of feasible cases (36 cases, see Table 3.4) This indicates that, under the resolution parameters, optimal solutions were found for problems for the aforementioned problems, unlike for the Upper-SW problems. For the latter, the total number of feasible points found was 36 (with a total of 50 cases considered), accompanied by a high optimality gap. Similarly, in Figure 3.2, the execution times are displayed. Upper-Profits and Upper-SW problems exhibited longer computation times, around 3600 seconds, whereas for problems with mixed constraints, the average execution time was approximately 42.92 seconds. According to the Tables 3.8 and 3.9, the solutions of the Upper-Profit and Upper-SW problems were the same, with the big difference that for the Upper-SW problems, they required considerably more time to find an optimal solution.

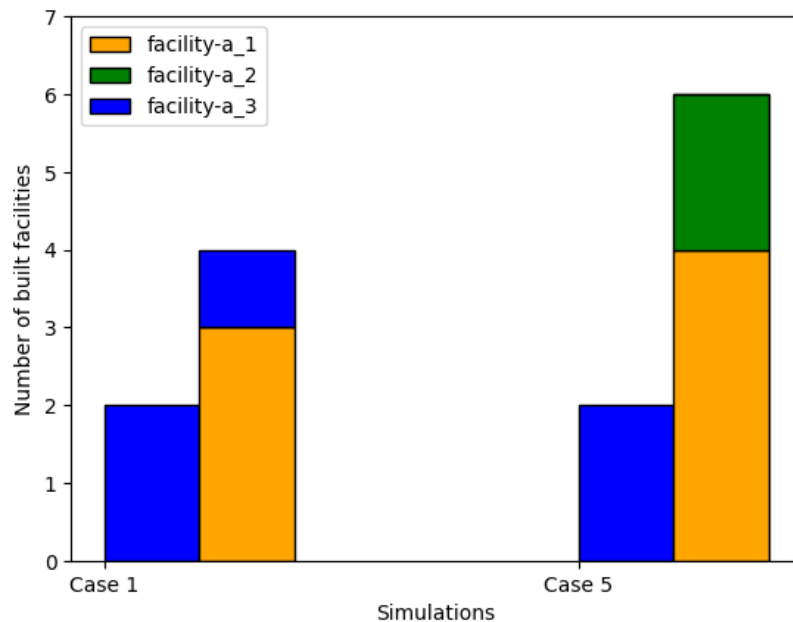


Figure 3.3: Each bar corresponds to the number of built facilities of type a_1 , a_2 or a_3 , for the different problems, these are, from left to right, 1-Upper-Profit, 2-Mixed-Profit, 3-Upper-SW, 4-Mixed-SW.

Figure 3.3 shows two instances out of the 50 simulations, summarizing the different solutions that were found. For the Upper-Profit, Upper-SW and Mixed-Profit problems, they produce the same solution, which is to build two facilities with the highest service cost (facility- a_3). On the other hand, for Mixed-SW, two different solutions were found, each one considering only the construction of two types of facilities, the first one, building three cheap facilities and one expensive, and the second one, building four cheap and two medium. This indicates, for this type of problem, that when considering different sets of parameters, it is essential, as a minimum, to contemplate the construction of a facility of type a_1 , and in most cases, the construction of a facility of type a_3 is also advisable. For more details see Table 3.4.

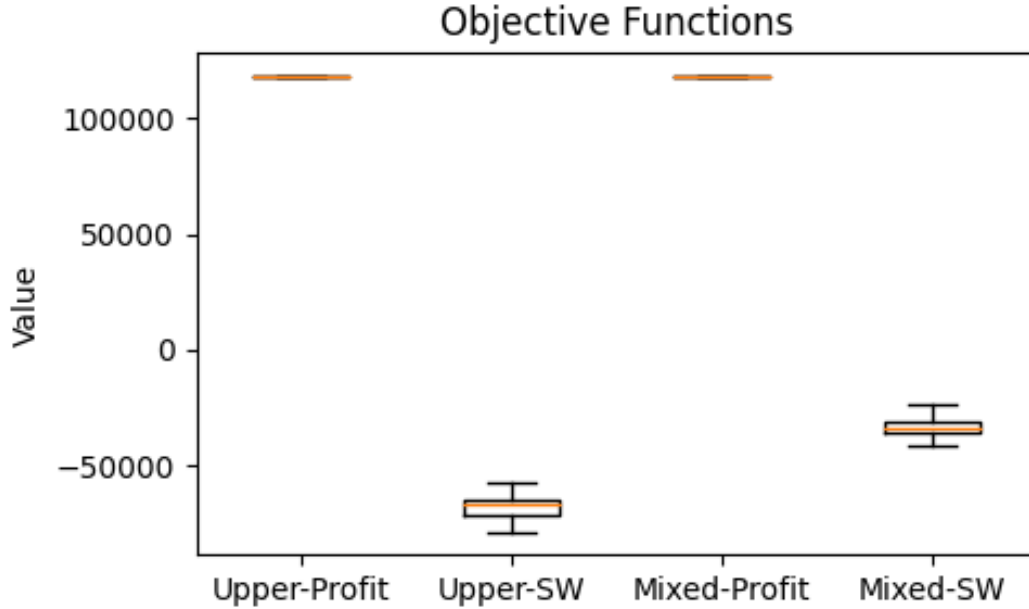


Figure 3.4: Values for the different functional objectives in each case study.

Figure 3.4 illustrates the distribution of objective function values. For the Upper-Profit and Mixed-Profit problems, the mean is the same since in all cases the same value of the objective function was obtained, as can be corroborated in the Table 3.8 and 3.10. On the contrary, a greater variation of the values of the objective function can be observed for the other two problems, where the mean of the found solutions of the Mixed-SW problem is better than that of the Upper-SW problem. As previously pointed out in Section 3.1 (see Example 3.1.2), bilevel problems with upper-level constraints pose a greater challenge for resolution. This is because the cardinality constraints at the upper level are, in fact, coupling constraints. Consequently, this may lead to problem infeasibility, a fact which is supported by simulations. For both Upper-Profits and Upper-SW problems, a feasible point could not be found within the specified computation time limit. Furthermore, for the Upper-SW problems, the discovered solutions exhibit a high gap and execution time, with an optimality gap and average execution time of 0.079 and 2199.38, respectively, (see Tables 3.5 and 3.6). All of the aforementioned stands in contrast to the Mixed problems, as optimal points were successfully identified in each case.

Note that in Upper-Profits and Upper-SW problems, in all cases they share the same solution, which makes sense since they have the same feasibility set (the same constraints) and only differ in the objective function. But there are also cases where it was not possible to find feasible points. This implies that the methodology employed for this type of problem may not be the most suitable in our case. It will be necessary to allocate significantly more time to find the feasible point in each case, as indicated.

Cases	Upper-Profit	Mixed-Profit	Upper-SW	Mixed-SW
1	0.0	0.0	0.112	0.039
2	0.004	0.0	0.104	0.047
3	0.0	0.030	0.0	0.038
4	0.008	0.0	0.379	0.038
5	0.0	0.0	0.036	0.0
6	-	0.0	-	0.008
7	-	0.0	-	0.042
8	-	0.0	-	0.045
9	0.0	0.0	0.038	0.029
10	-	0.0	-	0.0
11	-	0.0	-	0.0
12	0.008	0.0	0.022	0.002
13	0.0	0.0	0.174	0.023
14	0.0	0.0	0.047	0.037
15	0.0	0.0	0.0	0.048
16	0.0	0.0	0.049	0.038
17	0.0	0.0	0.010	0.047
18	0.0	0.0	0.035	0.009
19	0.0	0.0	0.297	0.025
20	0.0	0.0	0.007	0.010
21	-	0.0	-	0.042
22	0.0	0.0	0.0	0.016
23	-	0.0	-	0.020
24	0.0	0.0	0.048	0.013
25	0.0	0.0	0.028	0.026
26	-	0.0	-	0.049
27	0.0	0.0	0.0	0.006
28	0.0	0.0	0.032	0.0
29	0.0	0.0	0.039	0.042
30	0.0	0.0	0.047	0.001
31	0.0	0.0	0.0	0.003
32	0.0	0.0	0.224	0.0
33	0.0	0.0	0.375	0.044
34	0.007	0.0	0.004	0.0
35	0.0	0.0	0.127	0.037
36	0.0	0.0	0.049	0.035
37	0.0	0.0	0.0	0.012
38	-	0.0	-	0.001
39	0.0	0.0	0.058	0.028
40	-	0.0	-	0.041
41	0.0	0.0	0.033	0.028
42	-	0.030	-	0.020
43	0.0	0.0	0.249	0.039
44	0.0	0.0	0.0	0.015
45	-	0.0	-	0.030
46	0.0	0.0	0.156	0.0
47	-	0.0	-	0.040
48	-	0.008	-	0.021
49	0.0	0.0	0.0	0.034
50	0.004	0.0	0.062	0.035

Table 3.5: Optimality gap.

Cases	Upper-Profit	Mixed-Profit	Upper-SW	Mixed-SW
1	6.191	0.657	3740.590	15.263
2	3.208	0.784	3600.284	12.756
3	4.375	0.902	572.418	22.144
4	3.778	0.657	3600.290	15.902
5	7.727	0.687	753.646	17.362
6	3600	0.723	3600	17.299
7	3600	0.636	3600	18.949
8	3600	0.653	3600	14.346
9	12.823	3.879	1245.047	28.618
10	3600	0.725	3600	30.839
11	3600	0.752	3600	41.440
12	2.196	0.697	394.749	69.349
13	20.717	0.640	3600.326	88.868
14	3.522	0.748	1657.493	58.603
15	2.499	0.799	590.171	76.392
16	6.000	0.717	3028.510	75.185
17	15.552	0.622	412.490	98.379
18	3.669	0.710	866.065	94.647
19	5.649	0.795	3600.362	86.560
20	5.308	0.685	809.264	88.309
21	3600	0.749	3600	70.579
22	11.485	4.416	349.334	85.297
23	3600	5.123	3600	84.746
24	57.288	0.704	602.355	140.829
25	17.026	0.733	299.984	90.682
26	3600	0.687	3600	120.622
27	34.423	0.635	406.184	90.247
28	9.319	0.700	657.441	69.998
29	90.003	0.794	681.477	104.179
30	8.289	0.622	1665.688	94.690
31	4.044	0.639	315.150	73.569
32	13.707	3.822	3600.347	232.920
33	7.532	0.657	3600.226	773.350
34	5.791	0.651	437.842	53.886
35	21.394	0.673	3600.447	52.725
36	5.692	0.730	1282.929	47.173
37	13.253	0.708	544.162	45.824
38	3600	0.664	3600	86.840
39	11.93	0.754	3600.290	58.327
40	3600	0.764	3600	92.632
41	9.365	0.741	890.138	67.087
42	27.051	0.949	3600	284.789
43	152.249	0.619	3600.270	30.666
44	25.192	0.667	566.772	39.261
45	52.400	0.728	3600	46.766
46	27.463	0.723	3600.213	55.306
47	3600	0.712	3600	78.790
48	3600	0.691	3600	59.764
49	7.229	0.743	328.830	52.140
50	6.261	0.838	3600.087	87.288

Table 3.6: Execution time.

Cases	Upper-Profit	Mixed-Profit	Upper-SW	Mixed-SW
1	[0, 0, 150]	[0, 0, 150]	[0, 0, 150]	[58, 0, 92]
2	[0, 0, 150]	[0, 0, 150]	[0, 0, 150]	[60, 0, 90]
3	[0, 0, 150]	[0, 0, 150]	[0, 0, 150]	[59, 0, 91]
4	[0, 0, 150]	[0, 0, 150]	[0, 0, 150]	[57, 0, 93]
5	[0, 0, 150]	[0, 0, 150]	[0, 0, 150]	[80, 70, 0]
6	-	[0, 0, 150]	-	[60, 0, 90]
7	-	[0, 0, 150]	-	[60, 0, 90]
8	-	[0, 0, 150]	-	[60, 0, 90]
9	[0, 0, 150]	[0, 0, 150]	[0, 0, 150]	[57, 0, 93]
10	-	[0, 0, 150]	-	[60, 0, 90]
11	-	[0, 0, 150]	-	[60, 0, 90]
12	[0, 0, 150]	[0, 0, 150]	[0, 0, 150]	[60, 0, 90]
13	[0, 0, 150]	[0, 0, 150]	[0, 0, 150]	[60, 0, 90]
14	[0, 0, 150]	[0, 0, 150]	[0, 0, 150]	[60, 0, 90]
15	[0, 0, 150]	[0, 0, 150]	[0, 0, 150]	[60, 0, 90]
16	[0, 0, 150]	[0, 0, 150]	[0, 0, 150]	[60, 0, 90]
17	[0, 0, 150]	[0, 0, 150]	[0, 0, 150]	[60, 0, 90]
18	[0, 0, 150]	[0, 0, 150]	[0, 0, 150]	[60, 0, 90]
19	[0, 0, 150]	[0, 0, 150]	[0, 0, 150]	[58, 0, 92]
20	[0, 0, 150]	[0, 0, 150]	[0, 0, 150]	[60, 0, 90]
21	-	[0, 0, 150]	-	[56, 0, 94]
22	[0, 0, 150]	[0, 0, 150]	[0, 0, 150]	[60, 0, 90]
23	-	[0, 0, 150]	-	[60, 0, 90]
24	[0, 0, 150]	[0, 0, 150]	[0, 0, 150]	[60, 0, 90]
25	[0, 0, 150]	[0, 0, 150]	[0, 0, 150]	[60, 0, 90]
26	-	[0, 0, 150]	-	[60, 0, 90]
27	[0, 0, 150]	[0, 0, 150]	[0, 0, 150]	[60, 0, 90]
28	[0, 0, 150]	[0, 0, 150]	[0, 0, 150]	[60, 0, 90]
29	[0, 0, 150]	[0, 0, 150]	[0, 0, 150]	[60, 0, 90]
30	[0, 0, 150]	[0, 0, 150]	[0, 0, 150]	[60, 0, 90]
31	[0, 0, 150]	[0, 0, 150]	[0, 0, 150]	[60, 0, 90]
32	[0, 0, 150]	[0, 0, 150]	[0, 0, 150]	[60, 0, 90]
33	[0, 0, 150]	[0, 0, 150]	[0, 0, 150]	[59, 0, 91]
34	[0, 0, 150]	[0, 0, 150]	[0, 0, 150]	[60, 0, 90]
35	[0, 0, 150]	[0, 0, 150]	[0, 0, 150]	[60, 0, 90]
36	[0, 0, 150]	[0, 0, 150]	[0, 0, 150]	[60, 0, 90]
37	[0, 0, 150]	[0, 0, 150]	[0, 0, 150]	[60, 0, 90]
38	-	[0, 0, 150]	-	[60, 0, 90]
39	[0, 0, 150]	[0, 0, 150]	[0, 0, 150]	[60, 0, 90]
40	-	[0, 0, 150]	-	[59, 0, 91]
41	[0, 0, 150]	[0, 0, 150]	[0, 0, 150]	[57, 0, 93]
42	-	[0, 0, 150]	-	[60, 0, 90]
43	[0, 0, 153]	[0, 0, 150]	[0, 0, 153]	[58, 0, 92]
44	[0, 0, 150]	[0, 0, 150]	[0, 0, 150]	[60, 0, 90]
45	-	[0, 0, 150]	-	[60, 0, 90]
46	[0, 0, 156]	[0, 0, 150]	[0, 0, 156]	[80, 70, 0]
47	-	[0, 0, 150]	-	[60, 0, 90]
48	-	[0, 0, 150]	-	[60, 0, 90]
49	[0, 0, 150]	[0, 0, 150]	[0, 0, 150]	[59, 0, 91]
50	[0, 0, 150]	[0, 0, 150]	[0, 0, 150]	[55, 0, 95]

Table 3.7: Distribution for cars in facilities.

Cases \ Obj.Function	Profit-Suppliers	Benefit-Follower	Social Welfare
1	118400.0	-192008.923	-73608.923
2	118400.0	-180380.928	-61980.928
3	118400.0	-187135.487	-68735.487
4	118400.0	-184822.077	-66422.077
5	118400.0	-188947.843	-70547.843
6	-	-	-
7	-	-	-
8	-	-	-
9	118400.0	-181038.676	-62638.676
10	-	-	-
11	-	-	-
12	118400.0	-175394.128	-56994.128
13	118400.0	-186857.391	-68457.391
14	118400.0	-183407.952	-65007.952
15	118400.0	-183990.818	-65590.818
16	118400.0	-190945.839	-72545.839
17	118400.0	-182369.999	-63969.999
18	118400.0	-184728.078	-66328.078
19	118400.0	-190713.112	-72313.112
20	118400.0	-189697.1	-71297.1
21	-	-	-
22	118400.0	-187520.686	-69120.686
23	-	-	-
24	118400.0	-186880.104	-68480.104
25	118400.0	-185280.004	-66880.004
26	-	-	-
27	118400.0	-194307.029	-75907.029
28	118400.0	-180294.034	-61894.034
29	118400.0	-181783.172	-63383.172
30	118400.0	-186053.14	-67653.14
31	118400.0	-188242.251	-69842.251
32	118400.0	-193139.608	-74739.608
33	118400.0	-182683.563	-64283.563
34	118400.0	-189754.889	-71354.889
35	118400.0	-183520.064	-65120.064
36	118400.0	-179026.6	-60626.6
37	118400.0	-184985.892	-66585.892
38	-	-	-
39	118400.0	-185249.908	-66849.908
40	-	-	-
41	118400.0	-184816.079	-66416.079
42	-	-	-
43	118400.0	-192116.082	-73716.082
44	118400.0	-189325.82	-70925.82
45	-	-	-
46	118400.0	-197089.986	-78689.986
47	-	-	-
48	-	-	-
49	118400.0	-185171.809	-66771.809
50	118400.0	-182578.032	-64178.032

Table 3.8: Values in [USD] for the configuration Upper-Profit. The Social Welfare is given by the sum of the profit of the leader and the benefit of the followers.

Cases \ Obj.Function	Profit-Suppliers	Benefit-Follower	Social Welfare
1	118400.0	-192008.923	-73608.923
2	118400.0	-180380.928	-61980.928
3	118400.0	-187135.487	-68735.487
4	118400.0	-184822.077	-66422.077
5	118400.0	-188947.843	-70547.843
6	-	-	-
7	-	-	-
8	-	-	-
9	118400.0	-181038.676	-62638.676
10	-	-	-
11	-	-	-
12	118400.0	-175394.128	-56994.128
13	118400.0	-186857.391	-68457.391
14	118400.0	-183407.952	-65007.952
15	118400.0	-183990.818	-65590.818
16	118400.0	-190945.839	-72545.839
17	118400.0	-182369.999	-63969.999
18	118400.0	-184728.078	-66328.078
19	118400.0	-190713.112	-72313.112
20	118400.0	-189697.1	-71297.1
21	-	-	-
22	118400.0	-187520.686	-69120.686
23	-	-	-
24	118400.0	-186880.104	-68480.104
25	118400.0	-185280.004	-66880.004
26	-	-	-
27	118400.0	-194307.029	-75907.029
28	118400.0	-180294.034	-61894.034
29	118400.0	-181783.172	-63383.172
30	118400.0	-186053.14	-67653.14
31	118400.0	-188242.251	-69842.251
32	118400.0	-193139.608	-74739.608
33	118400.004	-182683.567	-64283.563
34	118400.0	-189754.889	-71354.889
35	118400.0	-183520.064	-65120.064
36	118400.0	-179026.6	-60626.6
37	118400.0	-184985.892	-66585.892
38	-	-	-
39	118400.0	-185249.908	-66849.908
40	-	-	-
41	118400.0	-184816.079	-66416.079
42	-	-	-
43	118400.0	-192116.082	-73716.082
44	118400.0	-189325.82	-70925.82
45	-	-	-
46	118400.0	-197089.986	-78689.986
47	-	-	-
48	-	-	-
49	118400.0	-185171.809	-66771.809
50	118400.0	-182578.032	-64178.032

Table 3.9: Values in [USD] for the configuration Upper-SW. The Social Welfare is given by the sum of the profit of the leader and the benefit of the followers.

Cases \ Obj.Function	Profit-Suppliers	Benefit-Follower	Social Welfare
1	118400.0	-197079.792	-78679.792
2	118400.0	-192893.792	-74493.792
3	118400.0	-192503.584	-74103.584
4	118400.0	-195156.416	-76756.416
5	118400.0	-197723.344	-79323.344
6	118400.0	-196573.104	-78173.104
7	118400.0	-196031.472	-77631.472
8	118400.0	-196372.176	-77972.176
9	118400.0	-190960.224	-72560.224
10	118400.0	-193892.608	-75492.608
11	118400.0	-198713.424	-80313.424
12	118400.0	-184258.256	-65858.256
13	118400.0	-198810.976	-80410.976
14	118400.0	-194218.752	-75818.752
15	118400.0	-193770.304	-75370.304
16	118400.0	-200664.464	-82264.464
17	118400.0	-193122.384	-74722.384
18	118400.0	-195364.624	-76964.624
19	118400.0	-199020.64	-80620.64
20	118400.0	-199469.088	-81069.088
21	118400.0	-188747.104	-70347.104
22	118400.0	-198564.912	-80164.912
23	118400.0	-195226.304	-76826.304
24	118400.0	-198062.592	-79662.592
25	118400.0	-197079.792	-78679.792
26	118400.0	-200064.592	-81664.592
27	118400.0	-200191.264	-81791.264
28	118400.0	-195032.656	-76632.656
29	118400.0	-193744.096	-75344.096
30	118400.0	-192467.184	-74067.184
31	118400.0	-198860.48	-80460.48
32	118400.0	-198282.448	-79882.448
33	118400.0	-198372.72	-79972.72
34	118400.0	-198110.64	-79710.64
35	118400.0	-194310.48	-75910.48
36	118400.0	-188171.984	-69771.984
37	118400.0	-196345.968	-77945.968
38	118400.0	-194843.376	-76443.376
39	118400.0	-195379.184	-76979.184
40	118400.0	-196839.552	-78439.552
41	118400.0	-195804.336	-77404.336
42	118400.0	-195559.728	-77159.728
43	118400.0	-197950.48	-79550.48
44	118400.0	-198723.616	-80323.616
45	118400.0	-198599.856	-80199.856
46	118400.0	-200050.032	-81650.032
47	118400.0	-194362.896	-75962.896
48	118400.0	-195682.032	-77282.032
49	118400.0	-197898.064	-79498.064
50	118400.0	-193802.336	-75402.336

Table 3.10: Values in [USD] for the configuration Mixed-Profit. The Social Welfare is given by the sum of the profit of the leader and the benefit of the followers.

Cases \ Obj.Function	Profit-Suppliers	Benefit-Follower	Social Welfare
1	79286.4	-116808.313	-37521.913
2	77248.0	-107396.016	-30148.016
3	78267.2	-115354.264	-37087.064
4	80305.6	-103580.714	-23275.114
5	-14096.0	-18173.792	-32269.792
6	77248.0	-106866.032	-29618.032
7	77248.0	-113747.088	-36499.088
8	77248.0	-109664.464	-32416.464
9	80305.6	-115952.899	-35647.299
10	77248.0	-108731.168	-31483.168
11	77248.0	-116420.304	-39172.304
12	77248.0	-98581.392	-21333.392
13	77248.0	-117139.568	-39891.568
14	77248.0	-113403.472	-36155.472
15	77248.0	-112652.176	-35404.176
16	77248.0	-104057.408	-26809.408
17	77248.0	-109133.024	-31885.024
18	77248.0	-111172.88	-33924.88
19	79286.4	-113031.318	-33744.918
20	77248.0	-110016.816	-32768.816
21	81324.8	-116710.164	-35385.364
22	77248.0	-110964.672	-33716.672
23	77248.0	-108712.24	-31464.24
24	77248.0	-113316.112	-36068.112
25	77248.0	-117452.608	-40204.608
26	77248.0	-121953.104	-44705.104
27	77248.0	-110653.088	-33405.088
28	77248.0	-97678.672	-20430.672
29	77248.0	-111235.488	-33987.488
30	77248.0	-106978.144	-29730.144
31	77248.0	-114049.936	-36801.936
32	77248.0	-107987.152	-30739.152
33	78267.2	-105036.16	-26768.96
34	77248.0	-107115.008	-29867.008
35	77248.0	-112344.96	-35096.96
36	77248.0	-106647.632	-29399.632
37	77248.0	-106662.192	-29414.192
38	77248.0	-109657.184	-32409.184
39	77248.0	-111860.112	-34612.112
40	78267.2	-119751.064	-41483.864
41	80305.6	-118155.885	-37850.285
42	77248.0	-109130.112	-31882.112
43	79286.4	-114573.572	-35287.172
44	77248.0	-112526.96	-35278.96
45	77248.0	-110388.096	-33140.096
46	-14096.0	-20675.2	-34771.2
47	77248.0	-111298.096	-34050.096
48	77248.0	-107939.104	-30691.104
49	78267.2	-108991.821	-30724.621
50	82344.0	-119177.968	-36833.968

Table 3.11: Values in [USD] for the configuration Mixed-SW. The Social Welfare is given by the sum of the profit of the leader and the benefit of the followers.

3.5 Conclusion

In this first part of the thesis, we delved into Single-Leader-Multi-Follower problems involving cardinality constraints. There is limited literature on optimization with cardinality constraints and, to our knowledge nothing on bilevel optimization with this kind of complex constraints; hence, we endeavored to develop both theoretical and practical results. First, we demonstrated the existence of solutions for SLMFG problems with cardinality constraints at the upper level. Additionally, equivalence results for global optimality were proven, coupled with reformulations of the original problem that facilitate numerical resolution. In a second approach, namely SLMFG problems with cardinality constraints at the lower level, we observed a loss of convexity in the followers' constraint set, making it challenging to guarantee solution existence. An alternative approach for a SLMF problem with cardinality constraints was proposed, considering such constraints split at both levels. This approach became tractable, largely due to the reformulation (see Section 3.1.2). In this latter case, solution existence was guaranteed for a specific scenario where follower constraint functions can be expressed as the difference of componentwise convex, weakly analytic, and continuous functions.

Furthermore, the application of this theme found its place in the facility location problem, involving the consideration of potential sites within a region for the construction of electric charging facilities, taking into account car preferences. For these simulations, two types of SLMF problems were considered (Upper - with cardinality constraints at the upper level and Mixed - with mixed cardinality constraints) alongside two different approaches for each problem-maximizing profits and maximizing social benefit, yielding a total of four problems for analysis. The results indicated that the methodology used to numerically solve Upper problems is inadequate, as in many cases, finding a feasible solution proved challenging, and the optimality gap of the solutions found is relatively high, it should be noted. In contrast, Mixed problems exhibited faster convergence and an optimality gap close to zero.

Part II

Economic Efficiency of Concentrated Solar Power plants

Chapter 4

Preliminaries

This chapter presents the fundamental preliminaries for the understanding and development of the second part of this work, which contains scientific contributions to the field of economic viability of CSP plants. In Section 4.1, the issues to be addressed in relation to Concentrated Solar Power plants (CSP plant) are presented. Section 4.2 describes the representation of a CSP plant through a black box model; and its importance in the formulation of optimization problems. Section 4.3 contains a description of the electricity market context considered. Section 4.4 specifies each of the economic indicators that will be used for the comparative study in Chapter 5. Then, Section 4.5 details the production strategies used for the comparative study (see Chapter 5), where different configurations for CSP plants are considered. Finally, the numerical methods used to solve each of the optimization problems addressed in this second part are presented.

4.1 Introduction

The growing awareness of the effects of climate change has encouraged the deployment of renewable energy sources for electricity generation, further supported by the fact that these sources come from free and inexhaustible natural resources. Consequently, the penetration of solar assets, particularly in the realm of concentrated solar power plants (CSP, see Figure 4.1), has rapidly grown and holds great potential for expansion in the coming years [80]. Here we focus on the study of concentrated solar power plants (CSP, see Figure 4.1), which are electrical energy systems that use mirrors to concentrate solar radiation, transform it into heat and feed a power generator to produce electricity [76, 117]. However, in these plants, the integration of energy storage systems presents a significant technical challenge, hindering their deeper penetration into the electricity markets. This challenge primarily lies in the storage systems' ability to handle the variability of solar output, ensuring a constant and reliable energy supply, which is crucial for their acceptance and success in the market [92, 98, 110].

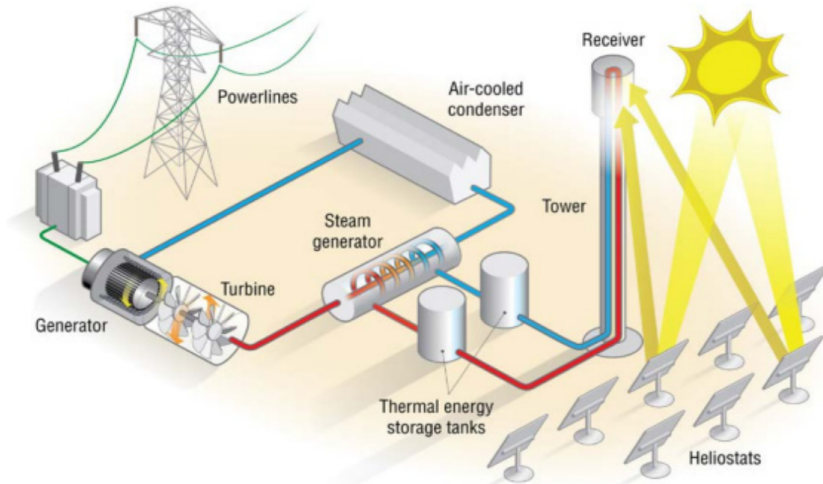


Figure 4.1: Concentrated Solar Power Plant (CSP plant). Image from [118].

Unlike other renewable energy systems, CSP plants allow the incorporation of storage systems for electricity production, which store heat in materials that change temperature (sensitive), phase (latent) or chemical composition (thermochemical) [78, 145]. Hence, several studies have been carried on to improve the implementation of these storage technologies [93, 78, 80]. Incorporating thermal energy storage (TES) into a CSP plant allows to manage the mismatch between energy supply and demand [142]; it allows to shift electricity production to periods of higher prices, providing greater profit opportunities to the system; and finally, the reliability and flexibility of a plant increases by improving the quality of the services provided [80]. One of the most used systems today is the sensible heat storage (SHS) that uses a storage of molten salt in two tanks. Its high implementation is due to the fairly economical and efficient storage medium. On the other hand, a storage system that has not yet been implemented industrially is thermochemical storage, which is based on reversible reaction heat storage. The advantages of this type of system are the ability to store energy for longer periods of time, its high volumetric energy density compared to the other technologies, its weak thermal losses and its operation within wider temperature ranges.

On the one hand, the high investment costs of solar thermal plants with storage capacity discourage private producers to install this type of plants. On the other one, without storage systems, solar plants are not very attractive in many geographical areas, such as in temperate/subtropical areas, since the production period does not coincide with the peak demand period [45, 46, 49, 80]. This has implied that storage systems are systematically included in the running CSP plants. These systems allow plants to continue their production after daylight, extending, in average, the production time in 7 hours, and some of them arriving to a continuous production 24/7 [102]. However, even in these cases, all working CSP plants require financial support/subsidies, either for their construction or for their operation [112, 75].

Despite these economical drawbacks, the interest on CSP and the number of projects that are operative or in construction is growing every day [144, 77, 75]. Furthermore, the NREL [44] contemplates new challenges for CSP production under atypical scenarios, in order to

maximize the participation of renewable energy sources in their (Californian) power generation mix. Other countries, including Chile and France, are also following this tendency of investigating the pathways for increasing the penetration of renewable energies [35, 108], in particular CSP involving a thermal storage system [81, 105, 91]. Under this context, the relevance to systematically study the different options of storage systems for CSP plants is clear. One of the objectives of this study is to investigate various aspects of the economic efficiency of such installations, focusing on two main axes: the optimal design of CSP projects and the optimal operation of existing plants.

4.2 Black-box model

The general model of a Concentrated Solar Power plant considers four main subsystems: a heliostat field (mirrors) that redirect the solar radiation to a focal point, a heat absorber, a power cycle, and a thermal energy storage system [138]. The heat absorber is commonly placed on the top of a central tower, at the focal point of the heliostat field. The heliostats reflect the solar radiation which intensity is given by the Direct Normal Irradiance (DNI), reaching extremely high temperatures (550-800 °C) [102], depending on the physical limitations of the heat transfer fluid. Through a primary circuit, the heat transfer fluid conveys the thermal energy captured either to the storage system, to the Rankine cycle or both.

The main principle we want to exploit is that CSP plants can be modeled as black-box components connected by the heat-transfer fluid loop, and possibly other thermally driven unit operations. The black-box model we propose to develop follows the approach presented in Figure 4.2. Here, we identify some nodes of the heat-transfer fluid, denoted by n_α (where α is the index of the node), as points to measure state variables of the heat transfer fluid. These state variables are the mass flow rate $\dot{m}_\alpha(t)$, measured in $[kg/s]$, which provides the variation of mass per unit of time, and the temperature T_α , measured in $[^\circ C]$.

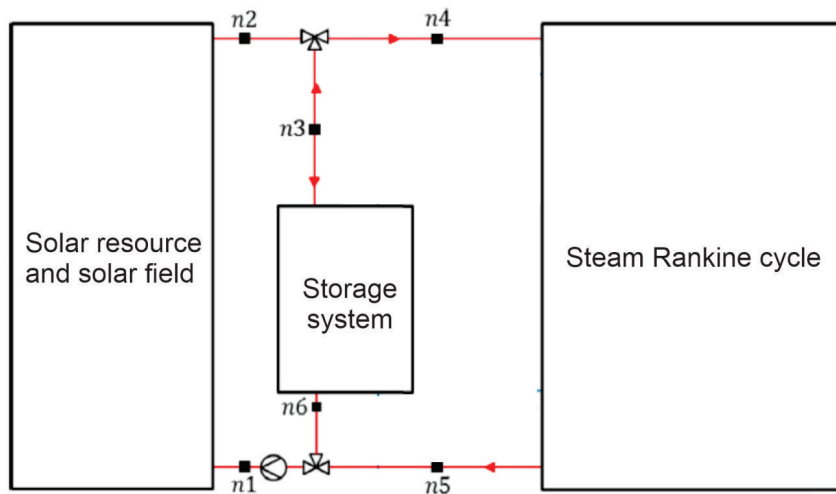


Figure 4.2: Scheme of the black-box model for a Concentrated Solar Power plant. The red circuit represents the main heat-transfer loop.

Four main designs typologies are available for CSP plants: parabolic through collector (PTC), solar tower also called central receiver systems (CRS), linear Fresnel reflectors (LFR), and parabolic dish collectors (PDC). The two first technologies have seen commercial large-scale deployment and exhibit a higher level of technological and commercial maturity, and account for the largest percentage of currently installed capacity worldwide [74, 25]. The Solar Towers, consist of an heliostat field that reflect the DNI to a focal point located at the top of the tower, where is placed a heat absorber [117]. Similarly, Parabolic troughs consist in a linear parabolic reflector which concentrates the DNI along its focal line, where a pipe acts as heat absorber [117].

Regardless the storage system, the heat exchange between the heat transfer fluid and the storage is given by the general equation

$$q_s = c \cdot \dot{m} \cdot \Delta T, \quad (4.2.1)$$

where q_s is the heat consumed by the storage system, c is the thermal capacity of the heat-transfer fluid, \dot{m} stands for the mass flow rate passing through the exchanger, and ΔT denotes the variation of temperature between the initial point and the final point of the heat exchanger. Finally, the Rankine cycle uses the heat to start a steam-based circuit that activates a sequence of turbines, producing electricity. Rankine cycles are well-known, both in the literature as in existing energy plants [109, 134].

For the Optimal Design problem, with the black-box models established for each component of the CSP plant, their interaction are modeled via a quasi-static model. The operation of the plant is divided in four phases, which are the Inactive phase, the Storage phase, the Storage-Production phase and the Discharge phase, and it is assumed that the transition in between them is instantaneous (the transient phases are not considered except for the start-up of the Power Block).

4.2.1 The Solar Resource and the Solar Field

The solar field is composed of a set of heliostats, whose function is to project the sun's rays to a specific point or sector called a receiver at the top of a tower, heating it up to approximately 565 °C [64].

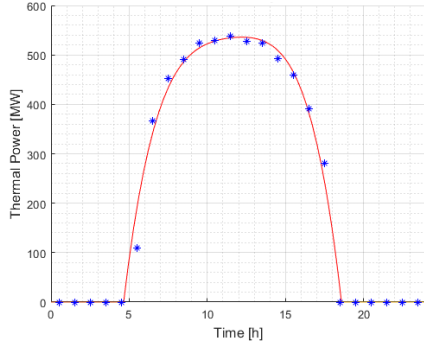


Figure 4.3: Data and Interpolation model - Summer day. California, $SM = 2.5$.

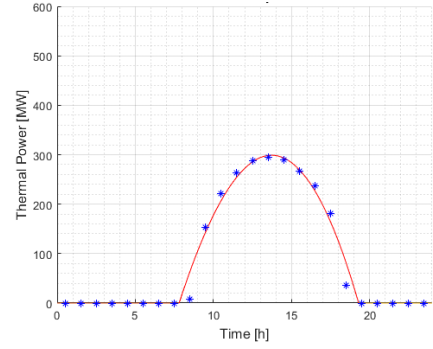


Figure 4.4: Data and Interpolation model - Summer day. Sevilla, $SM = 2.5$.

The intensity of the sun's rays depends on the place where the plant is installed. One way to represent solar irradiance is by means of the Direct Normal Irradiance (DNI), that is the amount of solar radiation that arrives in a direct line from the sun and strikes a surface perpendicularly. It does not include solar radiation that has been scattered or reflected by the atmosphere or surroundings. This measure is crucial for any solar technology that relies on the direct capture of sunlight, such as systems using mirrors or lenses to concentrate sunlight onto a small receiver [18]. For example, Figure 4.3 shows the irradiation of an average day in the summer season in California/USA. This curve is expressed by the Direct Normal Irradiance function, $DNI(\cdot)$, which depends on the time and the mirror field. Thanks to this curve, we model the useful thermal power function $q_{sol}(\cdot)$, whose expression represents the recovered thermal power from the solar field and considers the thermal losses at receiver. This is,

$$q_u(t) = K_{Hel} \cdot DNI(t), \quad \forall t \in [0, H], \quad (4.2.2)$$

where K_{Hel} is an efficiency constant depending on the thermal efficiency of the receiver, the optical efficiency of the mirrors field, and total surface of the heliostats (see [125]). Here, $[0, H]$ is a time interval (measured in hours).

In practice, the optical efficiency of the mirrors field is hard to model, thus the software *SAM* [103] is used to evaluate $q_{sol}(t)$ in terms of $DNI(t)$ and the Solar Multiple (SM) (which represents the ratio of the solar field size relative to the minimum size needed to generate the rated power of the turbine during peak solar radiation [100]). Actually, to obtain the new function $q_u(\cdot)$ the hourly average values of useful thermal power are simulated using *SAM* software and an polynomial approximation is done with the `polyfit` function in *MATLAB*. Then, the function of useful thermal power is

$$\forall t \in [0, 24], \quad q_{sol}(t) \begin{cases} p(t) & \text{if } t \in [t_{ini}^{sol}, t_{fin}^{sol}], \\ 0 & \text{otherwise.} \end{cases} \quad (4.2.3)$$

with the interpolation polynomial function $p(\cdot)$ and the times of sunlight, $t_{ini}^{sol}, t_{fin}^{sol}$.

4.2.2 The Steam Rankine Cycle or Power Block

The power block model has been reduced to a set of polynomial functions of degree 2 via quadratic regressions [124, 125]. These regressions were chosen to simplify the plant modeling

of the different connections and functionalities [103]. For the Rankine modeling, we mainly use three regressions, given by:

$$\begin{aligned}
\dot{W}_{elec}(t) &= f_a(\dot{m}_4(t), T_4(t), T_{out}(t)), \\
&= \mathbf{a}_1 + \mathbf{a}_2 T_4(t) + \mathbf{a}_3 T_4^2(t) + \mathbf{a}_4 T_{out}(t) + \mathbf{a}_5 T_{out}^2(t) + \mathbf{a}_6 \dot{m}_4(t) + \mathbf{a}_7 \dot{m}_4^2(t) \\
&\quad + \mathbf{a}_8 T_4(t) T_{out}(t) + \mathbf{a}_9 T_4 \dot{m}_4(t) + \mathbf{a}_{10} \dot{m}_4(t) T_{out}(t),
\end{aligned} \tag{4.2.4}$$

$$\begin{aligned}
\dot{W}_{elec}(t) &= f_b(q_R(t), T_4(t), T_{out}(t)), \\
&= \mathbf{b}_1 + \mathbf{b}_2 T_4(t) + \mathbf{b}_3 T_4^2(t) + \mathbf{b}_4 T_{out}(t) + \mathbf{b}_5 T_{out}^2(t) + \mathbf{b}_6 q_R(t) + \mathbf{b}_7 q_R^2(t) \\
&\quad + \mathbf{b}_8 T_4(t) T_{out}(t) + \mathbf{b}_9 T_4(t) q_R(t) + \mathbf{b}_{10} q_R(t) T_{out}(t).
\end{aligned} \tag{4.2.5}$$

$$\begin{aligned}
T_5(t) &= f_c(\dot{m}_4(t), T_4(t), T_{out}(t)), \\
&= \mathbf{c}_1 + \mathbf{c}_2 T_4(t) + \mathbf{c}_3 T_4^2(t) + \mathbf{c}_4 T_{out}(t) + \mathbf{c}_5 T_{out}^2(t) + \mathbf{c}_6 \dot{m}_4(t) + \mathbf{c}_7 \dot{m}_4^2(t) \\
&\quad + \mathbf{c}_8 T_4(t) T_{out}(t) + \mathbf{c}_9 T_4(t) \dot{m}_4(t) + \mathbf{c}_{10} \dot{m}_4(t) T_{out}(t).
\end{aligned} \tag{4.2.6}$$

$$\begin{aligned}
T_{12}(t) &= f_d(\dot{m}_4(t), T_4(t), T_{out}(t)), \\
&= \mathbf{d}_1 + \mathbf{d}_2 T_4(t) + \mathbf{d}_3 T_4^2(t) + \mathbf{d}_4 T_{out}(t) + \mathbf{d}_5 T_{out}^2(t) + \mathbf{d}_6 \dot{m}_4(t) + \mathbf{d}_7 \dot{m}_4^2(t).
\end{aligned} \tag{4.2.7}$$

$$\begin{aligned}
\dot{m}_{11}(t) &= f_e(\dot{m}_4(t), T_{out}(t)), \\
&= \mathbf{e}_1 + \mathbf{e}_2 T_{out}(t) + \mathbf{e}_3 T_{out}^2(t) + \mathbf{e}_4 \dot{m}_4(t) + \mathbf{e}_5 \dot{m}_4^2(t) + \mathbf{e}_6 \dot{m}_4 T_{out}(t).
\end{aligned} \tag{4.2.8}$$

$$\begin{aligned}
\dot{m}_4(t) &= f_h(\dot{W}_{elec}(t), T_4(t), T_{out}(t)), \\
&= \mathbf{h}_1 + \mathbf{h}_2 T_4(t) + \mathbf{h}_3 T_4^2(t) + \mathbf{h}_4 T_{out}(t) + \mathbf{h}_5 T_{out}^2(t) + \mathbf{h}_6 \dot{W}_{elec}(t) + \mathbf{h}_7 \dot{W}_{elec}^2(t) \\
&\quad + \mathbf{h}_8 T_4(t) T_{out}(t) + \mathbf{h}_9 T_4(t) \dot{W}_{elec}(t) + \mathbf{h}_{10} \dot{W}_{elec}(t) T_{out}(t).
\end{aligned} \tag{4.2.9}$$

Here, \dot{m}_α and T_α represent the mass flow and temperature at the node α (see Figure 4.2), and \dot{W}_{elec} , representing the electric power. Coefficients a, b, c, d, e and h were estimated with *SAM* software (see Table 4.1), for more detail [103]. Some of these regressions are “redundant”. For example, \dot{W}_{elec} can be expressed in terms of T_4 and T_{out} (outlet temperature in the Rankine steam loop, [124]) but also \dot{m}_4 can be expressed in terms of \dot{W}_{elec} , T_4 and T_{out} . This was done in order to avoid working with inverse functions or unnecessarily complex systems of equations. That is, f_h is an approximation of the inverse function of f_a with respect to the first entry. For the quadratic regressions used in the two-tank model, we will consider the temperature T_{out} as the ambient temperature T_{env} , which is fixed depending on the operating time interval of the plant and also takes different values depending on the day or night.

Coefficient index	a	b	c	d	e	h
1	-2.99	-5.53	-1.58e2	1.94e1	-5.75	9.92e1
2	-3.70e-3	1.44e-2	8.08e-1	1.10e-2	2.70e-1	-3.80e-1
3	1.17e-6	-2.01e-5	3.73e-5	2.25e-6	-2.80e-3	5.27e-4
4	6.75e-2	1.58e-2	3.47e-1	1.04	2.82	7.64e-1
5	6.18e-5	2.82e-5	9.48e-4	-1.23e-4	-5.69e-6	4.87e-3
6	4.88e-2	2.34e-1	-8.30e-2	-2.06e-2	-3.03e-3	1.31e1
7	8.76e-3	3.18e-4	2.67e-4	1.82e-5		-3.83e-3
8	-2.13e-4	-8.91e-5	1.32e-4			-1.72e-3
9	2.05e-4	2.29e-4	-8.14e-5			-1.37e-2
10	-5.24e-4	-9.73e-4	-4.69e-4			3.43e-2

Table 4.1: Coefficients of the quadratic regressions.

4.2.3 Storage System

In this work, two storage systems are considered. They are designed for the storage of sensible heat and chemical reaction enthalpy. The operation and composition of these systems will be briefly described below.

Storage - Two-tank indirect

Sensible heat storage is a technology currently implemented in most CSP power plants around the world. They can store thermal energy for up to 15 hours using a heat transfer medium such as molten salt [92]. Molten salts have a high storage efficiency that allows sensible heat storage to produce electricity during the peak power demand after sunset [123]. In recent years, studies have been carried out to improve these types of systems [143, 132].

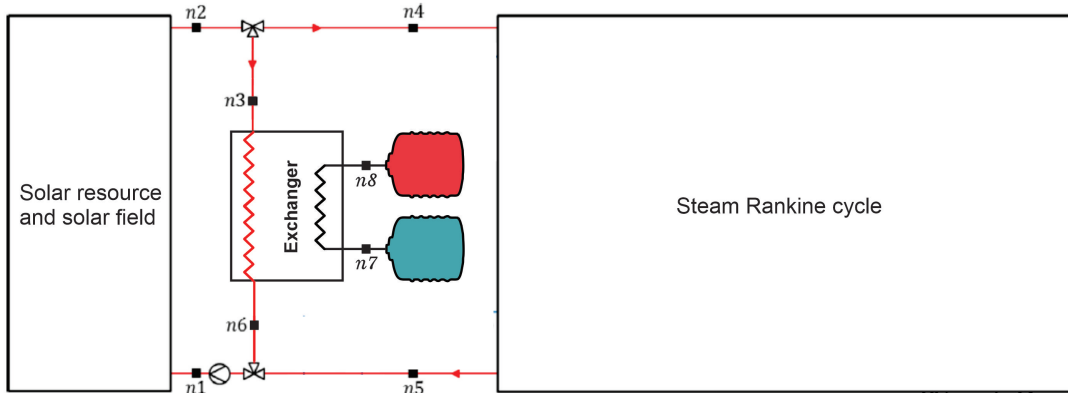


Figure 4.5: Schema in production phase.

We consider here an indirect sensible heat storage system, composed of two heat transfer loops, a heat exchanger and two tanks for the storage material (low temperature and high temperature). The plants use molten salt as storage material [66]. The integration of such Two-tank molten salt storage is illustrated in Fig. 4.5 (see also [2]).

During daytime operation of the plant, the solar field concentrates the solar irradiation on the receiver. Then, the heat transfer fluid (HTF) passes through it and conducts the collected heat to the heat exchanger (nodes 3 and 6, in Figure 4.5). The heat is thus transferred from HTF to the molten salt (Storage phase), which flows from the cold tank, with temperatures not lower than 290°C, to the hot tank, with temperatures not bigger than 560°C, where the heat will be stored. During the Storage-Production phase, one part of the HTF passes directly from solar field to the power block. For the Discharge phase, the molten salt flows from the hot tank to the cold tank and, by means of the heat exchanger, the stored heat is transferred to the HTF and finally is directed to the power block.

Storage - Thermochemical Reactor

Another type of heat energy storage is Thermochemical storage. It is not yet implemented in commercial CSP but its advantages in terms of heat storage and high temperature management are promising. In [125], an economic evaluation was performed for CSP plant projects using an innovative Thermochemical system, and this work includes this storage system in the comparative study.

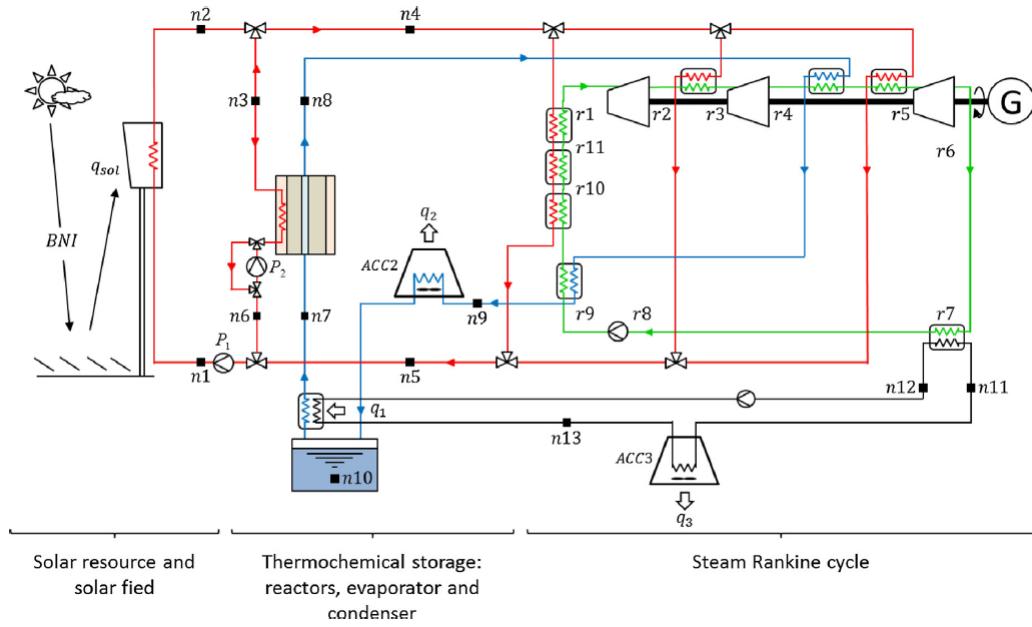
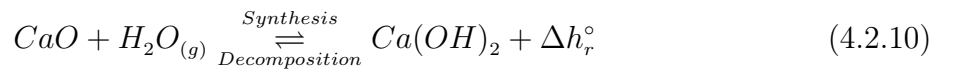
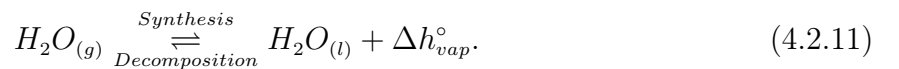


Figure 4.6: Concentrated Solar Power Plan with thermochemical storage.

The Thermochemical storage is based on a process that involves a fixed-bed Thermochemical reactor implementing the calcium oxide/calcium hydroxide ($CaO/Ca(OH)_2$) and water (H_2O) reactive pair. This storage is based on the association of two monovariant reversible transformations: a chemical reaction



and a liquid/gas phase change



where Δh_r° and Δh_{vap}° are respectively the standard molar enthalpy of reaction and vaporization. These transformations are defined by the thermodynamic operating conditions T_c (constraint temperature) and P_c (constraint pressure). The main advantages of $CaO/Ca(OH)_2$ Thermochemical storage are the intrinsic high energy density of this low cost and environmentally friendly reactive pair, and a non time-dependent energy storage capacity (as long as reactants are stored separately). Moreover, the power and temperature of the Storage/Discharge phases can be controlled not only by the mass flow rate and temperature of the heat transfer fluid, but also by the operating pressure of the reactor. In addition, these storage properties (power, energy density, ...) also depend on the physical characteristics of the reactor (dimension) and the way that the porous reactive solid is implemented in the reactor (apparent density, DEC, part of binder added to enhance heat transfer, ρ_{eng}). For more details, we refer to [125, 128, 140].

The integration of the Thermochemical storage system during these three different phases will be illustrated in figures 5.6, 5.7 and 5.8 in Chapter 5.

4.3 Spot Market

When setting a specific location for the planning of a CSP plant project, there are several considerations to take into account in addition to geographic characteristics, since each country presents various particularities in its electricity market, as well as high differences in its incentive schemes for promoting the deployment of renewable energy sources [53]. Aiming to consider such effects, the analysis for the CSP plant should consider that the location (and therefore its solar resource availability), as well as the features of the electricity market are fixed in advance.

There is a part of the electric energy that is exchanged through a so-called SPOT Market. These markets are also called "pay-as-clear", since this electricity would be paid according to the market price, instead of what is declared and/or ordered. Usually, the problem related to this market clearing is solved for each hour of the next day, and so, the market price is in fact a piecewise constant function $\lambda : [0, 24] \rightarrow \mathbb{R}_+$ such that

$$t \mapsto \lambda(t) = \sum_{k=1}^{24} \lambda_k 1_{[k-1, k]}(t) \quad (4.3.1)$$

where λ_k is a constant market price and $1_{[a, b]}(\cdot)$ is the indicator function of $[a, b]$, given by $1_{[a, b]}(t) = 1$ if $t \in [a, b]$ and 0 otherwise.

In this work, it is assumed that the production of the CSP plant is not sufficient to influence the market price. Moreover, it is assumed that the production offer is always fully accepted/bought. Therefore, an exogenous price function $\lambda(\cdot)$ is used, according to which the production is paid. This price function $\lambda(\cdot)$ is estimated by taking the average values of market prices from the historical data.

4.4 Economic Criteria

Once the context of Solar resource and market are chosen, the design and operation of the CSP plant must respond to an economic criterion. There are several criteria that can be chosen, where the most relevant for renewable energy projects have been summarized in [5]. In the same article, the authors show that these criteria are not equivalent in general, in the sense that optimizing with respect to one of them may lead to a quite different solution than optimizing with respect to another one. Therefore, the proposed model should be designed to switch between these criteria, depending on which is the best adapted one for the plant's market conditions. For example, if the CSP plant is designed under some public contract with a feed-in tariff (a fixed preferential price [33]), then the CSP plant should be designed to produce as much energy as possible minimizing the cost of production. This is a common scenario in several countries, where the economic criterion that must be chosen is the *Levelized Cost of Energy*.

In contrast, as described in [124, 125], a CSP plant can be conceived to participate in the SPOT market, as observed in many countries. Such is the case of the United States, France, Chile, and most countries in Europe and South America, where the market is managed by a regulator, usually called Independent System Operator (ISO), which fixes the market prices from the declarations/bids of the agents. The reader is referred to [1] for more information regarding the issue concerning the European market.

4.4.1 Levelized Cost of Energy (LCOE)

One of the most commonly used economic criteria in CSP plant projects is the *Levelized Cost of Energy (LCOE)*, which represents the annualized cost of a unit of energy (kWh) produced by the system (see, e.g., [5]). More precisely, it relates the total amount of costs involved in the project and the total amount of energy produced, over the lifetime of the project. It is expressed as follows:

$$LCOE = \frac{C_{invest} + \sum_{k=1}^N \frac{Cost_k}{(1+\iota_r)^k}}{\sum_{k=1}^N \frac{W_k}{(1+\iota_r)^k}} \quad (4.4.1)$$

where N represents the duration of the project (years), ι_r the nominal discount rate, $Cost_k$ is the annual cost of year k , C_{invest} the initial investment of the project, and W_k is the annual electrical energy produced.

4.4.2 Net Present Value (NPV)

In [125, 124], the Net Present Value (NPV) was used as indicator to evaluate a CSP plant project. This metric considers the revenues of the power plant during its lifetime, according to the variable prices of the SPOT market, as well as the investment, operation and maintenance

costs. More precisely,

$$NPV(N, \iota_r, \dots) = -C_{invest} + \sum_{k=1}^N \frac{(Rev_k - Cost_k)}{(1 + \iota_r)^k} \quad (4.4.2)$$

where N is the number of years of lifetime of the plant, Rev_k is the revenues of year k (implicit in this expression is the effect of market price variation for each year), and $Cost_k$ is the costs (operational and maintenance costs) of year k . As before, C_{invest} is the investment cost and ι_r is the real discount rate.

4.4.3 Internal Rate of Return (IRR)

The Internal Rate of Return (IRR) of a project is the real discount rate ι_r^* at which the Net Present Value of the project is zero. That is,

$$\iota_r^* : NPV(\cdot, \iota_r^*, \dots) = 0,$$

where $NPV(\cdot, \iota_r, \dots)$ is the expression of Eq.4.4.2 varying with respect to ι_r . This rate is used for depreciation of future flows and to determine their current values [5].

4.4.4 Conventional PayBack (CPB)

The conventional payback (CPB) evaluates the payback time based on the nominal discount rate ι . It does not take into account the inflation. The conventional payback is defined by:

$$CPB = \inf\{k \leq N | NPV(k, \cdot, \dots) \geq 0\},$$

where $NPV(k, \cdot, \dots)$ is the Net Present Value corresponding to the case of the project stopped after k years,

4.5 Production Strategies

In [124], it was corroborated how the use of a production strategy for a CSP plant, different from the classic one (using the energy stored after sunlight), can generate a higher profitability. This study was carried out considering the participation of the plant in a SPOT market. In this work three kind of production strategies will be considered: one of Classic strategies and two of Price Chasing. These are the following:

Classic production strategy: this is the typical strategy used in many plants around the world. It consists of, for each day, doing a Storage phase (according to the storage capacity and availability of heat energy) and immediately after discharging all the stored energy until the system is empty.

Price Chasing operation strategy : whenever storage is implemented in a CSP, the classic production strategy is perfectly adapted to a situation where the produced energy is sold at a fixed price. But it leads to a low economical efficiency of the CSP, actually to the need of subsidies (see e.g. [80]). When the energy price varies, like in deregulated market context, an alternative approach is to prefer a production targeted to periods during which the produced energy can be sold at advantageous prices, namely the peaks of spot/deregulated electricity markets. Note also that weekly storage strategy can also take advantage of low demand days, Sunday typically, to increase the discharge capacity during the week. Following [124], this production strategy will be called «Price Chasing strategy». In order to explore more deeply the Price Chasing strategy, we will here consider two different forms of it, one with one discharge per day and one with two discharges per day.

4.6 Optimization Algorithms

4.6.1 Interior point - Matlab

In the context of optimizing objective functions subject to nonlinear constraints, MATLAB[®] provides a tool known as *fmincon* [129]. This command relies on optimization methods that leverage information about the gradient of the objective function and constraints, resulting in an efficient search for the critical points of the problem.

In particular, *fmincon* serves to solve multivariable and nonlinear programming problems, with a distinctive feature, which is its ability to choose different optimization algorithms. These algorithms have different characteristics and are suitable for different types of problems, with one of the available algorithms being the Interior Point approach.

The Interior Point algorithm is exceptionally capable of addressing smooth nonlinear constraints in optimization problems, standing out for its robustness and efficiency. This method has proven to be very effective in a wide variety of situations, especially due to its sophisticated approach that handles constraints by introducing barriers that are iteratively modified. This allows for an efficient exploration of the solution space, ensuring stable and reliable convergence towards the optimum, even in large-scale problems. Its general applicability and the ability to handle inherent complexities in diverse applications establish it as a top-tier optimization method, widely endorsed in literature and engineering practices.[139, 26].

4.6.2 Bocop

The Bocop project [19] serves as an open-source toolbox designed to address optimal control problems through collaborative efforts with both industrial and academic partners. Optimal control, a discipline focusing on optimizing dynamic systems governed by differential equations, finds applications in diverse fields, including transportation, energy, process optimization, and biology. The original Bocop package employs a local optimization method, approximating the optimal control problem by transforming it into a finite-dimensional optimization problem (NLP) using time discretization, specifically utilizing the direct transcription approach. The ensuing NLP problem is then addressed using the well-established

software IPOPT, with sparse exact derivatives computed by ADOL-C [136].

The so-called direct approach involves converting the infinite-dimensional optimal control problem (OCP) into a NLP through time discretization applied to the state and control variables, as well as the dynamics equation. While these methods may exhibit lower precision compared to indirect methods based on Pontryagin's Maximum Principle, they offer greater robustness during initialization (in the sense of providing good convergence and stability in the solution of the problem). Moreover, their application is more straightforward, contributing to their widespread adoption in industrial settings.

Chapter 5

Multidimensional analysis for the techno-economic study of the CSP plant with different storage systems

In this chapter, the comparative study of the profitability and feasibility of a CSP plant, different storage systems, economic criteria and operation strategies will be considered (see subsections 4.2, 4.4 and 4.5. In Subsection 5.1, the transition from these control problems to classical optimisation formulations will be briefly explained. In 5.2, the optimization problems to be solved are detailed, giving a description of the dynamics of each of the storage systems under consideration, the composition of the objective function and the functionality for each of the variables that make up the problem. Finally, results and discussions will be presented in Subsection 5.3, and finally conclusions are given in Subsection 5.4.

5.1 Control problem

The aim of this study can be formally written as follows: given a location, a price curve, a solar field and a power block, the aim is to design the Storage System (Two-tanks and Thermochemical) and its operational use in order to maximize (minimize) the economic indicator over the lifetime (N years) of the project. Due to the fact that some of the variables correspond to the operational use of the storage (and are therefore functions), this maximization (minimization) problem is actually an optimal control problem.

The variables of the control problem should be thus optimized in a time interval $[0, H]$, with H being the number of hours of the plant project duration and defined as follows:

- ν - represents the vector of the physical variables that describe the Storage System dimensions;
- μ - represents the vector of operational variables composed of real-valued functions describing the operation of the Storage System;

- τ - represents the state of operation of the plant,

$$\tau : [0, H] \rightarrow \{I, S, \{S, P\}, D\}$$

describing the order and number of phases (Inactive/Storage/Storage-Production/Discharge) for each $t \in [0, H]$.

Depending on the Storage System, the physical and operation vectors will differ. For example, in the case of a Thermochemical storage system, the components of the vector of physical variables will correspond to the dimensions and amounts of chemical compounds for a Thermochemical reactor and the components of the vector of operations will correspond to the operating pressure and temperatures. For the case of a storage with two molten salt tanks, the components of the vector of physical variables will correspond to the volume of the tank and dimensions of heat exchanger while the components of the vector of operation variables will correspond to the mass flows of the heat transfer fluid and molten salt, which are controlled by pumps. On the other hand, the strategic variables will define the operation phase of the plant, determining the instants of time that the Storage System will be in some operation phase (Inactive, Storage and Discharge), that is, determining the order and number for each of the operation phases.

The set of possible physical variables will be denoted by V and the sets of feasible (functions-valued) operational and strategy variables will be respectively denoted by $\mathcal{U}(\nu)$ and $\mathcal{F}(\nu, \mu)$. Thus the optimal control problem can be formulated in the following abstract form:

$$\begin{aligned} & \max/\min_{\nu, \mu, \tau} \quad \text{Indicator}(\nu, \mu, \tau) \\ & \text{subject to} \quad \begin{cases} \nu \in V, \\ \mu \in \mathcal{U}(\nu), \\ \tau \in \mathcal{F}(\nu, \mu). \end{cases} \end{aligned} \quad (5.1.1)$$

5.1.1 From Control problem to the Optimization Problem

The idea of *Pre-scenarios*, which has been introduced in [124], consists of restricting the "profile" of the strategy functional variables (defining order and number of phases) in such a way that these restricted profiles can be described by vectors of real numbers.

In a pre-scenario, the functions fixing a certain operation (Storage/Production/Discharge) are defined on time intervals, $I_S = [t_{ini}^S, t_{fin}^S]$, $I_P = [t_{ini}^P, t_{fin}^P]$ and $I_D = [t_{ini}^D, t_{fin}^D]$. Thus, along with some simplifying assumptions, such as that the Storage and Discharge phases occur at a constant power rate, the reformulated optimisation problem consists, for what concerns the operational variables, on deciding the size of the intervals of each of the phases, and the constant values of the operational values within these intervals. This concept will be described in more detail below.

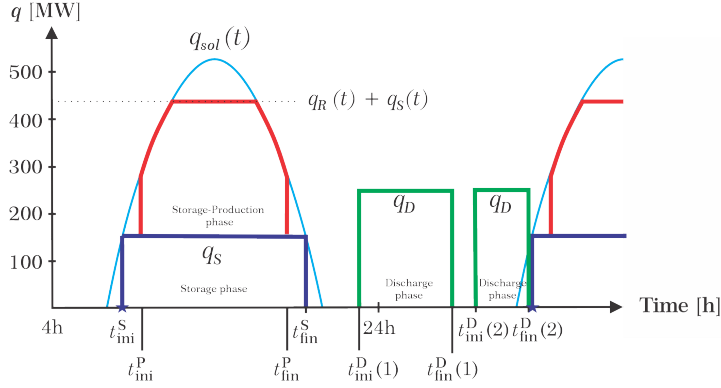


Figure 5.1: Example of a Pre-scenario for one day, one Storage phase, one Storage-Production phase and two Discharges phases.

The control problem described in (5.1.1) is hard to solve. Thus, in order to simplify this control problem and solve it in a differentiable optimization environment, a differentiable optimization problem will be proposed. This technique was introduced in [124] and here we summarize it for completeness.

First, assuming that the N years of the project are equal, a single model year is divided in p periods. Each periods Per_i , with $i \in \{1, \dots, p\}$, it is modeled as R_i repetitions of a cyclic stage S_i , with its own operational and strategy variables (μ_i, τ_i) . Also, the stage S_i has a fixed number of days $N_{Days}(i)$ and therefore a fixed number of hours H_i . Let $H(Per_i)$ the number of hours of the period Per_i , the only constraint for the stage S_i is that

$$R_i = \frac{H(Per_i)}{H_i} \text{ is a positive integer,}$$

that is, the duration of the stage S_i is a divisor of the duration of the period Per_i .

At this point, the original control problem was divided into control sub-problems coupled only by the physical variables ν . Therefore, since we are assuming that each stage is independent and cyclic, the approach will now be to solve the following problem decoupled by periods:

$$\begin{aligned} & \min/\max_{\nu, \mu_1, \dots, \mu_p, \tau_1, \dots, \tau_p} \quad \text{Indicator}(\nu, \mu_1, \dots, \mu_p, \tau_1, \dots, \tau_p) \\ & \text{subject to} \quad \begin{cases} \nu \in V, \\ \mu_i \in \mathcal{U}_i(\nu) \text{ and } \tau_i \in \mathcal{F}_i(\nu, \mu_i), \forall i \in \{1, \dots, p\}, \\ \text{IniCond}(S_i, \nu, \mu_i, \tau_i) = \text{FinCond}(S_i, \nu, \mu_i, \tau_i), \forall i \in \{1, \dots, p\}, \end{cases} \end{aligned} \quad (5.1.2)$$

where $\mathcal{U}_i(\nu)$ stands for all feasible operation functions

$$\mu_i : [0, H_i] \rightarrow \mathbf{R}_i^m$$

representing a cyclic operation for the stage S_i (that is, satisfying $\mu_i(0) = \mu_i(H_i)$). Analogously, $\mathcal{F}_i(\nu, \mu_i)$ stands for the strategy functions

$$\tau_i : [0, H_i] \rightarrow \mathbf{R}_i^l$$

representing a cyclic strategy for the stage S_i (that is, satisfying $\tau_i(0) = \tau_i(H_i)$). Finally, $\text{IniCond}(S_i, \nu, \mu_i, \tau_i)$ and $\text{FinCond}(S_i, \nu, \mu_i, \tau_i)$ represent the initial and final conditions for the stage S_i (which allows to close the cycle of the stage), for the dimensions ν , the operation μ_i and the strategy τ_i .

Daily pre-fixed strategies

Now the objective will be to reduce the optimal control problem (5.1.2) to one of real value differentiable optimization. For this, a pre-scenario will be set, that is, a plant production strategy will be pre-established, with a fixed number of phases (Storage, Storage-Production, Discharge), as well as the order of these on each day $k \in \{1, \dots, N_{days}(i)\}$ of each stage S_i .

In this part, we are going to assume that in our model the Storage and Discharge phases happen at a constant rate, that is, when the plant is inside of a phase, all its behavior is constant (static). In other words, the operational variables that describe the operation of the plant in each phase will be constant, and thus, we now aim to decide the value of those constants, and the initial and final times of each phase. By prefixing the number and order of such phases, the control problem 5.1.2 becomes parameterized.

Then, setting a stage S_i and a day $k \in \{1, \dots, N_{days}(i)\}$, the following definitions are included:

- The indices that will be representing the temporary variables, $(t_{ini}(i, j, k))$ and $t_{fin}(i, j, k)$, as well as other variables, for the different phases of Storage, Storage-Production, and Discharge, are:
 - i : It will represent index of the the stage S , with $i \in \{1, \dots, p\}$
 - k : It will represent index of the day k of stage S_i
 - j : It will represent the order index of the phase on day k
- The number of Storage phases $J_S(i, k)$. For each $j \in \{1, \dots, J_S(i, k)\}$, the variables $t_{ini}^S(i, k, j)$ and $t_{fin}^S(i, k, j)$ are introduced as the initial time and final time of the j th Storage phase of the k th day of the stage S_i .
- The number of Production phases $J_P(i, k)$. For each $j \in \{1, \dots, J_P(i, k)\}$, the variables $t_{ini}^P(i, k, j)$ and $t_{fin}^P(i, k, j)$ are introduced as the initial time and final time of the j th Storage-Production phase of the k th day of the stage S_i .
- The number of Discharge phases $J_D(i, k)$. For each $j \in \{1, \dots, J_D(i, k)\}$, the variables $t_{ini}^D(i, k, j)$ and $t_{fin}^D(i, k, j)$ are introduced as the initial time and final time of the j th Storage phase of the k th day of the stage S_i .

Figure 5.1 shows an example of a pre-scenario for one day, between the two blue stars, which is indicating that a day is not fixed and in fact a day k is measured from the initial storage instant $t_{ini}^S(i, k, 1)$ to the next day's initial storage time $t_{ini}^S(i, k + 1, 1)$.

In Problem (5.1.2), for each stage S_i one had the set

$$\mathcal{O}_i(\nu) = \{(\tau_i, \mu_i) : \mu_i \in \mathcal{U}_i(\nu), \tau_i \in \mathcal{F}_i(\nu, \mu_i)\}$$

that represents all physically possible operations of the CSP plant. This is a set of functions and therefore of infinite dimension. Nevertheless, when a pre-scenario is fixed, the admissible operations are restricted, considering only those which respect the pre-scenario strategy. Thus, a subset $\mathcal{O}'_i(\nu) \subseteq \mathcal{O}_i(\nu)$ of admissible operations can be constructed. Furthermore, this set can be described by real variables. Indeed, let $\tilde{\tau}_i \in \mathbb{R}^{a_i}$ denotes the vector of all time variables for all days of stage S_i , and $\tilde{\mu}_i \in \mathbb{R}^{b_i}$ denotes the vector of all operational variables for each one of the Storage and Discharge phases considered in the same stage. Thanks to the pre-scenario construction, there exists a subset $O_i(\nu) \subseteq \mathbb{R}^{a_i+b_i}$ and an invertible mapping

$$\phi_i : O_i(\nu) \rightarrow \mathcal{O}'_i(\nu)$$

such that each admissible operation in $\mathcal{O}'_i(\nu)$ can be uniquely identified with a vector $(\tilde{\tau}_i, \tilde{\mu}_i) \in O_i(\nu)$ through ϕ_i . This identification is called a parameterisation of the admissible operations and with it, it is possible to rewrite problem (5.1.2) as

$$\begin{aligned} & \min/\max_{\nu, \tilde{\mu}_1, \dots, \tilde{\mu}_p, \tilde{\tau}_1, \dots, \tilde{\tau}_p} \quad \text{Indicator}(\nu, \tilde{\mu}_1, \dots, \tilde{\mu}_p, \tilde{\tau}_1, \dots, \tilde{\tau}_p) \\ & \text{subject to} \quad \begin{cases} \nu \in V \subseteq \mathbb{R}^n, \\ (\tilde{\mu}_i, \tilde{\tau}_i) \in O_i(\nu) \subseteq \mathbb{R}^{a_i+b_i} \quad \forall i \in \{1, \dots, p\}, \\ \text{IniCond}(S_i, \nu, \tilde{\mu}_i, \tilde{\tau}_i) = \text{FinCond}(S_i, \nu, \tilde{\mu}_i, \tilde{\tau}_i), \\ \forall i \in \{1, \dots, p\}. \end{cases} \end{aligned} \quad (5.1.3)$$

Therefore, with the above parameterisation, Problem (5.1.3) is now a constraint real-valued optimization problem. It is therefore simpler and less expensive, in the sense of computational demand, than Problem (5.1.1).

According to the indicators in (4.4) and the implementation of pre-scenarios for solving optimization problems as described in the Section 5.1, for example, two objective functions, $\text{Indicator}(\cdot, \dots, \cdot)$, would be

$$NPV(\nu, \mu_1, \dots, \mu_p, \tau_1, \dots, \tau_p) = USF(N, \iota_r) \left[\sum_{i=1}^p R_i (\text{Rev}_i(\nu, \mu_i, \tau_i) - \text{Cost}_i(\nu, \mu_i, \tau_i)) \right] - C_{invest}(\nu)$$

and

$$LCOE(\nu, \mu_1, \dots, \mu_p, \tau_1, \dots, \tau_p) = \frac{USF(N, \iota_r) \cdot [\sum_{i=1}^p R_i \cdot \text{Cost}_i(\nu, \mu_i, \tau_i)] + C_{invest}(\nu)}{USF(N, \iota_r) \cdot \sum_{i=1}^p R_i \cdot W_i(\nu, \mu_i, \tau_i)}$$

with $USF(N, \iota_r)$ called the Uniform Series Factor (more details see [5]) given by the N years, the real discount rate ι_r and R_i is the number of repetitions of the stage S_i .

$Rev_i(\nu, \mu_i, \tau_i)$ and $Cost_i(\nu, \mu_i, \tau_i)$ stand for the revenues and costs of the stage S_i for the dimensions ν , the operation μ_i and the strategy τ_i .

5.2 Optimization Problem

This section is devoted to the detailed structure of problem (5.1.3), and how are all the variants considered in this work. In Subsection 5.2.1 we detail the equations governing each of the plant components. Then, the expressions of the revenues and costs which compose each of the economic indicators are described in Subsection 5.2.2. Subsequently, the constraints will be indicated in terms of the variables of the problem. Finally, the bounds for the problem variables are shown and the complete optimization problems to solve are exposed in the Subsection 5.2.4.

5.2.1 Modeling - Storage System

In order to reduce the notation of each variable and expression in the different phases of the plant, the sub-indices i, k, j will be omitted. Therefore, continuous equations are considered to represent the variation and evolution of temperatures, mass flows, powers, etc., for all $t \in I = [t_{ini}, t_{fin}]$. Note that, for the Storage and Discharge phases occurring at a constant rate (see, [125]), it is sufficient that these expressions are verified for $t = t_{ini}, t_{fin}$.

Two-tank molten salt storage

The operation of the Two-tank system with molten salt is determined by the heat transfer fluid inside the heat exchanger, which is controlled from pumps that regulate mass flow rates. This exchange operates in a counter current mode. For the Storage phase, the fluid in the red circuit (see Figure 5.2) passes from node 3 to node 6, and the flow of molten salt passes through the exchanger from the cold tank (node 7) to the hot tank (node 8). In the case of the Discharge phase, the fluids pass through the same nodes in opposite directions. For this reason, we will distinguish the operational variables as follows:

- $\mu^S(t) = (\dot{m}_3^S(t), \dot{m}_{salt}^S(t), T_7(t))$ represents the operational variables of the mass flows during the Storage phase, where the molten salt \dot{m}_{salt}^S (mass flow) moves from the cold tank (at temperature T_7) to the hot tank;
- $\mu^D(t) = (\dot{m}_3^D(t), \dot{m}_{salt}^D(t), T_8(t))$ represents the operational variables of the mass flows during the Discharge phase, where the molten salt \dot{m}_{salt}^D (mass flow) moves from the hot tank (at temperature T_8) to the cold tank.

Therefore the vector of operational variables is defined as

$$\mu(t) = (\dot{m}_3^S(t), \dot{m}_{salt}^S(t), T_7(t), \dot{m}_3^D(t), \dot{m}_{salt}^D(t), T_8(t)).$$

Now, the physical and operational variables will allow to determine the thermal power involved in each of the different phases, and the amount of energy which is stored or discharged during a day of operation :

- $q_S(t) = q_S(\nu, \dot{m}_3^S(t), \dot{m}_{salt}^S(t), T_7(t))$ represents the storage power corresponding to heat transfer from the heat transfer fluid to the molten salt flow;
- $q_D(t) = q_D(\nu, \dot{m}_3^D(t), \dot{m}_{salt}^D(t), T_8(t))$ represents the discharge power corresponding to heat transfer from the molten salt to the heat transfer fluid.

These two variables for the thermal powers, q_S and q_D , allow to calculate each operating mode.

Storage phase. In this phase, the solar field and the Storage System are active. The storage schema of the plant is shown in Fig. 5.2. Let's assume that this phase happens in a time interval $I_S = [t_{ini}^S, t_{fin}^S]$.

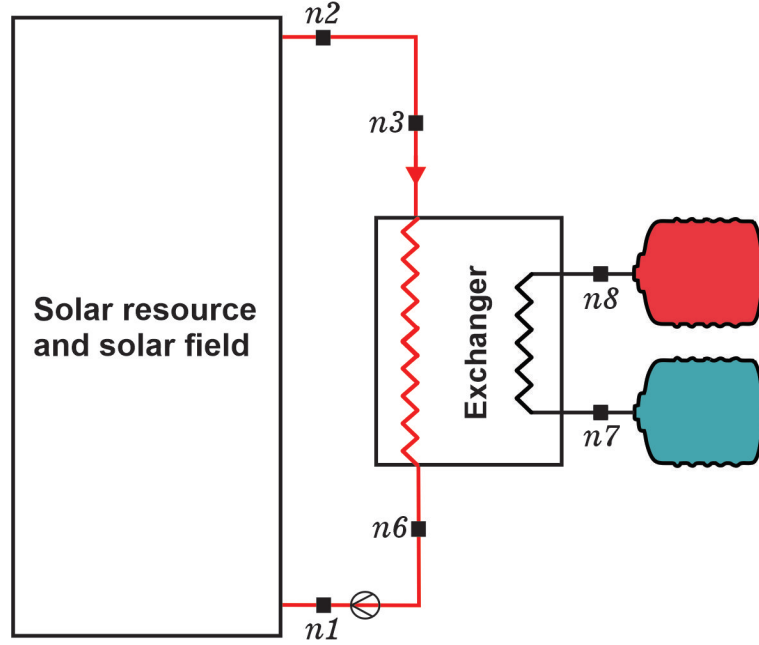


Figure 5.2: Two-tank molten salt storage. Scheme in Storage phase.

To simplify the modeling of the heat exchange, we assume that there is no heat loss. Therefore, the heat sent by the heat transfer fluid between nodes 3 and 6, and the heat received by the molten salt between nodes 7 and 8, is the same. This is represented by the following equations:

$$q_S(t) = C_{htf} \dot{m}_3^S(t) (T_3 - T_6(t)) \quad (5.2.1a)$$

$$q_S(t) = C_{salt} \dot{m}_{salt}^S(t) (T_8(t) - T_7(t)) \quad (5.2.1b)$$

where C_{htf} , C_{salt} are the heat capacity of the heat transfer fluid and molten salt, and $\dot{m}_3^S(\cdot)$, $\dot{m}_{salt}^S(\cdot)$ are the mass flow rates for each fluid. During the Storage phase, the CSP plant operates with a nominal temperature of $T_2 = 560^\circ\text{C}$ in the node 2. The thermal losses for the heat-transfer fluid are neglected and so, $T_2 = T_3$, $T_1(t) = T_6(t)$ and $\dot{m}_1(t) = \dot{m}_2(t) = \dot{m}_3(t) = \dot{m}_6(t)$, for any $t \in I_S$, as shown in Table 5.1. Note that if the plant is operating with a nominal temperature ($T_2 = 560^\circ\text{C}$), then in the storage phase the temperature will be the same at node 3. Similarly, temperatures at nodes 1 and 6 will coincide, but the values will depend according to the mass flow \dot{m}_3^S and the thermal power q_S .

Mass Flow	Temperature
$\dot{m}_1 = \dot{m}_2 = \dot{m}_3 = \dot{m}_6$	$T_3 = T_2 \quad ; \quad T_1 = T_6$

Table 5.1: Storage phase - Conditions for temperatures and mass flows.

For the heat exchanger, each side of the exchanger has an average temperature, that is

$$T_{htf}(t) = \frac{T_3 + T_6(t)}{2}, \quad \text{and} \quad T_{salt}(t) = \frac{T_7(t) + T_8(t)}{2}.$$

According to the previous assumptions, the thermal power inside the exchanger (which coincides with the exchanged heat q_S) is expressed as follows:

$$q_S(t) = \frac{1}{2} h_{conv} \cdot A_{exch} \cdot [(T_3 + T_6(t)) - (T_7(t) + T_8(t))], \quad (5.2.2)$$

with h_{conv} representing the convective heat transfer coefficient. Finally, the thermal power cannot exceed the available thermal power, leading to

$$C_{htf} \dot{m}_3^S(t) (T_3 - T_6(t)) \leq q_{sol}(t) \quad \forall t \in [t_{ini}^S, t_{fin}^S]. \quad (5.2.3)$$

Recall that $q_{sol}(\cdot)$ is the thermal power coming from the solar field (see Eq. 4.2.3).

Storage-Production phase. During the Storage phase, when the thermal power obtained from the solar field generates a non-negligible excess with respect to the consumption of the Storage System q_S , the operation of the plant switches to a Storage-Production phase. In this phase, we have one part of the recovered energy coming from the solar field which goes to the exchanger (nodes 3 and 6). The other part goes to the power block (nodes 4 and 5). All components are active in this phase, as shown in Fig. 5.3. Let's assume that this phase happens in a time interval $I_P = [t_{ini}^P, t_{fin}^P]$.

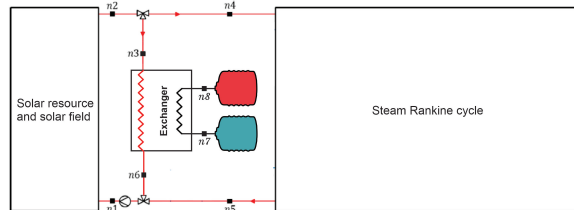


Figure 5.3: Two-tank molten salt storage. Scheme in Storage-Production phase.

Note that, both in the Storage and Storage-Production phases, the same vector μ^S will be used to describe the operation of the exchanger and the two tanks. Thus, the storage power during the Storage-Production phase coincides with $q_S(\cdot)$, that is, $q_P(t) = q_S(\dot{m}_3^S(t), \dot{m}_{salt}^S(t), T_7(t))$, for all $t \in I_P$. In addition, as in the Storage phase, the assumptions we are considering are summarized in Table 5.2.

Mass Flow	Temperature
$\dot{m}_1 = \dot{m}_2 ; \dot{m}_3 = \dot{m}_6 ; \dot{m}_4 = \dot{m}_5$	$T_2 = T_3 = T_4$

Table 5.2: Storage-Production phase assumptions.

The mass flow through node 2 will be divided into two parts, the first one directed to the Storage System and the second one to the power block. Therefore, according to the

conservation of flow of mass and energy, we have the following relationships:

$$\dot{m}_1(t) = \dot{m}_3^S(t) + \dot{m}_4(t), \quad (5.2.4)$$

$$\dot{m}_1(t)T_1(t) = \dot{m}_3^S(t)T_6(t) + \dot{m}_5(t)T_5(t). \quad (5.2.5)$$

Now, since the thermal power cannot exceed the available thermal power, the inequality (5.2.3) is replaced by

$$C_{htf}\dot{m}_3^S(t)(T_3 - T_6(t)) + C_{htf}\dot{m}_4(t)(T_4 - T_5(t)) \leq q_{sol}(t), \quad (5.2.6)$$

Finally, the following equations end the description of the operation of the plant in this phase,

$$q_R(t) = \min\{q_{sol}(t) - q_S(t), q_{nom_max}\}, \quad (5.2.7)$$

$$q_R(t) = C_{htf}\dot{m}_4^S(t)(T_4 - T_5(t)), \quad (5.2.8)$$

$$q_R(t_{ini}^P), q_R(t_{fin}^P) \geq q_{nom_min}, \quad (5.2.9)$$

$$\dot{W}_{elec}(t) = f_b(q_R(t), T_2, T_{env}^d), \quad (5.2.10)$$

$$\dot{m}_4(t) = f_f(\dot{W}_{elec}(t), T_2, T_{env}^d), \quad \forall t \in I_P, \quad (5.2.11)$$

with $q_R(\cdot) + q_S(\cdot)$ the thermal consumption of the plant and q_{nom_min} , q_{nom_max} being respectively the minimum and maximum power value at which the power block operates. These values correspond to 20% and 105% of the nominal value of the power block. The last quadratic regressions are determined given that the CSP plant continues to operate with a nominal temperature at node 2 of $T_2 = 560^\circ\text{C}$ and the average environment daylight temperature T_{env}^d (which is exogenous), is known.

Discharge phase. In this phase, only the Storage System and the Rankine cycle are active, as can be seen in the Fig. 5.4.

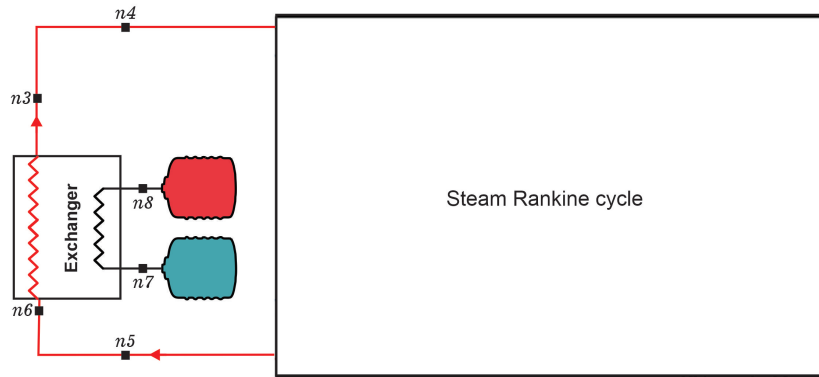


Figure 5.4: Two-tank molten salt storage. Schema in Discharge phase.

During this Discharge phase, the molten salt stored in the hot tank is conducted to the heat exchanger to transfer the stored heat energy to the heat transfer fluid. Subsequently this energy is transferred to the power block to finally produce electricity. Assuming that this phase happens in a time interval $I_D = [t_{ini}^D, t_{fin}^D]$, the system of equations representing

this phase is as follows:

$$q_D(t) = C_{htf} \dot{m}_3^D(t) (T_3(t) - T_6(t)) \quad (5.2.12a)$$

$$q_D(t) = C_{salt} \dot{m}_{salt}^D(t) (T_8(t) - T_7(t)) \quad (5.2.12b)$$

$$q_D(t) = -\frac{1}{2} h_{conv} A_{exch} ((T_3(t) + T_6(t)) - (T_7(t) + T_8(t))) \quad (5.2.12c)$$

$$T_5(t) = f_c(\dot{m}_3^D(t), T_4(t), T_{env}^i) \quad (5.2.12d)$$

where $q_D(\cdot)$ represent the thermal power transferred to the heat transfer fluid from the molten salt. The relations (5.2.12a - 5.2.12c) are similar to those expressed in (5.2.1a-5.2.1b and 5.2.2).

Note that, as shown in the Table 5.3, in this phase we have $T_6(t) = T_5(t)$, $T_3(t) = T_4(t)$ and $q_D(t) = q_P(t)$, for all $t \in I_D$.

Mass Flow	Temperature
$\dot{m}_3 = \dot{m}_4 = \dot{m}_5 = \dot{m}_6$	$T_3 = T_4 \quad ; \quad T_5 = T_6$

Table 5.3: Discharge phase assumptions.

Finally, using the quadratic regression f_b (see equation 4.2.5), we calculate the electrical power produced in this phase by

$$\dot{W}_{elec}(t) = f_b(q_D(t), T_4(t), T_{env}^i) \quad \forall t \in I_D.$$

where T_{env}^i is the temperature of the environment, which we assume constant while its value depends on the season $i \in \{1, \dots, 4\}$.

Volumes and Temperatures During the Storage and Discharge phases, the volume and temperature of the two tanks vary. In each of the phases, the temperature will only vary in one tank while remaining constant in the other. The variation is produced mainly by the new volume entering one of the tanks and its temperature. The volume's balance is given by the following expressions:

$$V_{cold}(t) = \begin{cases} V_{cold}(t_{ini}^S) - V_{new}^S(t), & \text{if } t \in I_S, \\ V_{cold}(t_{ini}^D) + V_{new}^D(t), & \text{if } t \in I_D. \end{cases}$$

$$V_{hot}(t) = \begin{cases} V_{hot}(t_{ini}^S) + V_{new}^S(t), & \text{if } t \in I_S, \\ V_{hot}(t_{ini}^D) - V_{new}^D(t), & \text{if } t \in I_D. \end{cases}$$

Here, the new incoming or outgoing volume of each of the tanks is given by

$$V_{new}^S(t) = \int_{t_{ini}^S}^t \frac{\dot{m}_{salt}^S(t)}{\rho_{salt}} dt,$$

$$V_{new}^D(t) = \int_{t_{ini}^D}^t \frac{\dot{m}_{salt}^D(t)}{\rho_{salt}} dt,$$

where ρ_{salt} is the density of molten salt.

Regarding the temperatures, since the variation in the cold tank is not really significant during the Storage phase, we assume that it remains constant during this phase, and similarly

for the hot tank temperature in Discharge phase. This assumption is made by the fact that the daily heat losses in the tanks are around 5°C (see [114]), which are negligible for this type of study. Then, the temperature variation in the cold tank is, $T_{cold}(t) = T_{cold}(t_{ini}^S)$ if $t \in I_S$, and

$$T_{cold}(t) = \frac{T_{cold}(t_{ini}^D) \cdot V_{cold}(t_{ini}^D) \cdot \rho_{salt} + T_7(t) \cdot \int_{t_{ini}^D}^t \dot{m}_{salt}^D(t) dt}{V_{cold}(t) \cdot \rho_{salt}}, \quad \text{if } t \in I_D. \quad (5.2.13)$$

For the hot tank, $T_{hot}(t) = T_{hot}(t_{ini}^D)$ if $t \in I_D$, and

$$T_{hot}(t) = \frac{T_{hot}(t_{ini}^S) \cdot V_{hot}(t_{ini}^S) \cdot \rho_{salt} + T_8(t) \cdot \int_{t_{ini}^S}^t \dot{m}_{salt}^S(t) dt}{V_{hot}(t) \cdot \rho_{salt}}, \quad \text{if } t \in I_S. \quad (5.2.14)$$

Finally, these volumes cannot exceed the maximum or minimum capacity allowed in the two tanks, that is, setting the physical characteristics of the tank (V), the capacities of both tanks will be limited, that is,

$$V_{min}(V) \leq V_{cold}(t), V_{hot}(t) \leq V_{max}(V), \quad \forall t \in I_{S,D}.$$

According to [131], a temperature range has been established for the stored molten salt in the tanks,

$$290^\circ\text{C} \leq T_{cold}(t), T_{hot}(t) \leq 560^\circ\text{C}, \quad \forall t \in I_{S,D}.$$

Thermochemical Storage

The model we use here has been mainly elaborated in [124, 125]. In order to keep a self-contained exposition, we present the main elements of the model.

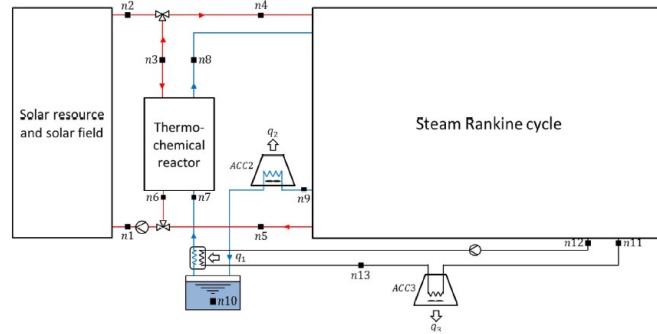


Figure 5.5: Concentrated Solar power plant with Thermochemical storage, including the thermal integration (original Figure from [124]).

When this type of storage is considered, the vector of physical variables ν is composed of four components: energy density DEC , apparent volumetric mass of conductive binder

ρ_{eng} , tubes' radius r_{sw} and the equivalent length of the tubes L . The equivalent length of the tubes corresponds to the product of the number of tubes in a module by the number of modules and by the length of each tube. Then, the vector of physical variables is represented as $\nu = (DEC, \rho_{eng}, r_{sw}, L)$.

The operation of the thermochemical reactor is defined by the pressure of the reactor $P_c(t)$ and the gap between operating and thermodynamic equilibrium temperatures $\Delta T_{eq}(t)$. This gap of temperature $\Delta T_{eq}(t)$ is expressed as the difference between the average temperature of the heat-transfer fluid (when passing through nodes 3 and 6), and the thermodynamic equilibrium temperature of the reversible reaction (4.2.10), $T_{eq}(P_c(t))$, which is given by

$$T_{eq}(P_c(t)) = \frac{94573}{121.186 - 8.314 \cdot \ln(P_c(t))} - 273.158. \quad (5.2.15)$$

Therefore it is assumed, as a first approximation, that

$$\frac{T_6(t) + T_3(t)}{2} = T_c(P_c(t), \Delta T_{eq}(t)) = T_{eq}(P_c(t)) + \Delta T_{eq}(t), \quad (5.2.16)$$

where $T_c(P_c(t), \Delta T_{eq}(t))$ stands for the operating temperature of the reactor. However, the operational variables ($P_c(t), \Delta T_{eq}(t)$) are different depending on the direction of the reaction that the reactor (4.2.10) performs. Thus, the following definitions are made:

- $\mu^S(t) = (P_c^S(t), \Delta T_{eq}^S(t))$ stands for the operational variables during the Storage process (decomposition reaction).
- $\mu^D(t) = (P_c^D(t), \Delta T_{eq}^D(t))$ stands for the operational variables during the Discharge process (synthesis reaction).

Finally, the vector μ of operational variables is defined as

$$\mu(t) = (P_c^S(t), \Delta T_{eq}^S(t), P_c^D(t), \Delta T_{eq}^D(t)).$$

As previously described, the physical and operational vectors (ν and μ respectively) define the thermal power stored or released by the reactor. These variables will allow to evaluate two important functions:

- $q_S(t) = q_S(\nu, P_c^S(t), \Delta T_{eq}^S(t))$ represents the storage power corresponding to heat flux from the heat transfer fluid to the reactor.
- $q_D(t) = q_D(\nu, P_c^D(t), \Delta T_{eq}^D(t))$ represents the discharge power corresponding to heat flux from the reactor to the heat transfer fluid.

The governing equations of these functions are the local mass balance and the energy balance equations in the porous reactive media, with source and sink terms related to the thermochemical reaction and depending on the reaction kinetics (see, e.g. [125]). This set of equations is solved by a finite elements method. Therefore, the above mentioned functions q_S and q_D are the solutions of a large differential system and no explicit formulae are available. We follow [124] and consider a Shepard Interpolation [120] based on simulated data.

Storage phase During the Storage phase, only the solar field and the Thermochemical reactor are active. The active schema of the plant is shown in Fig. 5.6. Let's assume that

this phase happens in a time interval $I_S = [t_{ini}^S, t_{fin}^S]$.

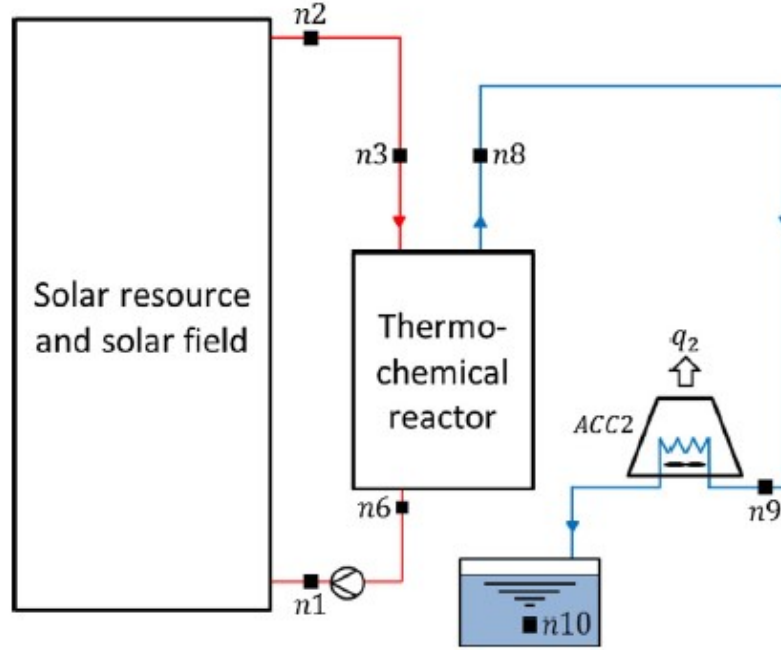


Figure 5.6: Thermochemical storage system. Schema in Storage phase. Copied from [124].

The exchange of heat between the heat-transfer fluid and the reactor is given by the following equation:

$$q_S(t) = C_{htf} \dot{m}_3(t) (T_3 - T_6(t)), \quad (5.2.17a)$$

where C_{th} is the thermal capacity of the heat-transfer fluid. It is assumed that, during the Storage phase, the CSP plant operates with a nominal temperature in the node 2 of $T_2 = 560^\circ\text{C}$. The thermal losses for the heat-transfer fluid are neglected and so, $T_2 = T_3$ and $T_1(t) = T_6(t)$ during this phase. Also, $\dot{m}_1(t) = \dot{m}_2(t) = \dot{m}_3(t) = \dot{m}_6(t)$, $\forall t \in I_S$.

Further, for ensuring the heat transfer and the decomposition reaction, it is imposed that the heat-transfer fluid always has a higher temperature than the thermodynamic equilibrium temperature of the reactor, that is,

$$T_6(t) \geq T_{eq}(P_c^S(t)), \forall t \in I_S. \quad (5.2.18a)$$

where the equilibrium temperature $T_{eq}(P_c^S(t))$ is given by Eq. (5.2.15).

Also, the thermal power cannot exceed the available thermal power.

$$C_{htf} \dot{m}_1(t) (T_2 - T_1(t)) \leq q_{sol}(t), \quad \forall t \in [t_{ini}^S, t_{fin}^S], \quad (5.2.19)$$

where $q_{sol}(\cdot)$ is the thermal power coming from the solar field.

The storage process consists in the decomposition reaction in Eq. 4.2.10 and 4.2.11. The water is pulled out from the reactor and stored in the reservoir (node 10) in liquid form. According to the values of physical variable ν , and the operational variable $\mu^S =$

$(P_c^S(t), \Delta T_{eq}^S(t))$, the thermal power that has to be dissipated (between nodes 8 and 10) in order to condensate the water is computed, and it is denoted by $q_{dis}(t) = q_{dis}(\nu, \mu^S(t))$. In this phase, q_{dis} coincides with the dissipated power q_2 , and it is calculated from the states of node 8 (which depends on $(\nu, \mu^S(t))$) and node 10 (which depends on the exogenous environmental conditions), and the thermal capacity of water.

Storage-Production phase

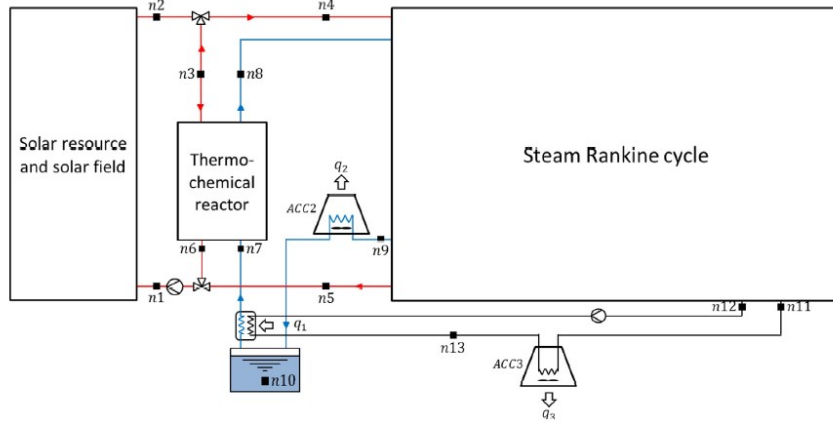


Figure 5.7: Thermochemical storage system. Schema in Storage-Production phase. Copied from [124].

As in the case of the Two-tank storage system, when the thermal power recovered from the solar field generates a non-negligible excess with respect to the q_S consumption of the Storage System, the operation of the plant switches to a Storage-Production phase. Let's assume that this phase happens in a time interval $I_P = [t_{ini}^P, t_{fin}^P]$. In this phase all the components are active as shown in the Fig. 5.7.

During this phase, part of the recovered power goes to the reactor and the other part goes to the power block. This latter thermal power will be denoted by $q_{th}(\cdot)$ and it varies in time. This variation is motivated by the fact that the plant tries to recover the maximum power from $q_{sol}(\cdot)$. Then, $\forall t \in I_P$, we have the inequality (5.2.19) is replaced by

$$C_{htf}\dot{m}_3(t)(T_3 - T_6(t)) + C_{htf}\dot{m}_4(t)(T_4 - T_5(t)) \leq q_{sol}(t), \quad \forall t \in I_P. \quad (5.2.20)$$

Also, thanks to the thermal integration (blue circuit, see Figure 5.7), part of the outlet thermal power q_{dis} can be recovered (between nodes 8 and 9) by the power block. This useful part, recovered at the instant $t \in I_P$ is denoted by $q_{dis}^u(t)$. Knowing the thermal power $q_{th}(\cdot)$ it is possible to determine the electrical power in this phase, as

$$\dot{W}_{elec}(t) = f_b(q_{th}(t) + q_{dis}^u(t), T_2, T_{11}), \quad \forall t \in I_P. \quad (5.2.21)$$

where f_b is one regressions shown in the equation 4.2.5. In this phase, we have $T_2 = T_4$, since the CSP plants continues to operate with a nominal temperature at node 2 of $T_2 = 560^\circ\text{C}$. All these functions finally are deduced by $q_{sol}(\cdot)$ and the variables ν and $\mu^S(\cdot)$.

The last quadratic regressions are determined given that the CSP plant continues to operate with a nominal temperature at node 2 of $T_2 = 560^\circ\text{C}$ and the average environment daylight temperature T_{env}^d (which is exogenous), is known.

Discharge phase

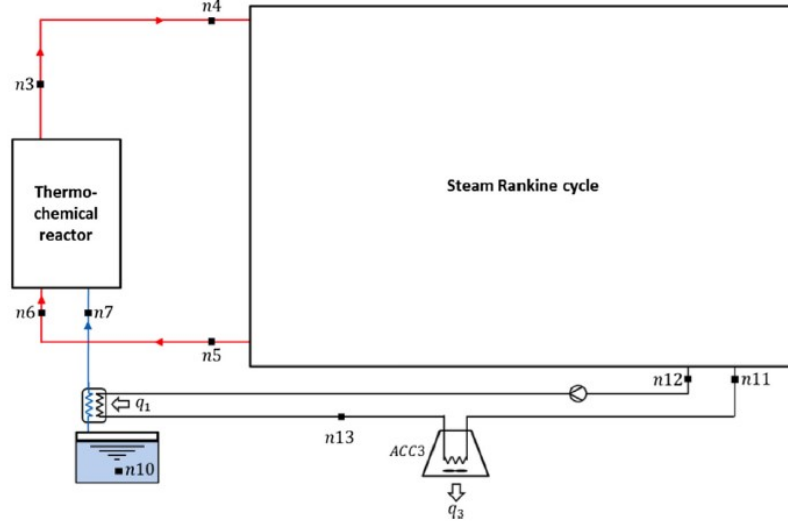


Figure 5.8: Thermochemical storage system. Schema in Discharge phase. Copied from [124].

In this phase, only the components of the Storage System and the power block are active, as shown in the Fig. 5.8. In the others phases, the heat transfer fluid goes from node to 3 to node 6, but at this stage, the transfer goes in the opposite direction.

The exchange of heat power between the heat-transfer fluid and the reactor is given by the following equation:

$$q_D(t) = C_{htf} \dot{m}_3(t) (T_3(t) - T_6(t)). \quad (5.2.22)$$

To calculate the electric power, we use the quadratic regressions f_b ,

$$\dot{W}_{elec}(t) = f_b(q_D(t), T_3(t), T_{11}(t)), \quad \forall t \in I_D. \quad (5.2.23)$$

For ensuring the heat power transfer and the synthesis reaction, it is necessary to impose that the heat-transfer fluid always has a lower temperature than the equilibrium temperature of the reactor, that is,

$$T_3(t) \leq T_{eq}(P_c^D(t)),$$

where the equilibrium temperature $T_{eq}(\cdot)$ is given by Eq. 5.2.15. During this synthesis reaction (Discharge phase), the water that was stored in the reservoir (node n_{10}) is evaporated and injected in the reactor. This process consumes a heat flux, q_1 , which depends on the reactor kinetics, that is, $q_1 = q_1(\mu^D)$. Through a thermal integration, the heat from the power block can provide the evaporation heat q_1 [125]. Thus,

$$q_1(t) = c_{cw} \dot{m}_{11}(t) (T_{12}(t) - T_{13}(t)), \quad \forall t \in I_D. \quad (5.2.24)$$

where c_{cw} is the average thermal capacity of coolant and the temperature in the node 12 is determined by the regression f_d (see Sec. 4.2.7).

Finally, we calculate the amount of electric power needed for the fan to dissipate during the cooling, from the thermal power dissipated (q_3) during the cooling process of the power

block with the following relation,

$$q_3(t) = \dot{m}_{11}(t) \cdot cp_{air} \cdot (T_{13}(t) - T_{11}(t)), \quad \forall t \in I_D. \quad (5.2.25)$$

$$W_{elec_q_3}(t) = 0.02 \cdot q_3, \quad \forall t \in I_D, \quad (5.2.26)$$

with cp_{air} thermal capacity of the coolant (black cycle, see Figure 5.7).

5.2.2 Objective Function

To be coherent with our approach, the objective function must be an economic criterion taking into account, at the same time, the storage design (investment cost) and the dynamic operation of the plant (operational costs and possibly incomes).

For the different indicators presented in Section 4.4, we must determine the initial investment of the project along with the costs and revenues related to the operation and production of the CSP plant. Thus, in the present Section, we begin to detail each of the terms that make up the economic indicator equations (see Section 4.4, equations 4.4.1 and 4.4.2), based on the reduced model of the plant and the pre-scenarios strategy. In this work, we will consider pre-scenarios, per day, with a single Storage and Production phase and one or several Discharge phases, similarly as shown in Figure 5.1.

Revenues

The revenues of the plant come from two sources: the electrical power produced during the Production-Storage phases,

$$Rev_i^P(\nu, \mu_i, \tau_i) = \sum_{k=1}^{N_{Days}(i)} \int_{t_{ini}^P(i,k)}^{t_{fin}^P(i,k)} \lambda(t) \dot{W}_{elec}(t) dt, \quad (5.2.27)$$

and the electrical power produced during the Discharge phases

$$Rev_i^D(\nu, \mu_i, \tau_i) = \sum_{k=1}^{N_{Days}(i)} \sum_{j=1}^{J(i,k)} \int_{t_{ini}^D(i,k,j)}^{t_{fin}^D(i,k,j)} \lambda(t) \dot{W}_{elec}(t) dt. \quad (5.2.28)$$

Thus,

$$Rev_i(\nu, \mu_i, \tau_i) = Rev_i^P(\nu, \mu_i, \tau_i) + Rev_i^D(\nu, \mu_i, \tau_i).$$

Common Storage System Costs

The costs associated with plant operation during the different time intervals corresponding to each phase, I_S , I_P , I_D , are listed below. The representation of these costs is the same, but the nature of the variables is not. The Inactive phase has no costs, since the plant is shut down. Therefore, there are no operating costs.

The following are the costs for each stage S_i and day $k \in 1, \dots, N_{days}(i)$:

- Heliostat operational cost: It consists in a constant energy requirement C_{start} of start-up and a marginal energy requirement C_{mov} of moving the Heliostats following the sun to

supply the useful heat

$$Cost_{hel}(i, k) = \lambda(i, t_{ini}^S(i, k)) \cdot C_{start} + \int_{t_{ini}^S(i, k)}^{t_{fin}^S(i, k)} \lambda(i, t) \cdot C_{mov} dt. \quad (5.2.29)$$

• Pumping cost of $\dot{m}_3^S(\cdot)$ - Storage and Storage-Production phases: During the Storage and Production phases, the red circuit is only pumped by the pump P_1 , and therefore, associated only with $\dot{m}_1^P(\cdot)$. This marginal cost is linear with respect to $\dot{m}_3^S(\cdot)$ so

$$Cost_{P_1}(i, k) = C_{P_1} \left(\int_{t_{ini}^S(i, k)}^{t_{ini}^P(i, k)} \lambda(i, t) \dot{m}_3^S(i, k) dt + \int_{t_{ini}^P(i, k)}^{t_{fin}^P(i, k)} \lambda(i, t) \dot{m}_1^P(i, k, t) dt + \int_{t_{fin}^P(i, k)}^{t_{fin}^S(i, k)} \lambda(i, t) \cdot \dot{m}_3^S(i, k) dt \right). \quad (5.2.30)$$

• Pumping cost of \dot{m}_R , Storage-Production phase: The power block must pump a vapor as heat-transfer fluid. Denoting by $\dot{m}_R(t)$ the mass flow rate of this fluid, it is known that it is proportional to $\dot{m}_4(t)$, $t \in I_P$ (as shown in the Figure 5.7). Nevertheless, the power consumption of pumping \dot{m}_R is quadratic. Thus, during the Storage-Production phases one has

$$Cost_{P_R}^P(i, k) = \int_{t_{ini}^P(i, k)}^{t_{fin}^P(i, k)} \lambda(i, t) (A_{P_R} \dot{m}_4(i, k, t)^2 + B_{P_R} \dot{m}_4(i, k, t) + C_{P_R}) dt, \quad (5.2.31)$$

where A_{P_R} , B_{P_R} and C_{P_R} are three constant real numbers.

• Pumping cost of \dot{m}_R , Discharge phase: similar to the previous cost, we have to

$$Cost_{P_R}^D(i, k, j) = \sum_{j=1}^{J(i, k, j)} \int_{t_{ini}^D(i, k, j)}^{t_{fin}^D(i, k, j)} \lambda(i, t) (A_{P_R} \dot{m}_4^D(i, k, j)^2 + B_{P_R} \dot{m}_4^D(i, k, j) + C_{P_R}) dt, \quad (5.2.32)$$

with the same constants A_{P_R} , B_{P_R} and C_{P_R} as above.

• Pumping cost of $\dot{m}_3^D(\cdot)$ - Discharge phase: In the Discharge phases, the active pump P_2 is at the node 4. As in the Storage phase, this cost is as follows,

$$Cost_{P_2}^D(i, k) = C_{P_2} \cdot \sum_{j=1}^{J(i, k)} \int_{t_{ini}^D(i, k, j)}^{t_{fin}^D(i, k, j)} \lambda(i, t) \dot{m}_3^D(i, k, j) dt. \quad (5.2.33)$$

• Maintenance: The operation and maintenance costs are divided into a fixed cost by capacity, set at 59.4 €/kWe/year and a variable cost (Var_{cost}) depending on the generated energy, fixed at 3.15 €/MWe (see [124]). Moreover, energy consumption of the heliostat field (tracking) and pumps are taken into account (using SAM default values). The variable costs are:

$$Cost_M(i, k) = Var_{cost} \cdot \left(\int_{t_{ini}^P(i, k)}^{t_{fin}^P(i, k)} \dot{W}_{elec}(t) dt + \sum_{j=1}^{J(i, k)} \int_{t_{ini}^D(i, k, j)}^{t_{fin}^D(i, k, j)} \dot{W}_{elec}(t) dt \right). \quad (5.2.34)$$

- Start-up cost of the power block: Before starting the power block and produce any power energy, the power block must be heated. The pre-heating requirement is modeled as a delay of one third of an hour in the effective production. Nevertheless, if the power block is already partially heated, this delay is attenuated. To compute this start-up cost, first the non-attenuated one is computed, that is

$$Cost_{fullStart}^P(i, k) = \int_{t_{ini}^P(i, k)}^{t_{fin}^P(i, k)+1/3} \lambda(i, t) \dot{W}_{elec}(t) dt \quad (5.2.35)$$

$$Cost_{fullStart}^D(i, k, j) = \int_{t_{ini}^D(i, k, j)}^{t_{fin}^D(i, k, j)+1/3} \lambda(i, t) \dot{W}_{elec}(t) dt. \quad (5.2.36)$$

Then, the effective start-up cost of the power block is obtained by considering an attenuation function $\varphi(t) = 1 - \exp(-3t/2)$ (as considered in [124]), which will take values depending on the difference in hours between the final and initial times of electric energy production (Production and Discharge phases),

$$Cost_{starR}^P(i, k) = \varphi(\Delta t) \cdot Cost_{fullStart}^P(i, k), \quad (5.2.37)$$

$$Cost_{starR}^D(i, k, j) = \varphi(\Delta t) \cdot Cost_{fullStart}^D(i, k, j), \quad (5.2.38)$$

thus, the smaller the time difference (Δt) the more attenuation will tend to be negligible. These expressions have been established with reference to those set forth in [124].

Costs of Thermochemical System

For the case of Thermochemical Storage System, it was taken advantage of the various exo- and endo-thermal components of the power block and the Thermochemical system by recovering thermal energy between them (see blue and black circuits in Figure 5.5). That will result in reducing the amount of wasted heat released to the ambient. The costs related with these integrated systems are:

- Pumping cost of $\dot{m}_{11}(\cdot)$ - Storage-Production phase and Discharge Phase: The black cycle of Fig. 5.5 is active during the Storage-Production phases and the Discharge phases and the coolant is pumped by the pump P_3 between nodes n_{12} and n_{13} . As above,

$$Cost_{P_3}^D(i, k) = C_{P_3} \cdot \int_{t_{ini}^P(i, k)}^{t_{fin}^P(i, k)} \lambda(i, t) \dot{m}_{11}^P(i, k, t) dt + C_{P_3} \cdot \int_{t_{ini}^D(i, k, j)}^{t_{fin}^D(i, k, j)} \lambda(i, t) \dot{m}_{11}^D(i, k, j) dt. \quad (5.2.39)$$

- Dissipation cost of q_2 - Storage Phase: During the Storage phase, the ventilator is used to dissipate $q_2(\cdot)$, which depends also on ν and $\mu^S(t)$,

$$Cost_{Diss2}^S(i, k) = \int_{t_{ini}^S(i, k)}^{t_{fin}^S(i, k)} \lambda(i, t) PC_{q_2}(\nu, P_c^S(i), \Delta T_{eq}^S(i), q_2(t)) dt, \quad (5.2.40)$$

where $PC_{q_2}(\cdot)$ is a nonlinear function that computes the electrical power consumption of the ventilator.

- Dissipation cost of q_3 : Storage-Production and Discharge phase: The power consumption is modeled as the 2% of the heat power q_3 that must be dissipated. Thus

$$Cost_{Diss_3}(i, k) = \int_{t_{ini}^P(i, k)}^{t_{fin}^P(i, k)} \lambda(i, t) \cdot 0.02 \cdot q_3(t) dt + \sum_{j=1}^{J(i, k)} \int_{t_{ini}^D(i, k, j)}^{t_{fin}^D(i, k, j)} \lambda(t) \cdot 0.02 \cdot q_3(t) dt. \quad (5.2.41)$$

The way to compute the heat power $q_3(\cdot)$ is described in Appendix 5.2.1.

- Investment cost: the total investment cost is calculated with the following formulation derived from SAM software:

$$Cost_0 = C_{land} + (C_{Str}(\nu) + C_{Rank} + C_{SF})(1 + \tau_c)[1 + \tau_s + 0.8\tau_t]$$

where τ_c is the contingency rate (fixed at 7%); τ_s is the rate which considers the EPC (engineer-procure-construct) and owner costs (fixed at 13%); τ_t is the sales tax (5%). For more details see [125]. The sub-costs of the power plant are calculated as follows:

(a) C_{land} and C_{SF} : the cost of the land and solar field, are approximated as functions of the Solar Multiple (SM):

$$C_{land} = 9000(414 \cdot SM + 51.6), \quad (5.2.42)$$

$$C_{SolarField} = 10^6(57.765 \cdot SM + 14.373). \quad (5.2.43)$$

(b) C_{Rank} : the cost of the power block is proportional to the design gross capacity. In this study C_{Rank} is 66M€.

(c) C_{Str} : the cost of the Storage System also considers the cost C_{acc2} of the ventilator that dissipates q_2 and the cost C_{hx} of the heater that uses q_1 to evaporate the water in node n_{10} . The final investment cost of the Storage System is given by

$$C_{Str} = 1.1(C_{reac}(\nu) + C_{acc2} + C_{hx}), \quad (5.2.44)$$

where the C_{reac} of the reactor is estimated in terms of the physical variables via consultation with an industrial partner, associated with the laboratory PROMES-CNRS, namely COLDWAY. This company manufactures Thermochemical reactors for different industrial processes. Given a vector $\nu = (DEC, \rho_{eng}, r_{sw}, L)$, a polynomial regression was obtained based on the estimations done by this company. The cost of the reactor can be expressed as

$$C_{reac} = \beta f_h(DEC, \rho_{eng}, r_{sw}) DEC \cdot L \cdot \pi(r_{sw}^2 - r_{diff}^2), \quad (5.2.45)$$

where f_h is a polynomial function, r_{diff} is a constant parameter and β is the ratio between the expected and estimated cost for the Thermochemical reactor. The correction coefficient β will take values between 1 and 3, with 1 being the optimistic case and 3 the pessimistic case [124].

Costs of Two-tank System

- Pumping cost of $\dot{m}_{salt}^S(\cdot)$ - Storage phase: In the Storage phases, the active pump is P_4 , which allows the flow of molten salt from cold tank to hot tank. This cost is as follows,

$$Cost_{P_4}^S(i, k) = C_{P_4} \cdot \int_{t_{ini}^S(i, k)}^{t_{fin}^S(i, k)} \lambda(i, t) \dot{m}_{salt}^S(i, k) dt. \quad (5.2.46)$$

- Pumping cost of $\dot{m}_{salt}^D(\cdot)$ - Discharge phase: In the Discharge phases, the active pump is P_4 , allowing the flow of molten salt from hot tank to cold tank and similarly as in the Storage phase, this cost is as follows,

$$Cost_{P_4}^D(i, k) = C_{P_4} \cdot \int_{t_{ini}^D(i, k, j)}^{t_{fin}^D(i, k, j)} \lambda(i, t) \dot{m}_{salt}^D(i, k, j) dt. \quad (5.2.47)$$

- Investment cost: The investment cost is according the three components, the solar field (which also considers the cost of the operation land) depending on the Solar Multiple (SM) indicator, the cost on the power block, which is constant, and the investment on the Two-tank storage system

$$Cost_{Inv} = C_{land} + (C_{Str}(V, A_{exch}) + C_{Rank} + C_{SF})(1 + \tau_c)[1 + \tau_s + 0.8\tau_t] \quad (5.2.48)$$

- C_{land} , C_{SF} and C_{Rank} : these costs are the same as those proposed for the Thermochemical system in the Subsection 5.2.2.
- C_{Str} : this cost is based on the estimated results of thermal energy storage in tanks, made in [140] and the estimate made in *SAM* [131]. The computation of the cost of the heat exchanger is given by the following expression

$$C_{HEexch} = C_0 \cdot \left(\frac{Q}{Q_0}\right)^M \cdot \frac{CEPCI}{CEPCI_{ref}}, \quad (5.2.49)$$

where C_{HEexch} is the cost of the exchanger with capacity Q (in this context, A_{exch}) and C_0 the known cost of an exchanger with capacity Q_0 . M is a constant that depends on the type of material in the exchanger. The evaluation of the investment cost for the Two-tank storage system is done on the basis of the estimated cost per unit of thermal energy, $C_{NREL} = 22\$/kWh_{th}$, estimated in the NREL reports [131]. Therefore, according to the above, the total cost of the Two-tank storage system is:

$$C_{Str}(V, A_{exch}) = C_{HEexch}(A_{exch}) + E_{max}(V) \cdot C_{NREL}, \quad (5.2.50)$$

with E_{max} representing the maximum energy produced per hour, during the time horizon.

5.2.3 Bounds

Table 5.4 shows the bounds for the variables of the optimization problem, which differ depending on the Storage System.

VARIABLE	RANGE
Two-tank System	
V	$[0, +\infty[$
A_{exch}	$[0, +\infty[$
\dot{m}_{salt}^S	$[0, 1500]$
\dot{m}_3^S	$[0, 1500]$
T_7	$[290, 560]$
\dot{m}_{salt}^D	$[0, 1500]$
\dot{m}_3^D	$[0, 1500]$
T_8	$[290, 560]$
Thermochemical System	
DEC	$[150, 300]$
ρ_{eng}	$[30, 70]$
r_{sw}	$[0.03, 0.09]$
L	$[0, +\infty)$
P_c^S, P_c^D	$[0.072, 2.753]$
T_{eq}^S	$[25, 125]$
T_{eq}^D	$[-150, -50]$
t_{ini}^S, t_{fin}^S	$[0, +\infty[$
t_{ini}^P, t_{fin}^P	$[0, +\infty[$
t_{ini}^D, t_{fin}^D	$[0, +\infty[$

Table 5.4: Optimization problem variables bounds.

The bounds for the variables corresponding to the Two-tank system have been deduced from [80, 90] and from the energy balance in the system. On the other hand, for the Thermochemical system, these bounds are based on the know-how of PROMES-CNRS, which are presented in [124]. At the end of Table 5.4, the strategic variables (time variables) are presented, which correspond to the initial and final time of each phase of the plant.

5.2.4 Structure of the optimization problem

Optimization Problem for Thermochemical Storage

In this case, according to Section 5.1 and the Subsection 5.2.1, the variables to be optimized would be the following:

- $\nu = (DEC, \rho_{eng}, r_{sw}, L)$.
- $\mu_i = (P_c^S(i, k), \Delta T_{eq}^S(i, k), P_c^D(i, k, j), \Delta T_{eq}^D(i, k, j))$.
- $\tau_i = (t_{ini}^S(i, k), t_{fin}^S(i, k), t_{ini}^D(i, k, 1), t_{fin}^D(i, k, 1), \dots, t_{ini}^D(i, k, j), t_{fin}^D(i, k, j))$, with $j \in J(i, k)$,

where the time intervals for each of the phases are denoted as, $I_S = [t_{ini}^S(i, k), t_{fin}^S(i, k)]$, $I_P = [t_{ini}^P(i, k), t_{fin}^P(i, k)]$ and $I_D = [t_{ini}^D(i, k, j), t_{fin}^D(i, k, j)]$. The optimization problem to solve would be the following:

$$\begin{aligned}
& \max_{\nu, \mu, \tau} \quad NPV = USF(N, \nu_r) \left[\sum_{i=1}^4 R_i (Rev_i(\nu, \mu_i, \tau_i) - Cost_i(\nu, \mu_i, \tau_i)) \right] - C_{invest}(\nu) \\
& \text{subject to } \left\{ \begin{array}{l}
q_S(i, k) = C_{htf} \dot{m}_3(i, k) (T_3 - T_6(i, k)), \\
T_8(i, k) = \frac{94573}{(121.186 - 8314 \cdot \log(P_c^S(i, k)))} - 273.15 \\
\dot{m}_8(i, k) = q_S(i, k) \cdot \frac{M_{water}}{dh_r} \\
T_{cond}^S(i, k) = 5120 / (13.7 - \log(P_c^S(i, k) / 1.013)) - 273.15 \quad \text{if } \tau_i = P, S \\
q_{desu}(i, k) = \dot{m}_8(i, k) \cdot c_{p_steam} \cdot (T_8(i, k) - T_{cond}^S(i, k)) \cdot \\
dh_{vap}(i, k) = -2451.7 \cdot T_{cond}^S(i, k) + 2.5033 \cdot 10^6 \cdot \\
q_{cond}(i, k) = \dot{m}_8(i, k) \cdot dh_{vap}(i, k) \cdot \\
q_2^S(i, k) = q_{desu}(i, k) + q_{cond}(i, k) \cdot \\
\dot{m}_1(i, k, t) = \dot{m}_3^S(i, k) + \dot{m}_4(i, k, t) \\
\dot{m}_1(i, k, t) T_1(i, k, t) = \dot{m}_3^S(i, k) T_6(i, k) + \dot{m}_5(i, k, t) T_5(i, k, t) \\
q_R(i, k, t) = q_{th}(i, k, t) + q_{dis}^u(i, k, t) \\
q_2(i, k, t) = q_{dis} - q_{dis}^u(i, k, t) \\
\dot{W}_{elec}(t) = f_b(q_R(i, k, t), T_2, T_{11}(i, k, t)) \quad \text{if } \tau_i = P \\
\dot{m}_{11}(i, k, t) = f_e(\dot{m}_4(i, k, t), T_{envDay}) \\
T_{12}(i, k, t) = f_d(T_2, \dot{m}_4(i, k, t), T_{envDay}) \\
q_3(i, k, t) = \dot{m}_{11}(i, k, t) \cdot cp_{11} \cdot (T_{12}(i, k, t) - T_{envDay}) \\
W_{q_3}(i, k, t) = 0.02 \cdot q_3(i, k, t) \\
q_D(i, k, j) = C_{htf} \dot{m}_3^D(i, k, j) (T_3(i, k, j) - T_6(i, k, j)) \\
\dot{W}_{elec}(i, k, j) = f_b(q_D(i, k, j), T_3(i, k, j), T_{11}(i, k, j)) \\
q_1(i, k, j) = c_{cw} \dot{m}_{11}(i, k, j) (T_{12}(i, k, j) - T_{13}(i, k, j)) \quad \text{if } \tau_i = D \\
q_3(i, k, j) = \dot{m}_{11}(i, k, j) \cdot cp_{air} \cdot (T_{12}(i, k, j) - T_{11}(i, k, j)) \\
\dot{W}_{elec_q_3}(i, k, j) = 0.02 \cdot q_3(i, k, j) \\
50 \leq q_S(i, k) \quad \text{if } \tau_i = S \\
T_{eq}(P_c^S(i, k)) \leq T_6(i, k) \\
q_{4_min} \leq q_R(i, k, t) \\
C_{htf} \dot{m}_3(i, k, t) (T_3 - T_6(i, k, t)) + C_{htf} \dot{m}_4(i, k, t) (T_4 - T_5(i, k, t)) \leq q_{sol}(i, t) \quad \text{if } \tau_i = P \\
50 \leq q_D(i, k, t) \\
T_3 \leq T_{eq}(P_c^D(i, k, t)) \quad \text{if } \tau_i = P \\
W_{Nom_min} \leq \dot{W}_{elec}^D(i, k, j) \leq W_{Nom_max}
\end{array} \right.
\end{aligned}$$

$$\left\{ \begin{array}{l} 290 \leq T_\alpha(i, k) \leq 590, \text{ with } \alpha=1, \dots, 6. \\ T_{env_min} \leq T_\alpha(i, k) \leq 200, \text{ with } \alpha=7, 11, 12, 13. \\ T_{env_min} \leq T_\alpha(i, k) \leq 590, \text{ with } \alpha=8, 9, 10. \\ 90 \leq \dot{m}_\alpha(i, k) \leq 2000, \text{ with } \alpha=1, 2, 3, 6. \\ 90 \leq \dot{m}_\alpha(i, k) \leq 600, \text{ with } \alpha=4, 5. \\ 200 \leq \dot{m}_\alpha(i, k) \leq 3000, \text{ with } \alpha=7, \dots, 10. \\ 0 \leq \dot{m}_\alpha(i, k) \leq 300, \text{ with } \alpha=11, 12, 13. \\ DEC \in [150, 300] \\ \rho_{eng} \in [30, 70] \\ r_{sw} \in [0.03, 0.09] \\ L \in [0, \infty [\\ P_c^S(i, k), P_c^D(i, k, j) \in [0.072, 2.753] \\ T_{eq}^S(i, k) \in [25, 125] \\ T_{eq}^D(i, k, j) \in [-150, -50] \\ t_{ini}^S(i, k), t_{fin}^S(i, k) \in [0, \infty [\\ t_{ini}^D(i, k, j), t_{fin}^D(i, k, j) \in [0, \infty [\\ \forall i \in \{1, \dots, p\}, \forall k \in \{1, \dots, N_{Days}(i)\}, \forall j \in \{1, \dots, J(i, k)\} \end{array} \right. \quad \text{if } \tau_i = S, P, D.$$

Optimization Problem for Two-tank Storage

In this case, as described in the Section 5.1 and the Subsection 5.2.1, the variables to be optimized would be the following:

- $\nu = (V, A_{exch})$.
- $\mu_i = (\dot{m}_3^S(i, k), \dot{m}_{salt}^S(i, k), T_7(i, k), \dot{m}_3^D(i, k, j), \dot{m}_{salt}^D(i, k, j), T_8(i, k, j))$.
- $\tau_i = (t_{ini}^S(i, k), t_{fin}^S(i, k), t_{ini}^D(i, k, 1), t_{fin}^D(i, k, 1), \dots, t_{ini}^D(i, k, j), t_{fin}^D(i, k, j))$, with $j \in J(i, k)$,

The optimization problem to solve takes the general form:

$\max_{\nu, \mu, \tau}$

$$NPV = USF(N, t_r) \left[\sum_{i=1}^p R_i(Rev_i(\nu, \mu_i, \tau_i) - Cost_i(\nu, \mu_i, \tau_i)) \right] - C_{invest}(\nu)$$

$$\text{subject to } \left\{ \begin{array}{l} \left\{ \begin{array}{l} q_S(i, k) = C_{htf} \dot{m}_3^S(i, k)(T_3 - T_6(i, k)), \\ q_S(i, k) = C_{salt} \dot{m}_{salt}^S(i, k)(T_8(i, k) - T_7(i, k)) \\ q_D(i, k) = \frac{1}{2} \alpha \cdot A_{exch} \cdot ((T_3 + T_6(i, k)) - (T_7(i, k) + T_8(i, k))). \end{array} \right. \quad \text{if } \tau_i = S \\ \left\{ \begin{array}{l} \dot{m}_1(i, k, t) = \dot{m}_3^S(i, k) + \dot{m}_4(i, k, t) \\ \dot{m}_1(i, k, t) T_1(i, k, t) = \dot{m}_3^S(i, k) T_6(i, k) + \dot{m}_5(i, k, t) T_5(i, k, t) \\ q_R(i, k, t) = q_{sol}(i, t) - q_S(i, k) \\ q_R(i, k, t) = C_{htf} \dot{m}_3^S(i, k)(T_4 - T_5(i, k, t)) \\ \dot{W}_{elec}(i, k, t) = f_b(q_R(i, k, t), T_2, T_{env}^d) \\ \dot{m}_4(i, k, t) = f_f(\dot{W}_{elec}(i, k, t), T_2, T_{env}^d) \end{array} \right. \quad \text{if } \tau_i = P \\ \left\{ \begin{array}{l} q_D(i, k, j) = C_{htf} \dot{m}_3^D(i, k, j)(T_3(i, k, j) - T_6(i, k, j)) \\ q_D(i, k, j) = C_{salt} \dot{m}_{salt}^D(i, k, j)(T_8(i, k, j) - T_7(i, k, j)) \\ q_D(i, k, j) = \frac{1}{2} \alpha \cdot A_{exch} \cdot ((T_3(i, k, j) + T_6(i, k, j)) - (T_7(i, k, j) + T_8(i, k, j))) \\ T_5(i, k, j) = (\dot{m}_3^D(i, k, j), T_4(i, k, j), T_{env}^n) \\ \dot{W}_{elec}(i, k, j) = f_b(q_D(i, k, j), T_4(i, k, j), T_{env}^n) \end{array} \right. \quad \text{if } \tau_i = D \\ \left\{ \begin{array}{l} V_{cold}(t_{fin}^S(i, k)) = V_{cold}(t_{ini}^S(i, k)) - V_{new}^S(t_{fin}^S(i, k)), \\ V_{hot}(t_{fin}^S(i, k)) = V_{hot}(t_{ini}^S(i, k)) + V_{new}^S(t_{fin}^S(i, k)), \\ V_{hot}(t_{fin}^D(i, k, j)) = V_{cold}(t_{ini}^D(i, k, j)) + V_{new}^D(t_{fin}^D(i, k, j)), \\ V_{hot}(t_{fin}^D(i, k, j)) = V_{hot}(t_{ini}^D(i, k, j)) - V_{new}^D(t_{fin}^D(i, k, j)), \\ T_{cold}(t_{fin}^S(i, k)) = T_{cold}(t_{ini}^S(i, k)), \\ T_{hot}(t_{fin}^S(i, k)) = \frac{T_{cold}(t_{ini}^S(i, k)) \cdot V_{hot}(t_{ini}^S(i, k)) \cdot \rho_{salt} + T_8(t_{fin}^S(i, k)) \cdot \int_{t_{ini}^S(i, k)}^t \dot{m}_{salt}^S(t_{fin}^S(i, k)) dt}{V_{hot}(t_{fin}^S(i, k)) \cdot \rho_{salt}}, \\ T_{cold}(t_{fin}^D(i, k, j)) = \frac{T_{cold}(t_{ini}^D(i, k, j)) \cdot V_{cold}(t_{ini}^D(i, k, j)) \cdot \rho_{salt} + T_7(t_{fin}^D(i, k, j)) \cdot \int_{t_{ini}^D(i, k, j)}^t \dot{m}_{salt}^D dt}{V_{cold}(t_{fin}^D(i, k, j)) \cdot \rho_{salt}}, \\ T_{hot}(t_{fin}^D(i, k, j)) = T_{cold}(t_{fin}^D(i, k, j)), \\ 50 \leq q_S(i, k) = \frac{2 \cdot C_{htf} C_{salt} \dot{m}_3^S(i, k) \dot{m}_{salt}^S(i, k) \cdot \alpha \cdot A_{exch} \cdot (T_2 - T_7(i, k))}{2 \cdot C_{htf} C_{salt} \dot{m}_3^S(i, k) \dot{m}_{salt}^S(i, k) + C_{htf} \dot{m}_3^S(i, k) \alpha A_{exch} + C_{salt} \dot{m}_{salt}^S(i, k) \alpha A_{exch}} \\ 260 \leq T_6(i, k) = \frac{-q_S(i, k)}{C_{htf} \dot{m}_3^S(i, k)} + T_3 \leq 590 \\ 220 \leq T_8(i, k) = \frac{q_S(i, k)}{C_{salt} \dot{m}_{salt}^S(i, k)} + T_7(i, k) \leq 600 \\ C_{htf} \dot{m}_3^S(i, k)(T_3 - T_6(i, k)) \leq q_{sol}(i, t) \\ q_{4_min} \leq q_R(i, k, t) \\ C_{htf} \dot{m}_3^S(i, k)(T_3 - T_6(i, k)) + C_{htf} \dot{m}_4(i, k, t)(T_4 - T_5(i, k, t)) \leq q_{sol}(i, t) \\ 50 \leq q_D(i, k, j) \\ 260 \leq T_3(i, k, j) \\ 260 \leq T_5(i, k, j) = f_c(\dot{m}_3^D(i, k, j), T_4(i, k, j), T_{env}^n) \leq 590 \\ 220 \leq T_7(i, k, j) = \frac{-q_D(i, k, j)}{C_{salt} \dot{m}_{salt}^D(i, k, j)} + T_8(i, k, j) \leq 600 \\ W_{Nom_min} \leq \dot{W}_{elec}^D(i, k, j) \leq W_{Nom_max} \\ V_{min}(V) \leq V_{cold}, V_{hot} \leq V_{max}(V) \\ 280^\circ\text{C} \leq T_{cold}, T_{hot} \leq 590^\circ\text{C} \end{array} \right. \quad \text{if } \tau_i = S, P, D. \end{array} \right.$$

$$\left\{ \begin{array}{l} \left\{ \begin{array}{l} V_{cold}(0) = V_{cold}(H_i) \\ V_{hot}(0) = V_{hot}(H_i) \\ T_{cold}(0) = T_{cold}(H_i) \\ T_{hot}(0) = T_{hot}(H_i) \end{array} \right. \quad \forall i \in \{1, \dots, p\} \\ \left\{ \begin{array}{l} V \in [0, \infty[\\ A_{exch} \in [0, \infty[\\ \dot{m}_{salt}^S(i, k) \in [0, 900] \\ \dot{m}_3^S(i, k) \in [0, 900] \\ T_7(i, k) \in [290, 560] \\ \dot{m}_{salt}^D(i, k, j) \in [0, 900] \\ \dot{m}_3^D(i, k, j) \in [0, 900] \\ \hat{T}_8(i, k, j) \in [290, 560] \\ t_{ini}^S(i, k), t_{fin}^S(i, k) \in [0, \infty[\\ t_{ini}^D(i, k, j), t_{fin}^D(i, k, j) \in [0, \infty[\end{array} \right. \\ \forall i \in \{1, \dots, 4\}, \quad \forall k \in \{1, \dots, N_{Days}(i)\}, \quad \forall j \in \{1, \dots, J(i, k)\} \end{array} \right.$$

5.3 Results and Discussion

In this section, we present the different simulations carried out for the comparative study with different «profiles», that is different economic indicators; different production strategies; different storage systems; and even possibly different price scenarios or different correction coefficients β . The model proposed in the previous sections has been implemented in the case of Californian markets, more precisely with the data corresponding to the network node of Daggett. Thus the solar resource (used with $SM = 2.5$) and market prices are the ones corresponding to this location. Nevertheless, as in many deregulated market around the world, the prices on the Californian electricity market has been subject to important perturbations in the recent years and it is quite difficult to determine a «mean profile» of prices. Therefore we decided to focus on a scenarios analysis, emphasizing the potential influence of such perturbations on the results. The Price-Pessimistic scenario (PP) corresponds to the price profiles of year 2016 (with low prices) which was also used in [124, 125], thus allowing to compare both studies. An optimistic scenario has been elaborated on the base of the mean price in California in 2021. But in order to avoid that this sensitivity analysis would be perturbed by a difference of profiles instead of the difference of mean prices, the Price-Optimistic scenario (PO) corresponds to the prices profile of 2016 shifted by the difference of mean prices between 2021 and 2016, that is by $16.3\$/MWh$. The mean price of 2021 was preferred to the ones of 2022 which are quite extreme (reaching often $124\$/MWh$). In fact, between 2020 and 2021 the average price difference was also high, equal to 14.64. Finally, a Price-Medium scenario (PM) is considered for the difference between the average price of the years 2020 and 2021, and the average price of the year 2016, that is by $9\$/MWh$.

The real discount rate is set as $\iota_r = 0.03$ and the number of years as $N = 30$. In some simulations a sensitivity analysis on these parameters will be done. We consider $p = 4$ seasons, with a stage of $N_{days} = 7$ each. For $i = 1, \dots, 4$ (each index representing a season), the curves of useful power $q_{sol}(\cdot, i)$ (see Subsection 4.2.1) and electricity price $\lambda(\cdot, i)$ (see 4.3), are taken from [124, 125], whose data comes from the SAM software and the average electricity prices for each day during each season of year 2016 (Price-Pessimistic scenario).

5.3.1 Computational Implementation

The solution of the different optimisation problems were obtained with MATLAB® version 9.9.0.1570001 (R2020b) using the *fmincon* function with the interior point algorithm [129].

This implementation required a large computational processing capacity, mainly due to the number of variables of these problems (see 5.2.4 and 5.2.4), which varies depending on the type of Storage System and production strategy. Moreover, for certain configurations, convergence problems occur. Hence, it has been needed to look for an alternative approach to obtain optimal results in a reasonable time.

When considering the Two-tank system, we propose to split the search for a best local minimum by two loops, as shown in Algorithm 1. In this case, the physical variable V , which represents the maximum volume of molten salt used during the model year (and therefore for the entire time horizon N), is left fixed and the problem is solved for the rest of the variables. In this way, we get a while loop with a subroutine of iterations corresponding to the command *fmincon* (the number of iterations for this subroutine can also be fixed). For each iteration of the while loop of the variable V , the convergence is verified, based on different tolerance criteria, towards an optimal value of V^* .

Algorithm 1: Double loop - Interior point

Input: $x_0 = (V_0, A_{exch}^0, \dots, \cdot) \in \mathbb{R}^n$,
 $k = 0, exitflag = 2, \varepsilon > 0$,
 $V_0 = 10000, V_A = V_0 + 2\varepsilon$,
 $x_0^{aux} = (A_{exch}^0, \dots, \cdot) \in \mathbb{R}^{n-1}$;

- 1 **while** $|V_0 - V_A| > \varepsilon$ and $k < maxiter$ and $exitflag = 2$, **do**
- 2 $V_0 = V_A$;
- 3 $[x, fval, exitflag, output] = fmincon(fun, x_0^{aux}, \dots, \cdot)$ $V_A = \max\{V_i\}$, // $i = 1, \dots, 4$.
- 4 $k = k + 1$
- 5 $V = V_A$;
- 6 **return** $x = (V, A_{exch}, \dots, \cdot)$;

Now when considering Thermochemical storage, before executing the optimization process, the physical variables have been rescaled to avoid numerical instabilities.

In what follows, we provide a comparison of the results of the optimization process for different economic criteria. We compare the Two-tank system with the Thermochemical system under the different values of beta (see cost equation 5.2.45) for the cost estimation of the reactor.

5.3.2 LCOE sensitivity to discharge duration

For this first analysis, the economic indicator LCOE is used and the discharge duration for the two storage systems in question were varied. Different price scenarios (PP, PM, PO) were considered but their influence is minor since the LCOE criterion doesn't take into account revenues/incomes of the plant. Thus the different of price scenario only acts on the

costs associated to the use of electricity (pumping, heliostats, dissipation). More important influence of the price scenarios will be observed in the forthcoming subsections where NPV criterion will be used. Here since we focus only on LCOE criterion, the price profile is not taken into account (for revenues/incomes) and the Discharge strategy is only the Classical one.

As can be observed in Figures 5.9 and 5.10, in all cases the Two-tank system is the most economically efficient to implement. Furthermore, it can be observed that the compensation of the income generated from considering more time in the Discharge phase is maintained for all cases for the Two-tank system, hence its slow decrease. For the Thermochemical system, in the optimistic case ($\beta = 1$, continuous red curve), the results found indicate that if we consider a Discharge phase greater than 10 hours, the costs of producing electricity increase. This is reflected mainly when comparing the results of 10h and 12h, where we can observe a change in the behavior of the curve (continuous red, Figure 5.9 - 5.10), and this is due to the cost of considering a larger Thermochemical reactor to discharge energy for a longer time is not compensated by the production of electrical energy. In the other cases ($\beta = 2, 3$), we can notice a more sensitive behavior of the curves that represent them, since when considering higher costs for the Storage System, they present a peak for the 6 hours of duration and then a valley approximately in the 10 hours of duration, which is due to insufficient production of electric energy and to an excessively large design of the Storage System. Finally, if we compare the most viable cases of both systems (12h duration for Two-tanks and 10h duration for Thermochemical reactor with $\beta = 1$), we have that the cost of energy production is reduced by approximately 27%.

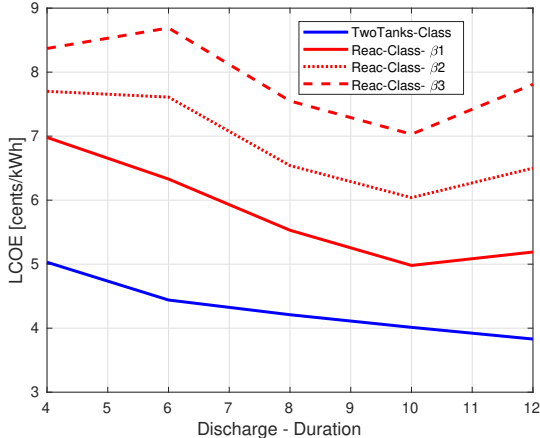


Figure 5.9: LCOE values, changing the discharge duration with the classic strategy, $SM = 2.5$, $N = 30$ years and $\iota_r = 3\%$. PP scenario.

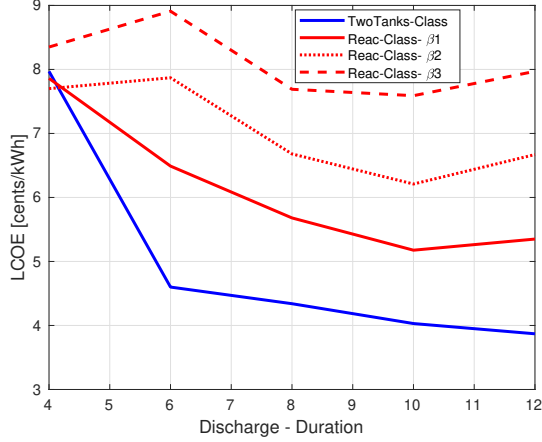


Figure 5.10: LCOE values, changing the discharge duration with the classic strategy, $SM = 2.5$, $N = 30$ years and $\iota_r = 3\%$. PO scenario.

The results in Figure 5.9 and 5.10, show very low LCOE values for both storage systems, which are comparable to those estimated in [78, 108, 71, 128]. Let us nevertheless recall that, fossil fuel technologies have a projected LCOE for the year 2035 in the range of approximately 3.49-7.09 cents/kWh [86].

5.3.3 Sensitivity analysis based on NPV criterion

In this subsection, the optimization (actually maximization) will be done using the NPV economical criterion, thus taking into account the revenues generated by electricity sales. Thus the different price scenarios will clearly have an influence on the results.

NPV sensitivity to discharge duration

The sensitivity analysis being here focusing on the Discharge duration, only the Classical strategy will be considered. Tables 5.5 - 5.7 and Figures 5.11- 5.12 show the NPV values with respect to the variation of the discharge duration. For the PP scenario, we can notice the strong evolution of the curves corresponding to the Thermochemical system, as they decay rapidly after 6 hours of discharge duration (see Figure 5.11). The best configuration corresponds to "Reac-Class- β_1 " with a discharge duration equal to 6 hours. For the Two-tank system, the behavior of the blue curve is opposite to the others, since it has a slow and constant growth from a certain point. For this system, the best configuration corresponds to "Two-tanks-Class" with 12 hours discharge duration. It is clear that for both storage systems, the plant project does not recover the investment (negative NPV). A similar analysis happens for the PM scenario.

Time	4h	8h	12h
Incomes PP	133.55	166.45	174.75
NPV PP[M€]	-134.36	-129.73	-158.40
Incomes PM	177.74	230.95	233.69
NPV PM[M€]	-94.44	-62.12	-104.00
Incomes PO	215.25	277.64	293.76
NPV PO[M€]	-60.38	-19.45	-15.18

Table 5.5: Thermochemical reactor system with Classical strategy, $\beta = 1$.

Time	4h	8h	12h
Incomes PP	135.14	170.15	177.08
NPV PP[M€]	-151.95	-157.81	-246.66
Incomes PM	180.74	230.92	235.61
NPV PM[M€]	-110.78	-98.01	-392.02
Incomes PO	218.0	277.90	287.51
NPV PO[M€]	-77.28	-54.21	-146.66

Table 5.6: Thermochemical reactor system with Classical strategy, $\beta = 2$.

Time	4h	8h	12h
Incomes PP	152.61	184.65	207.89
NPV PP[M€]	-104.50	-91.96	-89.05
Incomes PM	203.62	246.79	260.96
NPV PM[M€]	-58.46	-39.81	-45.69
Incomes PO	245.13	297.25	339.60
NPV PO[M€]	-22.62	8.40	28.87

Table 5.7: Two-tank system with Classical strategy.

Additional results have shown that the variations of NPV when one considers either one Discharge phase or two Discharge phases are minor. Thus in the forthcoming subsection, and for simplicity, we will essentially consider configurations with only one Discharge phase.

For the PO scenario, the Thermochemical system continues to show greater sensitivity to the change in discharge duration. Here, the best configuration is "Reac-Class- β_1 ", with a duration of 8 hours. Note that, the NPV value improved by 3 times (on negative values) compared to the PP scenario. For the case of "Reac-Class- β_2 ", we have a variation in the behavior of the NPV curve coinciding with the first case in that the best configuration corresponds to a duration of 8h. Finally, for the "Reac-Class- β_3 ", the results are analogous to those deduced with the PP scenario.

When considering the PO scenario the NPV values increase of more than 100 M€ in most cases, which allowed that for a period of 30 years and under plant configurations with a duration in the Discharge phase of more than 6 hours, it was possible to obtain a positive NPV, i.e., the plant recovers the investment.

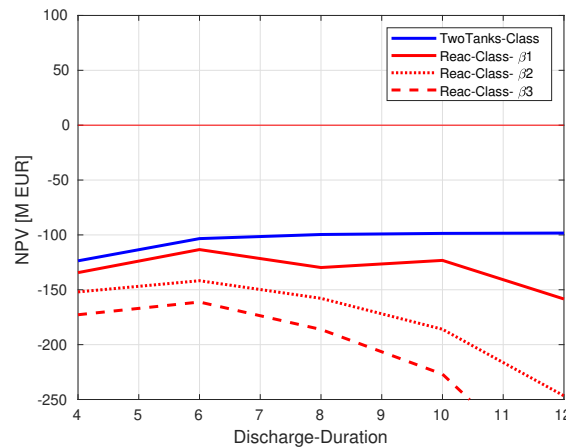


Figure 5.11: NPV values, changing the discharge duration with the classic strategy, $SM = 2.5$, $N = 30$ years and $\iota_r = 3\%$. Price-Pessimistic scenario.

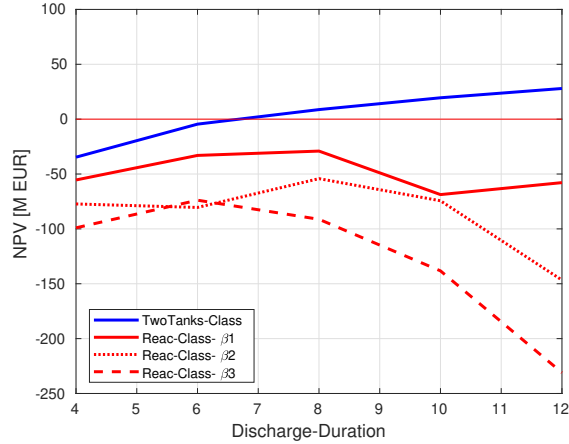


Figure 5.12: NPV values, changing the discharge duration with the classic strategy, $SM = 2.5$, $N = 30$ years and $\iota_r = 3\%$. Price-Optimistic scenario.

Optimal production profiles

In parallel to the optimization of the sizing of the storage systems, the optimization problems are also aimed at optimizing the plant production operations. According to the production strategies described in Subsection 4.5, the optimized strategies found for both storage systems will be analyzed. Finally, the consideration of different price scenarios does not represent important variations in the operating profiles. Therefore, the price scenarios in question will not be specified in this subsection.

Thermochemical system In this subsection, our aim is to combine the most innovating approaches, that are Thermochemical system and Price Chasing strategy (see [124, 125]).

Figures 5.13 and 5.14 show the operational profiles of the plant with the Thermochemical storage system using Price Chasing as production strategy, for 7 days (upper graph) together with the electricity production and price curve for the same time horizon (lower graph), corresponding to Winter season.

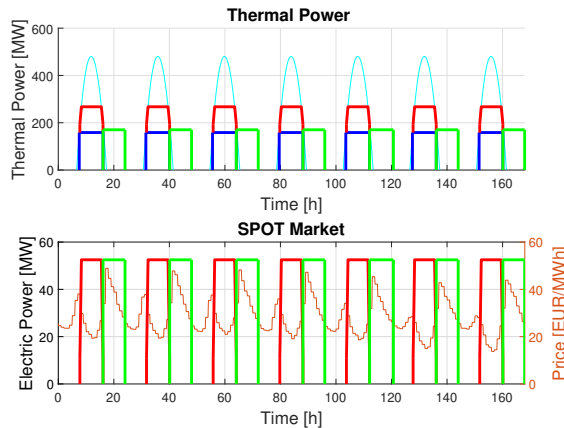


Figure 5.13: Winter season, Thermochemical system with Price Chasing strategy - 1 Discharge phase.

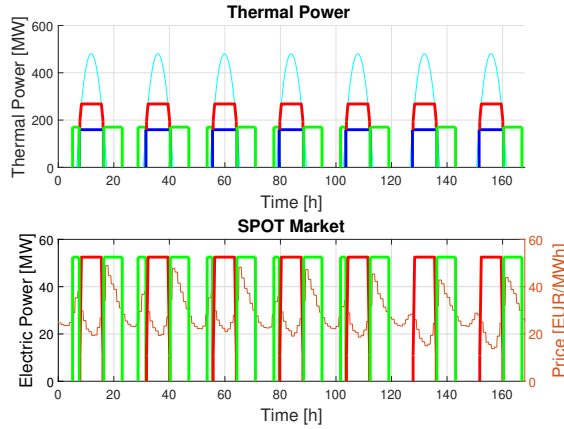


Figure 5.14: Winter season, Thermochemical system with Price Chasing strategy - 2 Discharge phases.

It can be observed that in the case of a single discharge (Figure 5.13), the discharge takes place immediately after the end of the Storage phase, mainly for two reasons: the first one is due to the highest peaks of the price curve, approximately after the beginning of the night; and the second one, due to the cost that would entail to restart the power block. Then, Figure 5.14 shows the operational profile for two Discharge phases per day, where Discharge phases are carried out in those time intervals where the value of the electricity price is higher. One can indeed observe that the optimisation aligns both Discharge phases with price peaks.

Similarly, in Figures 5.15 and 5.16, the operation profiles in the summer season are shown. In both cases, a continuous production of electrical energy is obtained and considering two Discharge phases instead of one does not have any relevant effect. The relevance of multiple Discharge phases is related to the storage capacity of the plant. Indeed, in the case of the Winter season (Figure 5.14), the amount of stored energy was not enough to have a continuous production.

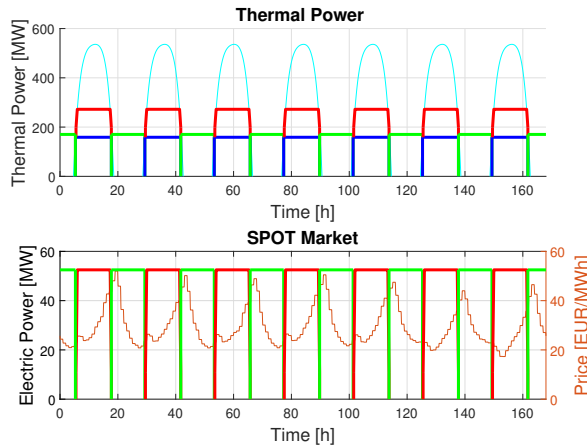


Figure 5.15: Summer season, Thermochemical system with Price Chasing strategy - 1 Discharge phase.

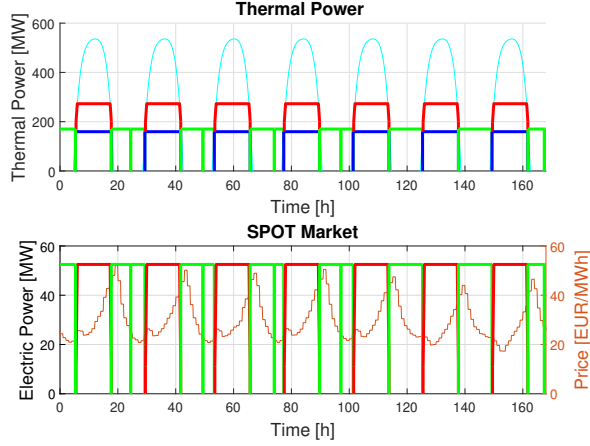


Figure 5.16: Summer season, Thermochemical system with Price Chasing strategy - 2 Discharge phases.

Here, the production strategy used is Price Chasing, with which a positive NPV is obtained for the price (PO) and cost coefficient $\beta = 1$. We can also see the large effect of considering a specific production strategy for the plant. Indeed, when comparing Classical and Price Chasing strategies combined with Thermochemical system, then with Classical strategy positive NPV is never reached (see Table 5.5) while with Price Chasing strategy, in the PO scenario, a positive NPV is obtained for the configuration “Reac-PC-1D- β_1 ” (see Table 5.8). Now, if we compare the configurations “Reac-Class- β_1 -6h” (see figures 5.11 and 5.12) and “Reac-PC-1D- β_1 ” (see tables 5.8 and 5.9), we note that in this case, the implementation of the Price Chasing strategy increases the NPV by approximately 40 M€ (with respect to $N = 30$ years), for the PP and PO price scenarios.

Parameter	$\beta = 1$	$\beta = 2$	$\beta = 3$
Incomes PP	195.98	171.03	163.59
NPV PP [M€]	-94.12	-117.15	-134.63
Incomes PM	274.03	246.60	224.26
NPV PM [M€]	-29.40	-62.39	-84.16
Incomes PO	334.94	321.91	287.15
NPV PO [M€]	24.20	-14.44	-40.74

Table 5.8: Economic results considering different β for Thermochemical storage system and Price Chasing strategy with one Discharge phase. $SM = 2.5$, $N = 30$ years and $\iota_r = 3\%$.

Parameter	$\beta = 1$	$\beta = 2$	$\beta = 3$
Incomes PP	190.65	165.79	162.28
NPV PP [M€]	-99.61	-123.99	-138.06
Incomes PM	271.48	243.46	224.63
NPV PM [M€]	-30.73	-61.79	-83.33
Incomes PO	332.71	295.76	286.84
NPV PO [M€]	23.61	-14.65	-39.06

Table 5.9: Economic results considering different β for Thermochemical storage system and Price Chasing strategy with two Discharge phases. $SM = 2.5$, $N = 30$ years and $\iota_r = 3\%$.

Two-tank system In Figures 5.17 and 5.18, the operational profiles of the plant with a Two-tank system are shown. These profiles correspond to the Classical 12-hour discharge duration strategy, which according to the sensitivity analysis performed in the Subsection 5.3.3, is the most cost-efficient. A negative effect of this strategy with fixed discharge duration

is that the plant must discharge regardless of the market value price: first, in Figure 5.17, it can be observed that the Discharge phase for each day ends in the price valleys that occurs in the evening hours; second, the cost related to the large sizing of the Storage System for discharges of such a length is quite high.

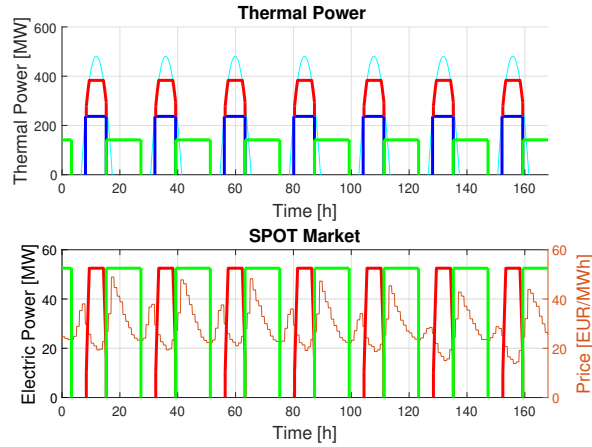


Figure 5.17: Winter season, Two-tank storage system with Classical production strategy.

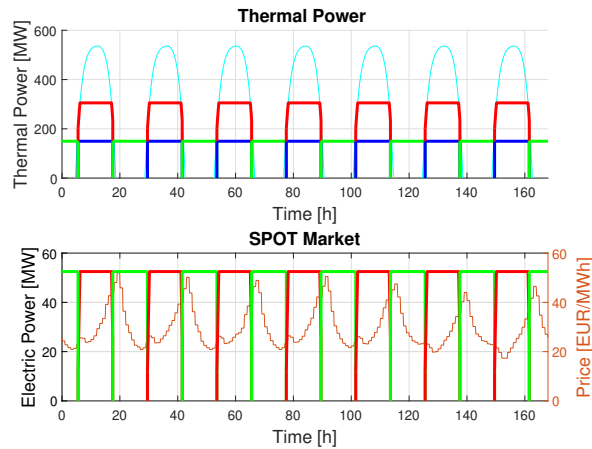


Figure 5.18: Summer season, Two-tank storage system with Classical production strategy.

If we compare this Storage System with the best configurations for each production strategy, Two-Tanks-Class-12h and Two-tanks-PC-1D, this is opposite to what happens with the Thermochemical system, since the Classical strategy is more cost-effective, increasing the NPV value by approximately 16 M€ for the PO price scenarios and a period of 30 years (see Table 5.10). As can be checked in Table 5.10, in this case, the Storage System has been sized larger for the case of the Price Chasing strategy, and therefore it is more costly.

Strategy	Classical-12h	Price Chasing
Incomes	339.60	357.16
Operational cost	11.32	11.44
Maintenance cost	25.40	26.62
Storage system cost	44.97	88.09
Solar field cost	148.06	148.06
Power block cost	69.67	69.67
NPV PO [M€]	28.87	13.29

Table 5.10: Economic results for the Two-tank system considering different strategies of production and the PO price scenario. $SM = 2.5$, $N = 30$ years and $t_r = 3\%$.

5.3.4 Conventional Payback

It is well-known that in the case of CSP equipped with Two-tanks storage system one cannot reach a valuable CPB (i.e. a CPB value lower than the project duration) without subsidies [99]. Thus here we only focus on Thermochemical storage system.

In order to identify the time needed to obtain or recover the investment in a CSP plant, the optimization problem to be solved will be to maximize the NPV indicator, varying the parameter corresponding to the number of years, N , as well as considering different production strategies for each of the storage systems. For this indicator, the case studies corresponding to the Price Chasing strategies are also considered. Therefore, we will detail the most relevant configurations for the CSP plant according to the type of Storage System.

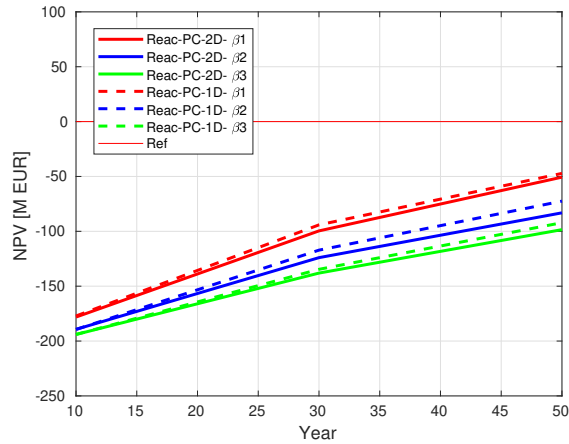


Figure 5.19: Thermochemical system, Price Chasing strategy with one and two Discharge phases, different values for cost parameter β , $SM = 2.5$, $t_r = 3\%$ and PP scenario.

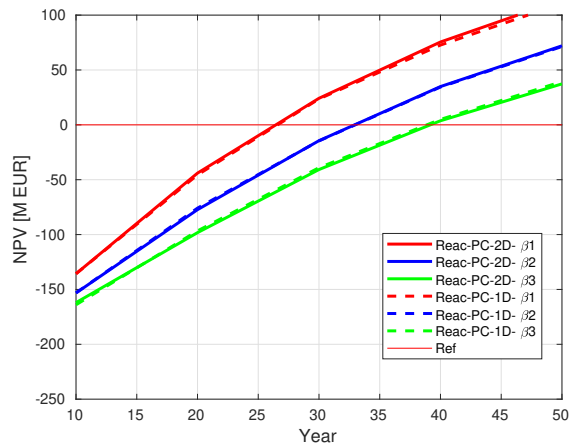


Figure 5.20: Thermochemical system, Price Chasing strategy with one and two Discharge phases, different values for cost parameter β , $SM = 2.5$, $t_r = 3\%$ and PO scenario.

In the Figures 5.19-5.20, we analyzed configurations with the Thermochemical system and the Price Chasing production strategy (one and two Discharge phases). For the PP

scenario, we can notice that the different configurations require more than 50 years to recover the investment. Under such conditions, this type of systems cannot become economically competitive. A similar case happens with the Thermochemical system worked out in [21]. For the PO scenario, the first configurations to recover the investment correspond to the optimistic cost cases ($\beta = 1$) with the Price Chasing strategy of one and two Discharge phases. A time horizon of 26 years, respectively 28 years is necessary to obtain a positive NPV. But for $\beta = 2$ (resp. 3), our results show that 30 years (resp. 40 years) are necessary. Finally, we can note that in the case of the PP scenario, we can observe a similar behavior of the curves for all the β cases, with a small difference between both curves of the same color, with the strategy of a single Discharge phase (1D) better than that of two Discharge phases (2D). In the case of the PO scenario, we can analyse that the difference between the one and two discharge strategies is negligible.

It is important to emphasize that, to our knowledge, it is the first time that an optimal configuration of a storage in a CSP plant attains a positive NPV with a "reasonable" time horizon (less that 30 years).

5.3.5 Internal Rate of Return

Another approach consists in analysing to what extent the possible fluctuations of the currency price can affect the economical efficiency of the CSP power plant with storage. Hence the importance of the parameter ι_r , which is used to depreciate future money transactions and determine their current values. The following results correspond to the maximization of the NPV indicator by varying the real discount rate until the initial investment is recovered. In this subsection, we decided to present the sensitivity analysis of the Internal Rate of Return only for the PM scenario, that is the mean price scenario.

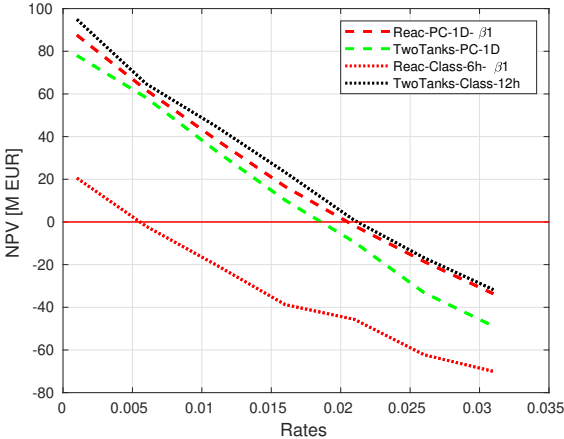


Figure 5.21: These simulations correspond to the Classical and Price Chasing strategies with both storage systems. $SM = 2.5$, $N = 30$ years and PM scenario.

Analyzing the evolution of the different curves for each configuration in Figure 5.21, we can observe that, as in the case study with the CPB indicator, the configuration of the Thermochemical system with the classic production strategy is the one that presents the most deficient results that is the plant can recover the investment only with very small rates. On the other hand, the other configurations recover the initial investment, within a period of 30 years, considering a rate up to approximately $\iota_r = 2\%$. Such a rate is particularly

reasonable with regards to real life data. This shows that, for each of these configurations, the CSP plant will be economically efficient for a large set of values of rate ι_r .

Finally the most favorable configurations, independently of the variations of the real discount rates, correspond to the Two-tank system with the Classical strategy (Two-tanks-Class-12h) and the Thermochemical system with the Price Chasing (Reac-PC-1D- β_1).

5.3.6 Comparison of some typical profiles

Comparing only the Price Chasing operation strategy with one Discharge phase for the two storage systems (see Table 5.11), the revenues produced with the Two-tank system are higher, but this implies a larger investment in the Storage System. In contrast, the Thermochemical storage is designed to be smaller, attacking only the first peak of prices. In other words, the Thermochemical system maintains a more efficient balance between investment costs and revenues, for all price scenarios.

YEAR	10	30	50
Two-tanks			
Incomes PP	94.73	219.21	287.93
NPV PP [M€]	-208.50	-108.67	-62.53
Incomes PM	124.57	288.06	378.28
NPV PM [M€]	-179.67	-42.08	24.73
Incomes PO	155.24	357.16	466.40
NPV PO [M€]	-168.34	13.29	134.63
Thermoch.			
Incomes PP	71.87	195.98	240.87
NPV PP [M€]	-177.14	-94.12	-47.20
Incomes PM	103.63	271.48	358.89
NPV PM [M€]	-152.85	-30.73	40.49
Incomes PO	118.85	332.71	439.16
NPV PO [M€]	-135.73	23.21	110.63

Table 5.11: Economic results for Thermochemical and Two-tank storage system (with Price Chasing strategy, one Discharge phase), considering different years.

Now, comparing the most relevant cases of a CSP plant with different storage systems and operating strategies (see Figures 5.22 and 5.23), we can highlight the configurations that have a better behavior compared to the rest.

When considering the PP scenario, a CSP plant with any of the configurations in question would not be able to recover the investment in less than 50 years.

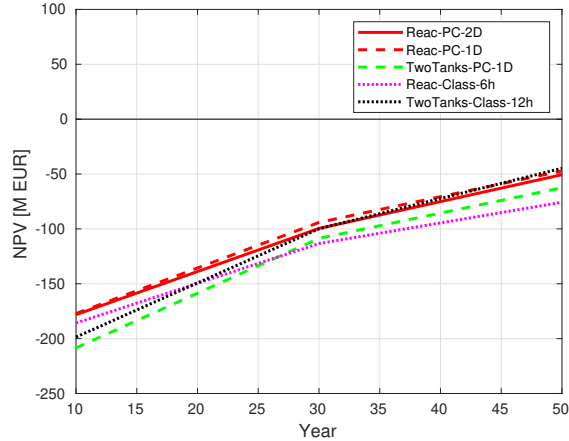


Figure 5.22: These curves correspond to the different storage systems with the Price Chasing and Classical operation strategies. $SM = 2.5$, $\iota_r = 3\%$ and PP scenario.

When considering the scenario PO, we can see in Figure 5.23 several changes in the results. First, we have that all the evaluated configurations, except the Reac-Class-6h, obtain a positive value for the NPV after 26 years. Excluding the Reac-Class-6h case and analyzing the evolution of the curves of the other configurations, we can notice that the best configuration corresponds to Reac-PC-1D, with a small advantage on the second configuration, that is Two-Tanks-Class-12h. The Thermochemical system presents a higher cost-efficiency in the operation of the plant.

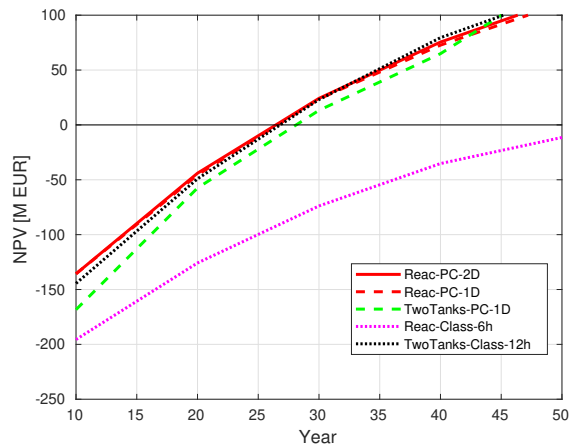


Figure 5.23: These curves correspond to the different storage systems with the Price Chasing and Classical operation strategies. $SM = 2.5$, $\iota_r = 3\%$ and PO scenario.

Let us emphasize that the optimization problems are solve using the all purpose optimization tool `fmincon` of Matlab (with interior point methods). The problem being highly non-convex, the obtained solutions (physical/operational variables) are only stationary point or at the best local minimums and they depend on the initial point. As a consequence the optimisation in the case of Price Chasing strategy (thus with an higher degree of liberty) could possibly not reach the same optimal value as the more restricted optimisation with Classical strategy. This situation can be observed in Figure 5.22 between the curves «Two tank-PC-1D»and «Two tanks-Class-12h». The difference, in terms of NPV values, is nevertheless no

significant for a -somehow classical- lifespan of the project of 30 years (see [31, 130]).

5.4 Conclusion

In conclusion, the main objective of this work was to develop a comparative study of the feasibility and economic efficiency of a CSP plant with different storage systems and production strategies, along with the impact of considering different pricing scenarios. In these cases studied, we have a parallel between technologies and strategies commercially implemented and those that are still in development phase.

First, when the sensitivity study was carried out using only the classical LCOE criterion, with Classical strategy and varying the discharge duration, in both the PP and PO scenarios, the Two-tank system with a duration of 12 hours for the Discharge phase was the most cost efficient to implement. On the other hand, it should be noted that for the Thermochemical system (optimistic case $\beta = 1$, 10 hours of Discharge phase) a very low value was also obtained. But of course, since the LCOE indicator does not take into account incomes, different price scenarios do not generate important variations of the LCOE (see Figure 5.9 and 5.10).

For the second sensitivity study, again with Classic strategy but using now the NPV criterion, in all prices scenarios the results also indicated that the Two-tank storage system was the most cost-effective. Moreover, in the case of the PO scenario, we obtained a positive NPV for Discharge phases longer than 7 hours. For the Thermochemical system the most cost-efficient corresponds to a Discharge phase of 8 hours (the best configuration) while the optimal duration is of 6 hours if the PP scenario is considered.

For the third case study, using the CPB criterion and for the PO scenario, we obtained that, after a period of 26 years, the investment is recovered with the configurations Reac-PC-1D and Two-Tanks-Class-12h. When the IRR criterion is used, the best configuration corresponds to Two-Tanks-Class-12h, obtaining a NPV equal to zero for a real discount rate $\iota_r = 2.1\%$ over a time horizon equal to 30 years. Note that the configuration Reac-PC-1D reaches extremely similar performance.

These case studies also enlighten how the consideration of different prices scenarios impacted the sizing, operation and economic benefit of the CSP. Notice that considering the NPV, CPB and IRR indicators using the PO scenario, we found that it was possible to recover the investment mainly in a period of 30 years. It is important to emphasize that no subsidies are considered in this work.

One of the main contribution of this work is not only to provide a large spectrum tool (with possible variations of the economical criterion, of the electricity price, of the real discount rate) but more importantly to emphasize the real pertinence of an optimisation process in which the optimal design of the storage and the optimal operation are jointly (and not sequentially) decided/computed. And this allows to prove that an economical equilibrium for CSP is possible both with Two-tanks and Thermochemical technologies.

Some possible extensions could be first to integrate to the configuration of a hybrid storage system (Two-tanks/Thermochemical), second, to investigate the feasibility of considering operating strategies for long periods of time like inter-seasonal strategies and third to reinforce the present analysis by using specific optimization methods to better embrace the high non-

convexity of the problem.

Chapter 6

Optimal Operation of a CSP plant under DNI perturbations using switch controls

Solar irradiation variability is one of the primary challenges confronting solar power plants [48]. The amount of solar radiation received varies throughout the day and year due to Earth's rotation and atmospheric factors. This leads to fluctuations in electricity production, making solar energy generation intermittent rather than constant. Additionally, the geographic location of a solar plant also influences the amount of solar radiation received, which can affect its efficiency. On the other hand, studies are currently being conducted to counteract the uncertain variability resulting from weather conditions, like the presence of clouds and rain can dramatically reduce the amount of sunlight reaching photovoltaic panels or mirrors in concentrated solar power plants [149]. Clouds can block direct sunlight and scatter radiation, diminishing the intensity of available solar energy. Rain can temporarily decrease panel efficiency by affecting their ability to capture and convert sunlight into electricity.

These variations and impacts related to solar irradiation variability and weather conditions pose a significant challenge for the integration of solar energy into electrical grids and ensuring stable and reliable production. Therefore, research and development of technologies and strategies to mitigate these effects are crucial to fully harness the potential of solar energy as a clean and sustainable energy source [48].

In this exploratory chapter, our main focus is to develop a sufficiently reduced differential model for implementing control operations that can react to these variations and maintain economical performance of the plant. This challenging task has at least three components that deserved to be explored: First, the differential system modeling the dynamics of the plant; Second, the operation of the Rankine cycle including possible shutdowns; and third, the operation under uncertain irradiation.

With respect to the first aspect, the differential system needs to balance the trade-off between representation of reality, and management of the model. If the model is too simple,

connection with real plants might be lost. If the model is too complicated, it might become impossible to find solutions to the induced control problems. Here, we propose a model that takes into account these aspects.

With respect to the second aspect, a natural consequence of variability of solar irradiation is that plants are not capable of maintaining continuous production. Thus, it becomes necessary to turn off the Rankine cycle, for a period of time. We will call this action as a *shutdown* of the Rankine cycle. In this work, we provide an initial exploration of how to deal with shutdowns, by including a binary control (the switch control) to alternate between two dynamics: one with the Rankine cycle on producing electrical power within its nominal range, and the other with the Rankine cycle off, where no electrical power is produced. We explore some scenarios that require one shutdown, and we look for the optimal one.

To model scenarios with disturbances, we assume that, in the presence of significant variations in solar irradiation, the capture of heat in the solar receiver is suspended. In the real context, strong disturbances can damage the solar receiver, therefore, one of the measures taken in this type of situation is to defocus the mirrors to reduce the solar concentration. This type of measures will be assumed to be pre-established in the dynamics of the model. This action is assumed and represented by the useful power function. In order to determine the optimal shutdown instant and duration, a series of optimal control problems will be solved for each critical scenario under consideration.

While this is an initial exploration of the problem of including switch controls, our developments here suggest that the proposed model is suitable for more complex scenarios. Moreover, eventually it might lead to new solutions on how to manage shutdowns of the Rankine cycle. The third aspect is left as a perspective of this work.

6.1 Dynamics of the reduced plant model

The model we will use to study and analyze the optimal shutdown of the Rankine Cycle is a system of ordinary differential equations consisting of four state variables and three control variables. This model represents the dynamics of a CSP plant with a two-tank storage system, similar to the one described in the previous chapter. The main difference is that we will consider a direct configuration, with the storage tanks as part of the main loop instead of the indirect configuration presented in Chapter 5. As shown in Figure 6.1, the plant's schematic includes strategically located nodes for which our model will provide information regarding temperatures, mass flows, thermal powers, and the amount of mass in the storage tanks.

In this model, we consider the use of molten salt as the heat transfer fluid, which circulates throughout the plant in a closed-loop system. Therefore, we assume that the total mass within the entire plant remains constant over time. We consider a fixed time horizon, that we denote by H , which will be in hours.

In the following figure, we present the reduced model of the CSP plant with the two-tank storage system.

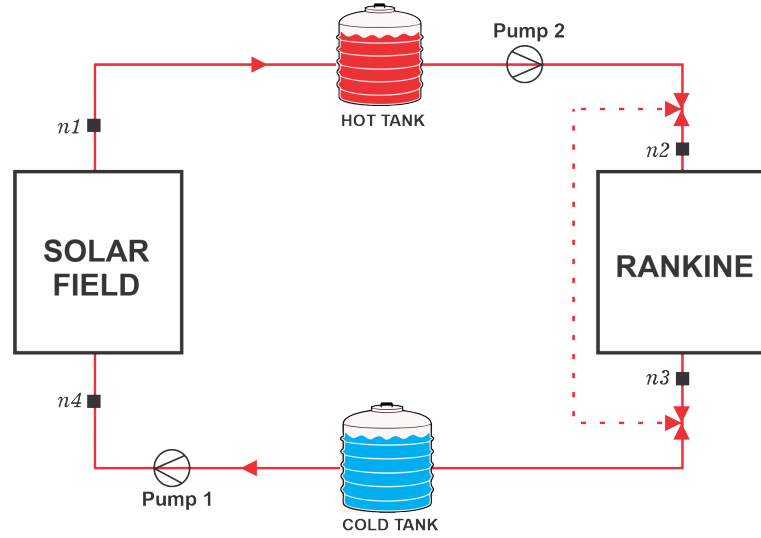


Figure 6.1: Scheme of a CSP plant reduced model.

As illustrated in Figure 6.1, the reduced model of the solar power plant comprises two black boxes: the Solar Receiver System and the Rankine Cycle. Additionally, the system incorporates two storage tanks and two pumps. Focusing on the Solar Receiver System, this component covers the process of capturing and transferring thermal energy to the heat transfer fluid as it enters the plant (node 1). The thermal power is subsequently represented by the function of useful thermal power (Q_u).

The two pumps control the movement of the heat transfer fluid throughout the plant. Pump 1 is responsible for directing the fluid from the blue tank to the red tank, where it receives the useful thermal power exchange between nodes 4 and 1, the flow of this fluid will be denoted by \dot{m}_{SF} . At the same time, Pump 2 works to transport the accumulated energy through the mass flow of the heat transfer fluid \dot{m}_R , from the red reservoir to the Rankine cycle, which occurs between nodes 2 and 3. In this process, thermal energy is converted into electrical energy. As a result, the now cooled heat transfer fluid is diverted to the blue tank to start the cycle once again.

As for the solar field component, we will simplify the heat transfer process by assuming that the thermal power entering the plant (from node 4 to 1) is described by an exogenous function, which we will refer to as the useful thermal power function (detailed for the first time in the previous chapter). This is expressed as:

$$Q_u(t) = c_p \cdot \dot{m}_{SF}(t) \cdot (T_1(t) - T_4(t)), \quad \forall t \in [0, H]. \quad (6.1.1)$$

To obtain this function, the hourly average values of useful thermal power are simulated using the SAM [103] software. This work will use this representation of the useful thermal

power, which is,

$$\forall t \in [0, 24], \quad Q_u(t) = \begin{cases} p(t) & \text{if } t \in [t_{ini}^{sun}, t_{fin}^{sun}], \\ 0 & \text{if not,} \end{cases} \quad (6.1.2)$$

with the polynomial interpolation function $p(\cdot)$ and the sunlight times, $t_{ini}^{sun}, t_{fin}^{sun}$. This implementation is explained in the Subsection 4.2.1. We will consider curves that represent critical scenarios in which there is no thermal power during certain time intervals.

From equation 6.1.3, the expression to represent the temperature variation at node 1 (T_1) is derived, that is,

$$T_1(t) = \frac{Q_u(t)}{c_p \cdot \dot{m}_{SF}(t)} + T_4(t). \quad (6.1.3)$$

Regarding the Rankine Cycle, we will assume that the plant being modeled retains the same nominal characteristics considered for the same component in Chapter 5. Therefore, we will also consider a quadratic approximation described in Subsection 4.2.2, which would represent, in this case, the variation of temperature at node 3. It will be defined based on the temperature at node 2 and the mass flow rate \dot{m}_R . Then, the quadratic regression is,

$$\begin{aligned} T_3(T_2(t), \dot{m}_R(t), T_a) = & c_1 + c_2 T_2(t) + c_3 T_2^2(t) + c_4 T_a + c_5 T_a^2 + c_6 \dot{m}_R(t) + c_7 \dot{m}_R^2(t) \\ & + c_8 T_2(t) T_a + c_9 T_2(t) \dot{m}_R(t) + c_{10} \dot{m}_R(t) T_a, \quad \forall t \in [0, H], \end{aligned} \quad (6.1.4)$$

where the values for the coefficients c_α , with $\alpha = 1, \dots, 10$, are in Table 4.1, and T_a stands for the ambient temperature.

For the reduced plant modeling, we relied on the articles [147, 146, 90]. On the one hand, they provide a detailed model of heat transfer from the receiver surface to the heat transfer fluid, which will then be transported throughout the plant. On the other hand, they specifically model and validate thermal energy storage systems with tanks, and subsequently conduct a study of control and operation strategies in scenarios with clear and cloudy days. In the Tables 6.3, 6.1 and 6.2, we describe the state and control variables, parameters and complementary functions used in the model (6.1.5-6.1.8).

Notation	Description	Unit/ Valor
T_1	Molten salt temperature at node 1	[°C]
T_3	Molten salt temperature at node 3	[°C]

Table 6.1: Complementary functions.

Notation	Description	Unit/ Value
A	Tank area	$[m^2]$
M	Mass	$[kg]$
c_p	Specific heat capacity t of salt	$[J/(kg \cdot ^\circ C)]$
T	Temperature	$[^\circ C]$
Q	Thermal power	$[W]$
α	Heat loss coefficient of the tanks	$[W/(m^2 \cdot ^\circ C)]$
η	Coefficient of performance	$[-]$
Acronyms		
a	Ambient	
$elec$	Electrical	
CT	Cold tank	
HT	Hot tank	
Nom	Nominal	

Table 6.2: Parameters and notations.

Notation	Description	Unit/ Value
T_2	Molten salt temperature at node 2 and hot tank	$[^\circ C]$
T_4	Molten salt temperature at node 4 and cold tank	$[^\circ C]$
M_{HT}	Mass of molten salt in the hot tank	$[kg]$
M_{CT}	Mass of molten salt in the cold tank	$[kg]$
\dot{m}_{SF}	Mass flow of salt controlled by pump 1	$[kg/s]$
\dot{m}_R	Mass flow of salt controlled by pump 2	$[kg/s]$

Table 6.3: State and control variables.

The equations that describe the model of this work are:

$$\frac{d(M_{HT})}{dt} = \dot{m}_{SF} - \dot{m}_R \quad (6.1.5)$$

$$\frac{d(M_{CT})}{dt} = \dot{m}_R - \dot{m}_{SF} \quad (6.1.6)$$

$$\begin{aligned} \frac{d(c_p \cdot (T_2 - T_{ref}^{hot}) \cdot M_{HT})}{dt} &= \dot{m}_{SF} \cdot c_p \cdot (T_1(T_4, \dot{m}_{SF}) - T_{ref}^{hot}) - \dot{m}_R \cdot c_p \cdot (T_2 - T_{ref}^{hot}) \\ &\quad - \alpha \cdot A \cdot (T_2 - T_a) \end{aligned} \quad (6.1.7)$$

$$\begin{aligned} \frac{d(c_p \cdot (T_4 - T_{ref}^{cold}) M_{CT})}{dt} &= \dot{m}_R \cdot c_p \cdot (T_3(T_2, \dot{m}_R, T_a) - T_{ref}^{cold}) - \dot{m}_{SF} \cdot c_p \cdot (T_4 - T_{ref}^{cold}) \\ &\quad - \alpha \cdot A \cdot (T_4 - T_a) \end{aligned} \quad (6.1.8)$$

Equations (6.1.5)-(6.1.6) are the mass balance of the tanks, which are representing the mass flow of molten salt into and out of each tank. We assume that this fluid system is controllable using Pump 1 and Pump 2 (see Figure 6.1), and whose representation will be

through the mass flows \dot{m}_{SF}, \dot{m}_R .

The temperature at node 2 (or in the hot tank) is represented by equation (6.1.7). In this expression we follow the variation of energy at the Hot tank, considering the incoming energy to the tank, coming from the solar field, minus the energy directed to the power block and the energy lost with respect to the ambient temperature (T_a). Also, in this equation, we have the function that describes the behavior of temperature at node 1 (see equation 6.1.3), which is deduced of the equation (6.1.1). Analogously, the equation representing the temperature variation at node 4 (or in the cold tank) is described by (6.1.8), with the addition of a complementary second function that describes the temperature at node 3 (see eq. 6.1.4). Again, this is done by following the energy variations at the cold tank. Finally, the T_{ref}^{hot} and T_{ref}^{cold} temperatures represent a nominal reference temperature inside the tanks.

By isolating the time derivatives of the state variables M_{HT} , M_{CT} , T_2 and T_4 , we obtain the following simplified system:

$$\frac{d(M_{HT})}{dt} = [\dot{m}_{SF} - \dot{m}_R], \quad (6.1.9)$$

$$\frac{d(M_{CT})}{dt} = [\dot{m}_R - \dot{m}_{SF}], \quad (6.1.10)$$

$$\frac{d(T_2)}{dt} = \frac{1}{M_{HT}} \left[\dot{m}_{SF}(T_1(T_4, \dot{m}_{SF}, \beta) - T_2) - \frac{1}{c_p} [\alpha \cdot A \cdot (T_2 - T_a)] \right], \quad (6.1.11)$$

$$\frac{d(T_4)}{dt} = \frac{1}{M_{CT}} \left[\dot{m}_R(T_3(T_2, \dot{m}_R, T_a) - T_4) - \frac{1}{c_p} [\alpha \cdot A \cdot (T_4 - T_a)] \right]. \quad (6.1.12)$$

To finish, we provide an expression of the electric power $\dot{W}_{elec}(t)$, produced by the system. According to [90], the estimation of the efficiency of the Rankine cycle is represented by, $\eta_R = \eta_{el} \cdot \eta_t$, where η_{el} is the efficiency of the generator and η_t is the efficiency of the turbines. Thus the net electrical power is given by

$$\dot{W}_{elec}(T_2(t), \dot{m}_R(t)) = Q_R(T_2(t), \dot{m}_R(t)) \cdot \eta_R \quad (6.1.13)$$

where Q_R is the heat power adsorbed by the Rankine cycle, that is,

$$Q_R(T_2(t), \dot{m}_R(t)) = c_p \cdot \dot{m}_R(t) \cdot (T_2(t) - T_3(T_2(t), \dot{m}_R(t), T_a)).$$

6.2 Plant dynamics with Switch Control

In real-life scenarios where a critical climatic situation arises for a Concentrated Solar Power (CSP) plant, one of the measures taken to safeguard the plant is to shutdown one or more of its components. In this section, we will introduce a switch control variable, into the previously presented model. This variable will enable the transition between the two dynamics corresponding to the operation being on and off in the Rankine cycle [17, 148].

The material considered for heat transfer throughout the plant is molten salt, which must be in constant motion along with minimum temperatures to prevent solidification [62]. Therefore, if the Rankine Cycle is turned off, the mass flow rate \dot{m}_R must continue its transition to node 3 through an auxiliary pathway (see, red dashed line in Figure 6.1). In contrast, the temperature at node 3 will be affected, and its value will be the same as that of node 2. In our model, this means to switch the expression of T_3 given by (6.1.12), by the expression $T_3 = T_2$.

To model this alternation for T_3 , we need to consider a control variable of the switch type, denoted as $v : [0, H] \rightarrow \{0, 1\}$, where 0 represents the off state, and 1 represents the on state. Thus, we seek to capture the ability to activate or deactivate the Rankine cycle if necessary. To depict this condition, the switch control variable would be included in equation 6.1.12 as follows:

$$\frac{d(T_4)}{dt} = \frac{1}{M_{CT}} \left[\dot{m}_R([v \cdot T_3(T_2, \dot{m}_R, T_a) + (1 - v) \cdot T_2]) - T_4 - \frac{1}{c_p} [\alpha \cdot A \cdot (T_4 - T_a)] \right].$$

Thus, the model that considers on/off in the Rankine cycle is:

$$\frac{d(M_{HT})}{dt} = [\dot{m}_{SF} - \dot{m}_R], \quad (6.2.1)$$

$$\frac{d(M_{CT})}{dt} = [\dot{m}_R - \dot{m}_{SF}], \quad (6.2.2)$$

$$\frac{d(T_2)}{dt} = \frac{1}{M_{HT}} \left[\dot{m}_{SF}(T_1(T_4, \dot{m}_{SF}, \beta) - T_2) - \frac{1}{c_p} [\alpha \cdot A \cdot (T_2 - T_a)] \right], \quad (6.2.3)$$

$$\frac{d(T_4)}{dt} = \frac{1}{M_{CT}} \left[\dot{m}_R([v \cdot T_3(T_2, \dot{m}_R, T_a) + (1 - v) \cdot T_2]) - T_4 - \frac{1}{c_p} [\alpha \cdot A \cdot (T_4 - T_a)] \right]. \quad (6.2.4)$$

When the Rankine cycle is running (between nodes 2 and 3), the temperature at node 3 is determined through the complementary function (6.1.4), but when the Rankine cycle is off, the mass flow continues its course through a circuit auxiliary, and therefore, the temperature of node 3 will coincide with that of node 2. Finally, the expression (6.1.13) representing the electrical power generated by the plant with the switch control would be as follows:

$$\dot{W}_{elec}(T_2(t), \dot{m}_R(t), v(t)) = Q_R(T_2(t), \dot{m}_R(t), v(t)) \cdot \eta_R \quad (6.2.5)$$

where Q_R is the heat power absorbed by the Rankine cycle, that is,

$$Q_R(T_2(t), \dot{m}_R(t), v(t)) = v(t) \cdot c_p \cdot \dot{m}_R(t) \cdot (T_2(t) - T_3(T_2(t), \dot{m}_R(t), T_a)).$$

6.3 Optimal control problem

In this section, we will describe the optimal control problem where the goal is to maximize operational incomes. For this, we will describe the revenues and costs generated by the plant

in its daily operations. In this part, we use a price function $\lambda(t)$, for the electric power. As in Chapter 5.1 we assume that λ is exogenous and that the plant's operation does not affect it.

6.3.1 Objective functional

- **Revenue:** The goal is to maximize the profit of the plant, which comes from the electrical energy produced in the time interval $[0, H]$. This, under the assumption that all the produced energy will be purchased. Then the Revenues derived from the produced energy are given by:

$$Rev(T_2(t), \dot{m}_R(t), v(t)) = \int_0^H \dot{W}_{elec}(T_2(t), \dot{m}_R(t), v(t)) \cdot \lambda(t) dt$$

- **Costs:** To maximize profit, one needs to take into account the operational costs of the plant, such as operation of the mirror field and pumping of the different heat transfer fluids. These operating costs are modeled as electricity consumption, which is purchased at the market price $\lambda(t)$. The operating cost functions are defined as follows:
 1. **Mass flow pumping cost \dot{m}_{SF} :** During power production, mass flow \dot{m}_{SF} is pumped by pump P_1 . This marginal cost is linear with respect to \dot{m}_{SF} so

$$Cost_{P_1}(\dot{m}_{SF}(t)) = C_{P_1} \cdot \int_0^H \lambda(t) \cdot \dot{m}_{SF}(t) dt$$

2. **Mass flow pumping cost \dot{m}_R :** During power production, mass flow $\dot{m}_R(t)$ is pumped by pump P_2 . This marginal cost is linear with respect to \dot{m}_R so

$$Cost_{P_2}(\dot{m}_R(t)) = C_{P_2} \cdot \int_0^H \lambda(t) \cdot \dot{m}_R(t) , dt$$

3. **Start-up - Rankine:** Before starting the Rankine cycle and producing electrical power, the Rankine cycle must be heated up. When the Rankine cycle is fully cold, the preheat requirement is modeled as a 20 *min* delay in actual production. However, depending of the form of the switch function $v : [0, H] \rightarrow \{0, 1\}$, this start-up cost becomes hard to model. As mentioned before, here we will only consider exploratory scenarios, where only one shutdown is needed. That is, the Rankine cycle will be on, except for a continuous interval of length Δt . In this situation, the start-up cost will be modeled with an average cost ($\bar{\lambda}$), the nominal thermal power of the plant (\dot{W}_{Nom}) and the attenuation function $\varphi(t) := 1 - \exp(-\frac{3}{2}t)$ (similar to the implementation made in equations 5.2.37 and 5.2.38), with the formula

$$Cost_{SU}(v(t)) = \frac{\varphi(\Delta t) \cdot \bar{\lambda} \cdot \dot{W}_{Nom}}{3}$$

where Δt is denoting the amount of time that the Rankine Cycle was off.

The objective functional will be the difference between previous revenues and costs.

6.3.2 Control Problem

Our objective functional is defined as follows:

$$J(\dot{m}_{SF}(t), \dot{m}_R(t), v(t)) = Rev(T_2(t), \dot{m}_R(t), v(t)) - Cost_{P_1}(\dot{m}_{SF}(t)) - Cost_{P_2}(\dot{m}_R(t)) - Cost_{SU}(v(t)) \quad (6.3.1)$$

The resulting optimal control problem is then given by:

$$\max J(\dot{m}_{SF}(t), \dot{m}_R(t), v(t)) \quad (6.3.2)$$

subject to the model (6.2.1), considering initial conditions:

$$T_4(t_{ini}) = T_1^0 \quad T_2(t_{ini}) = T_4^0 \quad (6.3.3)$$

$$M_{salt_CT}(t_{ini}) = M_{salt_CT}^0 \quad M_{salt_HT}(t_{ini}) = M_{salt_HT}^0 \quad (6.3.4)$$

and with the control constraints:

$$0 < \underline{\dot{m}_{SF}} \leq \dot{m}_{SF}(t) \leq \overline{\dot{m}_{SF}}, \quad 0 < \underline{\dot{m}_R} \leq \dot{m}_R(t) \leq \overline{\dot{m}_{Rank}}, \quad (6.3.5)$$

$$v(t) \in \{0, 1\}, \quad \forall t \in [t_{ini}, t_{fin}]. \quad (6.3.6)$$

Finally, for all $t \in [0, H]$, we include the following physical constraints:

$$T_2(t) \in [290, 565], \quad T_4(t) \in [290, 565]. \quad (\text{Temperatures range for the salt}) \quad (6.3.7)$$

$$M_{HT}(t) + M_{CT}(t) = M_{Total} \quad (\text{Mass balance between the two tanks}) \quad (6.3.8)$$

$$\dot{W}_{Nom}^{min} \cdot v(t) \leq \dot{W}_{elec} \leq \dot{W}_{Nom}^{max} \cdot v(t) \quad (\text{Nominal maximum Power}) \quad (6.3.9)$$

$$\dot{m}_{SF}, \dot{m}_R, M_{HT}, M_{CT} \geq 0 \quad (6.3.10)$$

The restriction on \dot{W}_{elec} means that either the Rankine cycle is off and so $\dot{W}_{elec} = 0$, or it is on and then \dot{W}_{elec} is within the range of nominal values $[\dot{W}_{Nom}^{min}, \dot{W}_{Nom}^{max}]$.

6.4 Simulations - Search for the optimal shutdown.

Up to now, we have presented a model with arbitrary switch control $v : [0, H] \rightarrow \{0, 1\}$, that can model any possible shutdown operation. However, the problem in full generality becomes hard to solve. In this first preliminary study of the problem, we want to study the pertinence of this model by considering controls where only one shutdown is needed, that is, where v takes the form

$$v(t) = \begin{cases} 0 & \text{if } t \in [h, h + \Delta t] \\ 1 & \text{otherwise.} \end{cases}$$

Here, we search for the optimal shutdown of the Rankine cycle, in the sense that we want to determine the optimal v described above.

In order to determine the optimal shutdown of the Rankine cycle, we must find the starting moment of shutdown and its duration. Identifying this initial moment is not straightforward, as it can be influenced by various factors, including variations in the useful power curve, electricity market prices, the amount of heat stored in the tanks, and more. To address these factors, we will solve a series of optimal control problems, each one associated with a prefixed switch control. Since, we study the case of a single switch for the Rankine cycle, the switch control is fully determined the initial shutdown time h and its duration Δt .

According to [124], the Rankine Cycle needs on average 20 minutes to warm up and start working. Therefore, we will consider Δt time windows, where the Rankine cycle will be off; we will start by considering a Rankine stop of 20 minutes from instant 0. Then, we will shift the window by moving its initial time according to a discretization of the $[0, H]$. This is shown in the following figure:

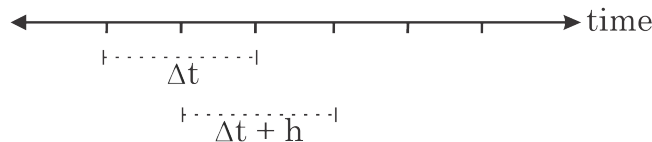


Figure 6.2: Methodology to find the optimal shutdown.

For every initial time h and every time window Δt , we will solve the optimal control problem described in Section 6.3.2, by imposing the following switch: the Rankine cycle must be turned off on the interval $[h, h + \Delta t]$, and turned on otherwise. The methodology is summarized in the following pseudo-code.

Algorithm 2: Routine - Bocop

Input: Initial condition $x_0 = (T_2^0, T_4^0, M_{HT}^0, M_{CT}^0, \dot{m}_{SF}^0, \dot{m}_R^0)$,
 $times = [h_0, h_1, \dots, H]$,
 $window = [20, 25, 30, \dots, 60]$,
 1 **for** h *in* $times$ **do**
 2 **for** Δt *in* $window$ **do**
 3 Define $v_{aux} : [0, H] \rightarrow \{0, 1\}$ as

$$v_{aux}(t) = \begin{cases} 0 & \text{if } t \in [h, h + \Delta t], \\ 1 & \text{otherwise.} \end{cases}$$

 4 Solve optimal control problem of Section 6.3.2 imposing $v = v_{aux}$.
 5 **Set** $x^*(h, \Delta t) = (T_2^*, T_4^*, M_{HT}^*, M_{CT}^*, \dot{m}_{SF}^*, \dot{m}_R^*)$ as the found solution.
Output: The full vector $x^* = (x^*(h, \Delta t) : (h, \Delta t) \in times \times window)$.

To solve these optimal control problems (6.3.2)-(6.3.10), the specialized software BOCOP was used [19]. Since we wish to solve various control problems by varying the time window and shifting it along the time horizon, we propose the Algorithm 2, where two loops have been created, corresponding to the variation of the time window and the shift of the off interval $[H, H + \Delta t]$. Some parameters were artificially set, while others were chosen as described in the literature [128, 90, 146, 24, 124]. See Table 6.4 table for more details.

Notation	Description	Unit	Value
A_{tank}	Tank area	$[m^2]$	1842.54
c_p	Specific heat capacity of the molten salt	$[J/(kg \cdot ^\circ C)]$	1560
T_{amb}	Ambient temperature	$[^\circ C]$	29.65
α_{tank}	Tank-Ambient Heat Loss Coefficient	$[W/m^2 \cdot ^\circ C]$	0.4
η_R	Rankine effectiveness coefficient	$[-]$	0.8

Table 6.4: Parameters and notations.

As illustrated in Figure 6.2, an optimal shutdown (if it exists) will be sought, For this, a day will be considered, in which a first analysis will be to shift the 20 minutes of shutdown (this time is set according to [124], where before starting the Rankine cycle and producing electrical energy, the Rankine cycle must be preheated, which was estimated at 20 min) during the whole time horizon $[0, 24]$. Then, a second analysis will be to extend the shutdown duration of the Rankine cycle by 5 more minutes and to shift this duration over the entire time horizon. These analyses will be done until a shutdown with duration of 60 minutes is considered.

6.4.1 Case 1: Useful thermal power Without perturbations

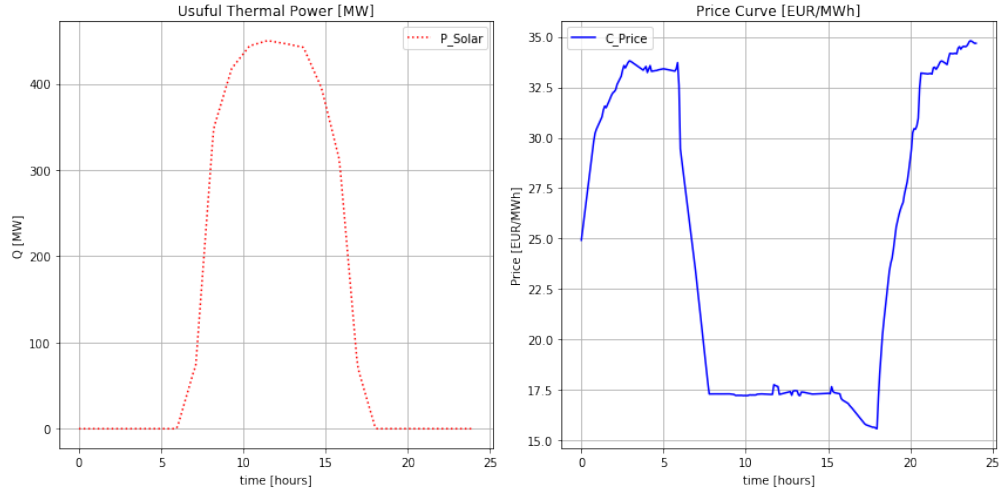


Figure 6.3: Exogenous functions. Useful thermal power and price function.

The first case to be analyzed is to consider a scenario without any type of disturbances. For this purpose, two exogenous curves (see Figure 6.3) representing the useful thermal power and a price curve will be considered. Both curves have been defined from the values studied and analyzed in Chapter 5.

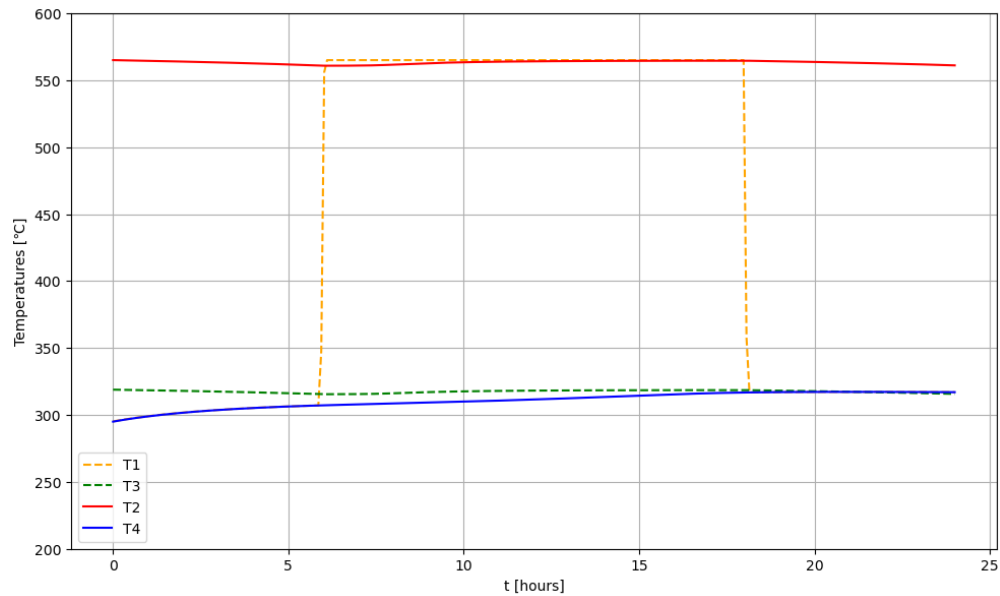


Figure 6.4: state variables and complementary functions of temperatures T_1 , T_2 , T_3 and T_4 , without shutdown of the Rankine cycle.

The temperatures found for the heat transfer fluid, which is Molten Salt, are within safe ranges for the preservation of the material, i.e., $T \in [290, 565]$ (see Figure 6.4). This graph shows the variation of Temperature 1 (yellow curve) only since it corresponds to the temperature of the molten salt coming from the receiver. With respect to the controls, we can observe how the control of mass flow between nodes 4 and 1 (\dot{m}_{SF}) exhibits a behavior similar to that of the solar radiation curve. Indeed, this relationship is described by Equation 6.1.1, where, upon solving for Temperature 1, the mass flow becomes the quotient of useful thermal power. On the other hand, there is no variation in mass flow \dot{m}_R over the time

horizon. Consequently, given that this same mass flow passes through the Rankine cycle, we obtain constant electrical power production (see Figure 6.6).

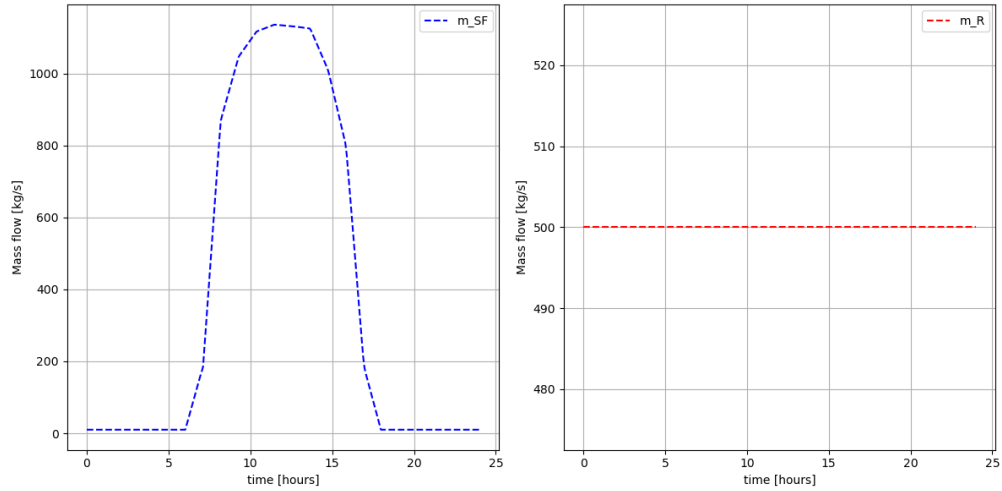


Figure 6.5: Control variables, mass flows \dot{m}_{SF} and \dot{m}_R , without shutdown of the Rankine cycle.

For the case without shutdown of the Rankine Cycle, it was found that the profits per day of 26840.56 [€]. No additional simulations were carried out since in this case a continuous production is already achieved.

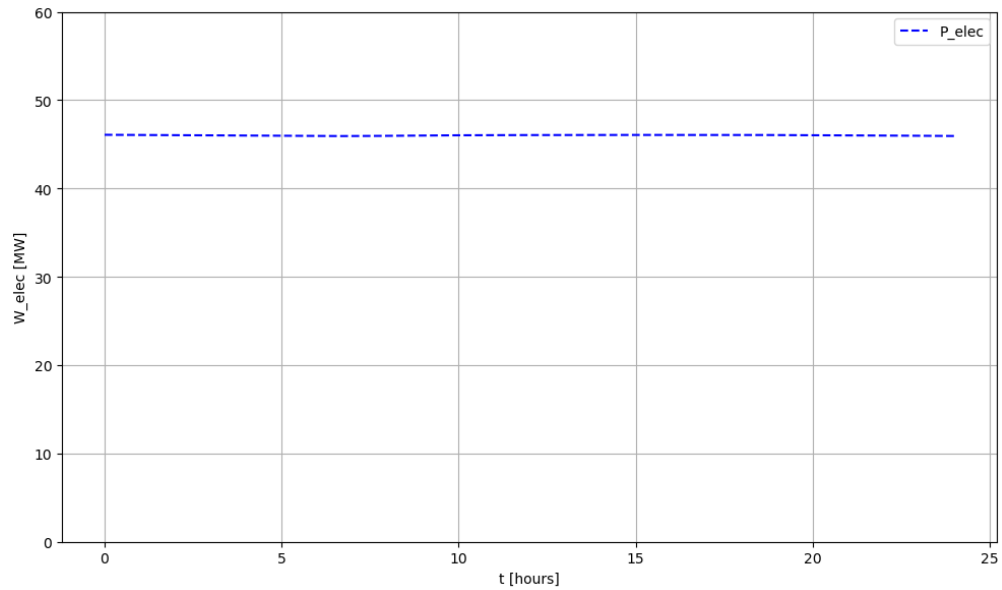


Figure 6.6: Electrical power in a nominal range of 40 to 55 MW, without shutdown of the Rankine cycle.

6.4.2 Case 2: Useful thermal power with continuous perturbation

For the second study scenario, we have considered a more extended disturbance, lasting approximately 3 continuous hours (see Figure 6.7). Table 6.5 presents the results for the optimal shutdown, occurring at time $t = 5.83$ hours in the time horizon, with a duration of 20 minutes.

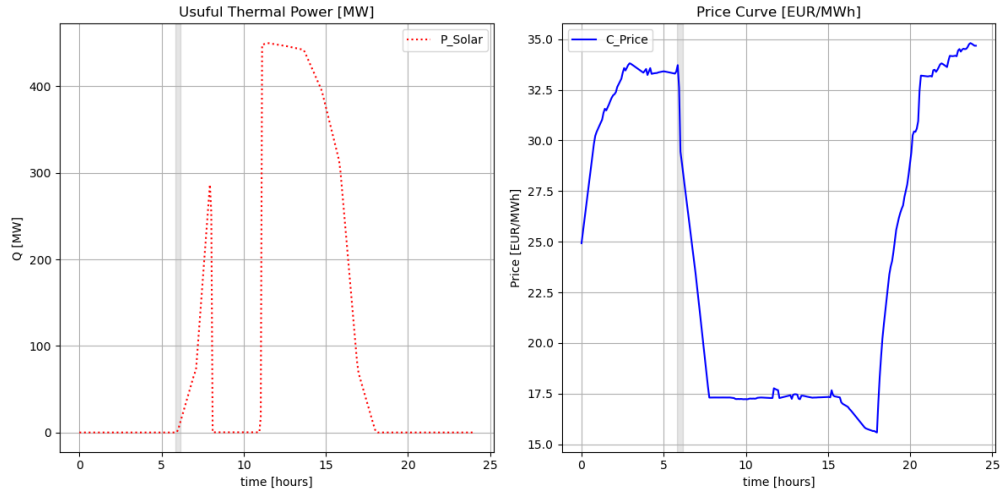


Figure 6.7: Exogenous functions. Useful thermal power and price function.

Duration - OFF	Initial time	Value - Objective function [€]
0 min	-	infeasible
20 min	5h_50min	26398.14
30 min	3h_40min	26074.82
40 min	12h_40min	26280.14
50 min	14h_10min	26125.23
60 min	19h_40min	25413.25
1h_10min	20h	25059.52
1h_20min	17h_50min	25473.63
1h_30min	8h_40min	25533.58

Table 6.5: Case 2, time and economic results. For every fixed duration value, only the optimal Initial time is displayed.

According to the found results, it was not possible for the plant to operate without considering a shutdown of the Rankine cycle (see Table 6.5). On the other hand, the optimal solution suggests that by shutting down the Rankine cycle at $t = 5.83$ for 20 minutes, a greater gain is achieved compared to different shutdown scenarios (Duration-OFF, first column in Table 6.5).

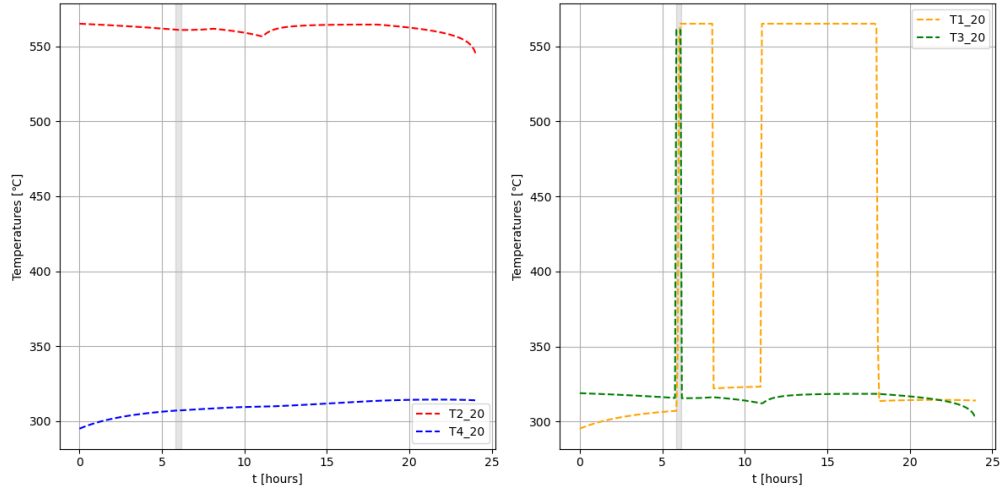


Figure 6.8: State variables and complementary functions of temperatures T_1 , T_2 , T_3 and T_4

In Figure 6.8, the dynamic change in the model when shutting down the Rankine cycle is evident, as the temperature at node 3 changes at $t = 5.83$ from being around 290°C to changing to another temperature close to 550°C , for 20 minutes. However, overall, the temperatures remain within a safe range that preserves the properties of the heat transfer fluid (molten salt) and the functionality of the plant. In Figure 6.9, it can be observed how the plant utilizes a significant portion of the stored heat energy for electricity production until around 11:00 hours, coinciding with the end of the continuous disturbance. Subsequently, it begins to store energy until approximately 17:00 hours, with the aim of using this energy during the period without sunlight. Finally, a stable production of electrical energy is achieved without considerable variations throughout the time horizon (as shown on the right side of Figure 6.10).

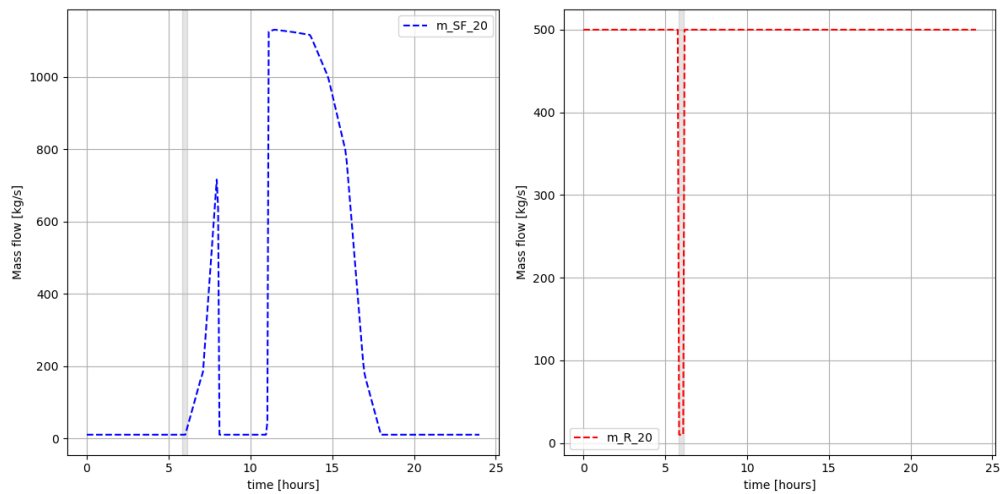


Figure 6.9: Control variable, mass flows with shutdown of the Rankine cycle at time $t=5.83$ (5 hours and 50 minutes), during 20 minutes.

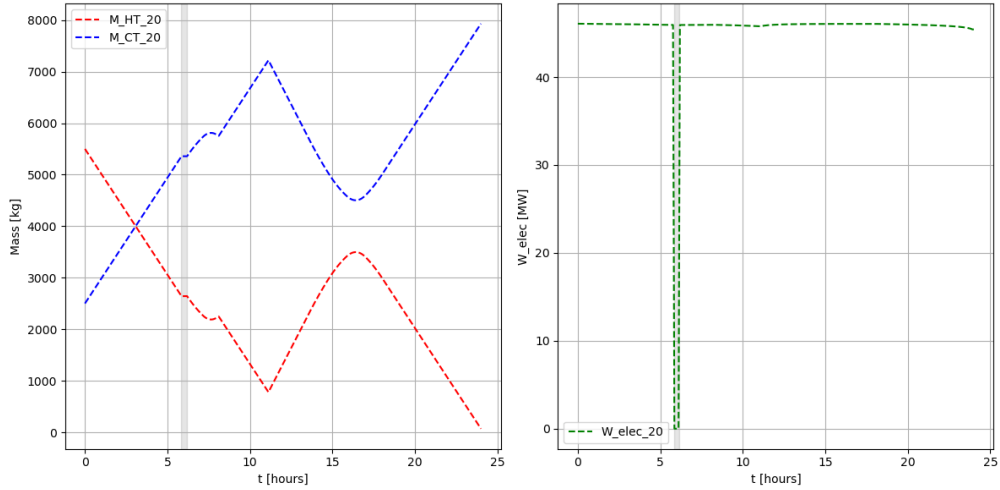


Figure 6.10: Mass in the cold and hot tanks and electric power.

6.4.3 Case 3: Useful thermal power with discontinuous perturbations

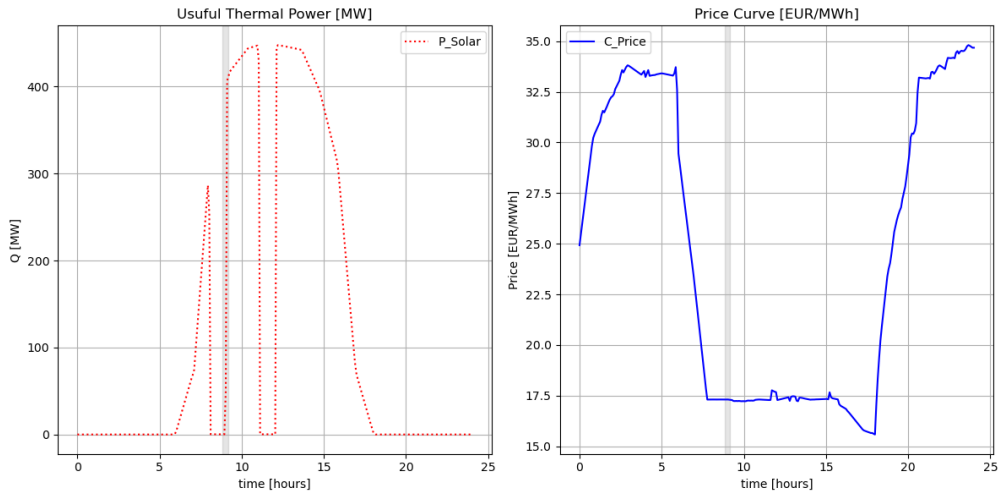


Figure 6.11: Exogenous functions. Useful thermal power and price function.

Now let us consider a scenario with strong intermittent perturbations in the useful thermal power curve, with two time intervals whose useful power will be zero. The price curve remains the same as the one used previously (see Figure 6.11). For this case, we proceeded in the same way, considering different time windows, starting from instant 0 and shifting it along the time horizon.

According to the results, the optimal shutdown would occur at time $t = 8.83$ within the time horizon of one day, lasting 30 minutes (see Table 6.6). In this scenario, unlike the previous one, finding an optimal shutdown proved to be challenging (and even impossible) for many cases. One reason for these infeasibilities is the intermittency in capturing heat energy, as maintaining stable conditions within nominal ranges poses a significant challenge for the

Duration - OFF	Initial time	Value - Objective function [€]
0 min	-	infeasible
20 min	-	infeasible
30 min	8h_50min	26449.85
40 min	12h	26286.19
50 min	3h_10min	25512.60
60 min	-	infeasible
1h_10min	-	infeasible
1h_20min	-	infeasible
1h_30min	12h_30min	25528.05

Table 6.6: Case 3, time and economic results. For every fixed duration value, only the optimal Initial time is displayed.

plant.

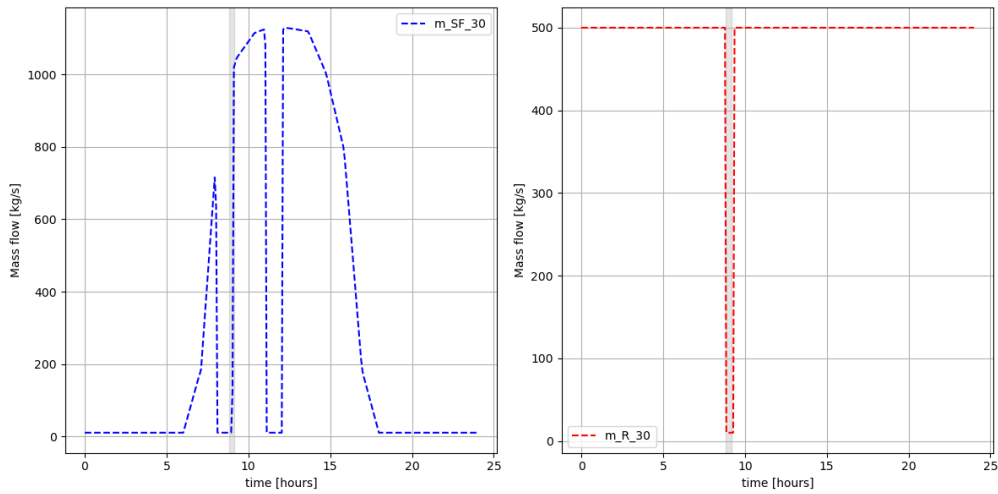


Figure 6.12: Control variable, mass flows with shutdown of the Rankine cycle at time $t=5.83$ (5 hours and 50 minutes), during 20 minutes.

As per the optimal solution, the behavior of the optimal controls aligns with what is expected. On one hand, control \dot{m}_{SF} follows the useful thermal power curve, as indicated by the expression for temperature T_1 (see 6.1.3). This control must maintain conditions to recover all useful thermal energy. On the other hand, control \dot{m}_R exhibits a constant and stable behavior, ensuring that electrical energy production also occurs at a constant and stable rate (see Figure 6.14).

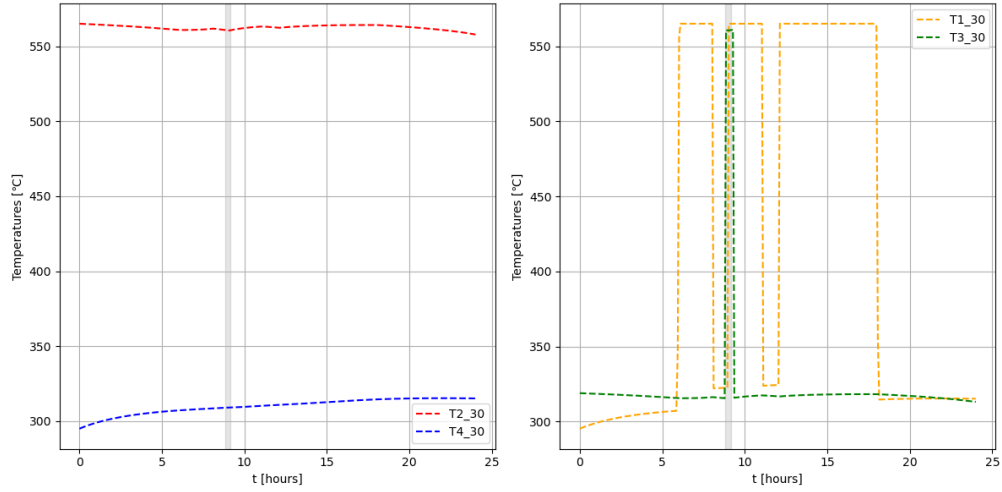


Figure 6.13: State variables and complementary functions of temperatures T_1 , T_2 , T_3 and T_4

In Figure 6.11, it is observed that the optimal shutdown occurs at the end of the first disturbance, coinciding with the timeframe when the hot tank has the least amount of mass (see Figure 6.14) and market prices are at their lowest throughout the time horizon. Temperatures remain within the nominal safety range for both the plant and the heat transfer fluid (see Figure 6.13), resulting in a stable production of electrical energy.

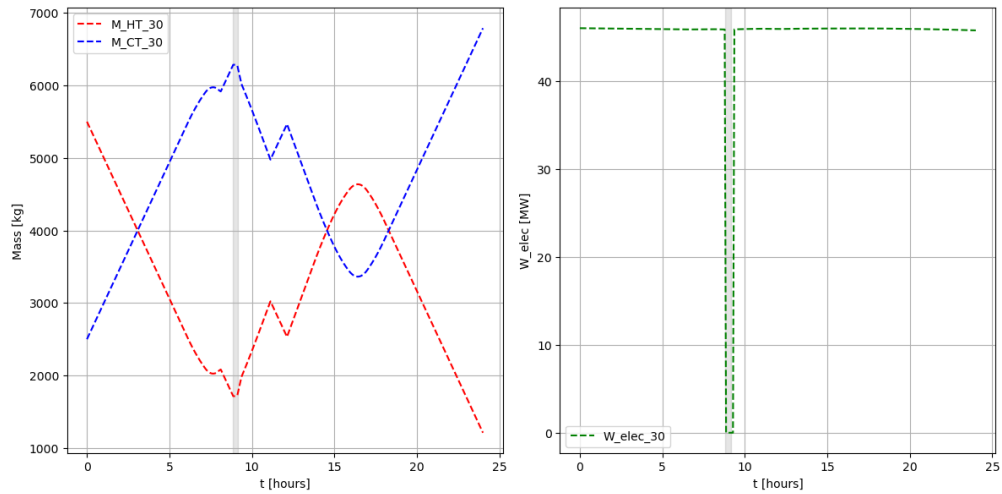


Figure 6.14: Mass in the cold and hot tanks and electric power.

6.5 Conclusion

In this study, we developed a simplified model for a Concentrated Solar Power (CSP) plant, allowing us to conduct simulations considering the shutdown of the Rankine cycle. Our intention is to further explore this model, considering not only a single switch but a finite number of switches per day. The most relevant perspective of this chapter is to pave the way for the consideration of stochastic disturbances, enabling the exploration of more realistic scenarios.

The constructed model was numerically validated for a single switch, and the challenge lay in considering multiple switches, as it is computationally demanding. The model achieves a good balance between the levels of detail found in the literature, providing crucial information about temperatures, mass flows, tank masses, and generated electrical power.

Notably, independently of the various disturbances, the control variable \dot{m}_R consistently exhibited a stable behavior, consequently ensuring a stable electrical energy production. This stability can be attributed primarily to the decoupled dynamics, where the storage system acts as a buffer against different disturbances, enabling the mass flow to remain constant and/or within a nominal range.

Chapter 7

Final Conclusion

In the initial part of this research, we focused on bilevel problems with cardinality constraints, an area that has received little attention to date. We achieved explored mainly two possible ways to include cardinality constraint, namely at the upper level and in a mixed form between upper level and lower level. Sufficient conditions for the existence of solutions, equivalent reformulation and application to a problem of optimal location for charging station of electric vehicles have been addressed. These investigations not only contribute to the knowledge to under explored fields but also open the door to new areas of theoretical analyses and applications. Specifically, in this thesis, we concentrated on models where there is one leader and multiple followers interacting with each other. As a natural extension of this work, the case with multiple leaders and followers could be explored, as well as the development of an alternative numerical method to solve problems with cardinality constraints at the upper level since the obtained results in this last situation leads to an certain inefficiency in terms of convergence speed and optimality gap.

In the second part of this research work, the primary objective was to assess and compare the practicality and economic efficacy of various storage systems and production strategies within a Concentrated Solar Power (CSP) plant, taking into account diverse pricing scenarios. The findings indicated that the Two-tank storage system is the most cost-effective option, evaluated using criteria such as: Levelized Cost of Electricity (LCOE), Net Present Value (NPV), Internal Rate of Return (IRR) and Conventional PayBack (CPB). But this analysis also enlighten promising results for the the Thermochemical storage system, for example showing that under certain electricity market configurations the initial investment and operating costs can be balanced with the revenues, and this before the 30 years lifespan of the project. In this first study, we underline the importance of considering different pricing scenarios. Possible extensions of this research include delving into hybrid storage systems and exploring inter-temporal strategies.

For the optimal operation problem, the last part of the PhD, a simplified model for a Concentrated Solar Power (CSP) plant was developed, allowing simulations with possible the shutdown of the Rankine cycle. The constructed model was numerically validated for a

single switch, and the challenge lay in considering multiple switches, as it is computationally demanding. The model achieves a good balance between the levels of detail found in the literature, providing crucial information about temperatures, mass flows, tank masses, and generated electrical power. Additionally, the incorporation of a switch variable decouples part of the dynamics, allowing us to build a sufficiently simplified model for controlling and optimizing processes to maximize plant profits. The intention is to further explore this model, considering not only a single switch but a finite number of switches per day. The significant perspective of this chapter is to pave the way for the consideration of stochastic disturbances, enabling the exploration of more realistic scenarios.

Part III

Bibliography

Bibliography

- [1] ACER. Public description - electricity market design report. https://www.acer.europa.eu/sites/default/files/documents/Publications/Final_Assessment_EU_Wholesale_Electricity_Market_Design.pdf, 2022. (accessed on April, 2024).
- [2] Guruprasad Alva, Yaxue Lin, and Guiyin Fang. An overview of thermal energy storage systems. *Energy*, 144:341–378, 2018.
- [3] Jean-Pierre Aubin and Hélène Frankowska. *Set-valued analysis*. Modern Birkhäuser Classics. Birkhäuser Boston, Inc., Boston, MA, 2009. Reprint of the 1990 edition [MR1048347].
- [4] D. Aussel. New developments in quasiconvex optimization. In *Fixed point theory, variational analysis, and optimization*, pages 171–205. CRC Press, Boca Raton, FL, 2014.
- [5] D Aussel, P Neveu, D Tsuanyo, and Y Azoumah. On the equivalence and comparison of economic criteria for energy projects: Application on pv/diesel hybrid system optimal design. *Energy Conversion and Management*, 163:493–506, 2018.
- [6] Didier Aussel, Cécile Egea, and Martin Schmidt. A tutorial on solving single-leader-multi-follower problems using sos1 reformulations, 2023. preprint - optimization-online:23744.
- [7] Didier Aussel and Anton Svensson. Some remarks about existence of equilibria, and the validity of the EPCC reformulation for multi-leader-follower games. *J. Nonlinear Convex Anal.*, 19(7):1141–1162, 2018.
- [8] Didier Aussel and Anton Svensson. Towards tractable constraint qualifications for parametric optimisation problems and applications to generalised nash games. *Journal of Optimization Theory and Applications*, 182:404–416, 2019.
- [9] Didier Aussel and Anton Svensson. A short state of the art on multi-leader-follower games. In *Bilevel optimization—advances and next challenges*, volume 161 of *Springer Optim. Appl.*, pages 53–76. Springer, Cham, [2020] ©2020.
- [10] Goran Banjac and Paul J Goulart. A novel approach for solving convex problems with

- cardinality constraints. *IFAC-PapersOnLine*, 50(1):13182–13187, 2017.
- [11] B. Bank, J. Guddat, D. Klatte, B. Kummer, and K. Tammer. *Nonlinear parametric optimization*. Birkhäuser Verlag, Basel-Boston, Mass., 1983.
- [12] Bernd Bank, Jürgen Guddat, Diethard Klatte, Bernd Kummer, and Klaus Tammer. *Non-linear parametric optimization*. Springer, 1983.
- [13] Evelyn Martin Lansdowne Beale and John A Tomlin. Special facilities in a general mathematical programming system for non-convex problems using ordered sets of variables. *OR*, 69(447-454):99, 1970.
- [14] Yasmine Beck, Ivana Ljubić, and Martin Schmidt. A survey on bilevel optimization under uncertainty. *European J. Oper. Res.*, 311(2):401–426, 2023.
- [15] Yasmine Beck and Martin Schmidt. A gentle and incomplete introduction to bilevel optimization. 2021.
- [16] Carlos Benavides, Marcelo Matus, Erick Sierra, Rodrigo Sepúlveda, Ana María Ruz, and Felipe Gallardo. Value contribution of solar plants to the Chilean electric system. *AIP Conference Proceedings*, 2126(1):170001, 07 2019.
- [17] Sorin C Benghea and Raymond A DeCarlo. Optimal control of switching systems. *automatica*, 41(1):11–27, 2005.
- [18] Philippe Blanc, Bella Espinar, Norbert Geuder, Christian Gueymard, Richard Meyer, Robert Pitz-Paal, Bernhard Reinhardt, David Renné, Manajit Sengupta, Lucien Wald, et al. Direct normal irradiance related definitions and applications: The circumsolar issue. *Solar Energy*, 110:561–577, 2014.
- [19] Frédéric J Bonnans, Pierre Martinon, and Vincent Grélard. *Bocop-A collection of examples*. PhD thesis, Inria, 2012.
- [20] Gabriel Boulnois. *Intégration d’un procédé de stockage thermo-chimique à une centrale solaire thermodynamique: de l’expérimentation à l’échelle matériau aux performances énergétiques à l’échelle système*. PhD thesis, Université de Perpignan, 2016.
- [21] Rubén Bravo, Carlos Ortiz, Ricardo Chacartegui, and Daniel Friedrich. Hybrid solar power plant with thermochemical energy storage: A multi-objective operational optimisation. *Energy Conversion and Management*, 205:112421, 2020.
- [22] Max Bucher and Alexandra Schwartz. Second-order optimality conditions and improved convergence results for regularization methods for cardinality-constrained optimization problems. *J. Optim. Theory Appl.*, 178(2):383–410, 2018.
- [23] Oleg P. Burdakov, Christian Kanzow, and Alexandra Schwartz. Mathematical programs with cardinality constraints: reformulation by complementarity-type conditions and a regularization method. *SIAM J. Optim.*, 26(1):397–425, 2016.

- [24] Juan Ignacio Burgaleta, Santiago Arias, and Diego Ramirez. Gemasolar, the first tower thermosolar commercial plant with molten salt storage. *SolarPACES, Granada, Spain*, pages 20–23, 2011.
- [25] Richard Burrett, Corrado Clini, Robert Dixon, Michael Eckhart, Mohamed El-Ashry, Deepak Gupta, Amal Haddouche, David Hales, Kirsty Hamilton, Chatham House, et al. Renewable energy policy network for the 21st century. *REN21 Global Status Report*, 2009.
- [26] Richard H Byrd, Mary E Hribar, and Jorge Nocedal. An interior point algorithm for large-scale nonlinear programming. *SIAM Journal on Optimization*, 9(4):877–900, 1999.
- [27] Antonio C Caputo, Pacifico M Pelagagge, and Paolo Salini. Manufacturing cost model for heat exchangers optimization. *Applied Thermal Engineering*, 94:513–533, 2016.
- [28] Jean-Philippe Chancelier and Michel De Lara. Hidden convexity in the l_0 pseudonorm. *J. Convex Anal.*, 28(1):203–236, 2021.
- [29] Jean-Philippe Chancelier and Michel De Lara. Capra-convexity, convex factorization and variational formulations for the l_0 pseudonorm. *Set-Valued Var. Anal.*, 30(2):597–619, 2022.
- [30] T-J Chang, Nigel Meade, John E Beasley, and Yazid M Sharaiha. Heuristics for cardinality constrained portfolio optimisation. *Computers & Operations Research*, 27(13):1271–1302, 2000.
- [31] Chukwubuikem Chukwuka and Komla Agbenyo Folly. Overview of concentrated solar power. *Journal of Energy and Power Engineering*, 7(12):2291, 2013.
- [32] Steve Cohen. The growing awareness and prominence of environmental sustainability. *State of the Planet, September*, 19, 2022.
- [33] T. Couture and Y. Gagnon. An analysis of feed-in tariff remuneration models: Implications for renewable energy investment. *Energy Policy*, 38(2):955 – 965, 2010.
- [34] Toby Couture and Yves Gagnon. An analysis of feed-in tariff remuneration models: Implications for renewable energy investment. *Energy policy*, 38(2):955–965, 2010.
- [35] M. Cruciani. Marketing renewable energy in France. In *Marketing Renewable Energy*, pages 303–329. Springer, 2017.
- [36] Teodora Dan and Patrice Marcotte. Competitive facility location with selfish users and queues. *Operations Research*, 67(2):479–497, 2019.
- [37] Himadry Shekhar Das, Mohammad Mominur Rahman, Shuhui Li, and Chee Wei Tan. Electric vehicles standards, charging infrastructure, and impact on grid integration: A technological review. *Renewable and Sustainable Energy Reviews*, 120:109618, 2020.

- [38] Fabrizio De Luca, Vittorio Ferraro, and Valerio Marinelli. On the performance of csp oil-cooled plants, with and without heat storage in tanks of molten salts. *Energy*, 83:230–239, 2015.
- [39] S. Dempe and J. Dutta. Is bilevel programming a special case of a mathematical program with complementarity constraints? *Math. Program.*, 131(1-2):37–48, 2012.
- [40] Stephan Dempe. *Foundations of bilevel programming*. Springer Science & Business Media, 2002.
- [41] Stephan Dempe, Vyacheslav Kalashnikov, Gerardo A. Pérez-Valdés, and Nataliya Kalashnykova. *Bilevel programming problems*. Energy Systems. Springer, Heidelberg, 2015. Theory, algorithms and applications to energy networks.
- [42] Stephan Dempe and Alain Zemkoho. Bilevel optimization. In *Springer optimization and its applications*, volume 161. Springer, 2020.
- [43] Stephan Dempe and Alain Zemkoho, editors. *Bilevel optimization—advances and next challenges*, volume 161 of *Springer Optimization and Its Applications*. Springer, Cham, [2020] ©2020.
- [44] P. Denholm, Y.-H. Wan, M. Hummon, and M. Mehos. An analysis of concentrating solar power with thermal energy storage in a California 33% renewable scenario - NREL/TP-6A20-58186. Technical report, National Renewable Energy Lab.(NREL), Golden, CO (United States), 2013.
- [45] Paul Denholm, Matthew O’Connell, Gregory Brinkman, and Jennie Jorgenson. Over-generation from solar energy in california. a field guide to the duck chart. Technical report, National Renewable Energy Lab.(NREL), Golden, CO (United States), 2015.
- [46] Paul Denholm, Yih-Huei Wan, Marissa Hummon, and Mark Mehos. Analysis of concentrating solar power with thermal energy storage in a california 33% renewable scenario. Technical report, National Renewable Energy Lab.(NREL), Golden, CO (United States), 2013.
- [47] Nishith B Desai, Maria E Mondejar, and Fredrik Haglind. Techno-economic analysis of two-tank and packed-bed rock thermal energy storages for foil-based concentrating solar collector driven cogeneration plants. *Renewable Energy*, 186:814–830, 2022.
- [48] Maimouna Diagne, Mathieu David, Philippe Lauret, John Boland, and Nicolas Schmutz. Review of solar irradiance forecasting methods and a proposition for small-scale insular grids. *Renewable and Sustainable Energy Reviews*, 27:65–76, 2013.
- [49] Alexander W Dowling, Tian Zheng, and Victor M Zavala. Economic assessment of concentrated solar power technologies: A review. *Renewable and Sustainable Energy Reviews*, 72:1019–1032, 2017.
- [50] Johan Edman and Johan Windahl. Dynamic modeling of a central receiver csp system in modelica. In *Proceedings of the 11th International Modelica Conference, Versailles*,

France, September 21-23, 2015, number 118, pages 585–594. Linköping University Electronic Press, 2015.

- [51] Andreas Ehrenmann. *Equilibrium problems with equilibrium constraints and their application to electricity markets*. PhD thesis, University of Cambridge Cambridge, 2004.
- [52] Juan F Escobar and Alejandro Jofré. Monopolistic competition in electricity networks with resistance losses. *Economic theory*, 44:101–121, 2010.
- [53] EUPHEMIA. Public description - PCR market coupling algorithm. <https://www.nordpoolgroup.com/globalassets/download-center/single-day-ahead-coupling/euphemia-public-description.pdf>, 2019. 55 pp.
- [54] Mingbin Feng, John E Mitchell, Jong-Shi Pang, Xin Shen, and Andreas Wächter. Complementarity formulations of l_0 -norm optimization problems. *Industrial Engineering and Management Sciences. Technical Report. Northwestern University, Evanston, IL, USA*, 5, 2013.
- [55] Mingbin Feng, John E. Mitchell, Jong-Shi Pang, Xin Shen, and Andreas Wächter. Complementarity formulations of l_0 -norm optimization problems. *Pac. J. Optim.*, 14(2):273–305, 2018.
- [56] Lara Fernández Fernández. *Análisis de los efectos por el uso de aditivos en ciclos Brayton supercríticos de CO₂*. PhD thesis, Industriales, 2023.
- [57] Jonathan E Fieldsend, John Matatko, and Ming Peng. Cardinality constrained portfolio optimisation. In *Intelligent Data Engineering and Automated Learning—IDEAL 2004: 5th International Conference, Exeter, UK. August 25-27, 2004. Proceedings 5*, pages 788–793. Springer, 2004.
- [58] Matteo Fischetti, Ivana Ljubić, Michele Monaci, and Markus Sinni. Interdiction games and monotonicity, with application to knapsack problems. *INFORMS J. Comput.*, 31(2):390–410, 2019.
- [59] Aoife M Foley, IJ Winning, and BP Ó Ó Gallachóir. State-of-the-art in electric vehicle charging infrastructure. In *2010 IEEE Vehicle Power and Propulsion Conference*, pages 1–6. IEEE, 2010.
- [60] G.B. Folland. *Real Analysis: Modern Techniques and Their Applications*. Pure and Applied Mathematics: A Wiley Series of Texts, Monographs and Tracts. Wiley, 2013.
- [61] Masao Fukushima and Gui-Hua Lin. Smoothing methods for mathematical programs with equilibrium constraints. In *International Conference on Informatics Research for Development of Knowledge Society Infrastructure, 2004. ICKS 2004.*, pages 206–213. IEEE, 2004.
- [62] Roberto Gabbrielli and C Zamparelli. Optimal design of a molten salt thermal storage tank for parabolic trough solar power plants. 2009.

- [63] Alfredo Peinado Gonzalo, Alberto Pliego Marugán, and Fausto Pedro García Márquez. A review of the application performances of concentrated solar power systems. *Applied Energy*, 255:113893, 2019.
- [64] WR Gould. Solarreserve’s 565 mwt molten salt power towers. In *17th International SolarPACES Symposium*, 2011.
- [65] Monique Guignard. Generalized kuhn–tucker conditions for mathematical programming problems in a banach space. *SIAM Journal on Control*, 7(2):232–241, 1969.
- [66] Mukrimin Sevket Guney. Solar power and application methods. *Renewable and Sustainable Energy Reviews*, 57:776–785, 2016.
- [67] Lei Guo, Gui-Hua Lin, and Jane J Ye. Solving mathematical programs with equilibrium constraints. *Journal of Optimization Theory and Applications*, 166:234–256, 2015.
- [68] Gurobi Optimization, LLC. Gurobi Optimizer Reference Manual, 2022.
- [69] Scott Hardman, Alan Jenn, Gil Tal, Jonn Axsen, George Beard, Nicolo Daina, Erik Figenbaum, Niklas Jakobsson, Patrick Jochem, Neale Kinnear, et al. A review of consumer preferences of and interactions with electric vehicle charging infrastructure. *Transportation Research Part D: Transport and Environment*, 62:508–523, 2018.
- [70] S Hemavathi and A Shinisha. A study on trends and developments in electric vehicle charging technologies. *Journal of energy storage*, 52:105013, 2022.
- [71] Catalina Hernández Moris, Maria Teresa Cerda Guevara, Alois Salmon, and Alvaro Lorca. Comparison between concentrated solar power and gas-based generation in terms of economic and flexibility-related aspects in chile. *Energies*, 14(4):1063, 2021.
- [72] Ronald A Howard and James E Matheson. Risk-sensitive markov decision processes. *Management science*, 18(7):356–369, 1972.
- [73] Ming Hu and Masao Fukushima. Multi-leader-follower games: models, methods and applications. *J. Oper. Res. Soc. Japan*, 58(1):1–23, 2015.
- [74] IEA. Technology Roadmap: Solar Thermal Electricity. Technical report, International Energy Agency, 2014.
- [75] IEA. Renewables 2019. <https://www.iea.org/reports/renewables-2019>, 2019. (accessed on May, 2021).
- [76] IEA. *Concentrated Solar Power (CSP)*, 2020. (accessed on May, 2021).
- [77] IEA. Concentrated Solar Power (CSP). <https://www.iea.org/reports/concentrating-solar-power-csp>, 2020. (accessed on May, 2021).
- [78] Rhys Jacob, Soheila Riahi, Ming Liu, Martin Belusko, and Frank Bruno. Techno-economic impacts of storage system design on the viability of concentrated solar power

- plants. *Journal of Energy Storage*, 34:101987, 2021.
- [79] Christian Kanzow, Andreas B. Raharja, and Alexandra Schwartz. Sequential optimality conditions for cardinality-constrained optimization problems with applications. *Comput. Optim. Appl.*, 80(1):185–211, 2021.
- [80] Imane Khamlich, Kuo Zeng, Gilles Flamant, Jan Baeyens, Chongzhe Zou, Jun Li, Xinyi Yang, Xiao He, Qingchuan Liu, Haiping Yang, et al. Technical and economic assessment of thermal energy storage in concentrated solar power plants within a spot electricity market. *Renewable and Sustainable Energy Reviews*, 139:110583, 2021.
- [81] Imane Khamlich, Kuo Zeng, Gilles Flamant, Jan Baeyens, Chongzhe Zou, Jun Li, Xinyi Yang, Xiao He, Qingchuan Liu, Haiping Yang, Qing Yang, and Hanping Chen. Technical and economic assessment of thermal energy storage in concentrated solar power plants within a spot electricity market. *Renewable and Sustainable Energy Reviews*, 139:110583, 2021.
- [82] Thomas Kleinert, Martine Labbé, Ivana Ljubić, and Martin Schmidt. A survey on mixed-integer programming techniques in bilevel optimization. *EURO J. Comput. Optim.*, 9:Paper No. 100007, 21, 2021.
- [83] Thomas Kleinert and Martin Schmidt. Why there is no need to use a big-m in linear bilevel optimization: A computational study of two ready-to-use approaches. *Computational Management Science*, 20(1):3, 2023.
- [84] Thomas Kleinert and Martin Schmidt. Why there is no need to use a big- M in linear bilevel optimization: a computational study of two ready-to-use approaches. *Comput. Manag. Sci.*, 20(1):Paper No. 3, 12, 2023.
- [85] Christoph Kost, Johannes N Mayer, Jessica Thomsen, Niklas Hartmann, Charlotte Senkpiel, Simon Philipps, Sebastian Nold, Simon Lude, Noha Saad, and Thomas Schlegl. Levelized cost of electricity-renewable energy technologies. 2013.
- [86] Christoph Kost, Johannes N Mayer, Jessica Thomsen, Niklas Hartmann, Charlotte Senkpiel, Simon Philipps, Sebastian Nold, Simon Lude, Noha Saad, and Thomas Schlegl. Levelized cost of electricity-renewable energy technologies. 2018.
- [87] N. Krejić, E. H. M. Krulikovski, and M. Raydan. A Low-Cost Alternating Projection Approach for a Continuous Formulation of Convex and Cardinality Constrained Optimization. *Oper. Res. Forum*, 4(4):Paper No. 73, 2023.
- [88] Evelin H. M. Krulikovski, Ademir A. Ribeiro, and Mael Sachine. On the weak stationarity conditions for mathematical programs with cardinality constraints: a unified approach. *Appl. Math. Optim.*, 84(3):3451–3473, 2021.
- [89] Guijun Li, Tanxiaosi Luo, and Yanqiu Song. Climate change mitigation efficiency of electric vehicle charging infrastructure in china: From the perspective of energy transition and circular economy. *Resources, Conservation and Recycling*, 179:106048, 2022.

- [90] Xiaolei Li, Zhifeng Wang, Ershu Xu, Linrui Ma, Li Xu, and Dongming Zhao. Dynamically coupled operation of two-tank indirect tes and steam generation system. *Energies*, 12(9):1720, 2019.
- [91] Ming Liu, N.H. Steven Tay, Stuart Bell, Martin Belusko, Rhys Jacob, Geoffrey Will, Wasim Saman, and Frank Bruno. Review on concentrating solar power plants and new developments in high temperature thermal energy storage technologies. *Renewable and Sustainable Energy Reviews*, 53:1411–1432, 2016.
- [92] Ming Liu, NH Steven Tay, Stuart Bell, Martin Belusko, Rhys Jacob, Geoffrey Will, Wasim Saman, and Frank Bruno. Review on concentrating solar power plants and new developments in high temperature thermal energy storage technologies. *Renewable and Sustainable Energy Reviews*, 53:1411–1432, 2016.
- [93] Tianye Liu, Jingze Yang, Zhen Yang, and Yuanyuan Duan. Techno-economic feasibility of solar power plants considering pv/csp with electrical/thermal energy storage system. *Energy Conversion and Management*, 255:115308, 2022.
- [94] Giovanni Lugaresi. The cardinality-constrained approach applied to manufacturing problems. 2016.
- [95] Zhi-Quan Luo, Jong-Shi Pang, and Daniel Ralph. *Mathematical programs with equilibrium constraints*. Cambridge University Press, 1996.
- [96] Vladimir Marianov. Location of multiple-server congestible facilities for maximizing expected demand, when services are non-essential. *Annals of Operations Research*, 123:125–141, 2003.
- [97] Suwaiba Mateen, Mohmmad Amir, Ahteshamul Haque, and Farhad Ilahi Bakhsh. Ultra-fast charging of electric vehicles: A review of power electronics converter, grid stability and optimal battery consideration in multi-energy systems. *Sustainable Energy, Grids and Networks*, page 101112, 2023.
- [98] Marc Medrano, Antoni Gil, Ingrid Martorell, Xavi Potau, and Luisa F Cabeza. State of the art on high-temperature thermal energy storage for power generation. part 2—case studies. *Renewable and Sustainable Energy Reviews*, 14(1):56–72, 2010.
- [99] Pere Mir-Artigues, Pablo del Río, Natàlia Caldés, Pere Mir-Artigues, Pablo del Río, and Natàlia Caldés. Public support schemes for the deployment of plants. *The Economics and Policy of Concentrating Solar Power Generation*, pages 157–193, 2019.
- [100] MJ Montes, A Abánades, JM Martínez-Val, and M Valdés. Solar multiple optimization for a solar-only thermal power plant, using oil as heat transfer fluid in the parabolic trough collectors. *Solar energy*, 83(12):2165–2176, 2009.
- [101] MJ Montes, A Abánades, JM Martínez-Val, and M Valdés. Solar multiple optimization for a solar-only thermal power plant, using oil as heat transfer fluid in the parabolic trough collectors. *Solar energy*, 83(12):2165–2176, 2009.

- [102] NREL. Concentrating Solar Power Projects | Concentrating Solar Power | NREL. url=<https://www.nrel.gov/csp/solarpaces/>, n.d. (accessed June, 2020).
- [103] NREL. System Advisor Model (SAM);. url=<https://sam.nrel.gov/>, n.d. (accessed mARCH, 2022).
- [104] Dario Paccagnan, Basilio Gentile, Francesca Parise, Maryam Kamgarpour, and John Lygeros. Nash and wardrop equilibria in aggregative games with coupling constraints. *IEEE Transactions on Automatic Control*, 64(4):1373–1388, 2018.
- [105] A. Palacios, C. Barreneche, M.E. Navarro, and Y. Ding. Thermal energy storage technologies for concentrated solar power – a review from a materials perspective. *Renewable Energy*, 156:1244–1265, 2020.
- [106] Jong-Shi Pang and Masao Fukushima. Quasi-variational inequalities, generalized Nash equilibria, and multi-leader-follower games. *Comput. Manag. Sci.*, 2(1):21–56, 2005.
- [107] Bhubaneswari Parida, Selvarasan Iniyan, and Ranko Goic. A review of solar photovoltaic technologies. *Renewable and sustainable energy reviews*, 15(3):1625–1636, 2011.
- [108] C Parrado, A Marzo, E Fuentealba, and AG Fernández. 2050 lcoe improvement using new molten salts for thermal energy storage in csp plants. *Renewable and Sustainable Energy Reviews*, 57:505–514, 2016.
- [109] Angela M Patnode. Simulation and performance evaluation of parabolic trough solar power plants. 2006.
- [110] Ugo Pelay, Lingai Luo, Yilin Fan, Driss Stitou, and Mark Rood. Thermal energy storage systems for concentrated solar power plants. *Renewable and Sustainable Energy Reviews*, 79:82–100, 2017.
- [111] Juan Peypouquet. *Convex optimization in normed spaces: theory, methods and examples*. Springer, 2015.
- [112] I. Purohit and P. Purohit. Technical and economic potential of concentrating solar thermal power generation in india. *Renewable and Sustainable Energy Reviews*, 78:648–667, 2017.
- [113] Kevin Ramos, Fernando Cardoso Silva Sequeira, Napoleon Hill, and João Miranda Lemos. Model and control of a solar tower for energy production. 2015.
- [114] Sergio Relloso and Emilio Delgado. Experience with molten salt thermal storage in a commercial parabolic trough plant. andasol-1 commissioning and operation. In *Proceedings of the 15th SolarPACES Conference, Berlin*, 2009.
- [115] Ademir A. Ribeiro, Mael Sachine, and Evelin H. M. Krulikovski. A comparative study of sequential optimality conditions for mathematical programs with cardinality constraints. *J. Optim. Theory Appl.*, 192(3):1067–1083, 2022.

- [116] Nele Rietmann, Beatrice Hügler, and Theo Lieven. Forecasting the trajectory of electric vehicle sales and the consequences for worldwide co2 emissions. *Journal of Cleaner Production*, 261:121038, 2020.
- [117] Manuel Romero and José González-Aguilar. Solar thermal csp technology. *Wiley Interdisciplinary Reviews: Energy and Environment*, 3(1):42–59, 2014.
- [118] Praveen RP. Performance analysis and optimization of central receiver solar thermal power plants for utility scale power generation. *Sustainability*, 12(1):127, 2019.
- [119] David Salas and Anton Svensson. Existence of solutions for deterministic bilevel games under a general Bayesian approach. *SIAM J. Optim.*, 33(3):2311–2340, 2023.
- [120] Donald Shepard. A two-dimensional interpolation function for irregularly-spaced data. In *Proceedings of the 1968 23rd ACM National Conference*, ACM '68, page 517–524, New York, NY, USA, 1968. Association for Computing Machinery.
- [121] Vladimir Shikhman and Sebastian Lämmel. Cardinality-constrained optimization problems in general position and beyond. *arXiv preprint arXiv:2106.08083*, 2021.
- [122] Ankur Sinha, Pekka Malo, and Kalyanmoy Deb. A review on bilevel optimization: From classical to evolutionary approaches and applications. *IEEE Transactions on Evolutionary Computation*, 22(2):276–295, 2017.
- [123] Ramteen Sioshansi and Paul Denholm. The value of concentrating solar power and thermal energy storage. *IEEE Transactions on Sustainable Energy*, 1(3):173–183, 2010.
- [124] Salas, D and Tapachès, E and Mazet, N and Aussel, D. Economical optimization of thermochemical storage in concentrated solar power plants via pre-scenarios. *Energy Conversion and Management*, 174:932–954, 2018.
- [125] Tapaches, Emeric and Salas, David and Perier-Muzet, Maxime and Mauran, Sylvain and Aussel, Didier and Mazet, Nathalie. The value of thermochemical storage for concentrated solar power plants: economic and technical conditions of power plants profitability on spot markets. *Energy Conversion and Management*, 198:111078, 2019.
- [126] Mikhail V Solodov et al. Constraint qualifications. *Wiley Encyclopedia of Operations Research and Management Science*. Wiley, New York, 2010.
- [127] Rüdiger Stephan. Cardinality constrained combinatorial optimization: Complexity and polyhedra. *Discrete Optimization*, 7(3):99–113, 2010.
- [128] Spandan Thaker, Abayomi Olufemi Oni, and Amit Kumar. Techno-economic evaluation of solar-based thermal energy storage systems. *Energy Conversion and Management*, 153:423–434, 2017.
- [129] The MathWorks, inc. *MATLAB R2020b - Online Documentation*, 2022. (acceded between January 2021 and February 2022).
- [130] Franz Trieb, Tobias Fichter, and Massimo Moser. Concentrating solar power in a sustainable

future electricity mix. *Sustainability science*, 9:47–60, 2014.

- [131] Craig S Turchi, Matthew Boyd, Devon Kesseli, Parthiv Kurup, Mark S Mehos, Ty W Neises, Prashant Sharan, Michael J Wagner, and Timothy Wendelin. Csp systems analysis-final project report. Technical report, National Renewable Energy Lab.(NREL), Golden, CO (United States), 2019.
- [132] Ségolène Vannerem, Pierre Neveu, and Quentin Falcoz. Thermal cycle performance of thermocline storage: numerical and experimental exergy analysis. *Energy*, 278:127647, 2023.
- [133] Michal Červinka, Christian Kanzow, and Alexandra Schwartz. Constraint qualifications and optimality conditions for optimization problems with cardinality constraints. *Math. Program.*, 160(1-2):353–377, 2016.
- [134] M. J. Wagner. Simulation and predictive performance modeling of utility-scale central receiver system power plants. 2008.
- [135] M. J. Wagner and P. Gilman. Technical manual for the SAM physical trough model. Technical report, National Renewable Energy Lab.(NREL), Golden, CO (United States), 2011.
- [136] Andrea Walther and Andreas Griewank. Getting started with *adol-c*. *Combinatorial scientific computing*, 181:202, 2009.
- [137] Yunshi Wang, Daniel Sperling, Gil Tal, and Haifeng Fang. China’s electric car surge. *Energy Policy*, 102:486–490, 2017.
- [138] Lee A Weinstein, James Loomis, Bikram Bhatia, David M Bierman, Evelyn N Wang, and Gang Chen. Concentrating solar power. *Chemical Reviews*, 115(23):12797–12838, 2015.
- [139] Margaret Wright. The interior-point revolution in optimization: history, recent developments, and lasting consequences. *Bulletin of the American mathematical society*, 42(1):39–56, 2005.
- [140] Sike Wu, Cheng Zhou, Elham Doroodchi, and Behdad Moghtaderi. Techno-economic analysis of an integrated liquid air and thermochemical energy storage system. *Energy Conversion and Management*, 205:112341, 2020.
- [141] Zhuoyu Xiao and Jane J Ye. Optimality conditions and constraint qualifications for cardinality constrained optimization problems. *arXiv preprint arXiv:2209.08428*, 2022.
- [142] Fritz Zaversky, Javier García-Barberena, Marcelino Sánchez, and David Astrain. Transient molten salt two-tank thermal storage modeling for csp performance simulations. *Solar Energy*, 93:294–311, 2013.
- [143] Fritz Zaversky, Javier Pérez de Zabalza Asiain, and Marcelino Sánchez. Transient response simulation of a passive sensible heat storage system and the comparison to a conventional active indirect two-tank unit. *Energy*, 139:782–797, 2017.
- [144] H.L. Zhang, J. Baeyens, J. Degreve, and G. Cáceres. Concentrated solar power plants: Review and design methodology. *Renewable and sustainable energy reviews*, 22:466–481, 2013.
- [145] Huili Zhang, Jan Baeyens, Gustavo Cáceres, Jan Degreve, and Yongqin Lv. Thermal energy storage: Recent developments and practical aspects. *Progress in Energy and Combustion*

Science, 53:1–40, 2016.

- [146] Qiangqiang Zhang, Xin Li, Zhifeng Wang, Chun Chang, and Hong Liu. Experimental and theoretical analysis of a dynamic test method for molten salt cavity receiver. *Renewable Energy*, 50:214–221, 2013.
- [147] QQ Zhang, X Li, C Chang, H Liu, and ZF Wang. Transient analysis of a molten salt cavity receiver. *Energy Procedia*, 49:599–606, 2014.
- [148] Feng Zhu and Panos J Antsaklis. Optimal control of switched hybrid systems: a brief survey. *ISIS*, 3, 2011.
- [149] Adriana Zurita, Carlos Mata-Torres, José M. Cardemil, and Rodrigo A. Escobar. Assessment of time resolution impact on the modeling of a hybrid csp-pv plant: A case of study in chile. *Solar Energy*, 202:553–570, 2020.